Comparison between Calculation and Measurement of Inductive Pipeline Interference Voltages

PhD Thesis

Institute of Electrical Power Systems
Graz University of Technology

Author:
Dipl.-Ing. Christian Wahl, BSc

1st Reviewer & supervisor:
Em.Univ.-Prof. Dipl.-Ing. Dr. techn. Lothar Fickert
Graz University of Technology

2nd Reviewer:
Assoc. Prof. Dr. Petr Toman
Brno University of Technology

Co-supervisor:
Dipl.-Ing. Dr. techn. Ernst Schmautzer

Head of Institute: Univ.-Prof. DDipl.-Ing. Dr.techn. Robert Schürhuber

A - 8010 Graz, Inffeldgasse 18-I
Telefon: (+43 316) 873 – 7551
Telefax: (+43 316) 873 – 7553
http://www.ifea.tugraz.at
http://www.tugraz.at

Graz / April– 2021

Acknowledgements

Danke.

Thank you.

A special thanks to my supervisor, Em.Prof. Lothar Fickert, for his help and patience on this thesis.

A special thanks to Prof. Petr Toman, for reviewing this thesis.

A special thanks to Ernst Schmautzer, for helping me in any situation in projects or with technical questions in this thesis.

A special thank you goes out to my wife Sigrid for supporting me during all these years of writing this thesis as well as for the proofreading.

And thank you to my children, Sarah and Miriam, for showing me that other things are just as important in life.

Statutory Declaration

I declare that I have authored this thesis independently, that I have not used other than the declared sources / resources and that I have explicitly marked all material which has been quoted either literally or by content from the used sources.

date

signature

Abstract

Due to bundled energy routes, high voltage power systems (e.g. high voltage overhead power lines, railway lines and cables) are often located near buried isolated metallic pipelines. A high inductive interference from energy systems may cause hazardous AC pipeline voltages. High induced voltage levels can lead to dangerously high touch voltages and AC material corrosion. Therefore, especially in the planning stage, pipeline interference calculations are necessary. However, in practice, such calculations often diverge significantly from real measurements conducted on pipelines. This thesis aims to investigate this discrepancy in order to improve calculations.

To determine the impact of different formulas and their corresponding electric parameters on calculations of pipeline interference voltages, this thesis uses a new calculation model. A simple example is used to compare the results of these formulas and to identify important parameters.

In addition, this thesis focuses on the effect of different pylon types of overhead lines and their conductor configuration on the calculations. Since, often, several parallel pipelines, high voltage power systems and metallic structures are located near each other, simple as well as complex examples are looked at. This is necessary to understand the interactions between different systems and to improve calculations.

Field measurements of the electrical pipeline parameters and measurements of the pipeline voltages were used to determine the validity of calculation formulas and for the correct interpretation of the results.

Taking into account the findings of the previous parts of the thesis, calculations were compared to measurements conducted at different pipeline locations. Different comparison methods were developed to identify the various problems of the calculations for each measuring location. By identifying parameters and surrounding effects, calculation results could be improved to better match measurement data. Better calculations increase personnel safety and the durability of the pipeline. With more accurate calculations, it is often possible to avoid additional earthing systems or other countermeasures against high pipeline interference voltages, thus reducing costs.

Keywords: Pipelines, inductive interference, AC corrosion, calculation of pipeline parameters, interference of overhead lines, railways and cables, measurement of pipeline parameters, comparison of calculation and measurement

Kurzfassung

Aufgrund der Bündelung von Verkehrs- und Energietrassen befinden sich Hochspannungsanlagen wie z.B. Freileitungen, Bahnstrecken oder Erdkabeln oft im Nahbereich von in der Erde vergrabenen metallischen Rohrleitungen. Dies kann aufgrund von induktiver Beeinflussung zu hohen Wechselspannungen an Rohrleitungen (Rohrspannung) führen, welche die Personensicherheit gefährden sowie die Wechselstromkorrosion fördern. Um dies zu verhindern ist eine genaue Berechnung der Rohrspannungen, vor allem in der Planungsphase, notwendig. Diese berechneten Rohrspannungen liegen in der Praxis jedoch oft höher als die tatsächlich gemessenen Rohrspannungen. Das Ziel dieser Doktorarbeit ist es, diese Unterschiede herauszuarbeiten um die Berechnungen der Rohrspannungen zu verbessern.

Ein neues Berechnungsmodel wurde entwickelt, um die Auswirkungen der verschiedenen Berechnungsformeln und deren dazugehörigen elektrischen Parameter zu untersuchen. Dazu wurde ein einfaches Beispiel generiert um die Ergebnisse dieser Formeln vergleichen zu können und um die wichtigsten elektrischen Parameter festzustellen.

Des Weiteren wurde in dieser Doktorarbeit der Einfluss der verschiedenen Masttypen und deren Phasenleiterbelegungen sowie die Wirkung von Erdungsleitern von Freileitungen untersucht. Aufgrund der bereits erwähnten Bündelung von Energietrassen befinden sich Rohrleitungen, Hochspannungsanlagen und andere metallische Strukturen wie z.B. fremde Erdungsanlagen häufig nah beieinander, was zu komplexen Beeinflussungssituationen führt. Verschiedene Beispiele in dieser Arbeit betrachten unterschiedliche Kombinationen der verschiedenen metallischen Einbauten, um die Wechselwirkung zu verstehen und die Berechnungen der Rohrspannung zu verbessern.

Zusätzlich wurde in dieser Arbeit der generelle Ablauf der Messung an der Rohrleitung sowie die Interpretation der Messdaten besprochen. Um die Berechnungsformeln auf ihre Gültigkeit zu überprüfen, wurden Praxismessungen an einer Rohrleitung durchgeführt.

Unter Berücksichtigung der ersten Ergebnisse dieser Dissertation wurden die Berechnungen mit Messungen an verschiedenen Punkten der Rohrleitung verglichen. Dazu wurden unterschiedliche Methoden entwickelt, um die verschiedenen Berechnungsprobleme an den Messpunkten zu erkennen. Dadurch konnten verschiedene Berechnungsparameter sowie Umgebungsparameter gefunden werden, die einen signifikanten Einfluss auf die Berechnungen haben. Unter Berücksichtigung dieser Parameter können die Berechnungen der Rohrspannungen verbessert werden, damit diese näher an den Messungen liegen. Dies führt zu erhöhter Personen- und Materialsicherheit und häufig ist es möglich, kostenintensive Gegenmaßnahmen zu vermeiden.

Schlüsselwörter: Rohrleitungen, induktive Beeinflussung, Wechselstromkorrosion, Berechnung der elektrischen Kenndaten der Rohrleitung, Beeinflussung von Freileitungen, Messung der elektrischen Kenndaten der Rohrleitung, Vergleich der Rohrspannung zwischen Berechnung und Messung

Contents

List of Abbreviations

CC …….	abbr. for conductor configuration; the geometrical arrangement of the phase conductors in relation to the structure of an overhead line
EC …….	abbr. for earthing conductor
HVPS ……	abbr. for high voltage power system
OHL ……..	abbr. for overhead line
MI …….	abbr. for mutual impedance
PIV ……...	abbr. for pipeline interference voltage, which is the pipeline potential along the pipeline
SC ……..	abbr. for screening conductor
SPCR …….	abbr. for specific pipeline coating resistance

1 Introduction

1.1 Overview

In the past decades, many operators in the energy sector have been forced to share the same geographical corridors for their facilities. The reasons for this are mainly geographical, political and social in nature. Projects have to fulfil an optimal cost management, strict environmental regulations and have to consider the interests of citizens.

These bundled energy routes can create problems, especially when high voltage power systems (HVPS), e.g. overhead lines (OHLs), are located near buried isolated metallic pipelines. Such current-carrying power systems form electromagnetic fields following three mechanisms, namely capacitive, conductive and inductive coupling.

Capacitive coupling does not play a key role in the case of a buried, active pipeline. Conductive coupling, however, can appear when the buried pipeline's isolation has a coating holiday and lies in a potential gradient. There, with direct contact between metal and influenced soil, the pipeline is influenced and a pipeline interference voltage (PIV) appears. Inductive coupling has the most significant effect. Due to its typical behaviour, inductive coupling leads to high PIVs and therefore, inductive coupling will be the focus of this thesis.

Calculating the PIV is crucial for operators with contiguous and/or long parallel routes of influencing and influenced systems since high induced voltages and current levels may occur. High induced voltages and currents are potentially dangerous for the operating personnel due to high touch voltages, as well as for the pipeline equipment and the pipeline material due to alternating current (AC) corrosion.

To implement the correct and appropriate countermeasures, accurate pipeline interference calculations are necessary.

1.2 Motivation

During the completion of this thesis, a lot of projects for Austrian pipeline operators were handled. Almost all of the pipelines in Austria were found to be influenced by high voltage power systems, most of them over several kilometres and by more than one system. Thus, the traditionally calculated alternating current pipeline interference voltages are very high in some areas. Also, measurements conducted by operators showed deviating results. These measured PIVs were in some cases equal to or higher than the standardized calculations, but mostly they were significantly lower. This discrepancy has to be investigated to bring calculations and measurement data closer together to avoid excessive measures which are often cost-intensive. Therefore, the motivation for this thesis is to provide crucial new research into the different impact factors and their effect on PIV calculations. This includes a focus on the effect of possible surroundings, such as other metallic

structures in the area, which can influence the PIV significantly. Due to the immense complexity of calculating all these factors manually, this thesis provides a new mathematical model for calculations.

1.3 Scope of Research

This thesis introduces a proposal for a computer program which integrates a new mathematical model to calculate PIVs. It focuses on minimizing discrepancies between the standardized calculations of PIVs and the real data collected during measurements in the field.

The following chapters will highlight the importance of identifying the main factors which influence the inductive interference on buried metallic pipelines. This includes the screening factors and their influence on PIVs.

During the course of this thesis, in cooperation with pipeline operators, measurements were conducted which were then compared to the results of standardized calculation methods. The goal was to investigate which factors lead to possible discrepancies.

1.4 Research Methods

A new program had to be developed to investigate the effects of the different formulas for calculating the inductive pipeline interference voltage. This program was programmed in the commercial software Matlab® and has the advantage that many steps of the calculation are done automatically. In this way many different parameters of the formulas could be considered and at the same time a new mathematical model could be inserted. With the help of the software Simulink®, the newly developed program was verified by calculations with different samples and thus it could be shown that the mathematical method worked correctly. In addition, various different models of high voltage power systems and their effects on the pipeline interference voltage could be investigated.

For verifying the calculation formulas, a complex measurement was done with the help of a pipeline operator. Despite some problems during the measurement, it was possible to show that the formulas are also valid in practice and can be used accordingly in the calculations.

Several pipeline operators have performed long-term measurements on their pipelines to analyse the PIV along the pipeline. In addition, the PIV along the pipeline has been calculated. To analyse these measurements and calculations, new analytical methods had to be developed to compare the measurements and the calculations. As a result, various problems both in the calculation and in the measurement could be analysed, which make the comparison between the measurement and the calculation difficult.

1.5 Previous publications relevant to this thesis

The electrical description of pipelines by Carson [1] and Pollaczeck [2] stems from the beginning of the 20th century and is still used today to calculate the longitudinal impedance of a pipeline. A more detailed description of the electrical parameters of a pipeline was later added by Mikhailov and Rasumov [3] which included the calculation of the shunt admittance of a pipeline.

Carlson and Pollaczeck also described the mutual impedance, using the mirror conductor theory and a very complex formula. A later work of Dommel [4] extended this formula, making possible a faster calculation. However, this formula is complex to program and shows a calculation error at a certain distance between pipeline and influencing conductor. An easier alternative is offered by the formula of Dubanton [5], which can be used over the whole distance of two conductors without limitation.

In general, the calculation can be performed with the formulas mentioned above and with the nodal admittance matrix [6]. The mathematical model used in this thesis takes a different approach, however, using the model of Starr [7] and Clarke [8]. This model was actually invented to describe transformers mathematically. On this basis it was possible to create a new calculation program for pipeline inductive interference calculations in order to methodically investigate the various parameters of calculating the pipeline interference voltage.

For a long time, the AC interference was of little importance because pipelines used a bitumen coating which had a lower specific pipeline coating resistance and, therefore, lower pipeline interference voltages (PIVs). With the use of polyethylene coatings, the PIVs increased significantly, leading to various investigations into the topic. First standards ([9], [10], [11]) were developed and have been further developed over the years to the current valid standards in Austria with ÖVE/ÖNORM EN 50443 [12], ÖVE/ÖNORM EN 15280 [13], ÖNORM EN ISO 18086 [14] and TE 30 [15]. Most of them are also European standards with slightly different titles which means that they are valid for a number of countries.

In Austria, it was Muckenhuber [16] who researched this topic and published several publications. This led to the important doctoral thesis of Schmautzer [17], who provided a precise mathematical description of the interference model and developed one of the first fully automatic programs for calculating the influence. In the following years research on AC interference continued in German-speaking countries, but it remained a marginal topic in science. A particularly large amount of research in the field of AC corrosion was done by Büchler who investigated the chemical steps involved in corrosion. He also investigated which soils particularly accelerate corrosion [18], the effect of pipeline coating holiday geometry [19] and how high the value of AC voltage and AC density on the holiday must be to cause severe corrosion [20]. Many of his research results were adopted for current standards. Bette (for example: [21]) also describes AC interference and its physical effects on pipelines. However, his particular area of expertise is DC interference on pipelines, which can greatly impact the cathodic protection system of a pipeline [22].

Many pipeline interference calculations were done based of the previous publications of Muckenhuber and Schmautzer. Braunstein [6] also wrote his doctoral thesis in this field. His thesis deals with many aspects of pipeline interference. An important section is the investigation of the size of coating holidays and the surrounding parameters. It has been shown that coating holidays must be small enough to generate a high current density at this point on the metallic surface of the pipeline and thus trigger AC corrosion. Other important parameters are the specific soil resistance and especially the PIV in this location. In order to reduce AC corrosion, PIVs must be reduced and some suggestions for mitigating measures were offered in his thesis.

It is shown that a screening conductor in the right place can reduce the PIV accordingly, but this is only possible in specific cases. It is much more efficient to use isolation joints to separate strongly influenced areas from weakly influenced areas. However, this is usually only possible during the pipeline construction, as retrofitting is associated with enormous costs. His thesis shows that the installation of earthing systems is in most cases much cheaper and easier to handle.

The placement of earthing systems and the calculation of the necessary earth electrode resistance can often be difficult. The master thesis (Diplomarbeit) by Wahl [23] tests, with the help of different algorithms, whether an automatic placement of earthing systems and calculation of their earth electrode resistance is possible. It is shown that algorithms can help, but not always are the optimal results achieved. In addition, the costs for the measures were very high or an unrealistic earth electrode resistance for the earthing systems was calculated. However, an algorithm based on human behaviour shows that up to a certain point, the optimisation of earthing systems can be done by a program.

Based on the mathematical model of Starr [7] and Clarke [8], Steinkellner [24] described this model in more detail and was able to program a first version to calculate other problems, such as the phase conductor configuration of overhead lines. This basic programming was then later developed further and is described in more detail in this thesis as well as in the master thesis by Roßmann [25] and is the basis of the current calculation model.

The DC interference is not only to be found in Austria, but everywhere where pipelines and high-voltage systems are placed closely together. Research has been carried out to optimise the calculations (for example: [26], [27], [28]). The problem with the publications [26] and [27] is that a comparison between calculation and measurement was only done for specific projects. Unfortunately, no analysis of the influence of the different parameters in the calculations was conducted. In addition, the calculation corresponds almost exactly to the measurements and this must, unfortunately, be questioned. These publications do not explain how exactly the calculation results were achieved. Some research was done to investigate the influence of parameters on the calculations.

To investigate the influence of overhead lines on the PIV, Wahl [29] performed several calculations with different expansion stages of the same overhead line. It was shown that not only the maximum possible current has an effect, but especially the phase conductor configuration. It was found that the type of pylon of the overhead line has an impact. Another publication [30] showed that the impact of the specific soil resistivity and the specific pipeline coating resistance is very important. If both parameters have a low value, then the calculations show that PIV also decreases and therefore it is important to accurately determine the specific soil resistivity and the specific pipeline coating resistance. This was one of the first publications that showed why previously the AC interference was considered to be relatively unimportant. This could be attributed to the old bitumen pipeline coatings, which are a poor insulator against the surrounding soil.

Most of these publications only deal with the influence on overhead lines. [25] deals mainly with railway lines. Different possible configurations of railway lines such as several parallel railway rails, additional amplifying conductors or return conductors are calculated to investigate the effects on the PIV in more detail. It is shown that the usual reduction factors are basically correct for most cases, but that there may be more significant deviations.

In [31] and [32], the problems of calculating the inductive interference due to surrounding factors were examined in more detail. These factors exist particularly in surrounding metallic installations such as external earthing systems, house foundation earth electrodes or other metallic pipes. These factors were examined in detail and it could be shown by curve progressions of measured and calculated PIVs that these are usually very difficult to determine and often can only be estimated.

Because of the problem that calculations and measurements show such different values, the electrical description of the pipeline of [1], [2] and [3] has also been questioned. [33] did tests on a real pipeline and could measure both the longitudinal impedance and the shunt admittance. It has been shown that the electrical description including the corresponding formulas are valid.

1.6 Scientific Contribution

The main contributions to science are

- Finding the most suitable and effective formulas for calculating pipeline interference voltages (PIVs) by analysing various parameters for longitudinal impedance, shunt admittance and mutual impedance
- Developing a new method and a program introducing a much more efficient mathematical method for calculating PIV
- The integration of a standardized example with an appealing graphical analysis to compare the influence of different parameters on the PIV
- Investigation into the degree of influence of different calculation parameters on the PIV
    - Parameters which have a direct influence on the equivalent model of the pipeline
    - Influence of the different types of pylons and system design of overhead lines
    - The role of earthing conductors of overhead lines
    - Calculation of the reduction and amplification factor on the PIV for multiple configurations of overhead lines and metallic structures in the soil
- Methods to enable a comparison between calculation and measurement so that the calculations can be optimised
- Identification of various problems in calculations and measurements, which complicate the graphical and numerical analysis
- Showing different approaches to the analysis of entire pipelines

1.7 Research Questions

The research questions were defined as follows:

- Which calculation formula system should be used to achieve more accurate calculation results for pipeline and conductor parameters?
    - For discussion, see chapters 4.2 and 6.2.
- Which parameter in the pipeline itself has the most significant impact on the calculation of pipeline interference voltage?
    - See chapters 2.3, 4.3 and 4.4.
- How does the pylon type and the phase conductor configuration of influencing overhead lines impact the pipeline interference voltage?
    - See chapters 0 and 4.6.3

- How large is the influence of earthing conductors of overhead lines on the pipeline interference voltage?
    - See chapter 4.7.
- What happens to the pipeline interference voltage in cases of multiple configurations of metallic structures?
    - For the case of two parallel overhead lines next to a pipeline, see chapter 5.2.
    - For the case of an overhead line next to a pipeline and several metallic structures, see chapter 5.3.
    - For the case of two parallel overhead lines next to a pipeline and several metallic structures, see chapter 5.4.
    - For the case of an overhead line next to two parallel pipelines, see chapter 5.5.
- Which factors should be considered when comparing calculations and measurements of inductive pipeline interference voltage?
    - How can measurements be conducted and interpreted correctly?
        - See chapter 6.1.
    - What are the different approaches to comparing data and what are the advantages and disadvantages?
        - See chapter 7.1.
    - What problems arise when comparing measurement and calculation and how can discrepancies be interpreted?
        - See chapters 7.2 and 7.3
    - What do such comparisons look like for entire sections of a pipeline?
        - See chapter 7.4.
- How can conducted measurements improve the performance of calculations?
    - See chapters 7.2, 7.3 and 7.4.

2 Pipeline interference voltage calculations

The first part of this chapter shows why such calculations are necessary. It provides an overview of standards and regulations, including their limitations regarding induced pipeline interference voltages (PIVs). Also, a survey of actions against hazardous AC PIVs is presented. The second part outlines all necessary calculation steps for the computation of PIV.

2.1 Standards, Regulations and Limitations

For minimizing the risk of personal injuries (e.g. by touch voltages) and material damages (e.g. system disturbances, AC corrosion), European and Austrian standards and guidelines (TE 30 [15], ÖVE/ÖNORM EN 50443 [12], ÖVE/ÖNORM EN 15280 [13]) exist, which limit the maximum voltage for long-term and short-term interference. These standards and guidelines are applied to high voltage power lines (OHLs, buried isolated cables) with rated voltages equal to or higher than 110 kV as well as for railroad systems.

2.1.1 Touch voltages

The standards and guidelines [15] and [12] are to be applied to touch voltages. Despite their minor differences in content, particularly concerning details with regards to interference distances, they propose similar values for inadmissible high touch voltages in pipelines. The following Table 2-1 provides an outline of the limits for induced PIVs:

According to [15] and [12] the interference must be differentiated for the duration of the influence. With this, it is possible to define long-term and short-term interferences. Simply put, long-term interference describes interference over a longer period of time within high voltage power systems in normal operational mode. Short-term interference describes interferences with durations ≤ 0.5 seconds which can be found, for example, in short-circuit situations. In Austria, the time of failure for short-circuit situations of high voltage power systems with voltages higher than 220 kV, as well as railroad systems, is usually lower than 0.2 seconds. Therefore, based on Table 2-1 and Table 2-2, the limit for hazardous voltages in normal operational mode is 60 Volt and 1500 Volt in short-circuit situations.

Long term interference

Limit for PIV	Measures against inadmissible high touch voltages
$U_P \leq 60$ V	None
$U_P > 60$ V	Reducing the pipeline potential under $U_P \leq 60$ Volt with the installation of earthing systems or electrical disconnecting points (isolating joints) Reducing the touchable voltage smaller than $U_P \leq 60$ Volt with potential control and insulations of the local place, insulation of accessible pipeline facilities and measures on pipeline stations

Short term interference

Limit for PIV	Measures against inadmissible high touch voltages
$U_P \leq 1500$ V	None
1500 V < $U_P \leq 2000$ V	Reducing the pipeline potential under $U_P \leq 1500$ Volt with the installation of earthing systems or electrical disconnecting points (isolating joints) Reducing the touchable voltage smaller than $U_P \leq 1500$ Volt with potential control and insulations of the local place, insulation of accessible pipeline facilities and measures on pipeline stations
$U_P > 2000$ V	Usage of earthing systems for reducing the pipeline potential under $U_P \leq 1500$ Volt or with above described additional measures for U_P between 1500 and ≤ 2000 Volt

Table 2-1: Maximum PIV for long- and short term interference as well as necessary actions against to high PIVs, according to [15]

Time of failure [s]	Interference voltage (effective value) [V]
$t \leq 0{,}10$	2000
$0{,}10 < t \leq 0{,}20$	1500
$0{,}20 < t \leq 0{,}35$	1000
$0{,}35 < t \leq 0{,}50$	650
$0{,}50 < t \leq 1{,}00$	430
$1{,}00 < t \leq 3{,}00$	150
$t > 3{,}00$	60

Table 2-2: Maximum interference voltage for different time of failure, according to [12]

2.1.2 Risk of AC corrosion

For AC corrosion to appear, two circumstances must occur: First, the isolation of the pipeline coating must have an isolation defect, which is called a coating holiday, and second, the pipeline must be highly influenced. The Ph.D. thesis [6] also shows that some environmental factors play a role, for example soil resistivity and humidity as well as soil composition. To minimize the risk of AC corrosion on steel surfaces, the induced PIVs should not exceed a certain limit. According to [13], this limit is 15 Volt. Furthermore, this regulation also has other requirements which have to be considered:

The compliance with the AC current density requirement should always be verified by measurements and/or calculations. [6] describes the links between interference voltages, soil resistivity and the size of a possible coating holiday: First, interference currents caused by high induced voltages must exceed a certain limit. Second, in areas with a low soil resistivity, the induced pipeline current will flow more easily into the soil and does not stay inside the pipeline (the resistance ratio). Third, the coating holiday shape and size play a key role.

In theory, the size of the coating holiday must be large enough for the contact resistance between the soil and the steel to be low enough and to enable a high current flow into the soil. This assumption, however, is problematic because extensive coating holidays produce low current densities and therefore highly influenced pipelines with a large coating holiday show no signs of corrosion. Consequentially, a coating holiday needs to be the right size for AC corrosion to actually occur [6].

With research and practical experience over the years, a standardized coupon has been invented with a size of 1.5 cm^2 [13]. Coupons are buried in the ground next to pipelines suspected of having a high risk of. The advantage of coupons is that, after a certain time has passed, they can be excavated and checked for corrosion easily.

2.2 Basics of calculating the pipeline interference voltage

2.2.1 General induced voltage calculation

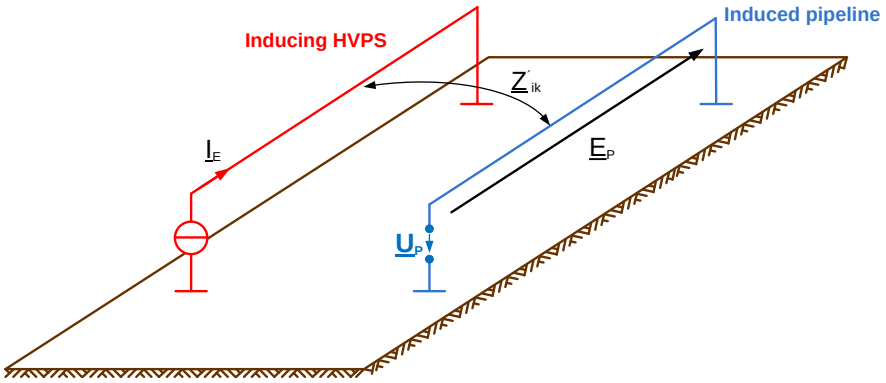

Figure 2-1: General example for the calculation of the induced voltage in a pipeline

Figure 2-1 shows a simple example of inductive interference between two conductors. This example describes an interfered pipeline and an interfering HVPS (high voltage power system). If the current $\underline{I}_E$ as well as the inductive coupling $\underline{Z}'_{ik}$ between pipeline and HVPS are known, the induced voltage $\underline{E}_P$ can be calculated. The pipeline itself is a closed conductor loop with a ground return on one side and an open side on the other end, where $\underline{E}_P$ as voltage per unit length ℓ is induced. The following simple formula (2-1) describes this figure:

$$\underline{E}_P = \underline{I}_E \cdot \underline{Z}'_{ik} \cdot \ell \qquad (2\text{-}1)$$

$\underline{E}_P$:	Electromotive force [Vm]
$\underline{U}_P$:	PIV [V]
$\underline{I}_E$:	Inducing current from a current-carrying HVPS [A]
$\underline{Z}'_{ik}$:	Inductive coupling impedance between both systems (mutual impedance) per unit length [Ω]
ℓ:	Distance of parallel route [m]

In reality, however, some problems may occur: In most cases, there is more than one current-carrying interfering conductor. In fact, most HVPS have many of them as well as often one or more than one EC (earthing conductor), which can reduce or amplify the interference voltage. These additional currents have to be calculated, as shown in chapter 2.4. Another problem is that real pipelines and ground conductors show not only longitudinal impedance – shunt admittances have to be considered as well, as will be shown in chapter 2.3.1.2.

2.2.2 Segmenting

Within a coupling between two conductors of a certain length, all parameters must be (approximately) homogenous because otherwise calculation formulas cannot be applied. This means that when a parameter changes, the section of this coupling has to be subdivided into smaller parts, which is called segmenting. When the distance x_{ik} between two coupled conductors is not constant, the distance should be divided up to improve accuracy.

The following Figure 2-2 shows a section with the length ℓ. It can be seen that the coupling distance x_{ik} is varying. Using a mean value between x_{ik1} and x_{ik2}, the coupling impedance cannot be calculated accurately because of a large deviation with regards to the real value. With segmenting, the length ℓ is subdivided into the segmenting lengths ℓ_{S1} to ℓ_{S6} and the mean value of the coupling distance is split up. This leads to a smaller error and improves the results of the calculation.

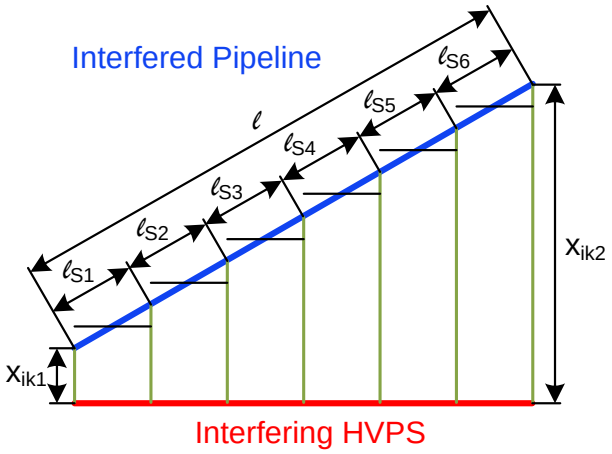

Figure 2-2: Model for segmenting an increasing distance between pipeline and HVPS

One disadvantage of this method is that the effort for creating simulations using a graphical interface (e.g. Matlab® Simulink) and calculations by hand is immense and at some point too extensive. Preferably, numerical calculations methods increasing the accuracy of calculations should not put a strain on human resources. Unfortunately, with the use of numerical methods to further improve the results, more time is needed for calculations and the requirements for the hardware needed increase.

2.2.3 Electric conductor equation

This chapter is mainly based on the works of Schmautzer [17], page 8 to 11 and Unger [34], but additional information can be found in Öding [35], page 305 to 307 and Klein [36]. When all parameters are homogenous within one segment, a general equation can be applied to electric conductors and therefore can be used for interfered pipelines, interfering HVPSs and other non-current-carrying conductors.

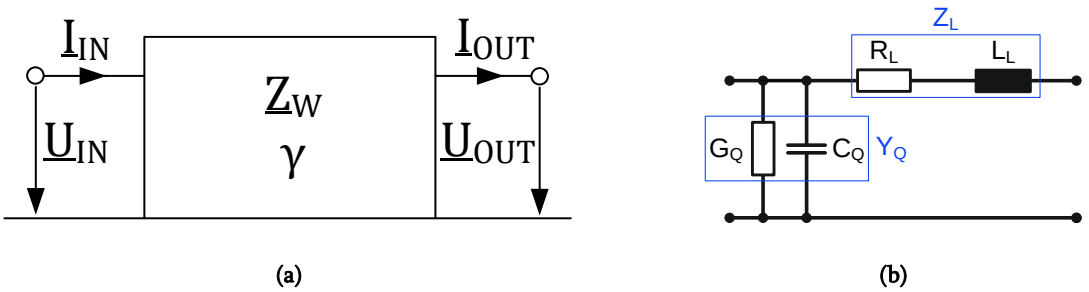

Figure 2-3: General model of a quadruple including the inner structure

Using a quadrupole and an inner structure, as shown in Figure 2-3 (a) and Figure 2-3 (b), an equivalent circuit without an inductive interference can be created, as illustrated in Figure 2-4. This model leads to the equations (2-2) and (2-3) for conductor voltages and conductor currents.

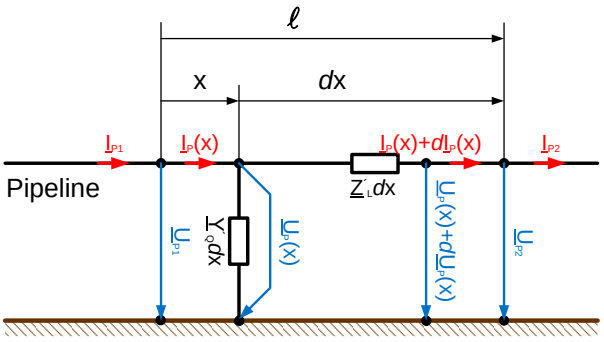

Figure 2-4: Equivalent circuit of a conductor segment without inductive interference

$$\underline{U}_P(x) - \underline{U}_P(x+dx) - \underline{I}_P(x) \cdot \underline{Z}'_L dx = 0 \tag{2-2}$$

$$\underline{I}_P(x) - \underline{I}_P(x+dx) - U_P(x) \cdot \underline{Y}'_Q dx = 0 \tag{2-3}$$

$\underline{U}_P$:	Conductor voltage [V]
$\underline{I}_P$:	Conductor current [A]
$\underline{Z}'_L$:	Specific longitudinal impedance [Ω/m]
$\underline{Y}'_Q$:	Specific shunt admittance [S/m]
ℓ:	Length of the segment [m]
x:	Integration variable

These two equations can be transformed into equations (2-4) and (2-5):

$$\frac{d\underline{U}_P}{dx} = -\underline{I}_P \cdot \underline{Z}_L' \tag{2-4}$$

$$\frac{d\underline{I}_P}{dx} = -\underline{U}_P \cdot \underline{Y}_Q' \tag{2-5}$$

These equations are the differential equations for conductors in steady-state condition and form a linear system of common first order differential equations. With reshaping and differentiation, the following wave equations can be established:

$$\frac{d^2\underline{U}_P}{dx} = \left(\underline{Z}_L' \cdot \underline{Y}_Q'\right) \cdot \underline{U}_P = \underline{\gamma}^2 \cdot \underline{U}_P \tag{2-6}$$

$$\frac{d^2\underline{I}_P}{dx} = \left(\underline{Z}_L' \cdot \underline{Y}_Q'\right) \cdot \underline{I}_P = \underline{\gamma}^2 \cdot \underline{I}_P \tag{2-7}$$

γ: Complex propagation coefficient with $\underline{\gamma} = \alpha + j\beta = \sqrt{(\underline{R}_L' + j\omega\underline{L}_L') \cdot (\underline{G}_Q' + j\omega\underline{C}_Q')} = \sqrt{\underline{Z}_L' \cdot \underline{Y}_Q'}$

Solving (2-6) and (2-7) leads to equations (2-8) and (2-9), where $\underline{U_1}$ and $\underline{U_2}$ are arbitrary values and are equal to integration constants.

$$\underline{U}_P = \underline{U}_1 \cdot e^{-\underline{\gamma}x} + \underline{U}_2 \cdot e^{\underline{\gamma}x} \tag{2-8}$$

$$\underline{I}_P = \frac{\underline{\gamma}}{\underline{Z}_L} \cdot \left(\underline{U}_1 \cdot e^{-\underline{\gamma}x} - \underline{U}_2 \cdot e^{\underline{\gamma}x}\right) = \frac{1}{\underline{Z}_W} \cdot \left(\underline{U}_1 \cdot e^{-\underline{\gamma}x} - \underline{U}_2 \cdot e^{\underline{\gamma}x}\right) \tag{2-9}$$

$\underline{U}_1$, $\underline{U}_2$: Integration constants

$\underline{Z}_W$: Characteristic wave impedance with $\underline{Z}_W = \sqrt{\frac{R' + j\omega L'}{G' + j\omega C'}}$

$\underline{U_1}$ and $\underline{U_2}$ are determined with boundary conditions at the beginning or the end of the conductor. The equations (2-10) and (2-11) can be formed by applying the conditions at the beginning of the conductors. This leads to results for $\underline{U_1}$ and $\underline{U_2}$, as shown in equations (2-12) and (2-13):

$$\underline{U}_P(0) = \underline{U}_{P1} = \underline{U}_1 + \underline{U}_2 \tag{2-10}$$

$$\underline{I}_P(0) = \underline{I}_{P1} = \frac{1}{\underline{Z}_W} \cdot \left(\underline{U}_1 - \underline{U}_2\right) \tag{2-11}$$

$$\underline{U}_1 = \frac{\underline{U}_{P1} + \underline{Z}_W \cdot \underline{I}_{P1}}{2} \tag{2-12}$$

$$\underline{U}_2 = \frac{\underline{U}_{P1} - \underline{Z}_W \cdot \underline{I}_{P1}}{2} \tag{2-13}$$

Equations (2-12) and (2-13) are then applied to the earlier equations (2-8) and (2-9). With the usage of exponential functions, they can be summarized to form the known electric conductor equations:

$$\underline{U}_{P2} = \underline{U}_{P1} \cdot \frac{e^{\underline{\gamma}\ell} + e^{-\underline{\gamma}\ell}}{2} - \underline{I}_{P1} \cdot \underline{Z}_W \cdot \frac{e^{\underline{\gamma}\ell} - e^{-\underline{\gamma}\ell}}{2} = \underline{U}_{P1} \cdot \cosh \underline{\gamma}\ell - \underline{I}_{P1} \cdot \underline{Z}_W \cdot \sinh \underline{\gamma}\ell \tag{2-14}$$

$$\underline{I}_{P2} = \underline{I}_{P1} \cdot \frac{e^{\underline{\gamma}\ell} + e^{-\underline{\gamma}\ell}}{2} - \frac{\underline{U}_{P1}}{\underline{Z}_W} \cdot \frac{e^{\underline{\gamma}\ell} - e^{-\underline{\gamma}\ell}}{2} = \underline{I}_{P1} \cdot \cosh \underline{\gamma}\ell - \frac{\underline{U}_{P1}}{\underline{Z}_W} \cdot \sinh \underline{\gamma}\ell \tag{2-15}$$

The above equations (2-14) and (2-15) can be rewritten as quadrupole, where $\underline{\boldsymbol{A}}$ represents the chain matrix. With this chain matrix, it is possible to connect different quadrupoles.

$$\begin{bmatrix} \underline{U}_{P1} \\ \underline{I}_{P1} \end{bmatrix} = \begin{bmatrix} \cosh \underline{\gamma}\ell & \underline{Z}_W \sinh \underline{\gamma}\ell \\ \frac{1}{\underline{Z}_W} \sinh \underline{\gamma}\ell & \cosh \underline{\gamma}\ell \end{bmatrix} \begin{bmatrix} \underline{U}_{P2} \\ \underline{I}_{P2} \end{bmatrix} = \underline{\boldsymbol{A}} \cdot \begin{bmatrix} \underline{U}_{P2} \\ \underline{I}_{P2} \end{bmatrix} \tag{2-16}$$

The induced voltage $\underline{\boldsymbol{E(x)dx}}$ has to be taken into account in interfered areas, as shown in Figure 2-5 and, therefore, equation (2-4) has to be expanded to equation (2-17). Equations (2-6) and (2-7) can be expanded to form equations (2-18) and (2-19).

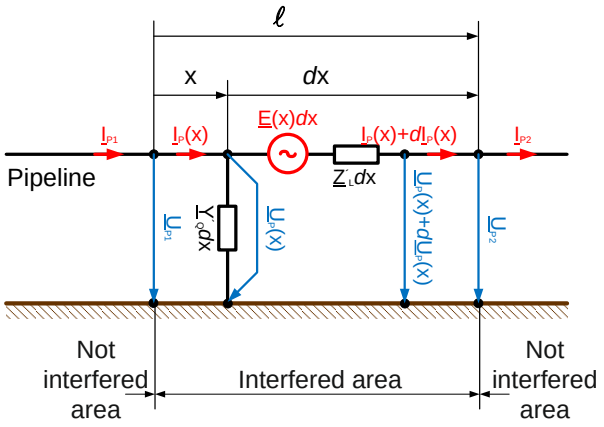

Figure 2-5: Equivalent circuit of a conductor segment with inductive interference

$$\frac{d\underline{U}_P}{dx} = -\underline{I}_P \cdot \underline{Z}_L' - \underline{E}(x)dx \tag{2-17}$$

$$\frac{d^2\underline{U}_P}{dx} = \left(\underline{Z}_L' \cdot \underline{Y}_Q'\right) \cdot \underline{U}_P + \frac{d\underline{E}(x)}{dx} = \underline{\gamma}^2 \cdot \underline{U}_P + \frac{d\underline{E}(x)}{dx} \tag{2-18}$$

$$\frac{d^2\underline{I}_P}{dx} = \left(\underline{Z}_L' \cdot \underline{Y}_Q'\right) \cdot \underline{I}_P - \underline{Y}_Q' \cdot \underline{E}(x) = \underline{\gamma}^2 \cdot \underline{I}_P - \underline{Y}_Q' \cdot \underline{E}(x) \tag{2-19}$$

Solving equations (2-18) and (2-19) is very complex and would go beyond the scope of this thesis. Two ways to handle these equations can be found in [17] and [37]. For more exact and less time consuming calculations, numerical methods are preferable to calculate PIVs.

The previous equations describe the general usage of this model. For calculating with discrete values, a lattice equivalent network is needed (see Figure 2-6). Choosing a Π-equivalent network instead of a T-network can be preferable because no inner node exists.

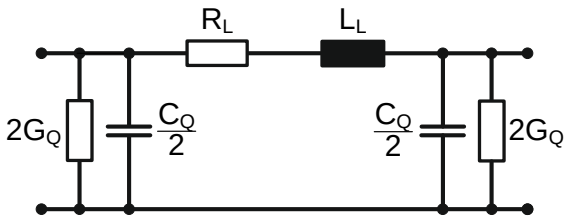

Figure 2-6: Π-equivalent network for the general conductor model

The equations are only valid for adequately short electrical conductors ([34], page 104 to 106), which is why segmenting is necessary: Every conductor is split into several shorter calculation segments to be able to use the discrete formulas (2-20) and (2-21), which provide approximately accurate results ([34], page 104).

$$\underline{Z}_L = \underline{Z}_W \sinh \underline{\gamma}\ell \approx \underline{Z}_W \cdot \underline{\gamma}\ell \left(1 + \frac{1}{6} \cdot \underline{\gamma}^2\ell^2\right) \approx (R' + j\omega L') \cdot \ell \tag{2-20}$$

$$\underline{Y}_Q = \frac{2}{\underline{Z}_W} \tanh \frac{\underline{\gamma}\ell}{2} \approx \frac{\underline{\gamma}\ell}{\underline{Z}_W} \left(1 - \frac{1}{12} \cdot \underline{\gamma}^2\ell^2\right) \approx (G' + j\omega C') \cdot \ell \tag{2-21}$$

With these formulas and the given Π-equivalent network, the initial Figure 2-1 can be extended to the following Figure 2-7.

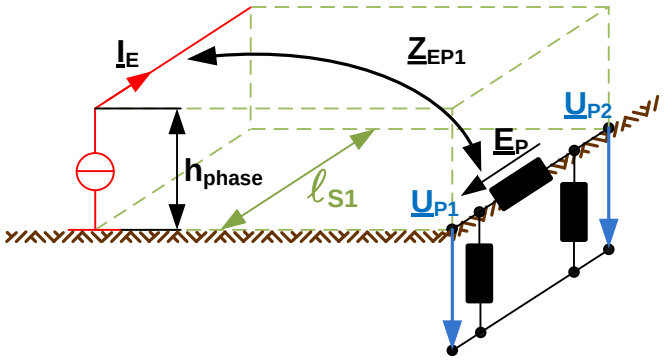

$\underline{E}_P$:	Electromotive force [Vm]
$\underline{U}_{P1}$, $\underline{U}_{P1}$:	PIV [V] on point 1 and 2
$\underline{I}_E$:	Inducing current from a current-carrying HVPS [A]
$\underline{Z}_{EP1}$:	Inductive coupling impedance between both systems (mutual impedance) for given distance [Ω]
ℓ_{S1}:	Distance of parallel route of a segment [m]
h_{phase}:	Height of the inducing conductor [m]

Figure 2-7: General example for the calculation of the PIV taking into account the PIE-equivalent network

2.2.4 General steps of calculating the pipeline interference voltage

Figure 2-8 shows the general method of calculating the pipeline interference voltage (PIV).

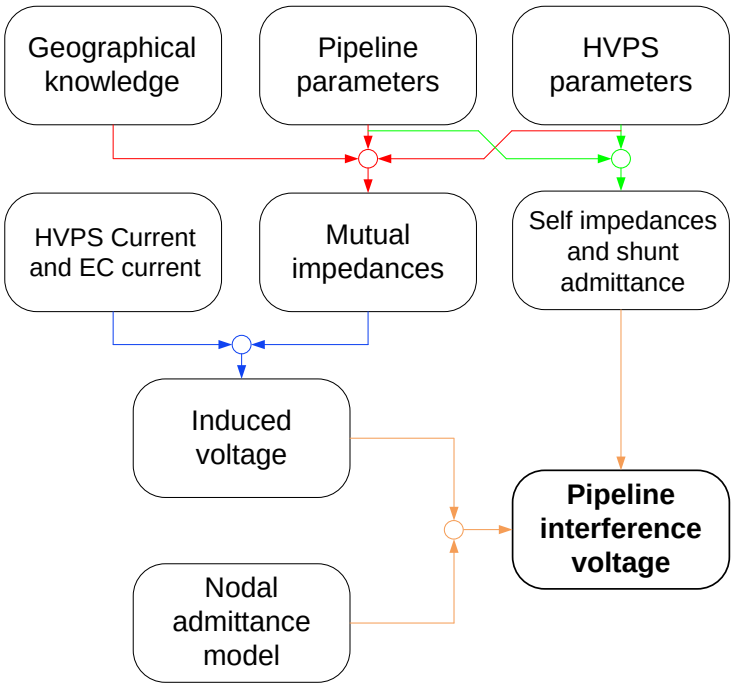

Figure 2-8: General steps of calculating the PIV

The first step is to calculate impedances and admittances. With knowledge of the geographical specifics between a pipeline and high voltage power systems (HVPSs), the mutual impedances can be calculated (red lines). The self-impedances as well as the shunt admittances are calculated taking into account material parameters and other essential information of the affected systems (green lines).

As a next step (blue lines), earthing conductor (EC) currents have to be calculated taking into account HVPS currents. In combination with the before calculated mutual impedances, the induced voltages can be determined.

As a final step, self-impedances, shunt admittances and induced voltages are combined with the nodal admittance model to calculate the PIV (orange lines). More details on the calculation methods will be presented in chapters 2 and 3.

2.3 Calculating impedances and admittances

2.3.1 Longitudinal impedance

2.3.1.1 Generally used formulas

As shown in Figures 2-3, 2-6 and 2-18, the longitudinal impedance is a part of the lattice equivalent network. It represents the material properties of the system (e.g. pipelines, earth conductors) and is strongly affected by variable parameters. These may be constituted by the system characteristics such as material or diameter as well as various surrounding factors including soil resistivity or interfering frequency. The longitudinal impedance is calculated using the following formula (2-22):

$$\underline{Z}'_L = (r'_e + r'_{Lo}) + j(\underline{x}'_L + \underline{x}'_{iLo}) \qquad (2\text{-}22)$$

$\underline{Z}'_L$:	Longitudinal impedance [Ω/m]
r'_e:	Earth resistivity [Ω/m]
r'_{Lo}:	Pipeline resistivity [Ω/m]
$\underline{x}'_L$:	Self reactance of ground return [Ω/m]
$\underline{x}'_{iLo}$:	Inner reactance [Ω/m]

This formula shows an ohmic and a reactance part. The formulas in Schmautzer [17], CIGRE [37] and Öding [35] are based on the initial publications by Carson [1] and Pollaczeck [2]. Additional publications from Michailow and Rasumov [3] are more pipeline-specific and improve the formulas, leading to more accurate results. Dubanton [5] uses his own derivation of the formula, which is calculated differently. The version offered by CIGRE also constitutes the official formula to calculate longitudinal values.

These formulas are often mentioned, calculated and compared in the following chapters and for easier reading, the following abbreviations are used:

"Formula S": Formula, which is described and used in the work of Schmautzer [17]

"Formula C": Formula, which is described and used in the work of CIGRE [37]

"Formula O": Formula, which is described and used in the book of Öding [35]

"Formula D": Formula, which is described and used in the work of Dubanton [5]

Table 2-3 lists all of the different formulas, taking into consideration the four parts of formula (2-22). These four parts of the formula can be described as follows:

r'_{Lo}: The pipeline resistivity per unit length, based on the ohmic resistance of a full conductor with skin effect. It is calculated using the formulas in Table 2-3, column 2. "Formula S" and "Formula C" use different formulas whereas "Formula O" and "Formula D" offer no definition. In these cases, "Formula O" is used because no significant difference between "Formula S" and "Formula C" was found in the calculations in the following pages 21 and 22.

r'_e: The earth resistivity per unit length is calculated in the same way as the Carson-based formula. "Formula D" uses another method of calculation and therefore r_e, $\underline{x}_{Lo}$ and $\underline{x}_L$ are calculated in a different way.

$\underline{x}'_{iLo}$: The inner reactance based again on the full ohmic conductor with/without skin effect. There are some differences between the three formulas which are based on Carson.

$\underline{x}'_L$: The self-impedance with ground return is calculated using the basic formulas by Carson. A mathematical conversion of "Formula C" leads to the result that all three formulas are equal.

As mentioned above, "Formula D" is different and can only be split into r_{Lo} and $\underline{Z}_{rest}$, where the last part is a complex value. $\underline{Z}_{rest}$ describes the other three parts as $\underline{Z}_{rest} = r_e + j(x_{Lo} + x_L)$.

Formula	r'_{Lo}	r'_e	X'_L	X'_{iLo}
"Formula S"	$\frac{\rho_L}{R_L^2 \cdot \pi}\left(\frac{R_L}{2 \cdot \delta_L} + \frac{1}{4}\right)$	$\frac{\omega \cdot \mu_0}{2 \cdot \pi} \cdot \frac{\pi}{4} = \frac{\omega \cdot \mu_0}{8}$	$\frac{\omega \cdot \mu_0}{2 \cdot \pi} \cdot \ln \frac{D_E}{R_L}$	$\frac{\rho_L}{2 \cdot R_L \cdot \pi \cdot \delta_L}$
"Formula C"	$\frac{\sqrt{\frac{\rho_L \cdot \mu_0 \cdot \mu_r \cdot \omega}{2}}}{\pi \cdot D}$	$\frac{\omega \cdot \mu_0}{8}$	$\frac{\omega \cdot \mu_0}{2 \cdot \pi} \cdot \ln\left(\frac{3.7}{D} \cdot \sqrt{\frac{\rho}{\omega \cdot \mu_0}}\right)$	$\frac{\sqrt{\frac{\rho_L \cdot \mu_0 \cdot \mu_r \cdot \omega}{2}}}{\pi \cdot D}$
"Formula O"	Not defined – Formula is taken from "Formula S"	$\frac{\omega \cdot \mu_0}{8}$	$\frac{\omega \cdot \mu_0}{2 \cdot \pi} \cdot \ln \frac{D_E}{R_L}$	$\frac{\omega \cdot \mu_0}{8 \cdot \pi}$
"Formula D"	Not defined – Formula is taken from "Formula S"	$\underline{z}_{rest} = j \cdot \frac{\omega \cdot \mu_0}{8} \cdot \left(\frac{1}{4} + ln \frac{2 \cdot \left(h_i + \underline{p}\right)}{R_L}\right)$		

r'e: Earth resistivity [Ω/m]
r'Lo: Pipeline resistivity [Ω/m]
x'L: Self-reactance of ground return [Ω/m]
x'iLo: Inner reactance [Ω/m]
f: Frequency [Hz]
ω: Singular frequency [1/s] with $\omega = 2 \cdot \pi \cdot f$
μr: Relative permeability – for steel approximately: 200
μ0: Magnetic field constant, $4\pi 10^{-7}$ [Vs/Am]
ρL: Specific resistivity of the material – for steel approximately: 0,16 [Ωmm²/m]
D: Pipeline diameter [m]m
RL: Pipeline radius [mm]
DE: Depth of equivalent earth return conductor [m]
ρ: Specific soil resistivity [Ωm]
k: Coefficient
C: Euler – Mascheroni constant (Euler's constant): ln(γ) = 0,5772156649
e: Euler`s number: 2,7182818284
γ: Euler`s constant: 1,791
δE: Penetration depth in earth [m]
hi: Vertical height of inducing conductor [m]

δL: Skin depth [mm] with

$$\delta_L = \sqrt{\frac{2 \cdot \rho_L}{\mu_0 \cdot \mu_r \cdot \omega}}$$

DE: Depth of equivalent earth return conductor [m] with

$$D_E = \sqrt{\frac{e^k}{\sqrt{\omega \cdot \mu_0 \cdot \frac{1}{\rho}}}} = \frac{e^{\frac{1}{2}+\ln 2-C}}{\sqrt{\omega \cdot \mu_0 \cdot \frac{1}{\rho}}} = \frac{1,8514}{\sqrt{2 \cdot \pi \cdot \mu_0 \cdot \sqrt{\frac{f}{\rho}}}} = 658,88 \cdot \frac{1}{\sqrt{\frac{f}{\rho}}} = 658,88 \cdot \sqrt{\frac{\rho}{f}}$$

or

$$D_E = \frac{\sqrt{2 \cdot e}}{\gamma} \cdot \delta_e = \frac{\sqrt{2 \cdot e}}{\gamma} \cdot \frac{2 \cdot \rho}{2 \cdot \pi \cdot f \cdot \mu_0} = 658,88 \cdot \sqrt{\frac{\rho}{f}}$$

p: Complex penetration earth [m] with

$$\underline{p} = \sqrt{\frac{1}{j\omega \cdot \mu_0 \cdot \frac{1}{\rho}}} = e^{-j\frac{\pi}{4}} \cdot \sqrt{\frac{1}{\omega \cdot \mu_0}} = (1-j) \cdot \sqrt{\frac{\omega \cdot \mu_0}{2 \cdot \rho}}$$

Table 2-3: Different formulas for calculating the longitudinal impedance of conductors

2.3.1.2 Mathematical comparison of the above-described formulas

It is to be assumed that the results of the above-described formulas differ. Most parameters are already given and therefore only a few may influence the results: frequency f, conductor radius r_i, respectively diameter D and the specific soil resistivity ρ. "Formula D" also uses the vertical height h_i, which is zero for this comparison and can be neglected.

An analysis of these parameters requires the use of two different graphs. First, the specific soil resistivity is varied between 5 Ω and 10,000 Ω and is calculated for the most common frequencies, 16.7 Hz (railway lines) and 50 Hz (overhead lines and underground power cables). Figure 2-9 shows the absolute values for a diameter of 100 mm according to the given four longitudinal calculation methods. Two groups have similar results: "Formula S" and "Formula C" (group one) plus "Formula O" and "Formula D" (group two). The common denominator in both groups is that with a rising soil resistivity the longitudinal impedance rises as well. The difference in value between the results of both groups remains more or less constant.

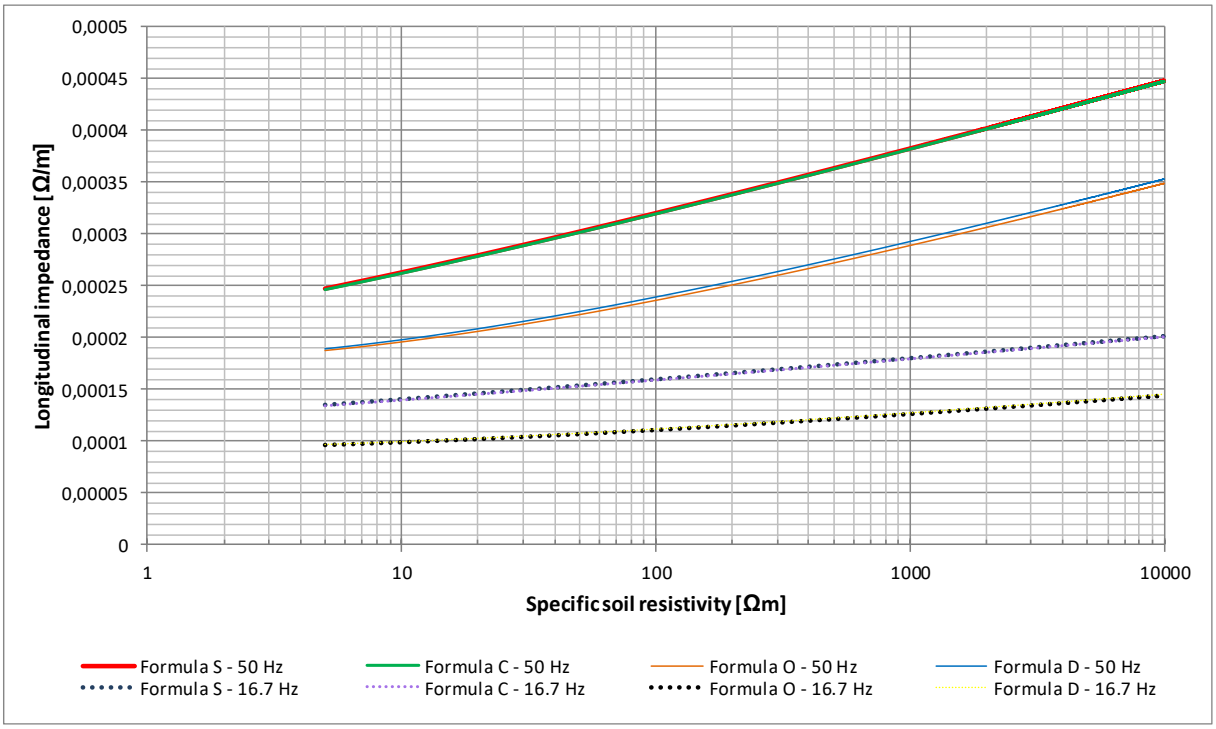

Figure 2-9: Comparison of the different formulas for the longitudinal impedance with varying specific soil resistivity

In the curve progressions for 50 Hz, the absolute value for 100 Ωm is 0.32 mΩ/m for group one and only 0.24 mΩ/m for group two. Most of the difference stems from the imaginary part of the formulas because the real part of the formulas is almost equal. Also, a frequency depending behaviour can be observed. It is interesting to note that with lower frequency, soil resistivity becomes less of an important factor. For a detailed analysis, the calculated real and imaginary parts can be seen in Appendix A.1, where the complete calculations are presented in concise charts.

The next parameter to consider is the conductor diameter, which varies between 4 and 1200 mm and concerns pipelines as well as conductors of HVPSs. The group classification in chart 2-9 can also be applied to the following chart 2-10. Correspondingly, the absolute values for the longitudinal impedances are again calculated for a frequency of 16.7 and 50 Hz. This chart clearly points out that the impedances decrease with a rising conductor diameter and conform to physical material properties.

It appears that all formulas show equal results with diameters higher than 500 mm. However, the research provided by this thesis does not concur with this statement. In chapter 4.2 an example calculated with a diameter of 1000 mm with exactly the same specific soil resistivity of 100 Ωm shows different results.

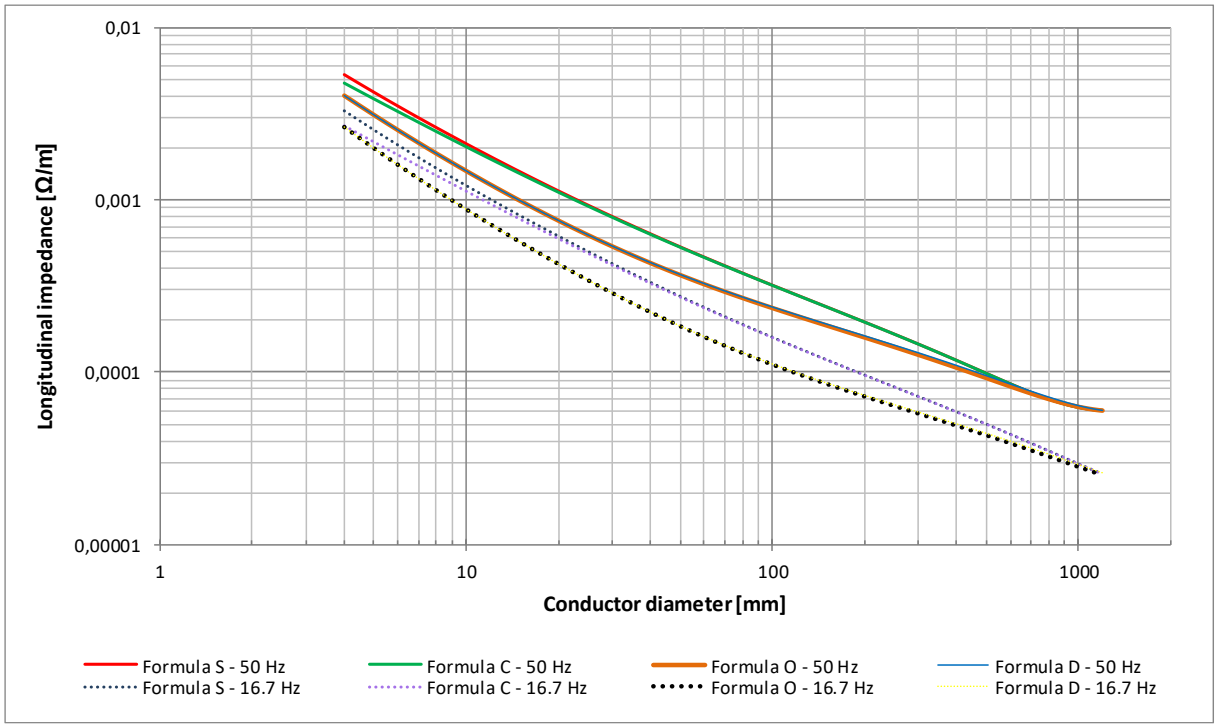

Figure 2-10: Comparison of the different formulas for the longitudinal impedance with varying conductor diameter

For a detailed analysis, the calculated real and imaginary parts can be seen in Appendix A.2, where the full calculations are presented in concise charts.

To summarize, the impedance does not remain constant when conductor diameter, soil resistivity and/or the frequency are varying parameters. The conductor diameter appears to be a more potent influencing parameter, irrespective of the frequency. Lower frequencies lead to a better conductance of a conductor and should lead to a better current distribution ability on the conductor and therefore to lower interference voltages. The value of the soil resistivity should always be carefully ascertained since otherwise, accurate calculations are not possible.

The diameter of a conductor has a greater impact than the soil resistivity, irrespective of the frequency, which also has to be considered for these calculations. But the question posed in this chapter was about which formula should be used for an accurate calculation. Considering only the diameter, every given formula would offer approximately the same result when used for diameters bigger than 500 mm. When multiple parameters are taken into account, however, it still remains unclear, which formula would provide the most accurate results. Therefore, chapter 4.2 will discuss this further and show how different formulas calculate the PIV. By presenting a simple calculation as an example, chapter 6.2 will then compare conducted measurements of pipeline parameters in the field with their corresponding calculations.

2.3.2 Shunt admittance

2.3.2.1 Pipelines

2.3.2.1.1 Specific pipeline coating resistance (SPCR)

As shown in Figures 2-3, 2-6 and 2-18, the shunt admittance is a part of the lattice equivalent network. As stated above, pipelines describe a closed conductor loop with a ground return. Therefore, the pipeline coating has to be considered. Calculating the shunt admittance is more problematic than calculating the longitudinal impedance because determining the value of the specific pipeline coating resistance (SPCR) r_u is very difficult due to coating holidays.

Pipeline manufacturers can only guarantee the value of the coating until the pipeline is dispatched. After its installation, however, it is nearly impossible to have a perfect coating due to coating holidays. Coating holidays occur because of material defects or disadvantageous environmental conditions (e.g. sharp-edged stones, ground vibration). Manufactures can only supply the value for a perfect coating. The real values have to be measured in the field or estimated based on experience.

In practice, a certain method is being used – based on information from various pipeline operators and [38]. However, some knowledge in the field of cathodic corrosion protection is essential: Cathodic corrosion protection systems only work with direct voltages. Pipelines are made of steel and have a free corrosion potential of U_{CSE_free} = -0.6 Volt. This potential can be accessed by coating holidays and after several chemical processes, steel degrades at the relevant spots and material corrosion occurs. To prevent this, the steel must have a more negative potential, which is created by a cathodic protection system. Therefore, the protection potential of at least U_{CSE_on} = -1.2 Volt is used. However, this depends on how old the pipeline is, how long the pipeline is, which pipeline coating material is used and which surrounding type of soil is present along the pipeline.

U_{CSE_on} is set via the protective current I_P, since the remaining properties of the pipeline cannot be influenced. The aim here is that the protective current I_P and the protective voltage U_{CSE_on} is applied at every point of the pipeline and thus the pipeline is protected.

In order to measure and calculate the correct DC-SPCR, the pipeline has to have been in operation long enough so that the material of the pipeline is strongly negatively polarised and can hold the negative potential for a specific period of time (usually a few hours), even when the power supply of the cathodic protection system is switched off. In this case, the protection potential must remain above the limit value of U_{CSE_off} = -0.85 volts for this duration.

Usually, it can be assumed that there is a voltage difference of at least 0.3 volts between U_{CSE_off} and U_{CSE_on} for pipelines which cannot hold the limit value of U_{CSE_off} = -0.85 volts for a longer period of time. But when U_{CSE_off} remains above the limit both measured voltages U_{CSE_off} and U_{CSE_on} can be used because these values provide a better overview of the electrical condition of the pipeline. With the knowledge of the required protective current I_P and the known surface of the pipeline, the current density can be calculated.

However, the current is measured inside the cathodic protection system installations. As a result, the current consumption by the anode field, the longitudinal impedance of the pipeline and parts of the electronics are also measured. This results in a falsification of the measured values, which becomes larger at lower protective currents I_P. This protective current is distributed over the entire pipeline and thus an average protective current density can be calculated ([38], page 95):

$$J_P = \frac{I_P}{A} \tag{2-23}$$

J_P:	Mean protective current density at any spot on the pipeline surface [A/m²]
I_P:	Complete protective current [A]
A:	Pipeline surface [m²]

With these variables, the SPCR r_u can be calculated with the following formula ([38], page 155):

$$r_u = \frac{U_{CSE\_off} - U_{CSE\_on}}{J_P} \tag{2-24}$$

r_u:	Specific coating resistance at any spot along the pipeline [Ωm²]
U_{CSE_Off}:	Switched off protection potential for a longer protected pipeline [V]
U_{CSE_On}:	Switched on protection potential[V]
J_P:	Mean protective current density at any spot on the pipeline surface [A/m²]

The following example shows a calculation example with real protection potentials:

- Characteristics of the pipeline: diameter = 100 mm; length = 10,000 m
- U_{CSE_off} = -1 Volt, U_{CSE_on} = -2 Volt
- I_P = 10 mA

$$J_P = \frac{I_P}{A} = \frac{0.01\ A}{3140\ m^2} = 3.18\frac{\mu A}{m^2} \tag{2-25}$$

$$r_u = \frac{U_{CSE\_off} - U_{CSE\_on}}{J_P} = \frac{-1\ V - (-2\ V)}{3.18\frac{\mu A}{m^2}} = 314{,}000\ \Omega m^2 \tag{2-26}$$

In practice, for older bituminous coatings, values for the coating resistance lie between 10^3 and 10^5 Ωm²; for newer polyethylene coatings between 10^5 and 10^7 Ωm². However, these calculations are based on direct current and it can be seen in chapter 6.2.3.2 that the SPCR behave differently for alternating current.

2.3.2.1.2 Generally used formulas and formula comparison

Unfortunately, not only does the SPCR r_u have a notable impact in the formula, but also, variable parameters including the pipeline radius R_L, conductor wall thickness t_L, coating thickness δ_c and the interfering frequency f.

Only “Formula S” [17] and “Formula C” [37] describe formulas to calculate the shunt admittance which is calculated using the following formula (2-27):

$$\underline{Y}'_Q = g'_Q + jb'_Q \tag{2-27}$$

$\underline{Y}'_Q$: Shunt admittance [S/m]
g'_Q: Galvanic conductance [S/m]
b'_Q: Capacitive conductance[S/m]

The galvanic conductance is predominantly affected by the material of the coating and the number of coating holidays. Due to their frequent occurrence, they appear as a constant earthing system. The following formulas (2-28) and (2-29) estimate the conductance. “Formula S” and “Formula C” use the same formula with the main impact factor being the estimated value for the coating.

$$g'_Q = \frac{2 \cdot R_L \cdot \pi}{r_u} \tag{2-28}$$

$$g'_Q = \frac{2 \cdot R_L \cdot \pi}{\rho_c \cdot \delta_c} = \frac{2 \cdot R_L \cdot \pi}{r_u} \tag{2-29}$$

g_Q':	Galvanic conductance [S/m]
R_L:	Pipeline radius [m]
r_u:	Specific coating resistance [Ωm²]
ρ_c:	Pipeline coating electrical resistivity [Ωm]
δ_c:	Thickness of the coating [m]

The capacitive conductance represents the capacity between the pipeline and the surrounding soil. It can be calculated using the “Formula S” (2-30) as well as “Formula C” (2-31) which show some minor differences.

$$jb'_Q = \omega \cdot \frac{2 \cdot \pi \cdot \varepsilon_0 \cdot \varepsilon_r}{\ln \frac{R_L + t_L}{R_L}} \tag{2-30}$$

$$jb'_Q = \omega \cdot \frac{\pi \cdot \varepsilon_0 \cdot \varepsilon_r \cdot 2 \cdot R_L}{\delta_c} \tag{2-31}$$

b_Q':	Capacitive conductance[S/m]
ω:	Singular frequency [1/s] with $\omega = 2 \cdot \pi \cdot f$
ε_0:	Electrical permittivity in the air: $8{,}85432 \cdot 10^{-12}$ [F/m]
ε_r:	Relative permittivity of the pipeline coating: typically: 5
R_L:	Pipeline radius [mm]
t_L:	Wall thickness of the metallic pipeline [mm] – typically between 5 and 15 mm
δ_c:	Thickness of the coating [mm] – factory coating typically around between 1 to 5 mm

Calculating the shunt admittance shows that the real part g_Q' in both formulas is the same and that two parameters can be varied: These are the pipeline radius R_L and the specific coating resistance r_U. The radius is always known but, as stated before, the resistance value can be only estimated.

When comparing the two formulas for the imaginary part b_Q', only the radius R_L and the frequency f appear to be a common variable. Both formulas include one pipeline parameter not taken into account by the other formula: “Formula S” includes the wall thickness of the pipeline t_L and “Formula C” the thickness of the coating δ_c. This fact makes comparing results between both formulas difficult and therefore, for achieving comparable results, the wall thickness is set at a fixed value of 5 mm and the coating thickness at 1 mm.

Figure 2-11 shows the shunt admittance y_Q' for a conductor diameter varying from 1 to 1000 mm with a range of coating resistances. Irrespective of the coating resistance and the formula used, it can be seen that with an increasing diameter, the value of the admittance increases steadily. This matches the physical behaviour because the reciprocal value decreases with larger radii due to a better contact with the soil.

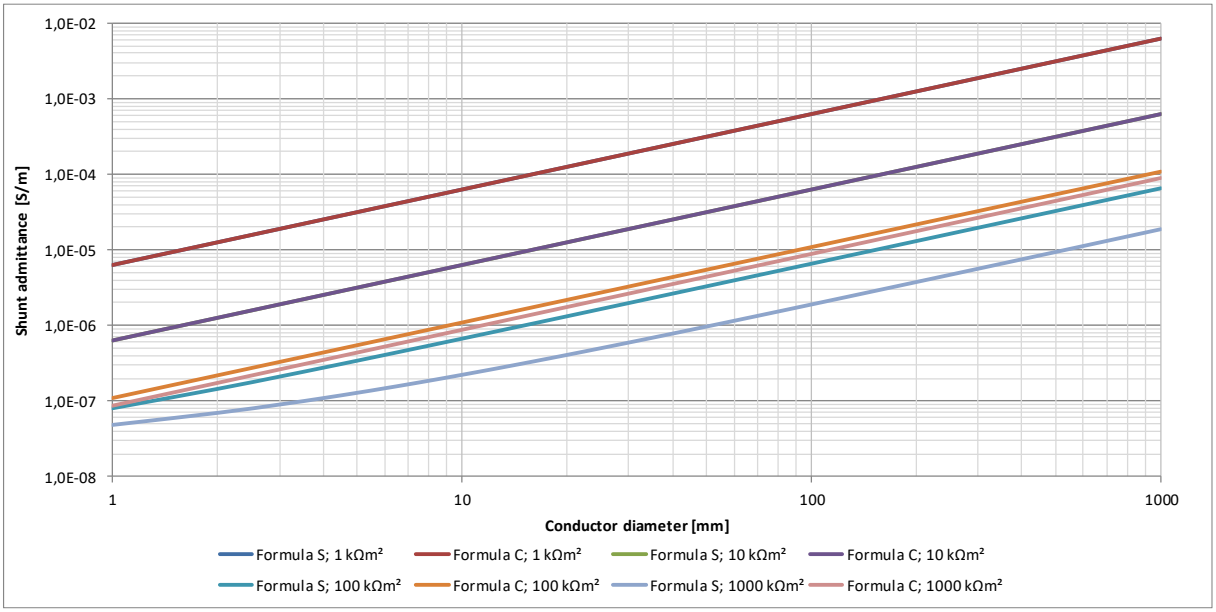

Figure 2-11: Comparison of both formulas for the shunt admittance with varying conductor diameter for different coating resistances

When comparing the lines for the different coating resistance values 1-10-100-1000 kΩm², two facts become apparent: First, the shunt admittance decreases with rising resistance values. This means that less contact to the soil increases isolation. Second, both formulas offer equal results for lower resistance values only. When comparing the values for a resistance value of 1000 kΩm² and a radius of 100 mm, "Formula S" has an admittance value of around 2 µS/m, while the result of "Formula C" is four times higher with a value of 8,5 µS/m.

The above described assumptions are valid for Figure 2-12 below. This figure utilizes the "Formula S" and "Formula C" for specific pipeline diameters (10-50-100-250-500 mm) to show at what point both formulas start offering diverging results. Both formulas are valid for a coating resistance of up to 30 kΩm², which is a common value for bitumen coated pipelines, independent of the pipeline radius. A higher coating resistance leads to diverging admittance values because the "Formula C" reaches the maximum admittance value for specific diameters earlier. When comparing both formulas for a coating resistance of 1000 kΩm², the "Formula S" applied to a diameter of 500 mm offers the same admittance value as the "Formula C" for a diameter of 100 mm. The meaning of this difference will be investigated in chapter 4.2, where the impact of the different results from both formulas will be calculated.

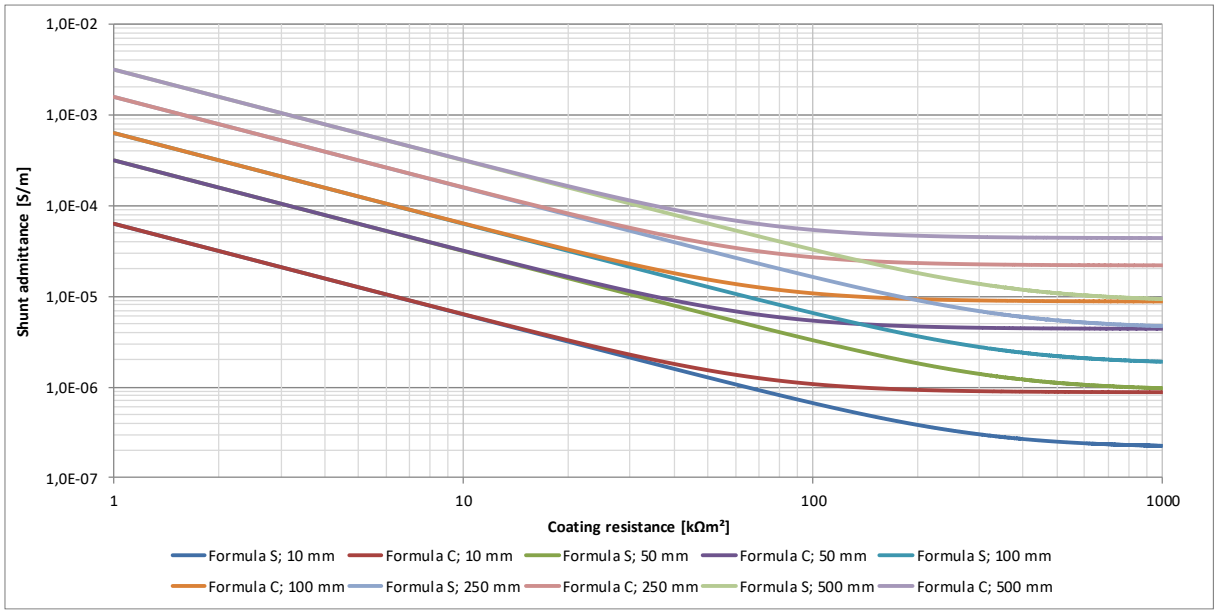

Figure 2-12: Comparison of both formulas for the shunt admittance with varying coating resistances for different pipeline diameters

As stated above, both formulas have an independent variable which can significantly impact the shunt admittance. Figure 2-13 (a) shows the results for the "Formula S" when varying the wall thickness of the pipeline for a coating resistance of 1000 kΩm². This figure shows a clear trend because with rising wall thickness, the shunt admittance slowly reaches a fixed value. For example, for a radius of 100 mm, the values vary from 3 µS/m (for 3 mm) to 0.9 µS/m (13 mm), which means that only one third of the 3 mm wall thickness is left. When comparing 7 with 13 mm, the value decreases from 1.3 µS/m to 0.9 µS/m, a much lower ratio. Converted into reciprocal value – which describes the physical behaviour of the pipeline – it shows that with an increase in wall thickness, the pipeline is better isolated against the surrounding soil.

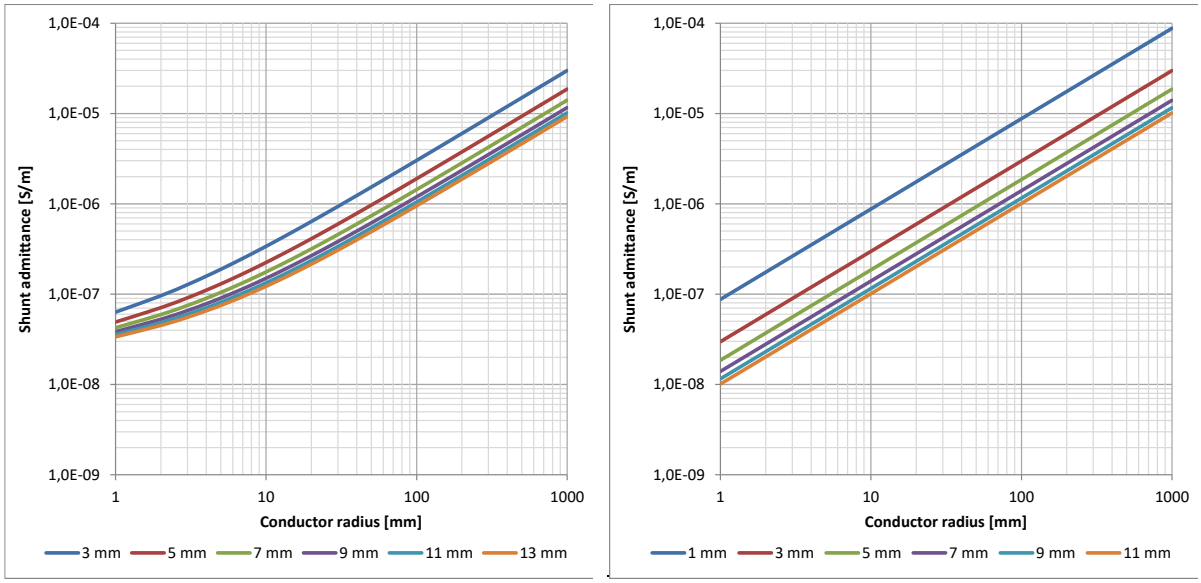

Figure 2-13: Impact of wall thickness (a) on the "formula S" and the coating thickness (b) on the "formula C"

Figure 2-13 (b) shows the calculation using the "Formula C" with a varying coating thickness. The difference between very thin and thick coatings is larger than for the wall thickness. Therefore, this parameter has a larger effect on the formula and has to be considered more closely. This case shows that with a rising coating thickness, the shunt admittance increases, which means that, considering the reciprocal value, the isolation against the surrounding soil is improving.

The figure also illustrates that with a rising coating thickness, an almost stable shunt admittance can be reached. In real life, however, pipelines usually have no coating thicknesses higher than 5 mm. In addition, with rising thickness, the possibility of coating holidays is reduced and the value of the coating resistance rises.

In summary, the theoretical calculations of the shunt admittance show that the results of both formulas are nearly equivalent when compared using the right parameters. When considering a coating resistance of more than 30 kΩm², the results diverge. The impact on the simple interference calculation example has to be examined. Also, the parameters specific to each formula have an impact on the calculations, and while the wall thickness is not as important, the coating thickness has to be determined more carefully, especially for lower thicknesses. The effects of these parameters will be shown in a simple calculation example in chapter 4.2.

2.3.2.2 Isolated conductors in the soil

Isolated conductors in the soil can be e.g. high voltage cables, where both the phase conductors and, if present, the shielding cable usually have no contact with the surrounding soil. Therefore, these conductors can be calculated with the above given formulas.

2.3.2.3 Blank conductors in the earth

Blank conductors are handled differently because an isolation layer does not exist. But the above given formulas can be used for the specific coating resistance r_u : the value of which represents the contact resistance between the conductor and the soil. For these cases, the formula of CIGRE cannot be used because there the coating thickness is zero. Alternatively, a coating resistance with the value of 1 Ω can be used for all formulas, as described above, and calculation errors can be minimized.

2.3.3 Mutual Impedance

The first efforts to calculate the mutual impedance used the infinite series of Pollaczek [2] and Carson [1] in 1926. Their methods are very time-consuming and in the following years, simpler but not exact calculation methods were developed. Figure 2-14 shows the mirror model of two conductors with earth return on which all calculations for the mutual impedance are based.

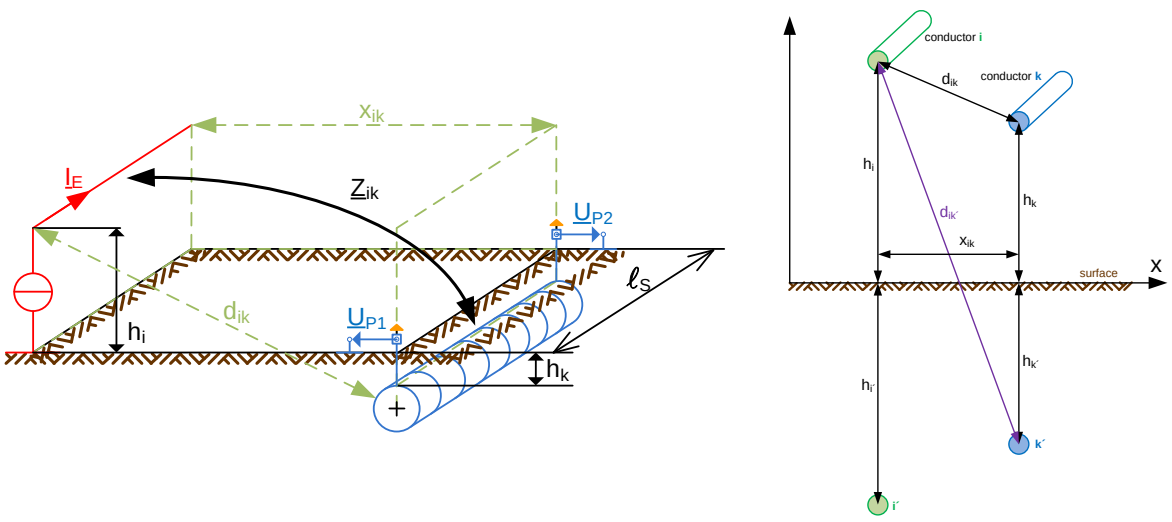

a) b)

$\underline{U}_{P1}$, $\underline{U}_{P1}$:	PIV [V] on point 1 and 2
$\underline{I}_E$:	Inducing current from a current-carrying HVPS [A]
$\underline{Z}_{ik}$:	Inductive coupling impedance between both systems (mutual impedance) for given distance [Ω]
ℓ_s:	Distance of parallel route of a segment [m]
h_i:	Vertical height of inducing conductor [m]
h_k:	Vertical height/depth of induced conductor [m]
h_i':	Mirrored conductor of the inducing conductor [m]
h_k':	Mirrored conductor of the induced conductor [m]
x_{ik}:	Horizontal distance between coupled conductors [m]
d_{ik}:	Distance between coupled conductors [m]
d_{ik}':	Distance between induced and mirrored conductor [m]

Figure 2-14: a) Example of an inductive interference with the distances between the conductors; b) Model for calculating the mutual impedance ([35], modified)

The geographical situation has to be constant between influencing and influenced system over the calculation length and segmenting is necessary. Another requirement is that the soil resistivity has to be homogeneous within a segment. The difference between the models of Pollazcek and Carson is that the conductor's height above the soil in Carson's version can be neglected [17]. This makes calculations easier, but heights are often included in the simplified methods.

The literature uses various simplified calculation methods such as the "expansion in series by Carson" [1] and its enhancements by "Dommel" [4], "Carson-Clem" [37], [39], expression in polynomial form [37] and "Complex Image Formula" by Dubanton [5], [40].

The enhanced "expansion in series by Carson" is used for calculations because of its implementation in the program KABEIN [17] which was initially used for calculating mutual impedances. In this thesis, all calculations use the faster and easier to implement formula "Complex Image Formula" which is based on the simplifications of Dubanton [5]. At the end of this chapter, calculation examples show that these calculation methods are very similar. All formulas consist of two parts: the part with the self impedance $\underline{Z}_{ii}$ and the more important part, which includes the mutual impedance $\underline{Z}_{ik}$. $\underline{Z}_{ii}$ is calculated in a similar way by different formulas (see chapter 2.3.1).

2.3.3.1 Carson-Dommel Formula

This chapter will first describe the series expansion. The general solution by Carson describes the infinite series for different cases between two conductors in the soil and/or in the air. But these formulas cannot be implemented for numerous calculations. Therefore, Carson describes his formula as a series expansion, which is not very user-friendly because of implementation and calculation time.

Later, Dommel enhanced this formula, making it applicable for a wider range of distances between two conductors. However, it needs complicated programming implementation and the calculation is not continuous over the whole range of distances [4]. Also the calculation time can be time consuming, depending on how many parts of the series expansions are calculated.

The following series expansion was invented by Dommel:

$$\underline{Z}'_{ik} = \frac{\omega \cdot \mu_0}{\pi} \cdot P_{ik} + i \cdot \frac{\omega \cdot \mu_0}{2 \cdot \pi} \cdot \left(\ln\left(\frac{d'_{ik}}{d_{ik}}\right) + 2 \cdot Q_{ik} \right) \tag{2-32}$$

Z_{ik}:	Mutual impedance [Ω/m]
ω:	Singular frequency [1/s] with $\omega = 2 \cdot \pi \cdot f$
μ_0:	Magnetic field constant, $4\pi 10^{-7}$ [Vs/Am]
d_{ik}:	$d_{ik} = \sqrt{x_{ik}^2 + (h_i - h_k)^2}$; Distance between coupled conductors [m]
d_{ik}':	$d_{ik}' = \sqrt{x_{ik}^2 + (h_i + h_k)^2}$; Distance between induced and mirrored conductor [m]
x_{ik}:	Horizontal distance between coupled conductors [m]
h_i:	Vertical height of inducing conductor [m]
h_k:	Vertical height of induced conductor [m]
P_{ik}, Q_{ik}:	Correction terms
ρ:	Specific soil resistivity [Ωm]

The correction terms P_{ik} and Q_{ik} are a series expansion. The first two elements are shown in formulas (2-33) and (2-34). Using a numerical method for calculating these series is recommended.

$$P_{ik} = \frac{\pi}{8} - b_1 \cdot x^1 \cdot \cos 1\theta + b_2 \cdot [(c_2 - \ln x) \cdot x^2 \cdot \cos 2\theta + x^2 \cdot \theta \cdot \sin 2\theta] + b_3 \cdot x^3 \cdot \cos 3\theta - d_4 \cdot x^4 \cdot \cos 4\theta - b_5 \cdot x^5 \cdot \cos 5\theta + b_6 \cdot [(c_6 - \ln x) \cdot x^6 \cdot \cos 6\theta + x^6 \cdot \theta \cdot \sin 6\theta] + b_7 \cdot x^7 \cdot \cos 7\theta - d_8 \cdot x^8 \cdot \cos 8\theta - \dots \quad (2\text{-}33)$$

$$Q_{ik} = \frac{1}{2} \cdot \ln \frac{e^k}{x} + b_1 \cdot x^1 \cdot \cos 1\theta - d_2 \cdot x^2 \cdot \cos 2\theta + b_3 \cdot x^3 \cdot \cos 3\theta - b_4 \cdot [(c_4 - \ln x) \cdot x^4 \cdot \cos 4\theta + x^4 \cdot \theta \cdot \sin 4\theta] + b_5 \cdot x^5 \cdot \cos 5\theta - d_6 \cdot x^6 \cdot \cos 6\theta + b_7 \cdot x^7 \cdot \cos 7\theta - b_8 \cdot [(c_8 - \ln x) \cdot x^8 \cdot \cos 8\theta + x^8 \cdot \theta \cdot \sin 8\theta] + \dots \quad (2\text{-}34)$$

x: $x = d'_{ik} \cdot \frac{1.85137}{\delta_E} = d'_{ik} \cdot \sqrt{\frac{\omega \cdot \mu_0}{\rho}}$

θ: $\theta \neq 0 = \arccos \frac{(h_i + h_k)}{d'_{ik}}$

e^k 1,85137

b_i: $b_i = b_{i-2} \cdot \frac{sign}{i \cdot (i+2)}$ with sign = +1 if i = 1 to 4, 9 to 12, otherwise -1 for 5 to 8, 13 to 16; The algebraic sign changes after four elements each.

c_i: $c_i = c_{i-2} + \frac{1}{i} + \frac{1}{i+2}$

d_i: $d_i = \frac{\pi}{4} \cdot b_i$

Starting values: $b_1 = \frac{\sqrt{2}}{6};\ b_2 = \frac{1}{16};\ c_2 = 1.36593$

If $\sqrt{\frac{\omega \cdot \mu_0}{\rho}} \cdot d'_{ik} > 6$ [17], then P_{ik} and Q_{ik} are calculated using the following formulas:

$$P_{ik} = \frac{\cos\theta}{x} - 2\frac{\cos 2\theta}{x^2} + \frac{\cos 3\theta}{x^3} + 3\frac{\cos 5\theta}{x^5} - 45\frac{\cos 7\theta}{x^7} \quad (2\text{-}35)$$

$$Q_{ik} = \frac{\cos\theta}{x} - \frac{\cos 3\theta}{x^3} + 3\frac{\cos 5\theta}{x^5} - 45\frac{\cos 7\theta}{x^7} \quad (2\text{-}36)$$

Exact calculations show that a change of the correction term by a factor of 6 is too high. The best calculation results can be reached when the correction term is changed by a factor of 3. Still, the change of the correction term leads to a point of discontinuity, depending on frequency and soil resistivity.

2.3.3.2 Complex Image Formula

The next method describes the "Complex Image Formula" (2-37) by Dubanton [5]. This method is much easier to implement in numerical calculations and can be applied over the complete frequency spectrum as well as over the full coupling distance between two conductors without any limitations. The formula is only applicable when the conductors lie above the ground. When conductors are buried in low depths like in these calculation examples, the formula is applicable by considering a small deviation in the calculation. [17].

$$\underline{Z'_{ik}} = j\omega \cdot \frac{\mu_0}{2 \cdot \pi} \cdot \ln \frac{\sqrt{(h_i + h_k + 2 \cdot \underline{p})^2 + x_{ik}^2}}{d_{ik}} \tag{2-37}$$

$$\underline{p} = \frac{1}{\sqrt{\frac{j\omega \cdot \mu_0}{\rho}}} = e^{-j\cdot\frac{\pi}{4}} \cdot \frac{1}{\sqrt{\frac{\omega \cdot \mu_0}{\rho}}} = (1-j) \cdot \sqrt{\frac{\omega \cdot \mu_0}{2 \cdot \rho}} \tag{2-38}$$

$\underline{Z_{ik}}$:	Mutual impedance [Ω/m]
ω:	Singular frequency [1/s]
μ_0:	Magnetic field constant, $4\pi 10^{-7}$ [Vs/Am]
$\underline{p}$:	Complex penetration depth in earth [m]
ρ:	Specific soil resistivity [Ωm]
d_{ik}:	$d_{ik} = \sqrt{x_{ik}^2 + (h_i - h_k)^2}$; Distance between coupled conductors [m]
x_{ik}:	Horizontal distance between coupled conductors [m]
h_i:	Vertical height of inducing conductor [m]
h_k:	Vertical height of induced conductor [m]

2.3.3.3 Comparative calculation

The following chart shows the comparative calculation of both formulas for a frequency of 50 Hz, a soil resistivity of 100 Ωm, a vertical height of the inducing conductor of 20 m and a height of -1 m for the induced conductor (pipeline).

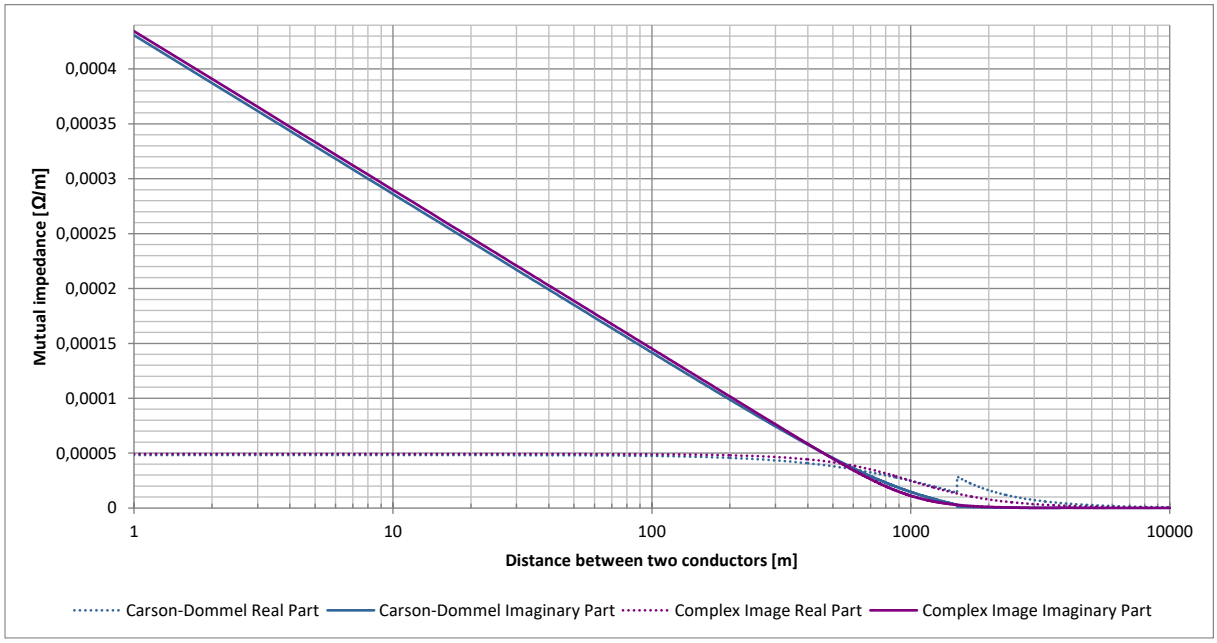

Figure 2-15: Comparison between both mutual impedance formulas under the same conditions (50 Hz, 100 Ωm)

Only minor differences can be seen until the correction terms in the Carson-Dommel formula change. Until this point, both formulas can be seen as fully valid. When, however, there is a greater distance between inducing and induced conductors, the Complex Image formula should be applied.

The full charts can be found in Appendix A.3. Therein, it is shows that with the Carson-Dommel formula, the point of discontinuity in most cases lies beyond 1000 m. The regulations in chapter 2.1 show that this covers most cases. Still, when using numerical methods, the Complex Image formula should be preferred because of its continuity over the full distance, its easier implementation and faster computation.

In addition, the chart shows why segmenting is necessary. The imaginary part changes very quickly in close vicinity to coupled conductors. Segmenting also improves the accuracy of calculating the mutual impedance.

2.4 Inducing currents

This chapter discusses the last aspect of the initial formula (2-1): the inducing currents of current-carrying conductors and systems. When giving an overview of all influencing systems, high voltage overhead lines (OHLs) are often the main cause of pipeline interference voltages (PIVs). For the most part, at normal operation, the inducing currents in such systems are symmetrical: every phase conductor has the same current with a proper phase shift. Calculations for normal operational modes include this assumption because asymmetrical currents cannot be known beforehand. For fault operation of three-phase systems, one-phase conductor systems and railway lines, however, this assumption is not valid.

Passive, non-current-carrying-conductors, e.g. earthing conductors (ECs) or return conductors, have to be taken into account because active conductors, such as phase conductors, induce currents into these passive conductors. Therefore, they will become current-carrying-conductors as well and will induce an interference voltage into other metallic structures such as pipelines. Consequently, any passive metallic structure located in a certain vicinity of a current-carrying-conductor plays an active role.

This chapter will explain how the EC currents from overhead lines (OHLs) are calculated when the mutual impedances have already been calculated and the phase conductor currents are known. Figure 2-16 a) shows the OHL pylon of the given system with the related mutual impedances and b) a distance between two pylons with corresponding self-impedances, voltages and currents.

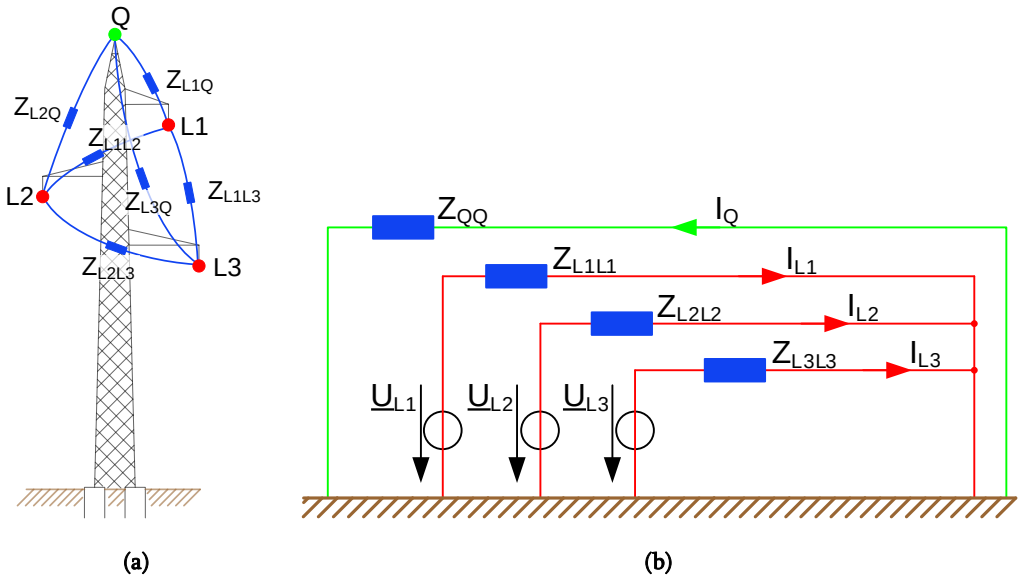

Figure 2-16: Calculating the EC current

This leads to the following matrix (2-39):

$$\begin{bmatrix} \Delta\underline{U}'_{L1} \\ \Delta\underline{U}'_{L2} \\ \Delta\underline{U}'_{L3} \\ 0 \end{bmatrix} = \begin{bmatrix} \underline{Z}'_{L1L1} & \underline{Z}'_{L1L2} & \underline{Z}'_{L1L3} & \underline{Z}'_{L1Q} \\ \underline{Z}'_{L2L1} & \underline{Z}'_{L2L2} & \underline{Z}'_{L2L3} & \underline{Z}'_{L2Q} \\ \underline{Z}'_{L3L1} & \underline{Z}'_{L3L2} & \underline{Z}'_{L3L3} & \underline{Z}'_{L3Q} \\ \underline{Z}'_{QL1} & \underline{Z}'_{QL2} & \underline{Z}'_{QL3} & \underline{Z}'_{QQ} \end{bmatrix} \begin{bmatrix} \underline{I}_{L1} \\ \underline{I}_{L2} \\ \underline{I}_{L3} \\ \underline{I}_{Q} \end{bmatrix} \tag{2-39}$$

$\Delta\underline{U}_{L1}$, $\Delta\underline{U}_{L1}$, $\Delta\underline{U}_{L1}$:	Potential difference along the conductor [V]
$\underline{Z}_{L1L1}$, $\underline{Z}_{L2L2}$, $\underline{Z}_{L3L3}$, $\underline{Z}_{QQ}$:	Longitudinal impedances [Ω/m]
Rest of $\underline{Z}_{xxx}$:	Mutual impedances [Ω/m]
$\underline{I}_{L1}$, $\underline{I}_{L2}$, $\underline{I}_{L3}$:	Given current from current-carrying conductors [A]
$\underline{I}_{Q}$:	Current in the EC [A]

The EC current can be calculated using the last line of equation (2-39):

$$\underline{I}_Q = -\frac{\underline{Z}'_{QL1} \cdot \underline{I}_{L1} + \underline{Z}'_{QL2} \cdot \underline{I}_{L2} + \underline{Z}'_{QL3} \cdot \underline{I}_{L3}}{\underline{Z}'_{QQ}} \tag{2-40}$$

Equation (2-40) describes a simplified but quick method to calculate $\underline{I}_Q$. When more systems are on an OHL, the formula is longer. For cases with more than one EC, there are two options: First, each EC current is calculated separately with equation (2-40) or second, a more complicated formula is used which is descripted in chapter 5.1.

With formula (2-40), the EC screening factor can be approximated. For this, only the zero-sequence-components of the currents are used, formula (2-40) can be simplified with $\underline{I}_{L1} = \underline{I}_{L2} = \underline{I}_{L3} = \underline{I}_0$ and $\underline{Z}'_{QL1} = \underline{Z}'_{QL2} = \underline{Z}'_{QL3} = \underline{Z}'_{QL}$ to form formula (2-41):

$$\underline{I}_Q = -\frac{\left(\underline{Z}'_{QL1} + \underline{Z}'_{QL2} + \underline{Z}'_{QL3}\right)}{\underline{Z}'_{QQ}} \underline{I}_0 = -\frac{\left(\underline{Z}'_{QL}\right)}{\underline{Z}'_{QQ}} 3 \cdot \underline{I}_0 = -(1 - \underline{r}_e) \cdot 3 \cdot \underline{I}_0 \tag{2-41}$$

$\underline{Z}_{QQ}$:	Longitudinal impedances from the EC [Ω/m]
$\underline{Z}_{QL1}$, $\underline{Z}_{QL2}$, $\underline{Z}_{QL3}$:	Mutual impedances [Ω/m]
$\underline{I}_0$:	Given current without angel from current-carrying conductors [A]
$\underline{I}_Q$:	Current in the EC [A]
$\underline{r}_e$:	EC screening factor [1]

This means that the current $(1 - \underline{r}_e) \cdot 3 \cdot \underline{I}_0$ flows inside the EC while the rest flows inside the soil. Transforming equation (2-41) enables the calculation of the EC screening factor. Equation (2-42) is influenced by conductor configuration and therefore not exact. Consequently, the distance between each phase conductor and the EC is not constant and the mutual impedance varies.

$$\underline{r}_e = \frac{\underline{I}_Q}{3 \cdot \underline{I}_0} - 1 \tag{2-42}$$

The following example represents a real pylon with one symmetrical system and one EC. The conductor configuration (CC) as well as the dimensioning is the same as in Figure 2-17. To calculate the impedances, the **"Formula S"** from chapter 2.3.1 and the **"Complex Image Formula"** from chapter 2.3.3 are used.

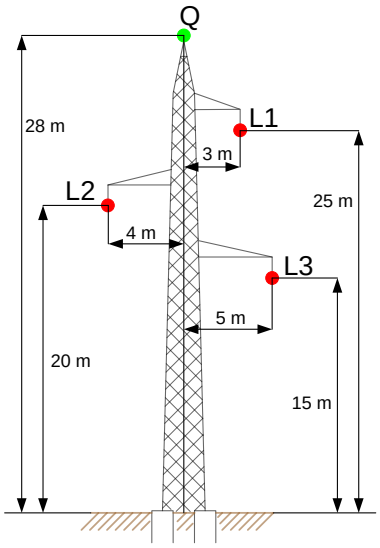

Figure 2-17: Example for calculating the earthing screening factor

The symmetrical system has a current of 1000 A in each conductor with the angles of L1 = 0°, L2 = 120° and L3 = 240°. The calculations are done for a length of 1000 m. The EC current is calculated with formula (2-40):

$$\underline{I_Q} = -(38.86 + i82.74)\ A = -94.14 \cdot e^{-i64.84} A$$

Bearing in mind formula (2-42), this leads to the screening factor:

$$\underline{r_e} = 0.968$$

In this example, the EC consist of a cable with a small diameter (12 mm) and therefore, only a small current flows through it. With better conductive cable material, the self-impedances would be lower and the EC currents significantly higher.

The inducing currents of railway lines are known to pipeline operators, but passive conductor currents from e.g. return conductors or rails are not known without calculations. Because different structures, such as two rail tracks with overhead traction lines and return conductors, can be in place, the screening factors are considered according to the standard ÖVE-B1/1976 [10] and are included in the calculations. The calculations are done beforehand because railway lines have several other active and passive conductors: an earthing conductor and a return conductor, a line feeder and railway tracks, which have to be considered as one system. In addition, the master thesis by Roßmann [25] shows that the usual screening factors of [10] have a good correlation with the

results of the detailed calculation models of different types of railway lines. However, it also states that other factors such as the position of the pipeline, the number of metallic structures or the earthing system of the rail tracks have a high impact. This makes calculating the passive conductor currents more difficult. But they can be calculated in the conventional way, as will be shown in chapter 5.1, or automatically by following the model in chapter 3.

2.5 Nodal admittance model and pipeline interference voltage

As stated above in chapter 2.2.2, segmenting is necessary. For each segment, an equivalent network for the pipeline can be generated, which has to be separated into influenced and non-influenced segments, as shown in Figure 2-18.

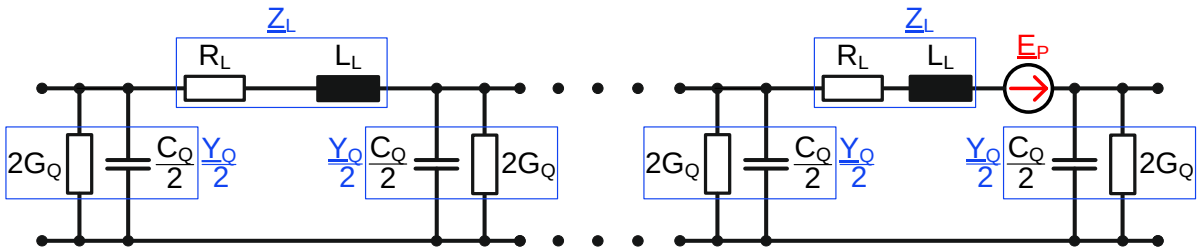

EP: Electromotive force [Vm] in the segment
ZL: Longitudinal impedance [Ω]
YQ/2: Shunt admittance [1/Ω]; Due to the model, half the value is used twice

Figure 2-18: Equivalent network, separated into non-influenced (left) and influenced (right) segments

The induced voltage $\underline{E_P}$ is usually calculated with formula (2-2). However, the situation is more complex when different currents $\underline{I}$ with different coupling impedances $\underline{Z_{ep}}$ have to be calculated, as shown in chapter 2.4 and illustrated in Figure 2-19.

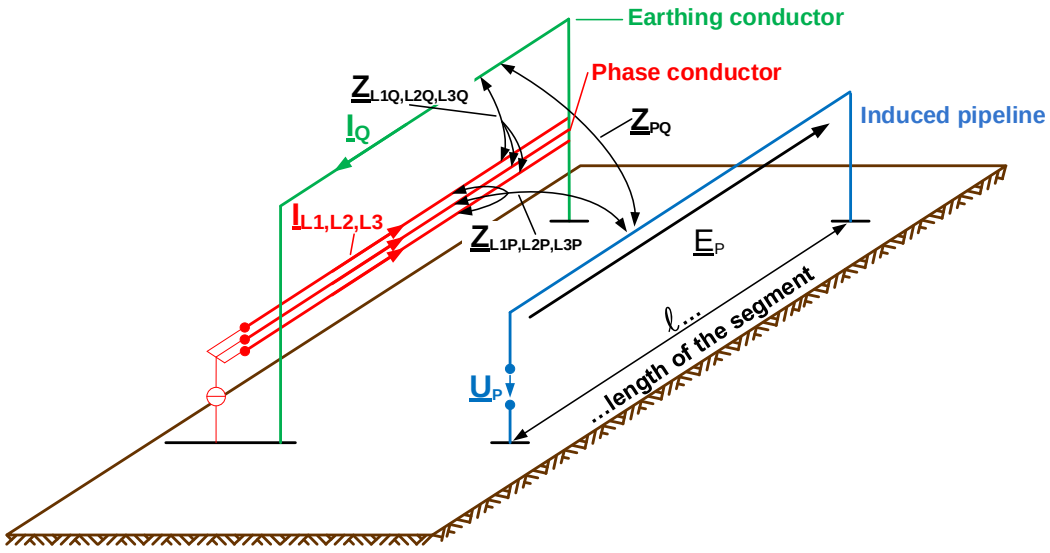

Figure 2-19: Example for the calculation of the induced voltage with multiple conductors

Therefore, formula (2-2) has to be extended to formula (2-43):

$$\underline{E}_{P\_segment} = \sum_{x=1}^{n} \underline{I}_x \cdot Z'_x \cdot \ell \tag{2-43}$$

$\underline{E}_P$:	Electromotive force [Vm] in the segment
$\underline{I}_x$:	Inducing current from a current-carrying conductor including calculated currents from e.g. ECs
$\underline{Z}'_x$:	Mutual impedance between conductor and pipeline
ℓ:	Length of the segment
n:	Number of current-carrying conductors in the segment

When all impedances and admittances as well as the inducing voltages are known, the pipeline can be modelled as an equivalent network and the pipeline interference voltage (PIV) can be calculated. A pipeline of two influenced and two non-influenced segments is shown in Figure 2-20 and consists of five nodes with the corresponding PIVs $\underline{U}_{P1}$ to $\underline{U}_{P5}$.

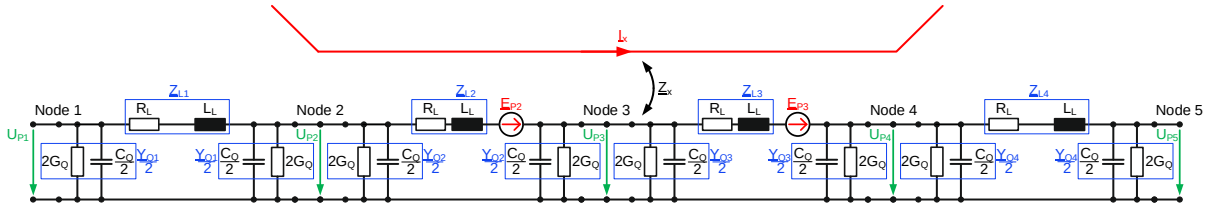

$\underline{E}_{P(x)}$:	Electromotive force [Vm] in the segment
$\underline{I}_x$:	Inducing currents from a current-carrying conductor including calculated currents from e.g. ECs
$\underline{Z}_x$:	Mutual impedances between conductors and pipeline

Figure 2-20: Equivalent network with four segments

As a next step, this example has to be converted into the nodal admittance model with a $\underline{Y}$– matrix (2-44), where the main diagonal consists of all elements connected to the node according to the position within the matrix. The minor elements are the negative longitudinal admittances between two nodes.

$$\underline{Y} = \begin{bmatrix} \frac{1}{\underline{Z}_{L1}} + \frac{\underline{Y}_{Q1}}{2} & -\frac{1}{\underline{Z}_{L1}} & 0 & 0 & 0 \\ -\frac{1}{\underline{Z}_{L1}} & \frac{1}{\underline{Z}_{L1}} + \frac{\underline{Y}_{Q1}}{2} + \frac{1}{\underline{Z}_{L2}} + \frac{\underline{Y}_{Q2}}{2} & -\frac{1}{\underline{Z}_{L2}} & 0 & 0 \\ 0 & -\frac{1}{\underline{Z}_{L2}} & \frac{1}{\underline{Z}_{L2}} + \frac{\underline{Y}_{Q2}}{2} + \frac{1}{\underline{Z}_{L3}} + \frac{\underline{Y}_{Q3}}{2} & -\frac{1}{\underline{Z}_{L3}} & 0 \\ 0 & 0 & -\frac{1}{\underline{Z}_{L3}} & \frac{1}{\underline{Z}_{L3}} + \frac{\underline{Y}_{Q3}}{2} + \frac{1}{\underline{Z}_{L4}} + \frac{\underline{Y}_{Q4}}{2} & -\frac{1}{\underline{Z}_{L4}} \\ 0 & 0 & 0 & -\frac{1}{\underline{Z}_{L4}} & \frac{1}{\underline{Z}_{L4}} + \frac{\underline{Y}_{Q4}}{2} \end{bmatrix} \tag{2-44}$$

The induced current matrix $\underline{\boldsymbol{I}}$ (2-45) consists of the induced voltages $\underline{\boldsymbol{E}}_{\boldsymbol{P2}}$ and $\underline{\boldsymbol{E}}_{\boldsymbol{P3}}$ which have to be converted into currents $\underline{I}_{EP2} = \frac{\underline{E}_{P2}}{\underline{Z}_{L2}}$ and $\underline{I}_{EP3} = \frac{\underline{E}_{P3}}{\underline{Z}_{L3}}$ because of the model used. On every node all known currents have to be summed up, e.g. node 1 is zero because no induced current can flow and on node 2, only the negative current of the first interfered segment is used.

$$\underline{I} = \begin{bmatrix} 0 \\ -\underline{I}_{EP2} \\ \underline{I}_{EP2} - \underline{I}_{EP3} \\ \underline{I}_{EP3} \\ 0 \end{bmatrix} \tag{2-45}$$

After all necessary parameters are determined, the PIV $\underline{\boldsymbol{U}}_{\boldsymbol{P(x)}}$ along the pipeline is calculated using the following equation (2-46):

$$\underline{U}_P = \underline{Y}^{-1} \cdot \underline{I} \tag{2-46}$$

Figure 2-21 shows the voltage along pipeline $\underline{\boldsymbol{U}}_{\boldsymbol{P(x)}}$. Between the nodes two and four lies the influenced area which shows rising PIVs. Outside of this area, the PIV is reduced, which is due to the shunt admittance. The red line shows the interference voltage distribution along the pipeline. The blue line shows the absolute value, which can be directly measured on the pipeline.

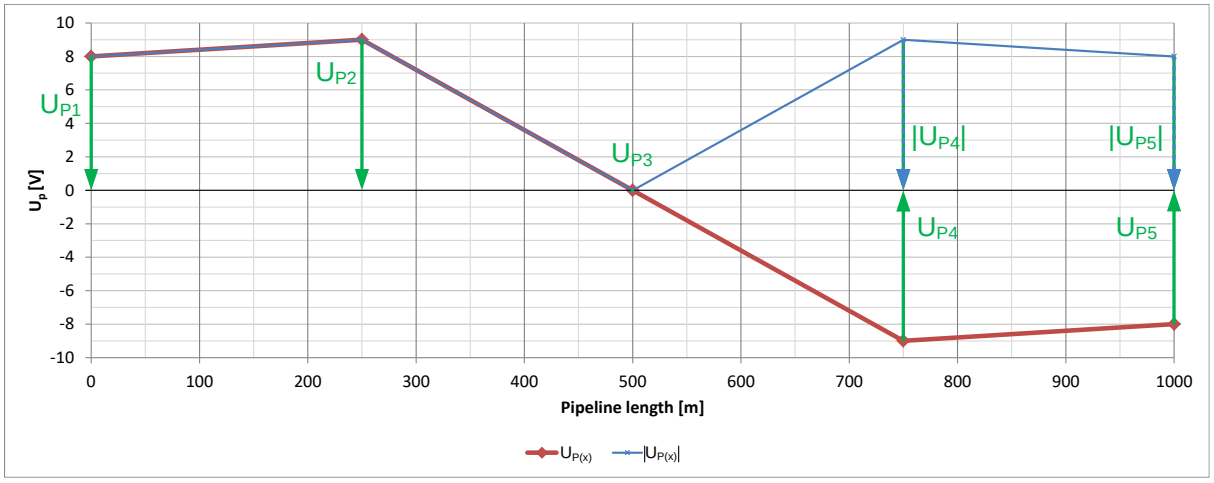

Figure 2-21: PIV for the example in Figure 2-20

3 Development of an efficient program for calculating the pipeline interference voltage

In the past, various specialised programs dealing with pipeline interference voltages were developed, causing a situation where there is a step by step calculation with a different program being used for each part of the calculation. In addition, the results have to be transferred manually between the programs. When a parameter changes, this can be especially challenging and time consuming because most of the calculation cycle has to be repeated.

Therefore, this process should to be optimised with the newly developed Matlab®-program "AiO", improving usability and efficiency. For this reason, a potent graphical and intuitive user-interface was designed to address the following issues:

- User-Interface (front end):
  - The geographical information can be easily inserted as well as all necessary information about the pipeline, HVPSs and other metallic structures.
  - Geographical information about existing digitalised systems can be changed e.g. the routing can be modified and whole systems can be deleted.
  - No knowledge about the different calculation steps is needed, offering an easy use of calculation methods.
  - It is possible to change calculation parameters with the user interface e.g. segmenting or interference strip size.
- Technical back end:
  - An internal data management system is integrated; therefore it can be easily expanded for other types of metallic structure
  - Automatic detection if an interference source is located near the pipeline within the user defined interference strip size. If this is the case, an automatic segmentation is made according to the user's specifications.
  - Using modern technologies ensures an efficient calculation program. However, big projects with small segments still need longer to calculate and have a large RAM usage
- Automated technology for this thesis includes:
  - A software-based implementation for varying two different parameters, for instance pipeline diameter and earth conductor height to optimise the inductive interference.
  - A direct Excel-export option for easy analysis of the impact of different parameters.

All these necessary requirements show that the nodal admittance matrix cannot be used anymore, that a modified calculation model is essential and that the Clarke-and-Starr-calculation model fulfils these requirements.

3.1 Selection of the programming environment

When using a Simulink® -model to solve interference problems, two main challenges arise:

- Calculating the impedances and admittances for parallel routing is easy but in cases, where the distance between influencing and influenced system is not constant, the relevant parameters have to be calculated for each segment. This can be done automatically and can be imported into the Simulink® -model. However, the number of segments has to be identical, which leads to problem number two.
- Very simplified calculation problems can be implemented in a relatively short time but with a more detailed segmenting or different metallic structures, the time needed to generate the proper structure increases significantly because Simulink® is a visual programming language (VPL). This means that for each segment, an equivalent quadrupole has to be added with the necessary parameters. Every change in structure can be easily programmed but drawing needs time and increases the risk of error.

Despite the disadvantages of Simulink®, the software can be used to verify the new Matlab® -based model, as will be shown in two examples in chapter 3.4. These examples will also illustrate the problems that arise with a fast-increasing number of elements.

3.2 Using the equivalent circuit by Clarke and Starr

As stated in chapter 2.5, the nodal admittance matrix can be used to calculate the PIV while the induced voltage must be calculated beforehand. Alternatively, the currents and other geographical information from high voltage power systems or other surrounding systems can be used instead of the induced voltage. For this, an equivalent circuit simulates the mutual impedance between all systems by simple impedance links. Frank M. Starr [7] and Edith Clarke [8] describe a method where a two-winding transformer is used as the basic equivalent circuit which is then modified into the following equivalent circuit:

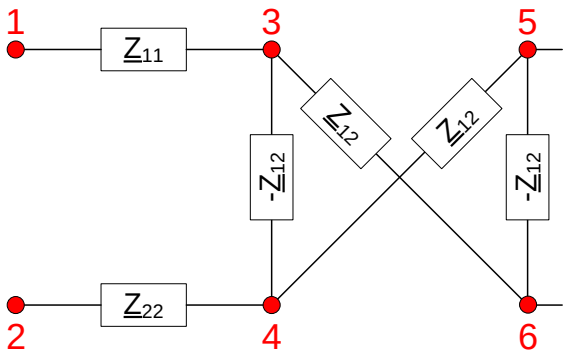

Figure 3-1: Simple model of the equivalent circuit by Clarke and Starr

In the equivalent circuit, $\underline{Z}_{11}$ and $\underline{Z}_{22}$ represent the self-impedances of each conductor and $\underline{Z}_{12}$ and $\underline{Z}_{12}$ the mutual impedances between two conductors. The values for $\underline{Z}_{12}$ and $\underline{Z}_{12}$ must be equal.

The advantage of this model is that it is a four-point network with voltage and current information. The arrangement of the elements is simple because the self-impedance is independent from the mutual impedance. Furthermore, it offers a mathematical description including a calculation of the interference problem. Adding the voltages and currents for two coupled conductor-earth-loops extends Figure 3-1 to Figure 3-2.

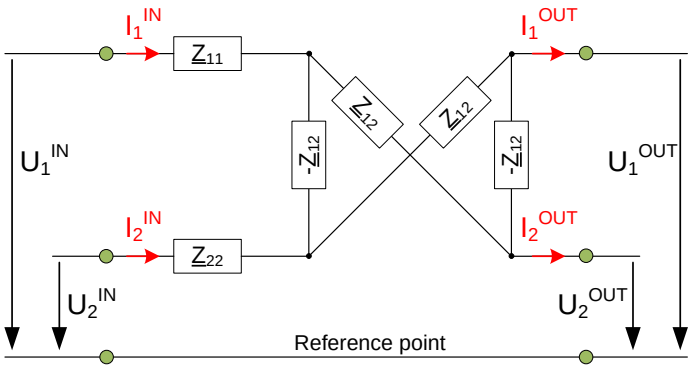

$\underline{Z}_{11}$:	Self-impedance of the first conductor
$\underline{Z}_{22}$:	Self-impedance of the second conductor
$\underline{Z}_{12}$ / $-\underline{Z}_{11}$:	Mutual impedance of the coupled conductors
$\underline{U}_1^{IN}$ / $\underline{U}_2^{IN}$:	Voltage at the beginning of this part of the first/second conductor
$\underline{U}_1^{OUT}$ / $\underline{U}_2^{OUT}$:	Voltage at the end of this part of the first/second conductor
$\underline{I}_1^{IN}$ / $\underline{I}_2^{IN}$:	Current at the beginning of this part of the second conductor
$\underline{I}_1^{OUT}$ / $\underline{I}_2^{OUT}$:	Current at the end of this part of the second conductor

Figure 3-2: Simple model of the equivalent circuit by Clarke and Starr; extended version

This model includes a system of equations:

$$\begin{bmatrix} U_1^{IN} \\ U_2^{IN} \end{bmatrix} = \begin{bmatrix} \underline{Z}_{11} & \underline{Z}_{12} \\ \underline{Z}_{12} & \underline{Z}_{22} \end{bmatrix} \begin{bmatrix} I_1^{IN} \\ I_2^{IN} \end{bmatrix} + \begin{bmatrix} U_1^{OUT} \\ U_2^{OUT} \end{bmatrix} \tag{3-1}$$

This model is able to describe complex interference problems without knowing the value of the impedances because they are calculated with the given formulas from chapter 2.3. However, the equivalent circuit of Clarke and Starr only works correctly with a correct numbering of the nodes. In Figure 3-1, the red number shows the best way to number the nodes.

When extending the problem to three conductors, the numbering of the nodes and branches has to be adapted. This can be seen in Figure 3-3 when comparing the numbers inside the light blue rectangle with the initial graphic (Figure 3-1; the number six is changed to seven). For an automatic calculation program with auto detect, this numbering of conductors poses a challenge.

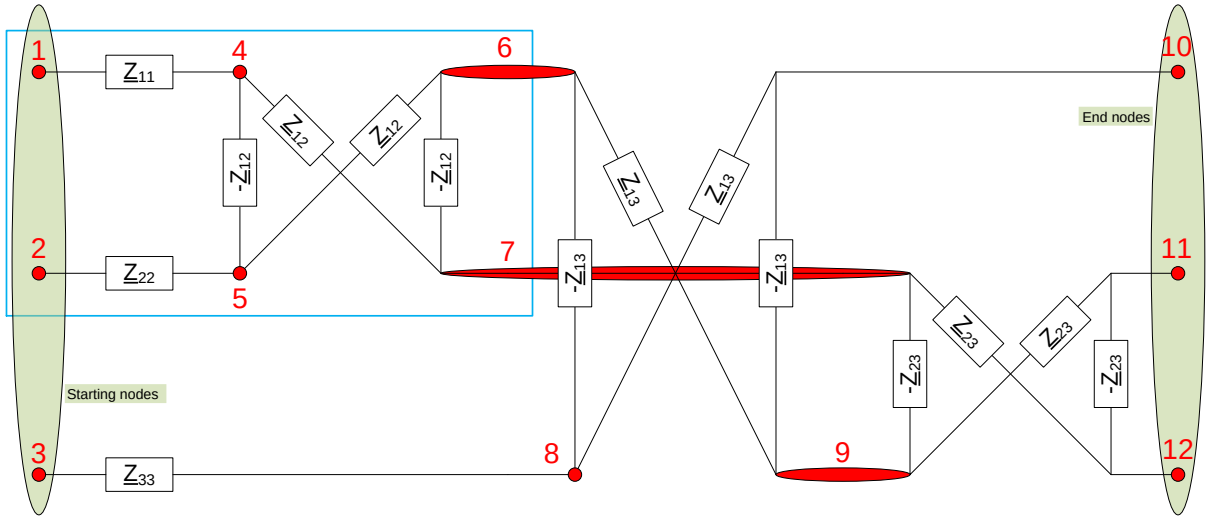

Figure 3-3: Equivalent circuit of Clarke and Starr with three conductors

The correct numbering is even more complicated in cases where a conductor or a metallic structure begins or ends, e.g. an influencing conductor stop its influence due to being outside of the interference strip.

The following example in Figure 3-4 shows two segments: the first one has two conductors while in the second one, a third conductor starts to interact with the other two conductors.

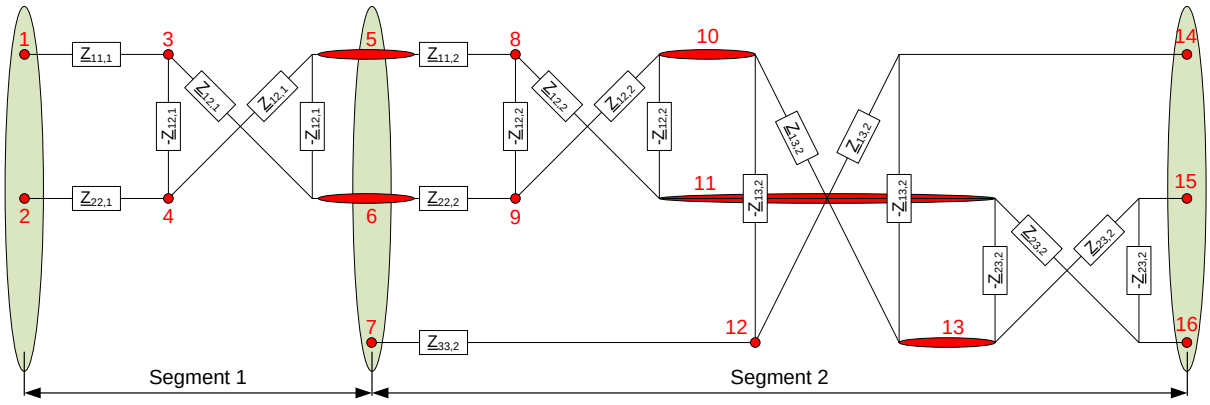

Figure 3-4: Equivalent circuit of Clarke and Starr with two segments and a change from two to three conductors

This example shows how the numbering in these situations must be handled. It is crucial that the nodes are numbered consecutively in ascending order at the beginning and end of a segment. This is also the case when a conductor disappears. More conductors create a more complex situation. The correct numbering is more difficult due to the different combinations: e.g. conductors 1,2,3,5 exist, then in the next segment number 4 is added and a few segments later, number 2 and 3 disappear. Also, these graphics show that complex computation models consist of more branches than nodes. Figure 3-4 consists of two segments, therefore, it may be assumed that with segmenting into smaller

parts, the complexity rises respectively and the handling of calculation resources is more challenging due to larger matrices.

A lot of these ideas have been described in the master thesis of Steinkellner [24], including the calculation of the increase of nodes as well as branches.

3.3 Calculation steps for the nodal analysis

The nodal analysis is used for complex electrical networks. Its significant advantage is that the number of independent nodes is equal to the number of unsolved equations. To use this method, preparations are required: the impedances must be changed to admittances and only current sources are allowed.

Other methods are more calculative, e.g. Kirchhoff's law. This chapter gives an overview of the calculations, a more exact description can be found in the master thesis of Roßmann [25].

3.3.1 Branch-node incidence matrix

The branch-node incidence matrix $\boldsymbol{C}$ is needed to uphold the structure of the interference example and constitutes the basis for the nodal analysis. Within the matrix, branches are assigned to rows and nodes to columns. When two nodes are connected, either a 1 or -1 are used; 1 designates an outgoing node, -1 an incoming. Making a branch-node incidence matrix from Figure 3-1 leads to Table 3-1.

Node	1	2	3	4	5	6	Branch
C =	1	0	−1	0	0	0	K1
	0	1	0	−1	0	0	K2
	0	0	1	−1	0	0	K3
	0	0	1	0	0	−1	K4
	0	0	0	1	−1	0	K5
	0	0	0	0	1	−1	K6

Table 3-1: Branch-node incidence matrix from Figure 3-1

Only a small example is being presented because larger examples lead to very large matrices $\boldsymbol{C}$, which would go beyond the scope of this chapter.

3.3.2 Incorporating external elements into the matrices

All elements, which are not longitudinal or mutual impedances, are external elements. Due to the different metallic structures such as pipelines, overhead lines (OHLs) or earthing systems, programming the auto-detection has to take into account which kind of structure is used and the right parameters. The following list shows the different parameters of external elements:

- **Buried metal structure:** Due to the direct contact with the soil, the shunt admittance has to be considered on every segment, even when the subdivisions are rather small.

- **Phase conductors:** At the beginning and end of the interference, the transformer impedance and the substation impedances have to be considered. Also, a current source parallel to the transformer impedance must be included.
- **ECs** above **ground:** At the beginning and end of the interference, the impedance of substations has to be included.
- **OHLs** in **general:** Usually, the pylon earthing systems should be considered, but in this thesis, they have been omitted. The main reasons for this are that it is difficult to get exact information about the distance between two pylons and the effective earthing resistance value of the pylons and it is not the goal of this thesis to simulate the exact current flow situation in OHLs because the focus lies on the calculation of the PIV.

An extension of Figure 3-1, with the external elements of a pipeline and a phase conductor, is shown in Figure 3-5. The pipeline uses the same shunt admittance while the phase conductor uses the parallel transformer impedance at the beginning and the substation impedance at the end. The reference node is needed as the remote earth or reference potential.

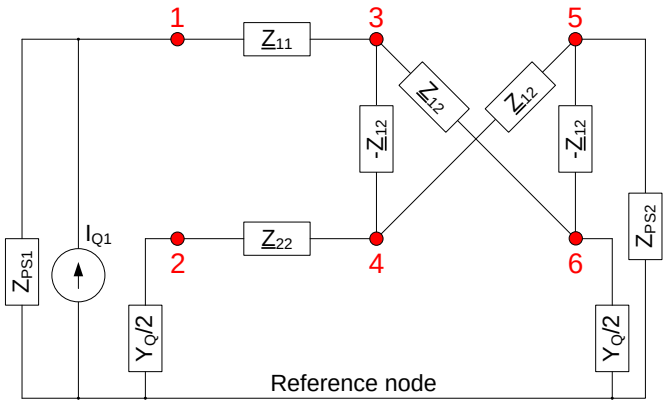

$\underline{Z}_{11}$:	Self-impedance of the first conductor
$\underline{Z}_{22}$:	Self-impedance of the second conductor
$\underline{Z}_{12}$ / $-\underline{Z}_{11}$:	Mutual impedance of the coupled conductors
$\underline{Y}_Q/2$:	Shunt admittance; due to the used Π-equivalent network, only half of the value is used at the start and end of a segment
$\underline{Z}_{PS1}$:	Transformer impedance and a substation impedance series
$\underline{Z}_{PS1}$:	Substation impedance

Figure 3-5: Simple example with the external elements for a pipeline and a phase conductor

With the external elements, the branch-node incidence matrix must be extended to update the structure. Also, the branch-current source matrix $\underline{I}_z$ can now be generated. The new elements are written in red.

$$\begin{array}{c} \text{Node} \\ \\ \\ \\ \\ \\ \\ \\ \\ \\ \end{array} \quad \begin{array}{c} 1 \quad 2 \quad 3 \quad 4 \quad 5 \quad 6 \\ \\ \\ \\ \\ \\ \\ \\ \\ \\ \end{array} \quad \begin{array}{c} \text{Branch} \\ \\ \\ \\ \\ \\ \\ \\ \\ \\ \end{array}$$

$$C = \begin{bmatrix} 1 & 0 & -1 & 0 & 0 & 0 \\ 0 & 1 & 0 & -1 & 0 & 0 \\ 0 & 0 & 1 & -1 & 0 & 0 \\ 0 & 0 & 1 & 0 & 0 & -1 \\ 0 & 0 & 0 & 1 & -1 & 0 \\ 0 & 0 & 0 & 0 & 1 & -1 \\ 1 & 0 & 0 & 0 & 0 & 0 \\ 0 & 1 & 0 & 0 & 0 & 0 \\ 0 & 0 & 0 & 0 & 1 & 0 \\ 0 & 0 & 0 & 0 & 0 & 1 \end{bmatrix} \begin{array}{l} \text{K1} \\ \text{K2} \\ \text{K3} \\ \text{K4} \\ \text{K5} \\ \text{K6} \\ \text{K7} \\ \text{K8} \\ \text{K9} \\ \text{K10} \end{array} \tag{3-2}$$

$$\underline{I}_z = \begin{bmatrix} 0 \\ 0 \\ 0 \\ 0 \\ 0 \\ 0 \\ I_{Q1} \\ 0 \\ 0 \\ 0 \end{bmatrix} \tag{3-3}$$

3.3.3 Branch-admittance matrix and nodal admittance matrix

The example in Figure 3-5 shows how to create the branch-admittance matrix $\underline{Y}_z$. This matrix is a diagonal matrix and therefore only the main diagonal has incorporated elements while all other parts equal zero. For this matrix, all elements must be admittances; therefore impedances have to be converted. The elements in red designate external elements, the other elements correlate with the longitudinal and mutual impedances.

$$\underline{Y}_z = \begin{bmatrix} \underline{Y}_{11} & & & & & & & & & \\ & \underline{Y}_{22} & & & & & & & & \\ & & \underline{Y}_{12} & & & & & 0 & & \\ & & & -\underline{Y}_{12} & & & & & & \\ & & & & -\underline{Y}_{12} & & & & & \\ & & & & & \underline{Y}_{12} & & & & \\ & & & & & & \underline{Y}_{PS1} & & & \\ & & 0 & & & & & Y_Q/2 & & \\ & & & & & & & & Y_Q/2 & \\ & & & & & & & & & \underline{Y}_{PS2} \end{bmatrix} \tag{3-4}$$

The three matrices $\boldsymbol{C}$, $\underline{\boldsymbol{I_Z}}$ and $\underline{\boldsymbol{Y_Z}}$ form the basis for calculations of voltages and currents in the interference example. First, the node-current source matrix $\underline{\boldsymbol{I}}$ and the nodal admittance matrix $\underline{\boldsymbol{Y}}$ are generated:

$$\underline{I} = -C^T \cdot \underline{I_Z} \tag{3-5}$$

$$\underline{Y} = C^T \cdot \underline{Y_Z} \cdot C \tag{3-6}$$

With (3-5) and (3-6), a matrix with the nodal voltages $\underline{\boldsymbol{U}}$ can be calculated:

$$\underline{U} = \underline{Y}^{-1} \cdot \underline{I} \tag{3-7}$$

Formula (3-7) does not directly calculate the pipeline interference voltage (PIV) along the pipeline, because the voltages are calculated separately for every node. This means that a node filter is necessary which can find the relevant nodes for the PIV. In the example in Figure 3-1, these are the nodes 1 and 5 and in Figure 3-4 the nodes 1, 5 and 14.

In addition, this model can calculate the branch voltages $\underline{\boldsymbol{U_Z}}$ and branch currents $\underline{\boldsymbol{I_{Zw}}}$. By using matrix with the node voltages $\underline{\boldsymbol{U}}$ in Formula (3-7), a matrix with the branch voltages $\underline{\boldsymbol{U_Z}}$ can be calculated. These values represent the voltage drop along the branches.

$$\underline{U_Z} = C \cdot \underline{U} \tag{3-8}$$

In the end, a matrix with the branch currents $\underline{\boldsymbol{I_{Zw}}}$, which flow along the branches between the nodes, can be calculated. For pipelines, this is the current which flows over the pipeline coating into the soil and is responsible for the pipeline interference voltage reduction in areas, where no interference exists.

$$\underline{I_{Zw}} = \underline{I_Z} + \underline{Y_Z} \cdot \underline{U_Z} \tag{3-9}$$

3.4 Model verification

The usage of the equivalent circuit in the Clarke and Starr matrix can be verified, by calculating the impact of the conductor configuration (CC) on the zero-sequence-currents for cases with parallel overhead lines [24]. Using this model to calculate the inductive coupling between pipelines and metallic structures is a new approach and therefore needs to be verified.

The conducted verification [24] shows that the Simulink®-model is useful and leads to correct results. Two situations were chosen: First, the interference area runs along the whole length of the pipeline (see chapter 3.4.1) and second, the interference area lies in the middle of the pipeline with two non-interference areas of the same length added on the left and right side, as calculated in chapter 3.4.2. The impedances and admittances were calculated beforehand by hand because the main goal was to test the node connection system between the segments as well as the complex branch-node matrices of the new calculation system. A one current-carrying phase conductor was used for easier comparison which was placed at a distance of 100 meters to the pipeline.

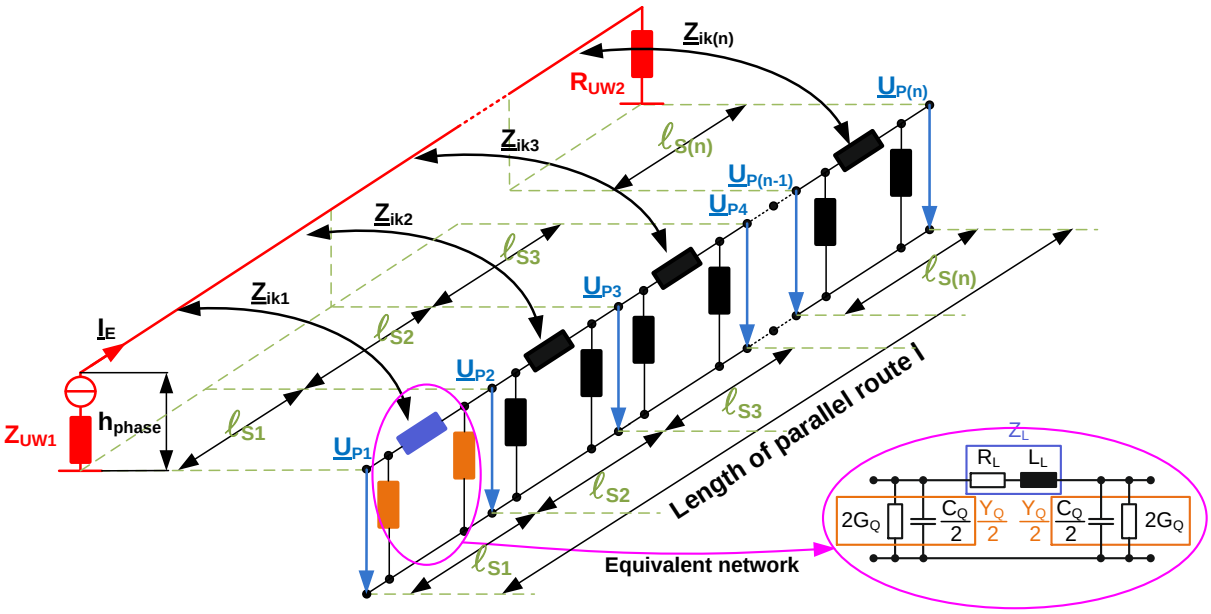

$\underline{U}_{P(n)}$:	PIV [V] on point (n)
$\underline{I}_E$:	Inducing current from a current-carrying HVPS [A]
$\underline{Z}_{ik(n)}$:	Inductive coupling impedance between both systems (mutual impedance) for a segment(n) [Ω]
$\ell_{S(n)}$:	Distance of parallel route of a segment (n) [m]
h_{phase}:	Vertical height of inducing conductor [m]
Z_{UW1}:	Impedance of the transformer with the connected earthing system [Ω]
R_{UW2}:	Impedance of the earthing system of the second power station[m]

Figure 3-6: Four segments of the inductive coupling with the lattice equivalent network of the pipeline; each segment consists of an equivalent network, as shown in this figure and in Figure 2-5

Figure 3-6 shows some segments of the first example, where the inducing phase conductor serve as a current source with the transformer admittance and both earthing systems visible; it also shows the inductive coupling on the pipeline, which is displayed as the known lattice equivalent network.

3.4.1 Overall interference of the pipeline

As explained above, the first example shows interference over the whole pipeline length ℓ. Figure 3-7 shows the parallel route between both systems over a length of 1000 m with a distance x_{ik} of 100 m. Also, the segmenting with a length of 50 m is added which is not necessary in this case due to homogenous conditions. The result, however, can be displayed in a more detailed fashion when segmenting is included.

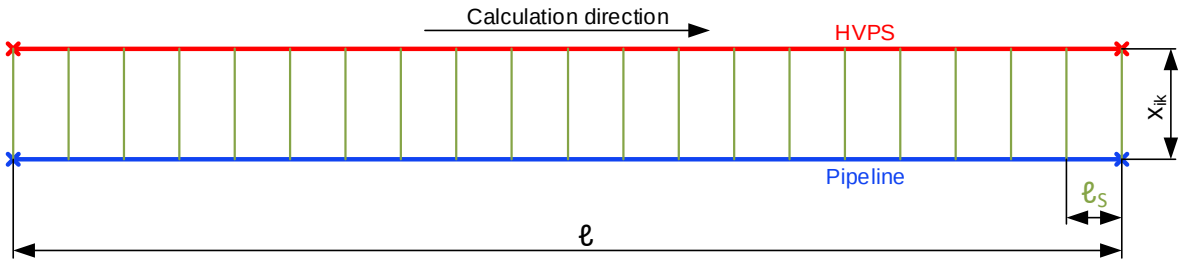

Figure 3-7: Parallel route between pipeline and high voltage power system over the whole length of the pipeline with segment lengths of 50 m

Figure 3-8 shows a part of the Simulink®-model with the Simulink®-built-in mutual impedances, the current source I_q and the shunt admittances, which are similar to Figure 3-6. The red line represents the phase conductor; the blue line is the pipeline. The full model can be found in Appendix B.

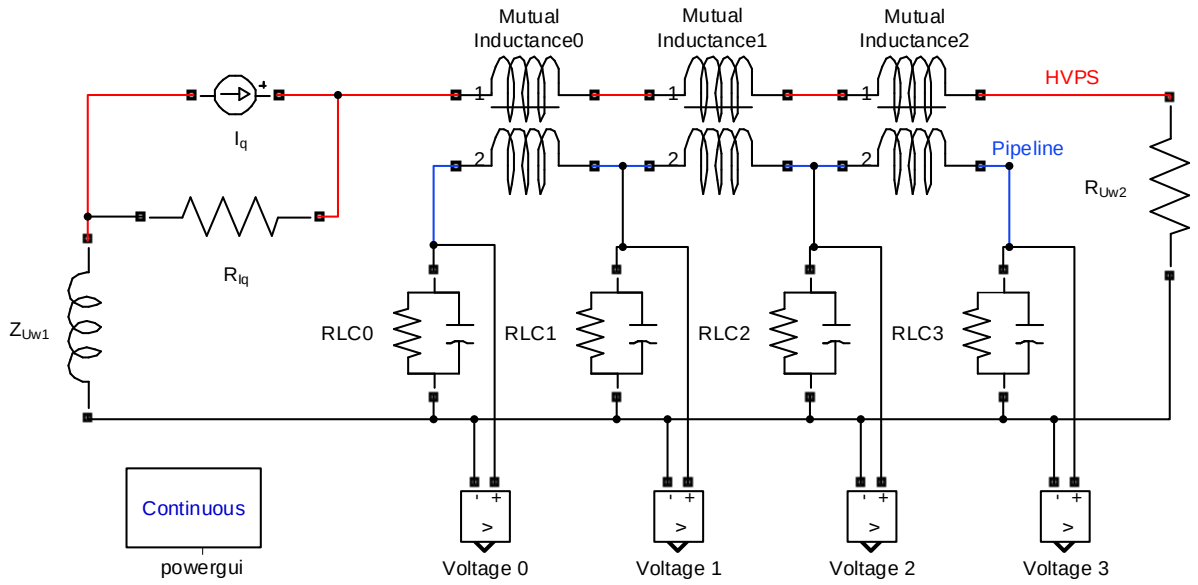

Figure 3-8: Simulink-model for the first verification example

When comparing the Simulink®-Model with "AiO", the pipeline interference voltage (PIV) along the pipeline has both the same curve progression and the maximum voltage value, as can be clearly

seen in Figure 3-9. These results show a typical curve progression for cases where influenced and influencing systems run exactly parallel to each other and where there is interference over the whole influenced system. Theoretically, the PIV between the pipeline lengths of 500 to 1000 m is negative due to inverted current flow but negative voltages cannot be measured and make it more complicated to compare. Therefore, such shapes, which are ideal for comparing different parameters, can only be seen in theoretical examples.

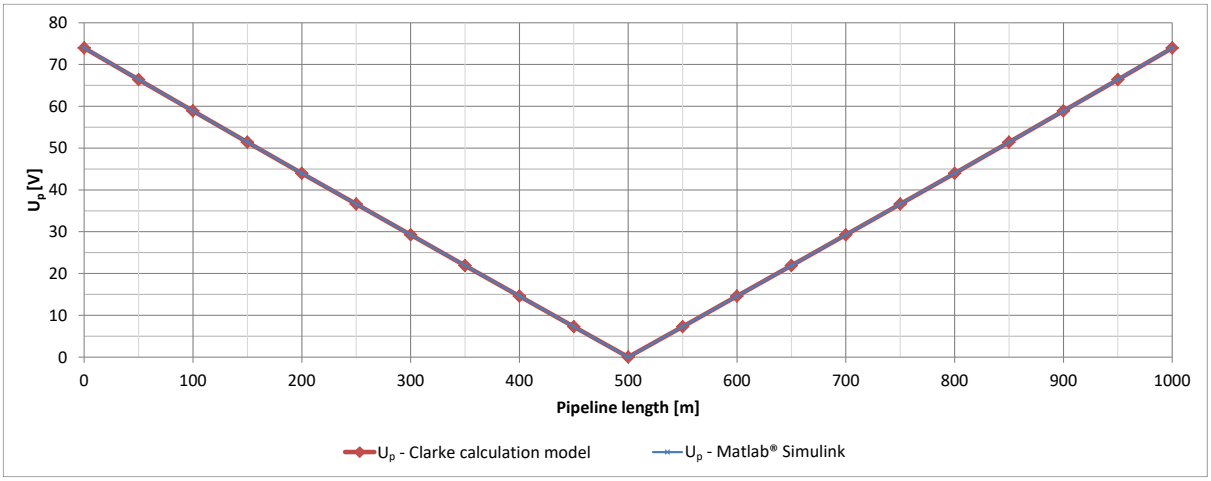

Figure 3-9: PIV along the pipeline for the Clarke calculation model and the Simulink®-model for the first verification model

The new program must have the same curve progression and values for the phase angle of the voltage as the already verified Simulink® model. Figure 3-10 shows that this is the case except for in the sector, where the voltage is zero. This small difference in the phase angle can occur due to the different accuracy of calculations, but appears in an area with a PIV around zero and therefore is not relevant. Another aspect is the nearly perfect 180 degree phase change in the middle of the pipeline. This phase change appears due to inverted current flow.

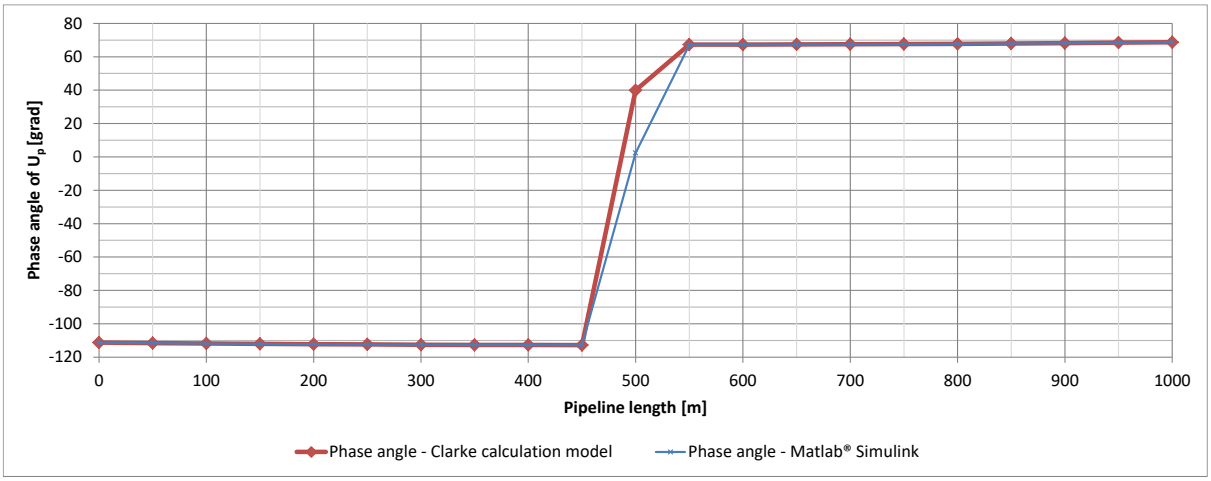

Figure 3-10: Phase angle of the PIV along the pipeline for both calculation models for the first verification model

3.4.2 Partial interference of the pipeline

As stated in chapter 3.4, the second example shows a partial interference in the middle, as illustrated in Figure 3-11. There is segmenting in the non-influenced segment which it is not displayed. The second example aims to verify whether the PIV decreases in the non-influenced segments.

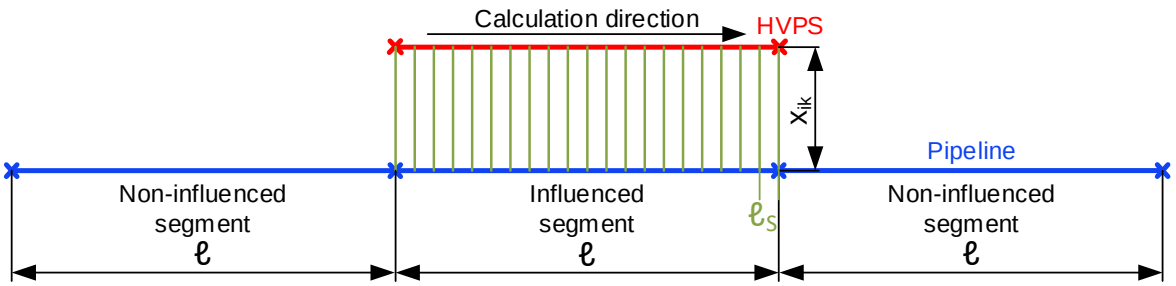

Figure 3-11: Parallel route between pipeline and HVPS in the middle segment of the pipeline with segments of 50 m length; the two other segments are non-influenced

This leads to the Simulink®-model in Figure 3-12, a more detailed model can be found in Appendix B:

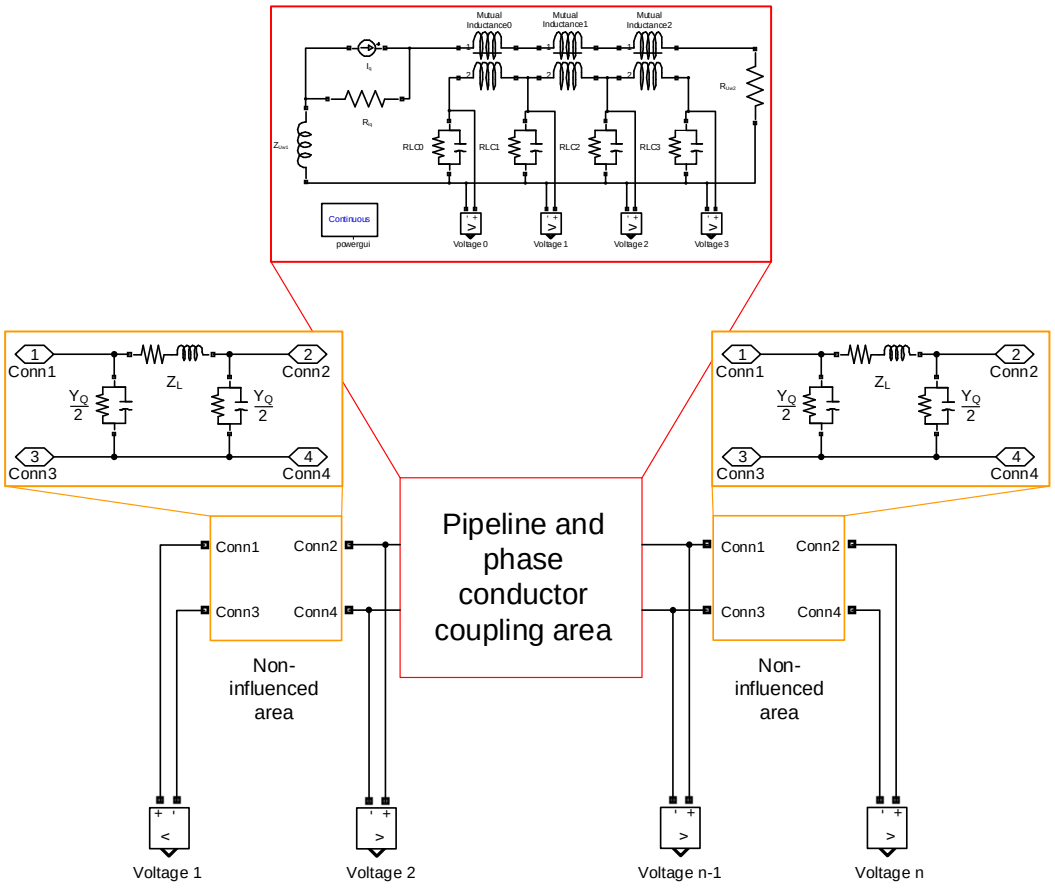

Figure 3-12: Simulink®-model for the second verification example

Figure 3-13 and Figure 3-14 show that both models are equivalent. When comparing Figure 3-9 to Figure 3-13, two important aspects can be seen: First, the peak PIV is lower in this example which can be explained by the current flow distribution over a larger area of the pipeline. Second, outside of the interference area, the PIV decreases slowly due to currents which can flow into the soil over the shunt admittance. The speed of the PIV decreasing is depends on the value of the shunt admittance: with e.g. lower specific pipeline coating resistances, the current can flow more easily into the soil.

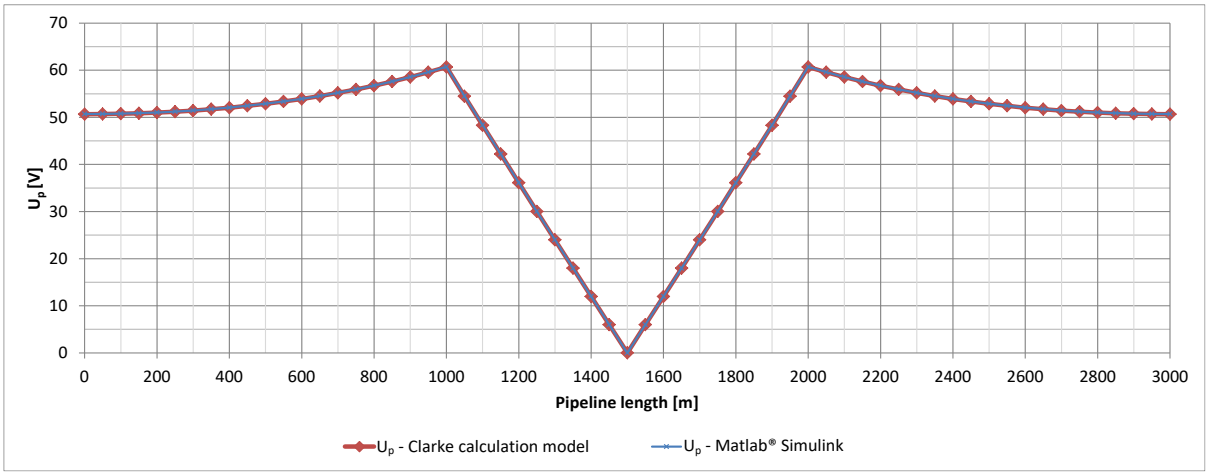

Figure 3-13: PIV along the pipeline for the Clarke calculation model and the Simulink®-model for the second verification model

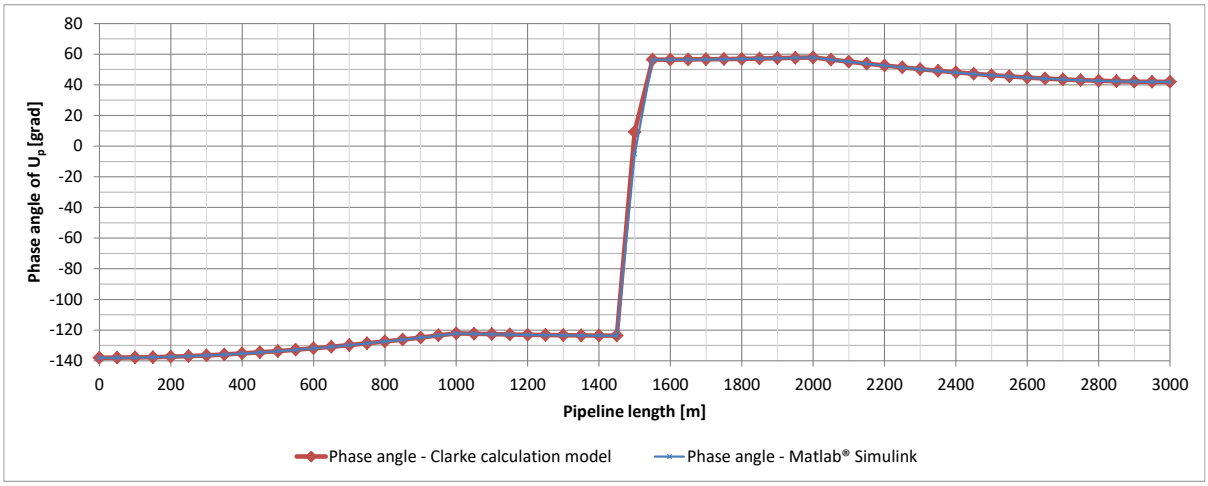

Figure 3-14: Phase angle of the PIV along the pipeline for both calculation models for the second verification model

In conclusion, these results prove that the newly developed Matlab®-program "AiO" can calculate pipeline interferences with the necessary accuracy and provide correct results. All further calculations in the next chapters are conducted with "AiO" and different aspects and factors of influencing and influenced metallic structures are investigated.

4 Investigation of the influence of different parameters on the calculation of the inductive interference voltage

4.1 Calculation example for easier comparison

The following example is necessary to account for the many different parameters for active and passive conductors. This makes comparing the results of varying parameters easier. In the following chapter of this thesis, this example is designated as the "standardized example" and does not follow any possible standardized examples from other publications, guidelines and norms. To keep it simple, the interference example in Figure 3-7 from the verification process in chapter 3.4.1 is used but instead assuming only one conductor for the high voltage power system (HVPS), an overhead line (OHL) with two symmetrical systems and one earthing conductor (EC) is used. Both, the interference example with the buried pipeline and the OHL pylon can be seen in Figure 4-1.

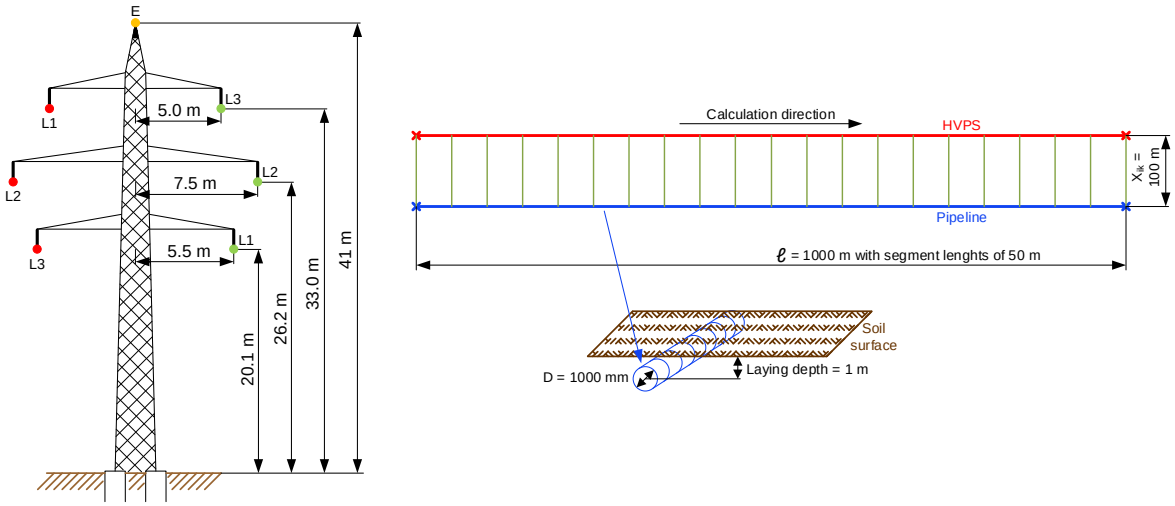

Figure 4-1: Geometrical parameters for the standardized calculation example

Figure 4-1 shows a "ton"-pylon as a double circuit line on the left side, which is very common in Austria. The dimensions are for a voltage level of 220 kV. Also, the conductor configuration (CC) can be read-out, which represents the best case. More information about the CC can be found in chapter 4.6.2.

The following additional data is necessary:

- Pipeline data:
  - Specific soil resistivity: 100 Ωm
  - Specific pipeline coating resistance: 1000 kΩm² with a thickness of 3 mm
  - Wall thickness: 10 mm

- OHL data:
  - Phase conductor diameter: 27 mm
  - EC diameter: 18 mm
  - Sag for all conductors: 10.9 m
  - Material: Steel-aluminium
  - Frequency: 50 Hz
  - Inducing current: 1000 A with the proper phase shifts (L1 = 0°, L2 = 120°, L3 = 240° or -120°)
  - External elements: At the beginning a combination of a transformer and a substation impedance with 0.2 + i177 Ω and at the end a substation impedance with 0.2 Ω
- Calculation formulas:
  - Self-impedances and shunt admittances: **"Formula S"** (see chapter 2.3.1.1)
  - Mutual impedances: **"Complex Image Formula"** (see chapter 2.3.3.2)
  - Pipeline interference voltage (PIV) along the pipeline: Matlab®-based program "AiO"

With this data and calculation formulas, the absolute value of the PIV as well as the phase angle along the pipeline is calculated. The result in Figure 4-2 (a) shows the typical curve progression for cases where influenced and influencing systems are exactly parallel to each other and where there is interference over the whole influenced system. Only for these special cases with very homogenous parameters, such a curve progression with the exact same values at the beginning and end of the pipeline can be calculated. Figure 4-2 (b) displays the phase angle of the PIV with a nearly perfect 180 degree phase change in the middle of the pipeline.

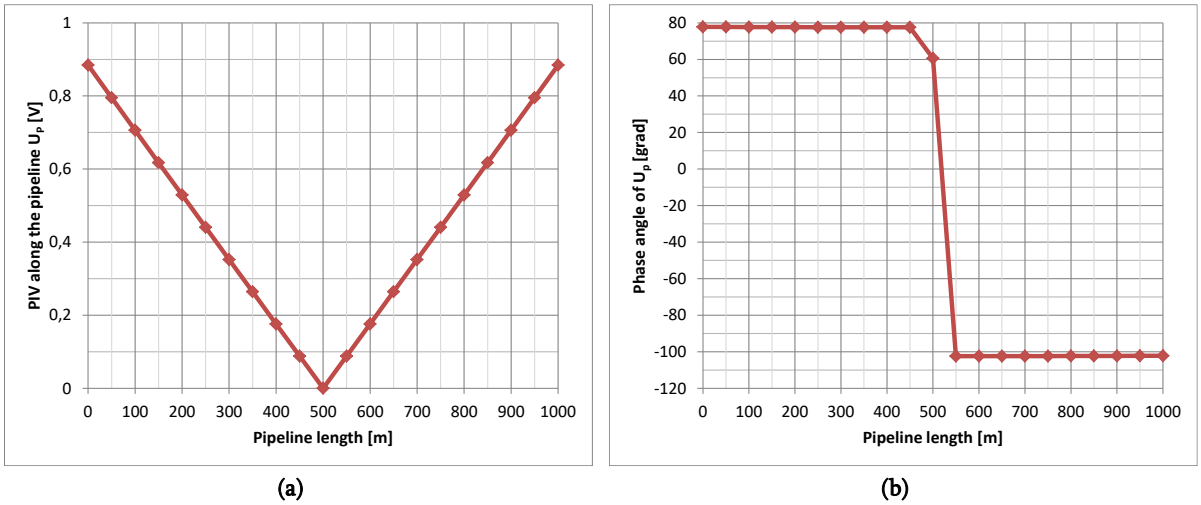

Figure 4-2: PIV and phase angle along the pipeline for the standardized example

The graph on the left shows that the maximum PIV on both ends of the pipeline is still quite small with a value of 0.88 V/km, despite a relative long and close vicinity of both systems. The reason for this is that the pylon configuration as well as the CC are ideal. This can also be seen in chapter 4.6, where the impact of different pylons and CCs on the absolute value of the PIV is investigated. The phase angle of the PIV shows another 180 degree phase change in the middle of the pipeline.

The example given above assumes a fixed vertical distance x_{ik} of 100 m. By varying this parameter, the mutual impedance changes and therefore, the induced voltage changes as well which leads to a different PIV progression. The upper part in Figure 4-3 shows a calculation where the vertical distance between the pipeline and OHL varies from -2000 to +2000 m. The original location of the above calculation is indicated in this figure and shows that only the maximum PIV is used. The blue curve shows the maximum PIV from each calculation; 4,001 calculations are conducted for this chart.

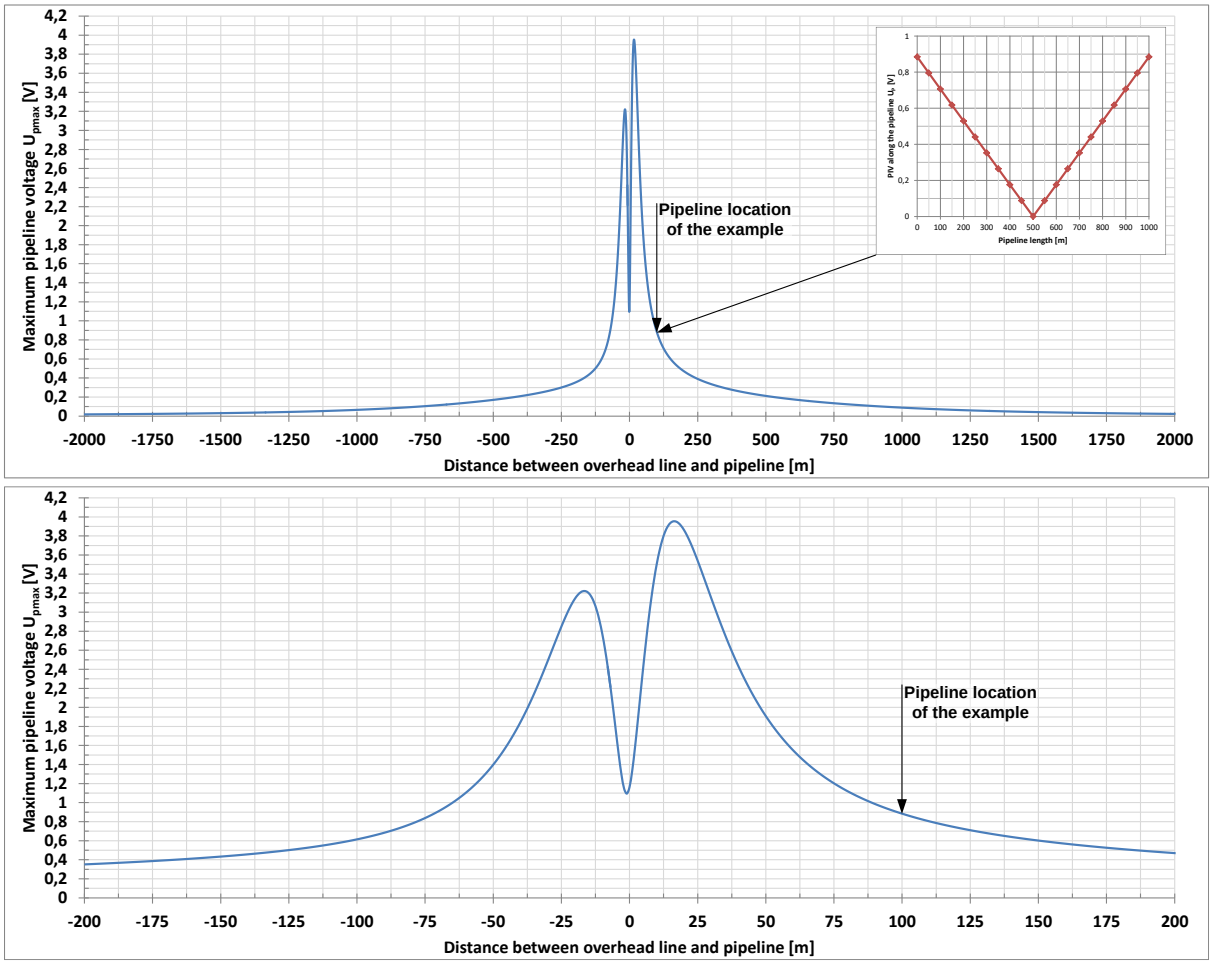

Figure 4-3: Maximum PIV for vertical distances from -2000 to 2000 m; the first graph shows the original calculation for a distance of 100 m, the lower graph is an enlarged version of the above picture with a vertical distance range of -200 to 200 m

The lower graph is enlarged to give a better view of the close vicinity of the pipeline. This unusual view of the PIV shows that when the pipeline is situated at a distance greater than 200 m from this OHL, the values are much lower than the highest value in this chart. When comparing the original calculation with a distance of 100 m to the lower graph with the outer distance of 200 m, the maximum PIV is already halved. The maximum PIV appears at a distance of around 17 m.

In addition, this example shows two interesting effects, which can only be understood when the magnetic flux density is taken into account. The first is that when the OHL runs directly above the pipeline (distance = 0 m), the maximum PIV falls dramatically. The reasons for this are that due to the symmetrical setup of the double circuit line, the magnetic fluxes of the single conductors mostly cancel each other out and that the dominating factor for the magnetic flux is the EC. In other words, when taking into account the mutual impedance formula, the three values for the three phase conductors add up to around zero, while the most dominating factor is the mutual impedance of the EC.

The second effect is that the maximum PIV value is not mirror-symmetrical over the entire vertical distance between pipeline and OHL. The cause of this is the EC, which deforms the symmetrical magnetic flux of the double circuit lines. Therefore, the magnetic field increases in some areas while in other areas it is decreasing. This effect also depends on the rotation direction of the magnetic flux. More details are discussed in [41], page 55, which gives a detailed analysis of the magnetic fields for different kinds of OHLs and also investigates the effects of ECs on the magnetic flux density.

4.2 Impact of the formula used for calculating conductor parameters

Calculating the conductor parameters has already been discussed in theory as well as shown by the parameter variation in chapter 2.3. It has been shown that for the longitudinal impedance, the four formulas can be split up into two groups due to their similar results. There are only two formulas to calculate the shunt admittance which differ under certain conditions such as a higher specific pipeline coating resistance or wall/coating thickness. Therefore, all in all, eight formula combinations have to be considered (see Table 4-1).

The impacts of these formulas will be described on the basis of the standardized example and a distance x_{ik} of 100 m. Calculating the maximum PIV $\underline{PIV}_{max}$ for each of the eight combinations leads to Figure 4-4, where, unfortunately, many of the curve progressions superimpose each other.

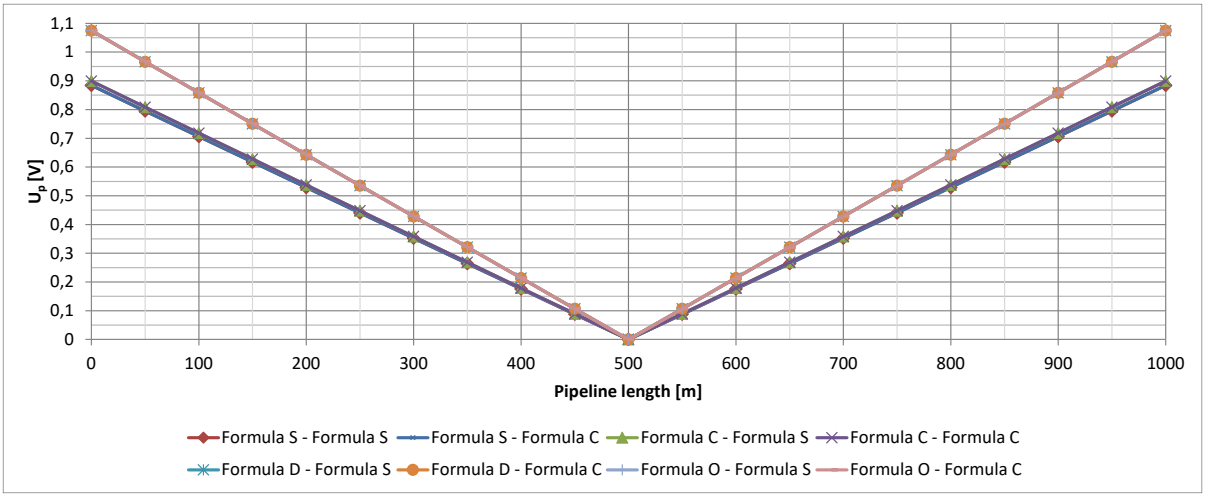

Figure 4-4: PIV along the pipeline according to the eight formula combinations for calculating the conductor parameters

The reason for this can be seen in Table 4-1, where the maximum PIV $\underline{PIV}_{max}$ is listed. First of all, comparing the two formulas for the shunt admittance shows no relevant difference and leads to the first result: both formulas are equal. Also, calculations were conducted, varying the wall and coating thickness. The outcome was that the impact of these two parameters is small and can be neglected. In its implementation, the "Formula S" for shunt admittances is easier to use because the value of the wall thickness is generally better known than the value of the coating thickness.

			Shunt admittance formula	
			Formula S	Formula C
			$\underline{PIV}_{max}$ [Volt/km]	
Longitudinal impedance formula	**Group one**	Formula S	0.884	0.884
		Formula C	0.899	0.899
	Group two	Formula D	1.075	1.075
		Formula O	1.075	1.075

Table 4-1: Comparing the maximum values of the PIV for the eight formula combinations

When comparing the results of the four longitudinal impedance formulas, the two formula groups "Formula S" – "Formula C" and "Formula D" – "Formula O" are again easy to spot due to similar or equal results. Table 4-1 shows that the values of the second group are about 20 % higher with the given parameters. When considering the results in light of the discussion in chapter 2.3.1, a part of the difference appears to be due to the differences in higher conductor diameters (Figure 2-10). Another significant part stems from the difference in calculating the specific soil resistivity (Figure 2-9).

The phase angles of $\underline{PIV_{max}}$ in Figure 4-5 show a very similar progression with slightly different values which have no effect on the PIV calculation. In the area where the voltage level equals zero, the differences between all formulas become apparent. This happens due to the calculation inaccuracy and disappears with smaller segments. Figure 4-5 is the last chart on phase angles because phase angles cannot be compared to conducted measurements and are not relevant for comparing the different parameters and other surrounding effects on the PIV.

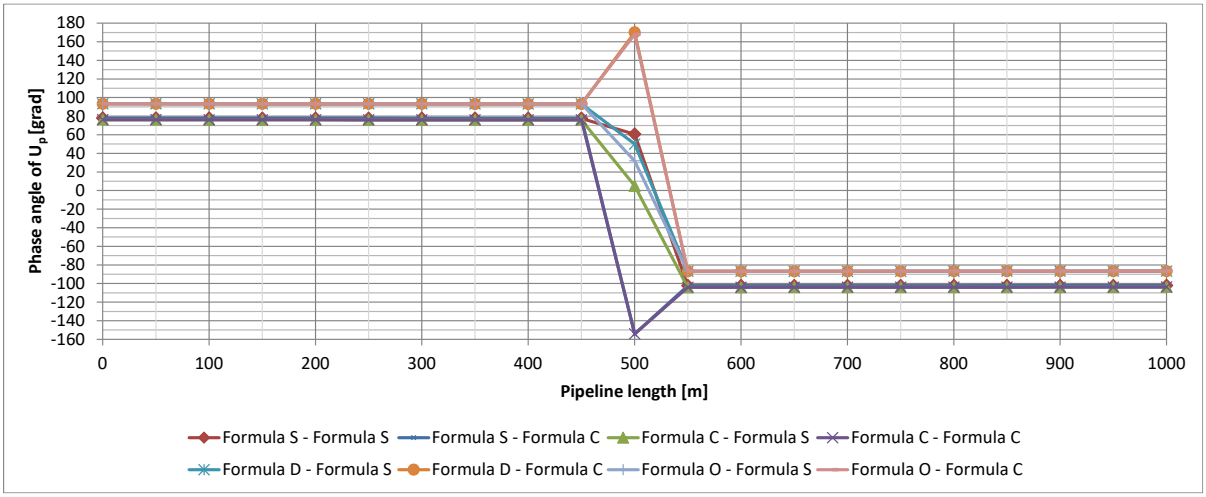

Figure 4-5: Comparing the phase angle of the PIV for the eight formula combinations

The standardized example includes only the influenced area and nothing else. The following example looks similar to the example in chapter 3.4.2, where the influenced area is flanked by two non-influenced areas. Both non-influenced areas are now 4000 m long, subdivided into 100 m segments. When comparing Figure 3-13 with the newly calculated Figure 4-6, the curve shape is very similar but the primary focus with this 9000 m long example is the effect of different formula combinations on the non-influenced areas.

The chart clearly shows that nothing changes and that the 20 % difference between both formula groups remains on the same level from one end to the other. Also, the shunt admittance has no effect, even when varying the thicknesses.

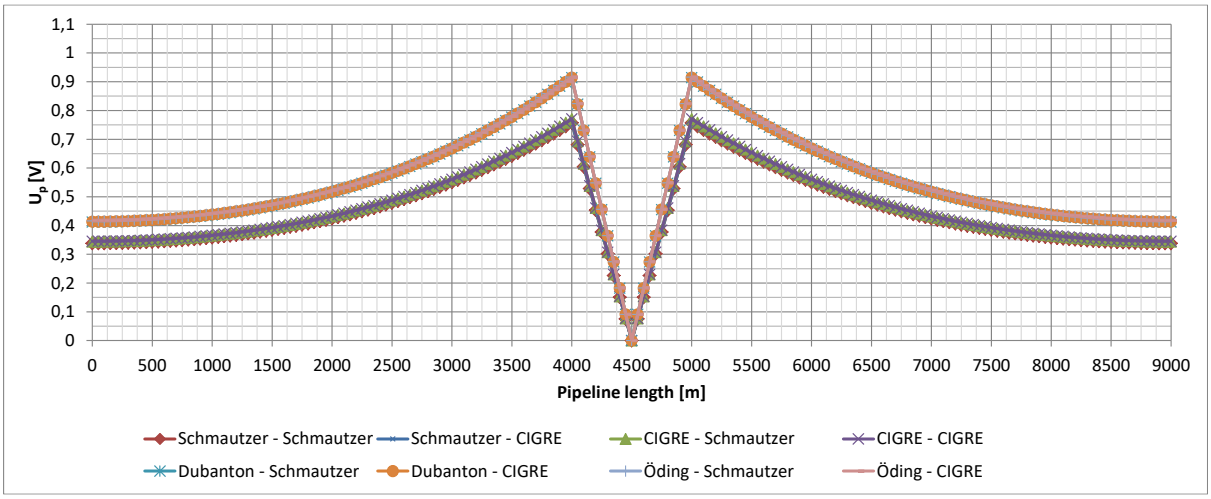

Figure 4-6: Comparing the maximum values of the PIV for the eight formula combinations for an example with one influenced and two non-influenced segments for a 9000 m long pipeline

Two changes in the parameters of the same example are also considered: the pipeline diameter is modified to 100 mm and the specific pipeline coating resistance is modified to 100 kΩm². The theoretical analysis in chapter 2.3.1.2 shows that the difference between both formula groups increases with a decreasing diameter (see Figure 2-10). Figure 2-12 in chapter 2.3.2.1 also shows that with smaller resistances, the gap between the values for the shunt admittance formulas decreases. Both results prove that the effect of smaller diameters is stronger than the effect of a lower admittance value. Therefore, the difference between both formula groups of the pipeline voltages along the pipeline increases to a value of around 26 %, as shown in Figure 4-7.

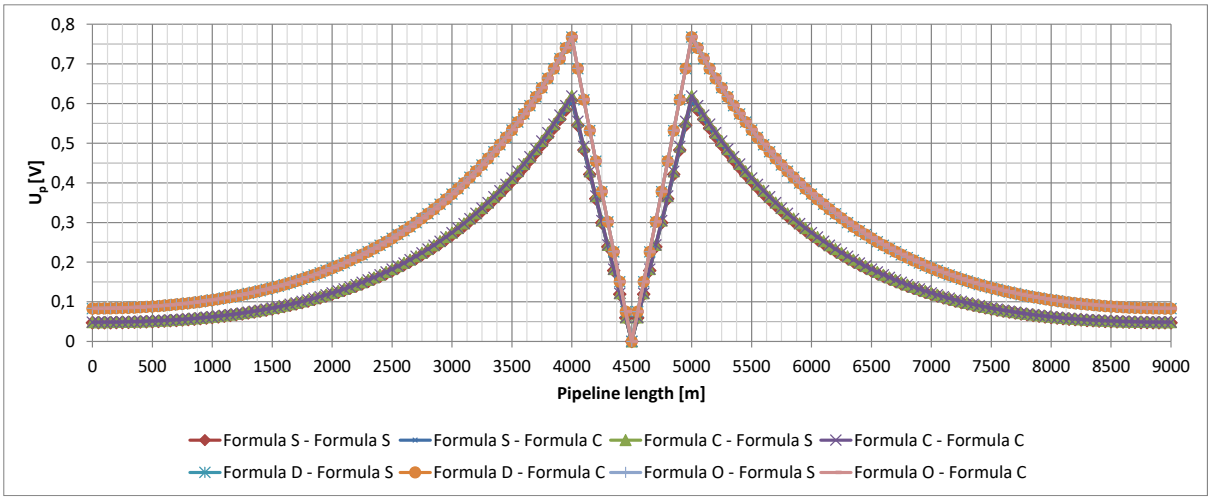

Figure 4-7: Comparing the maximum values of the PIV for the eight formula combinations for an example with one influenced and two non-influenced segments for a 9000 m long pipeline with modified parameters

When comparing Figure 4-6 to Figure 4-7, two additional effects can be seen. The maximum PIV_{max} is lower in the second figure which can be explained by a lower conductivity due to the smaller diameter of the pipeline. The second effect is how fast the PIV can be reduced in influenced areas and especially in non-influenced areas. The last example demonstrates the result of a lower coating resistance where the induced current can flow more easily into the surrounding soil.

In conclusion, it can be said that the formulas for the shunt admittance have no effect on the PIV calculation. It is unclear, which formula should be used for the longitudinal impedance. In the best case, the formulas of "Formula D" and "Formula O" reach nearly the same values when compared to the formulas of "Formula S" and "Formula C". In most other cases, the formulas of "Formula D" and "Formula O" calculate higher PIVs. The initial statement in chapter 1 was that conducted measurements show lower PIVs than calculations, therefore it is recommended to use either "Formula S" or "Formula C" because both formulas give very similar results.

4.3 Specific pipeline coating resistance

In the chapter above, the effect of the specific pipeline coating resistance (SPCR) has already been touched upon. The value of the SPCR has two effects: one is the decrease of the maximum PIV and the other is the speed of reducing the PIV along the pipeline. Generally it can be said that the lower the value of the SPCR resistance, the lower the PIV. Unfortunately, low resistances are not favoured by pipeline operators. The reason behind this is the cathodic protection system, which prevents the steel from corroding. When the coating is decreased, more cathodic protection current is needed and an increase in feeding points might have to be considered. Both are unpopular since they cause continuous costs for the protection current and create extra costs for construction and maintenance of the feeding points.

As stated in chapter 2.3.2, pipeline manufacturers can only guarantee the value of the coating at dispatch. The construction and operation of pipelines can change the coating resistance due to coating holidays, which appear because of sharp-edged stones, other natural events or human contact, e.g. chipping from excavators. These issues make the estimation of the coating resistance values very difficult since perfect pipeline coatings do not exist. The influence of the coating resistance has already been investigated in [30], where a practical example was examined for two different conductor configurations. This publication compared different coating resistance values with soil resistivity values. It was ascertained on page 10 that with rising coating values, the pipeline interference voltage rises as well. The exact value of this increase, however, depends on the soil resistivity.

This thesis shows, with the standardized example in chapter 4.1, which additional parameters have an impact on the PIV in addition to the pipeline coating. The assumption that with increasing coating resistances, the PIV rises as well is confirmed by Figure 4-8.

An additional effect is that the curve progression for lower values of coating resistances is not straight because a part of the induced voltage is already reduced. The induced voltages produce an induced current on the pipeline and as mentioned above, with lower coating resistances the induced current can flow more easily into the surrounding soil.

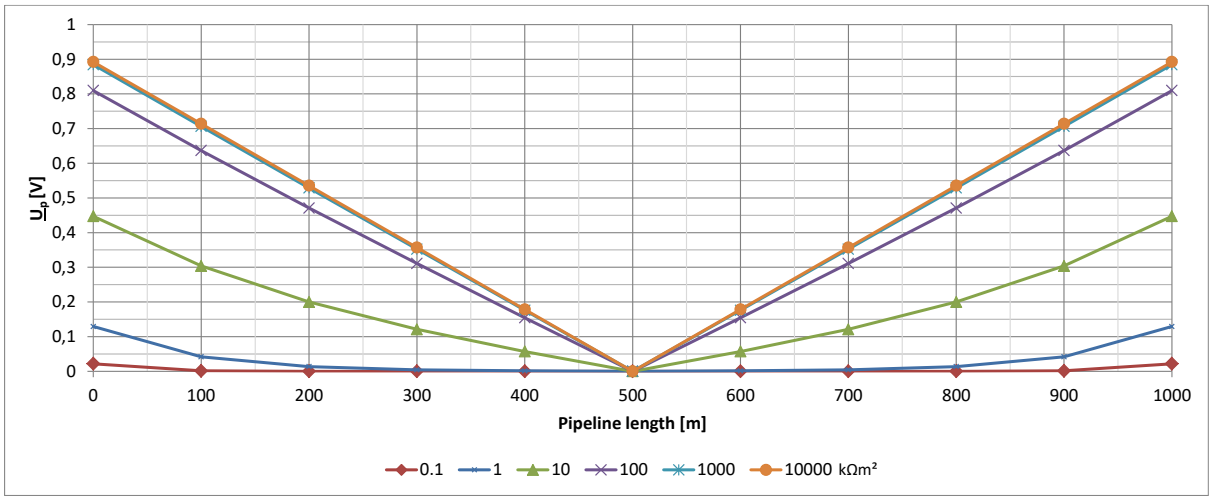

Figure 4-8: PIV along the pipeline with varying coating resistances

The same effect influences the maximum PIV. For higher coating resistances, the induced current is not able to flow into the soil, which is why there is an upper limit for the PIV. When comparing 1000 kΩm² and 10000 kΩm², only a minor visual difference can be observed. It is close to around 1 %. The specific resistance value of 100 kΩm² differs by about 10 % compared to the upper limit. This indicates a slower increase of the maximum PIV for higher specific coating resistances.

This effect can be seen in Figure 4-9, where the maximum PIV $\underline{PIV_{max}}$ is displayed for a range of 0.1 to 10000 kΩm² for the coating resistance. Irrespective of the pipeline diameter and the frequency from the interfering system, an upper limit is always reached and it is assumed that a lower limit exists around zero. Inadequate and old pipeline coatings have values around 10 kΩm² which can lead to a significant difference in the PIV compared to better coatings. In the standardized example (1000 mm, 50 Hz), $\underline{PIV_{max}}$ reaches only half the PIV for 10 kΩm² when compared to a value of 1000 kΩm².

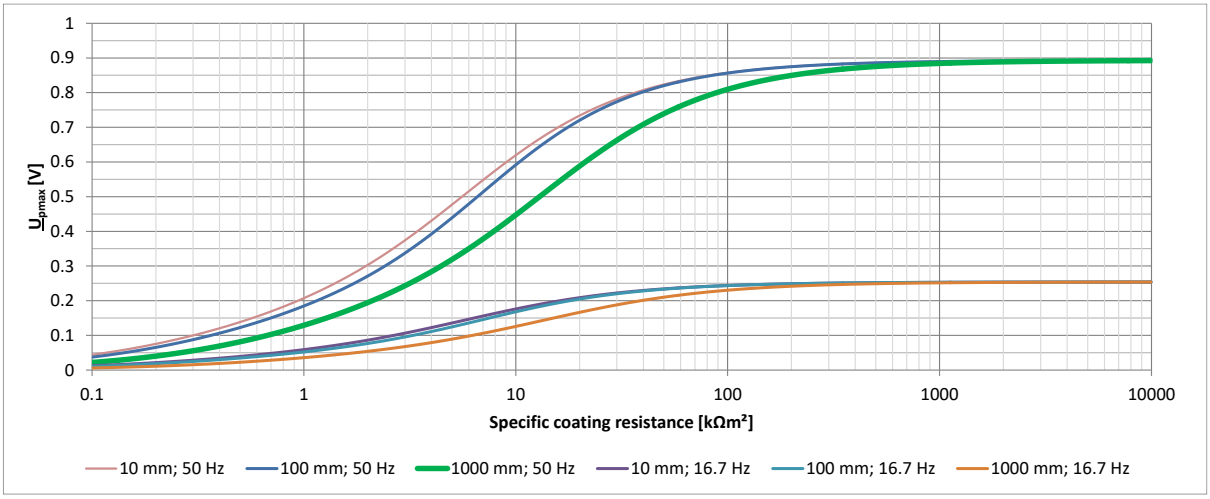

Figure 4-9: Maximum PIV for different pipeline diameters and influencing frequencies for a wide range of SPCR

The conductor diameter has an effect on the range of around 1 to 100 kΩm² which is especially relevant in the case of poorly coated cables or pipelines. When comparing the values for 10 kΩm², the difference between the diameters of 10 mm and 1000 mm is 0.17 V. Therefore, the values for 10 mm are 38 % higher than for 1000 mm. This leads to a first conclusion: metal structures have mostly small diameters and thus, the conductor diameter can be neglected. In the case of pipelines however, the diameter is can vary widely and therefore, the diameter has to be considered carefully.

A second conclusion is that the coating resistance shows an unexpected behaviour which can be explained with the physical effects. It can be stated that pipelines with a poor coating have a much lower maximum PIV and therefore, they are partially earthed. This conclusion leads back to the initial statement of the chapter: ascertaining the correct value for the coating including coating holidays is essential.

Figure 4-9 also shows the impact of the frequency. This is a theoretical scenario since 16.7 Hz will never appear in the pylon configuration of the standardized example. It shows similar effects compared to calculations with 50 Hz but on a much lower level. This difference can be returned to the longitudinal impedances because they are frequency-dependent. Still, this figure shows an impact of the coating resistance similar to a scenario with 50 Hz. Therefore, the argument for 50 Hz is valid for 16.7 Hz.

4.4 Specific soil resistivity

The specific soil resistivity is another important parameter for pipeline interference voltage (PIV) calculations. The surrounding soil is relevant to the maximum PIV because with a higher value for the soil resistivity, the induced current cannot flow into the soil. It is the same effect as described for the SPCR. The exact determination of the value of the soil resistivity is absolutely crucial when countermeasures against too high voltages are needed and earthing systems are put in place.

Earthing systems are defined locations, where the induced currents can flow into the soil and thereby reduce the PIV along a pipeline. As has been described and calculated in [6], a good conductivity for an efficient earthing system is needed. The conductivity depends on the type of earthing system in place, the quantity of material which is used and the surrounding soil. The calculation as well as the different types can be found in [23] and [42]. It can be seen in the formulas that the soil resistivity is the most dominant factor. The soil resistivity depends on the type of soil (see Table 4-2) as well as the soil humidity [43], [44].

Type of soil	range of variation of the specific soil resistivity [Ωm]	typical value of the specific soil resistivity [Ωm]
marsh	5 to 40	30
garden soil (clay, brickearth, humus)	20 to 200	100
sand (moist)	200 to 2500	400
weathered rock	500 to 1000	750
sand (arid)	200 to 2500	1000
granite, granite	2000 to 3000	2500
rock	2000 to 30,000	10,000

Table 4-2: Resistivity values for different types of soils [43]

According to Table 4-2, a wide range of soil resistivities is possible and the determination of the correct soil resistivity is a complex matter. Possible measuring techniques are described in [33] and are expensive when conducted in a number of locations.

The pipeline interference voltage depends on the value of the soil resistivity as shown in Figure 4-10. Again, the standardized example is used for the calculations. The soil resistivity varies from 1 to 10,000 Ωm. Also, specific pipeline diameters are used (10-100-1000 mm).

Figure 4-10 leads to the conclusion that the pipeline diameter is independent from the soil resistivity but is frequency selective. Figure 4-10 also shows that the PIV rises constantly with rising values of the soil resistivity which is consistent with the results in [30] where a specific example with specific soil resistivities was presented and the calculated results show a constant increase.

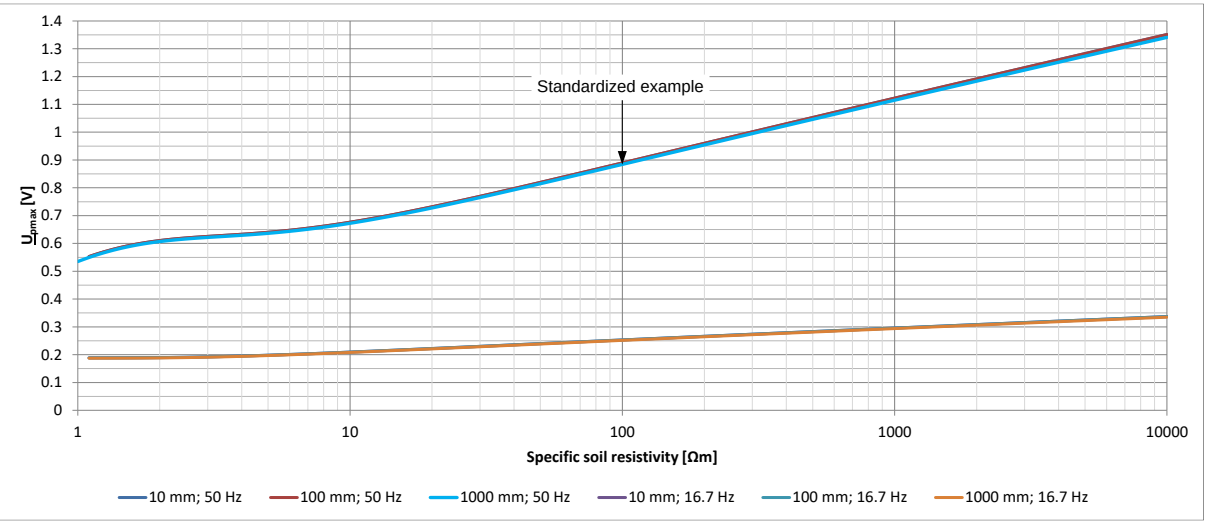

Figure 4-10: Maximum PIV for different pipeline diameters and influencing frequencies for a wide range of soil resistivities (50 Hz and 16.7 Hz)

In comparison to the standardized example, here the PIV can vary between +/- 50 % for a frequency of 50 Hz. According to Table 4-2, the soil resistivity shows values mostly between 30 and 2.000 Ωm. Conducted measurements in the field, however, often give values between 50 and 300 Ωm. By considering these real values, the range of the PIVs gets smaller; however, it still has an impact on the calculated results. Figure 4-10 shows that under the same conditions, the railroad-frequency of 16.7 Hz is low but still shows a constantly rising PIV.

[30] on page 10 also compared the values of the soil resistivity with the SPCR. The outcome is that with rising soil resistivity and rising SPCR, the maximum PIV rises with limits for low and high coating values.

Figure 4-11 shows something similar with different curve progressions for specific coating resistances. It can be clearly seen that the PIV rises when both parameters are increasing. The upper limit for high coating values is reached and shows the same curve for 1000 kΩm² and 10000 kΩm². When the pipeline coating is poor, the maximum PIV rises up to a certain level where it remains almost steady. Figure 4-11 gives the same conclusion as the curve progressions in [30] and therefore, both results have been confirmed by different calculation methods (chapter 2.5 versus chapter 3.3).

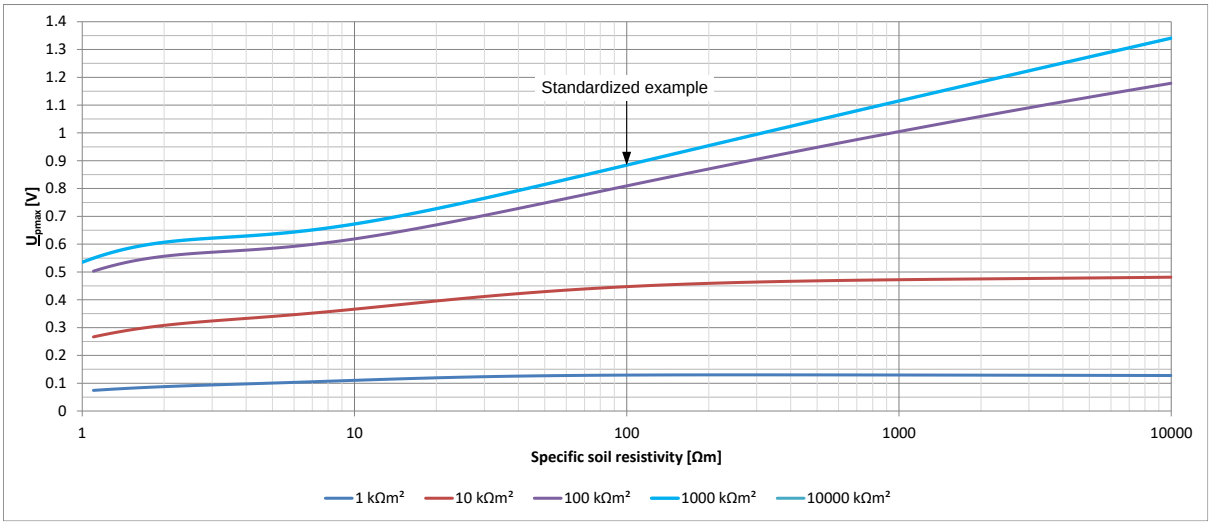

Figure 4-11: Maximum PIV for the relationship between SPCR and soil resistivity

4.5 Load currents

When using the general formula (2-2) to calculate the PIV, the current of the interfering systems is a direct proportionality factor. To calculate the worst-case scenarios for touch voltages, it is common practice to use the maximum operational currents or, depending on the type of influencing system, 60 to 95 % of this maximum load current to calculate the risk of AC corrosion [45].

Due to load safety or reliability reasons such as the commonly agreed (n-1)-criteria which prevent overhead line (OHL) overload situations in case of a failure of other coupled systems [45], or just due to the load flow situations, these maximum operational currents rarely occur. Typically, load currents are much lower than the maximum operational currents which simply reduce the PIVs. A comparison between both currents is shown for an OHL in Figure 4-12 and for railroads in Figure 4-13 [31]. The curve progressions are quite different because changes in the current flow situation in the OHL occur much slower and usually show a weekday/weekend as well as a day/night rhythm. On railway lines the current flows when power cars are moving. There, currents are not only time-dependent, they are also position-dependent due to the movement of the power car as well as e.g.

the type of energy supply and the position of other power cars. Figure 4-13 also shows that the currents have shape gradients which can be explained by the need for high currents for acceleration.

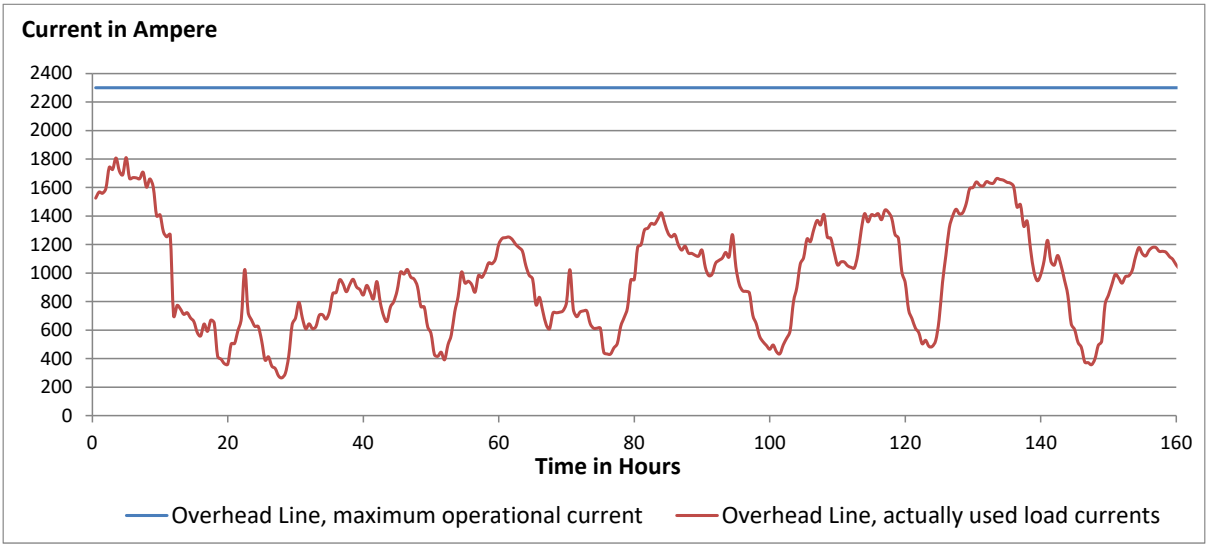

Figure 4-12: Maximum operational currents versus load currents for an 380-kV-OHL [31]

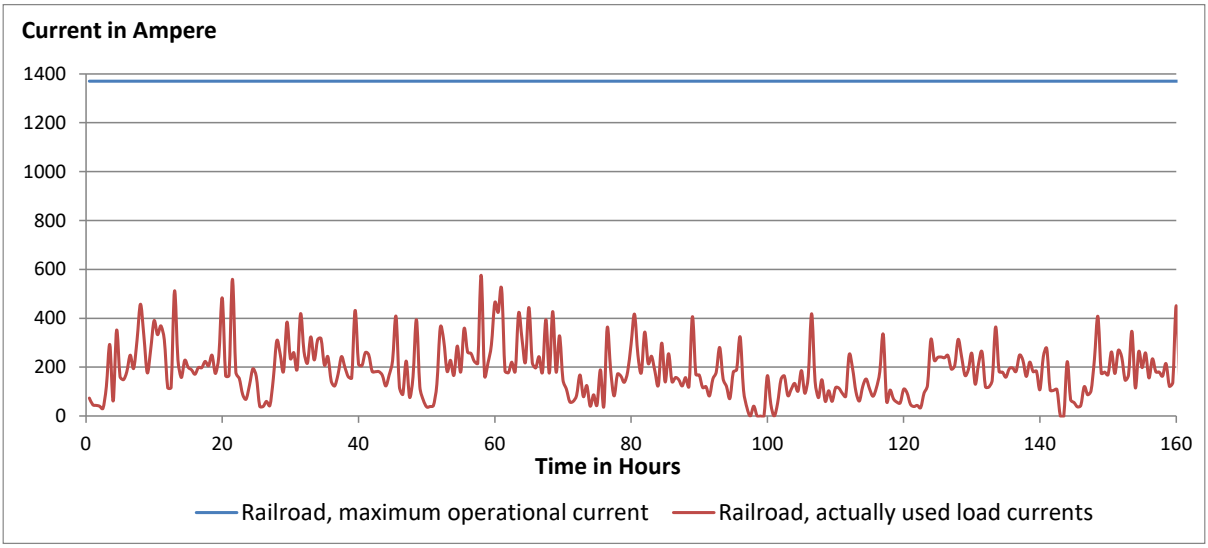

Figure 4-13: Maximum operational currents versus load currents for a 15-kV-railroad [31]

Furthermore, pipelines and other metallic structures are often interfered by several interfering systems with different maximum operational currents. The current can flow in both directions. In which direction depends on either on the OHL load flow situation or on the position of the power cars on the railroad tracks. The necessary data has to be provided by the system operators, which may cause further difficulties: While data about bygone load currents is provided, often no additional information about the current directions is added for confidentiality reasons.

Therefore, cases are challenging where multiple influences by different interfering systems occur, since they hold different load currents at the same time. Figure 4-14 illustrates such a situation with multiple influences, where two OHLs have different load currents due to their national importance and because of two railroad lines with a different workload.

Based on this figure, a correlation with conducted measurements is possible. However, it is difficult due to the time-dependent load currents without any knowledge about their direction as well as the different weighting of the systems due to different mutual impedances and system characteristics.

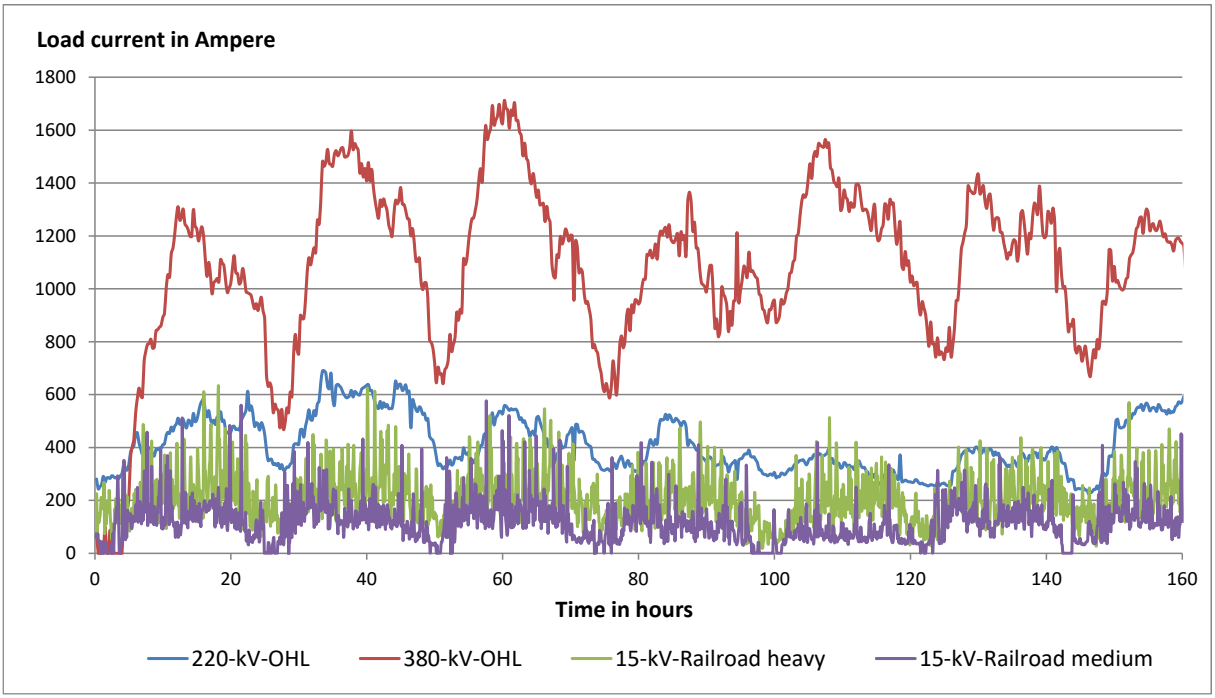

Figure 4-14: Different load currents for selected OHLs and railroads

4.6 Pylon type and conductor configuration of overhead lines

The pylon type and the conductor configuration (CC) as parameters for overhead lines (OHLs) have a strong effect on each other and cannot be considered separately. The influence on the pipeline interference voltages (PIVs) from different CCs as well as two types of pylons has already been explored in [46], with a set distance between pipeline and OHL. The conclusion was that the CC has considerable influence on the PIV and has to be considered in any case. Also, the pylon type has a less significant impact on the PIV.

[46] analysed the difference between one and two earthing conductors (ECs) with the outcome, that two ECs induce higher interference voltages into the pipeline. A different investigation was described in [41] with magnetic fields, magnetic flux and magnetic flux density. It examined the different parameters and showed that especially the CCs have a strong impact on the magnetic field.

No further research was conducted, however, on the consequences of interfering voltages on metallic structures. This chapter combines both approaches and analyses the effect of both parameters in different cases with the new mathematical model while varying the distance between pipeline and OHL.

4.6.1 Overhead line pylon type

The OHL pylon type is determined by the number of circuits, the voltage level, the minimum height and other surrounding factors. The minimum height is defined as the lowest conductor above earth including the maximum sag. It ranges from about 8 m for 110 kV lines to 12 m for 380 kV lines. These minimum heights are the ones predominantly used for comparing the different pylons.

Figure 4-15 a) shows the difference between the minimum height (1), the sag (2) and the mounted height of the conductor on the pylon (3).

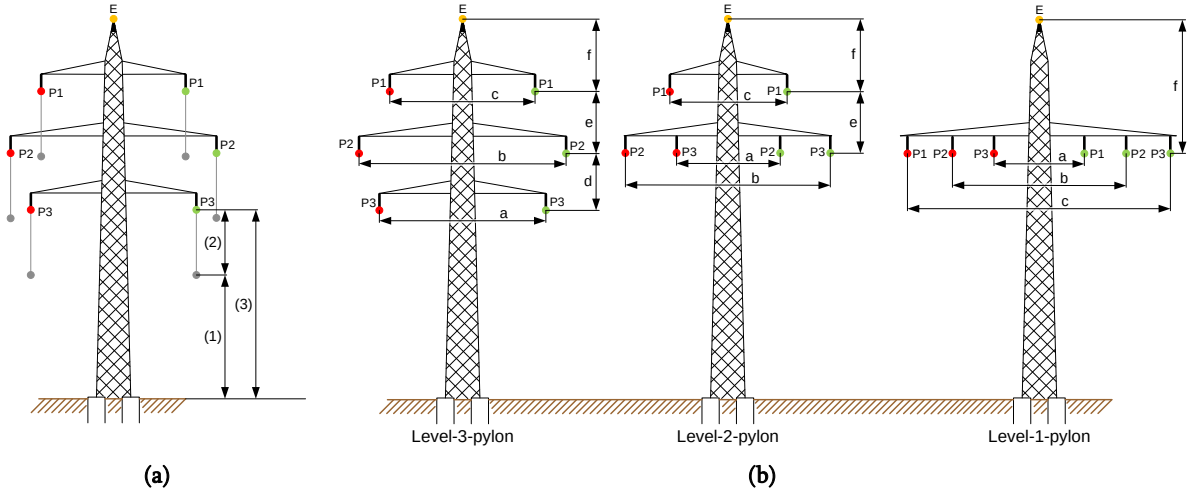

Figure 4-15: a) Definitions for the different heights between ground and conductors for an OHL pylon; b) Three pylon type examples for double circuit lines [[41], modified]

Pylons are categorised by conductor position. The conductor position depends on the number of phase conductor levels on the pylon, the voltage level of 110 kV, 220 kV and 380 kV and the number of circuits as well as the ECs. Figure 4-15 b) shows three examples of pylons and the corresponding values for the minimum and maximum distances in meter between conductors for different voltage levels, which can be found in Table 4-3. It should be noted that many more configurations of pylons types exist. Further information can be found in [41], page 51 to 55. The conductor positions on the pylons in Figure 4-15 and Figure 4-16 are referred to as P1, P2 and P3 and do not display the CC. Associated conductor positions are highlighted with the same colour. It is necessary for complex pylons with many circuits, to understand which conductor position belongs to each circuit.

voltage level		110 kV			220 kV		380 kV	
tower type (see Figure 4-15 b)		level-3	level-2	level-1	level-3	level-2	level-3	level-2
a	min	6.4 m	5.2 m	5.7 m	11.0 m	10.0 m	13.8 m	14.0 m
	max	8.4 m	6.8 m	6.4 m	12.0 m	14.8 m	19.0 m	15.2 m
b	min	6.4 m	12.4 m	12.9 m	14.0 m	20.4 m	18.8 m	25.4 m
	max	11.2 m	14.4 m	14.6 m	16.0 m	25.4 m	24.0 m	27.2 m
c	min	4.4 m	8.8 m	20.0 m	10.0 m	15.4 m	12.8 m	14.0 m
	max	6.6 m	10.4 m	23.0 m	11.0 m	20.1 m	15.0 m	19.8 m
d	min	3.2 m	0.0 m	0.0 m	6.1 m	0.0 m	7.2 m	0.0 m
	max	6.5 m	0.0 m	0.0 m	7.0 m	0.0 m	9.5 m	0.0 m
e	min	3.2 m	4.0 m	0.0 m	6.7 m	6.5 m	8.5 m	9.0 m
	max	6.5 m	4.3 m	0.0 m	7.0 m	9.5 m	9.6 m	11.5 m
f	min	3.1 m	4.7 m	5.0 m	5.5 m	6.5 m	6.5 m	8.6 m
	max	5.6 m	6.9 m	8.4 m	9.3 m	13.7 m	12.3 m	13.5 m

Table 4-3: Minimum and maximum dimensions for Austrian double circuit lines [41]

All over the world, OHL operators use widely different pylon types and therefore the different impact of OHLs on pipelines can be shown only for a selection of pylon types, which are displayed in Figure 4-16. The selection in this thesis focuses on widely used pylon types in Austria as well as pylons with a completely different phase conductor structure. In Austria, mostly level-3-pylons are used for all three voltage levels and, therefore, the chosen pylon type for the standardized example in chapter 4.1 is the most common type in Austria which is called “ton”.

The pylons in Figure 4-16 are used for different voltage levels in the following chapters and are designated with the abbreviation PY(x). The pylon dimensioning is different for every voltage level and can be found in the pylon description in each sub-chapter. As described before, the “ton”-pylon is predominantly used in Austria and, therefore, this type is used for 110 kV (PY7), 220 kV (PY1) and 380 kV (PY5) -voltage-levels.

This type is also used to show the effect on the pipeline interference voltage (PIV) because of the different pylon dimensions of PY1 and PY7. The “tan”-pylon is only used for 220 kV (PY2), the “quadruple”-pylon only for 380 kV (PY6) and the “danube”-pylon for 110 kV (PY8) and 220 kV (PY3). These types exist in Austria but are not often used. In contrast, the “single-circuit”-pylon is often built for 110 kV (PY10) for weaker OHLs. It represents an asymmetrical pylon due to its design.

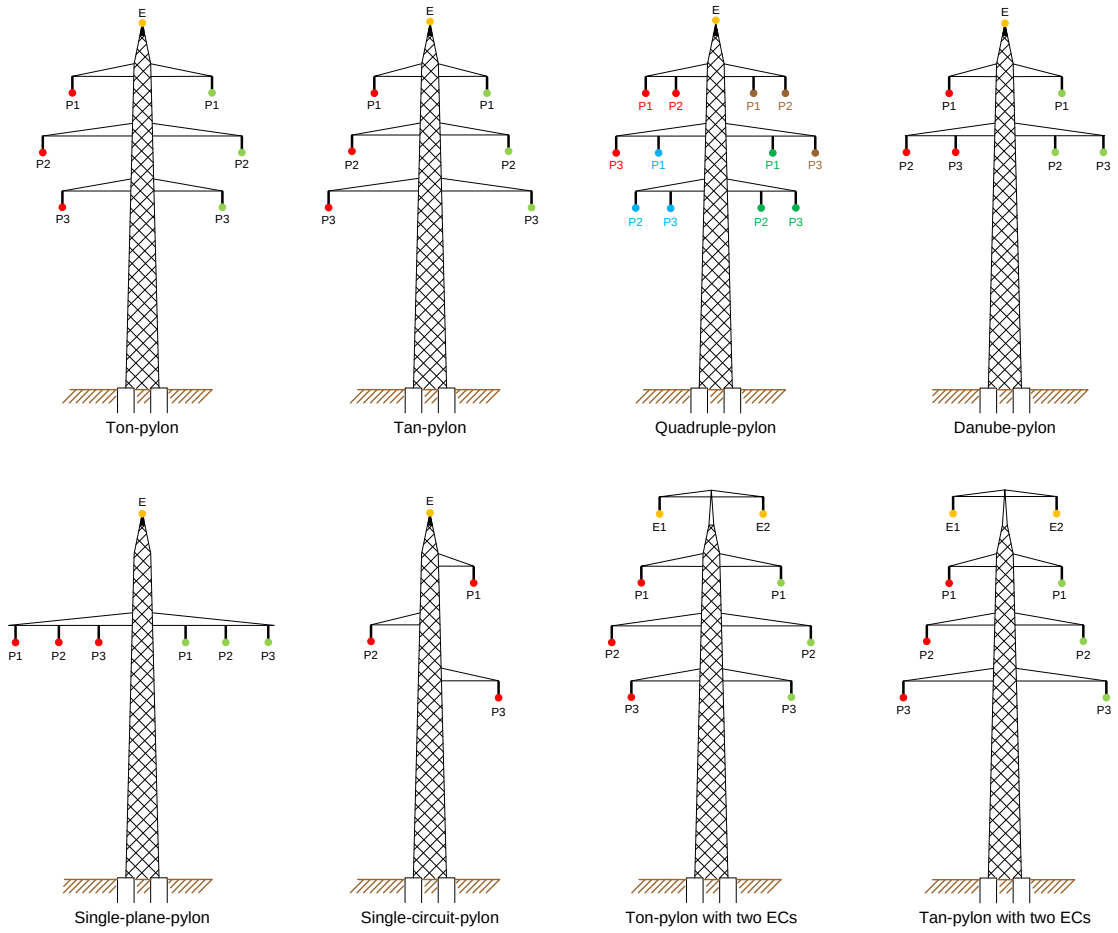

Figure 4-16: Different pylon types for comparing the effect on the PIV

All other types are typically not used within Austria but in other countries and, therefore, they should be part of the comparison between the different pylon types. The “single-plane”-pylon is used for 110 kV (PY9) and 220 kV (PY4). The “ton”-pylon with two earthing conductors (ECs) (PY13) as well as the “tan”-pylon with two ECs (PY14) are used for a 220 kV voltage level and are crucial for comparing the effect of an additional EC. PY15 (“ton”-pylon with no EC) and PY16 (“tan”-pylon with no EC) are not displayed in Figure 4-16 but are shown in chapter 4.7.1, where the influence on the PIV by the number of ECs is analysed.

4.6.2 Conductor configuration

The conductor configuration (CC) is simply the allocation of the electrical phases L1, L2 and L3 to the conductor positions P1, P2 and P3. An optimal CC is necessary to avoid asymmetries in the operational parameters of overhead lines (OHLs). OHLs are divided into nearly equal sections where the phase arrangement is periodically changed. Therefore, the CC has to be carefully taken into account in the vicinity of pipelines or other metallic structures due to its significant impact [41].

Theoretically, six CCs for one circuit and 36 combinations for two circuits are possible. This number rises significantly for more circuits. An overview of two lines with all possible combinations can be seen in Figure 4-17, as has been described in [41] and [47]. In this thesis it is not possible to analyse all different CCs for each pylon type due to the enormous effort necessary for these calculations.

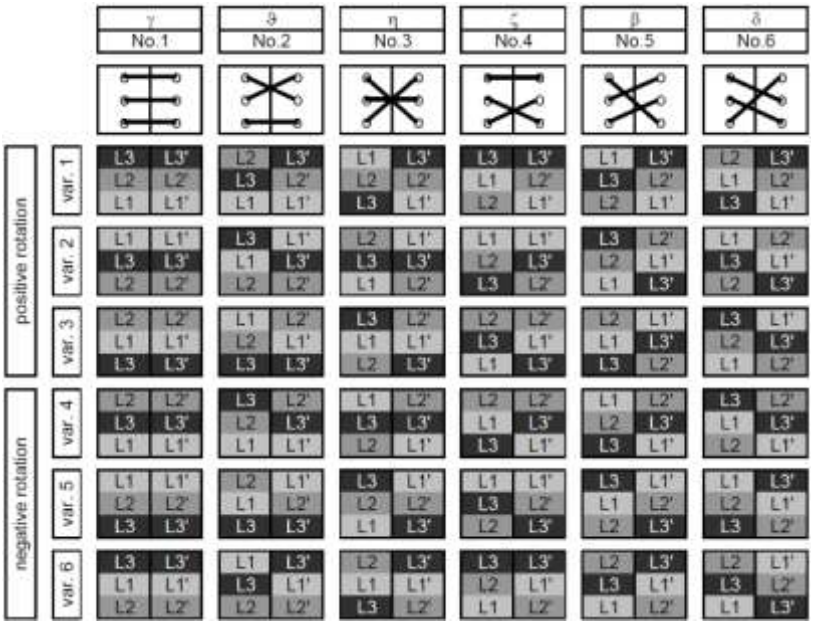

Figure 4-17: All possible CCs for a double circuit line [41]

Especially in [41], a wide range of CCs were calculated to find out, which of them show the most significant effect on the magnetic field. Inductive interference behaves similarly and therefore, chosen CCs from Figure 4-17 have to be taken into account and analysed. The pylon from the standardized example is used to show the difference between the various CCs when calculating pipeline interference voltages.

In Figure 4-18, the results of these calculations show that No.1 is the choice for worst-case-calculations and No. 3 for best-case-calculations. As has been stated in chapter 4.1, the magnetic field can have a positive (var.1) or negative rotation (var.4) and the maximum pipeline interference voltage (PIV) can be lower on one side than on the other side.

This effect can be seen when comparing Figure 4-3 to Figure 4-18. Looking at the conductor configuration (CC) No.3, var.1 from Figure 4-18, the maximum PIV lies around 0.88 V/km, which is equal to the distance of 100 m in Figure 4-3. With a distance of -100 m in Figure 4-3, a maximum PIV of around 0.6 V/km is reached, which can be found in Figure 4-18 as the CC No.3, var.4.

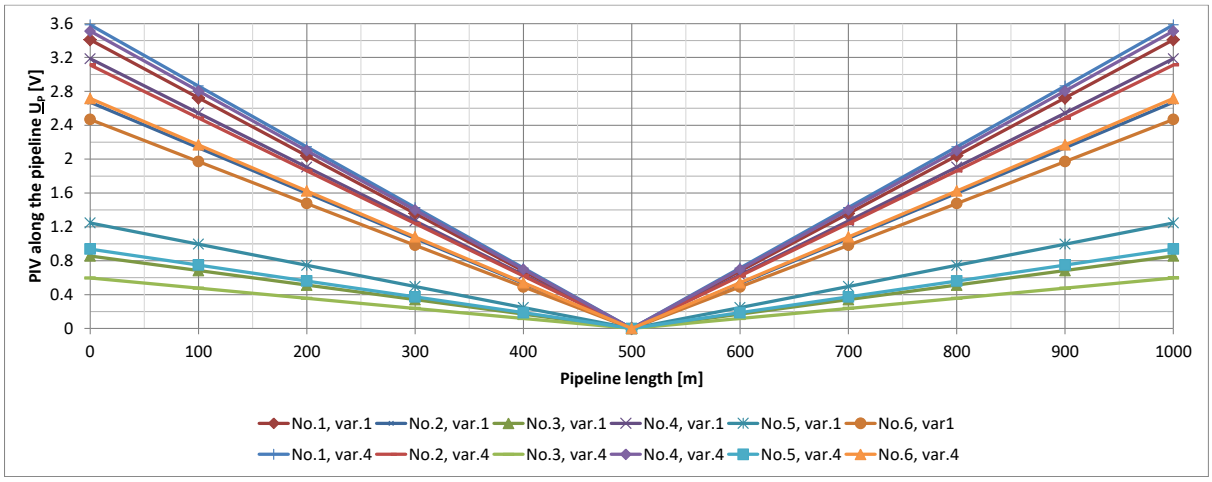

Figure 4-18: PIV along the pipeline by using the standardized example with different CCs

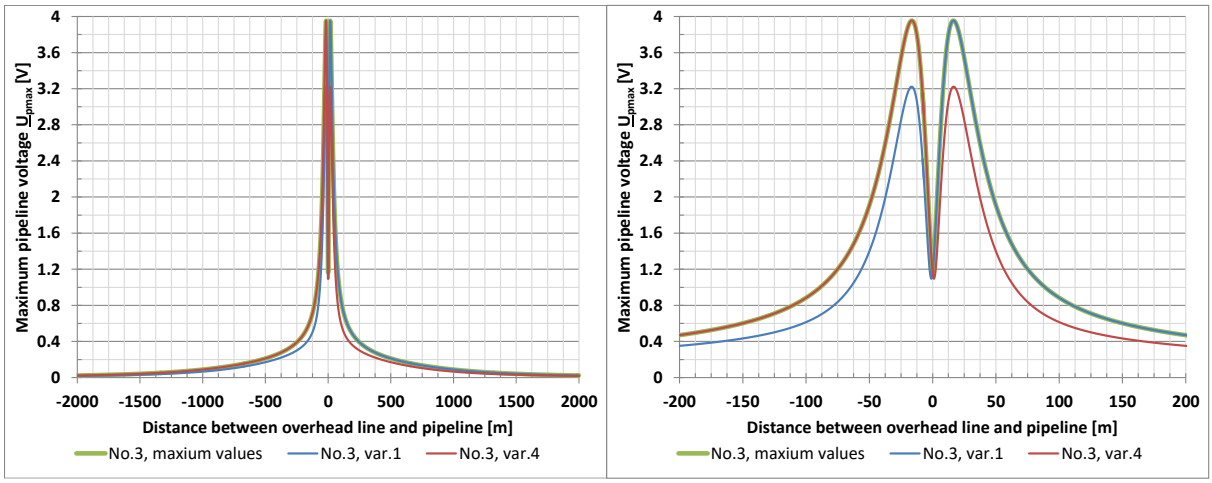

Figure 4-19: Using the maximum PIV from two associated CCs

To compare the different pylons and CCs, the maximum PIV must be used. Consequently, the maximum values from both rotation calculations must be combined. This can be shown in Figure 4-19 for the best case (No.3), where on the left side the distance between pipeline and OHL lies between -2000 and 2000 m and the right side is enlarged. The blue line (No.3, var.1) shows the same line as already displayed in Figure 4-3 and the red line (No.3, var.4) shows mirror-inverted values. The green line combines the maximum value from No.3, var. 1 and 4.

Due to the different pylon types, the best and worst CCs are not always the same. In the following chapter 4.6.3, the best and worst CC for each pylon is determined beforehand and will be described in the respective sub-chapters.

4.6.3 Comparison of different pylons of overhead lines in consideration of the conductor configuration

As has been stated before, considering the conductor configuration (CC) is essential for comparing the different pylon types for overhead lines (OHLs) because of their great impact on pipeline interference voltages (PIVs). The comparability between the different types can be problematic because the different voltage levels influence the dimension of a pylon. Therefore it is difficult to compare the calculated PIV results of the selected pylon types.

4.6.3.1 "Ton" versus "tan" pylon for a voltage level of 220 kV

First, the two most used pylon types in Austria "ton" (PY1) and "tan" (PY2) for a voltage level of 220-k are compared. The dimensions as well as the corresponding CC are shown in Figure 4-20.

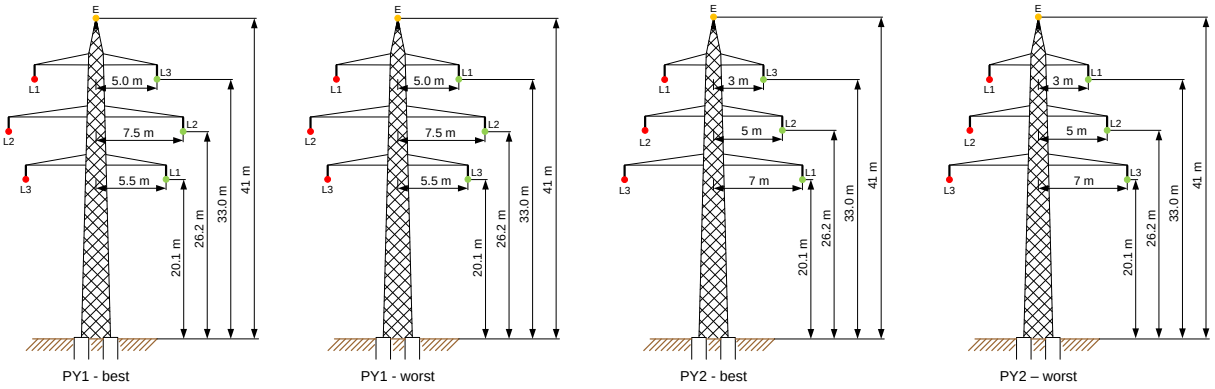

Figure 4-20: Dimensions of pylon types "ton" (PY1) and "tan" (PY2) with the corresponding best and worst CC

How to conduct the comparative calculations for the standardized example has already been described in chapter 4.1. The pipeline is fixed at 0 m and the respective OHL ranges between a vertical distance x_{ik} of plus/minus 2000 m with a total of 4001 steps. For each step, the PIV along the pipeline is calculated and the maximum PIV is recorded and plotted, which leads to Figure 4-21. The examples are theoretical and therefore, the calculations are (mostly) symmetrical between -2000 and 0 m and 0 m and 2000 m respectively. Thus, Figure 4-21 below is split into two curve progressions. The left side shows an overview of the maximum PIV for vertical distances between -2000 m and +250 m, while the right side of the chart shows an interesting section of the calculation steps. In this figure, the enlarged section shows steps between -25 to +200 m which is very useful to

illustrate the fast changes in the curve progression where there is a close proximity of OHL and pipeline.

Figure 4-21 shows almost no difference in pipeline interference voltages (PIVs) between the worst conductor configuration (CC) for PY1 and PY2 (both are designated in the key with "PYx – worst") but, as has been mentioned earlier, they are significantly higher than for the best CC. Much more interesting are the curve progressions for the best CC because a significant difference between both pylon types can be seen. This chart shows that the PIV from PY2 is almost always higher than the PIV from PY1, except for the spot, where the OHL is directly on top of the pipeline (0 m). In the case of the standardized example with a distance of 100 m, PY2 (with a value of 2.43 V/km) shows a nearly three-times higher value than PY1 with 0.88 V/km.

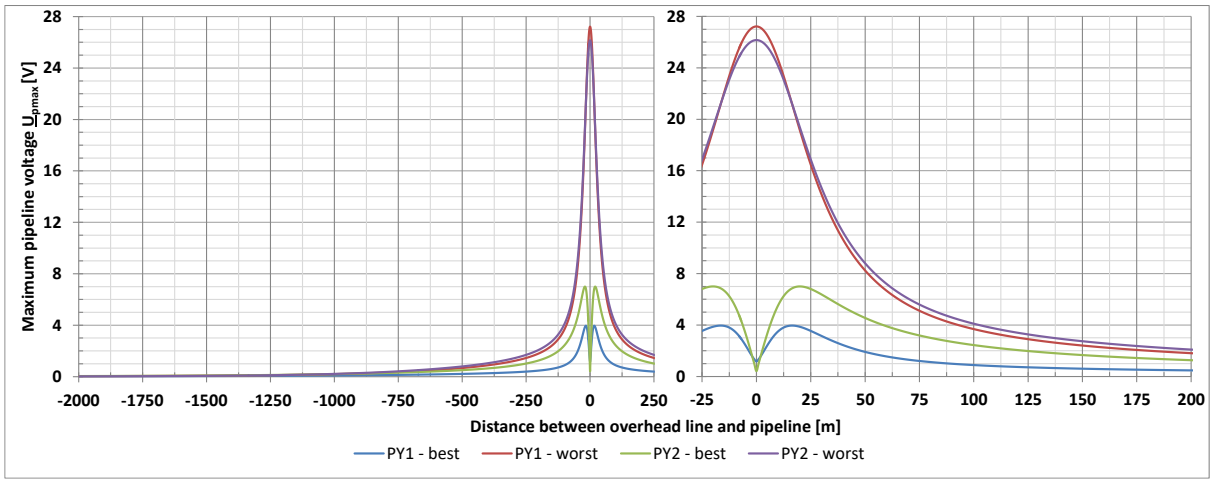

Figure 4-21: Maximum PIV for the pylon PY1 and PY2 with the best and worst CC

The PIV from both pylon types can be compared more easily when PY1 is fixed at a reference value of 1 over the whole distance and the PIV values for PY2 are calculated as the ratio between both pylon types. This is illustrated in Figure 4-22, where it can be clearly seen that the PIV from PY2 is almost always two times higher than from PY1, with a maximum of around 2.8 times at a distance of around 125 m. This leads to the conclusion that, for the two most common pylon types in Austria, in case of pipeline interference, the "ton"-pylon is recommended.

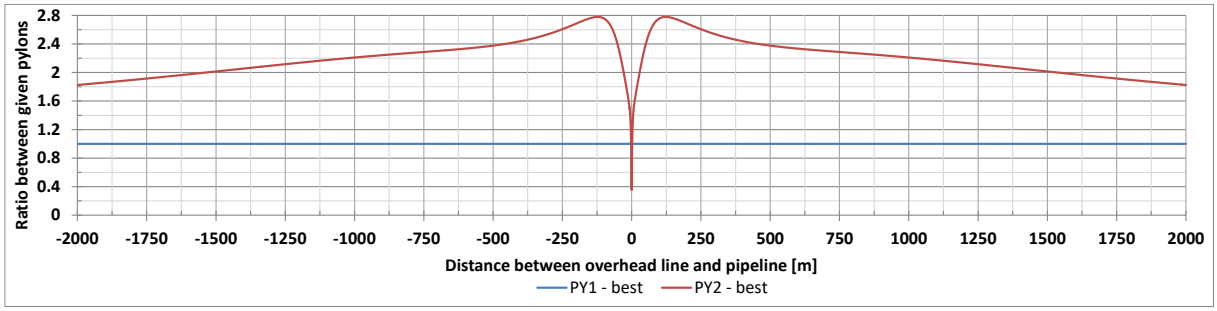

Figure 4-22: Ratio between PY1 and PY2 for the best CC; Ratio is related to the PIV values of PY1

4.6.3.2 Several pylon types for a voltage level of 220 kV

As has been stated in chapter 4.6.1, not only the most common pylons are included in this analysis, also unusual pylons are considered to find out which one has the best characteristics for pipeline interference and produces low pipeline interference voltages (PIVs). Figure 4-23 shows different kinds of pylon types, which have been explained above. Again, for each pylon type, the best and worst conductor configuration (CC) is identified and can be read out from the figure below.

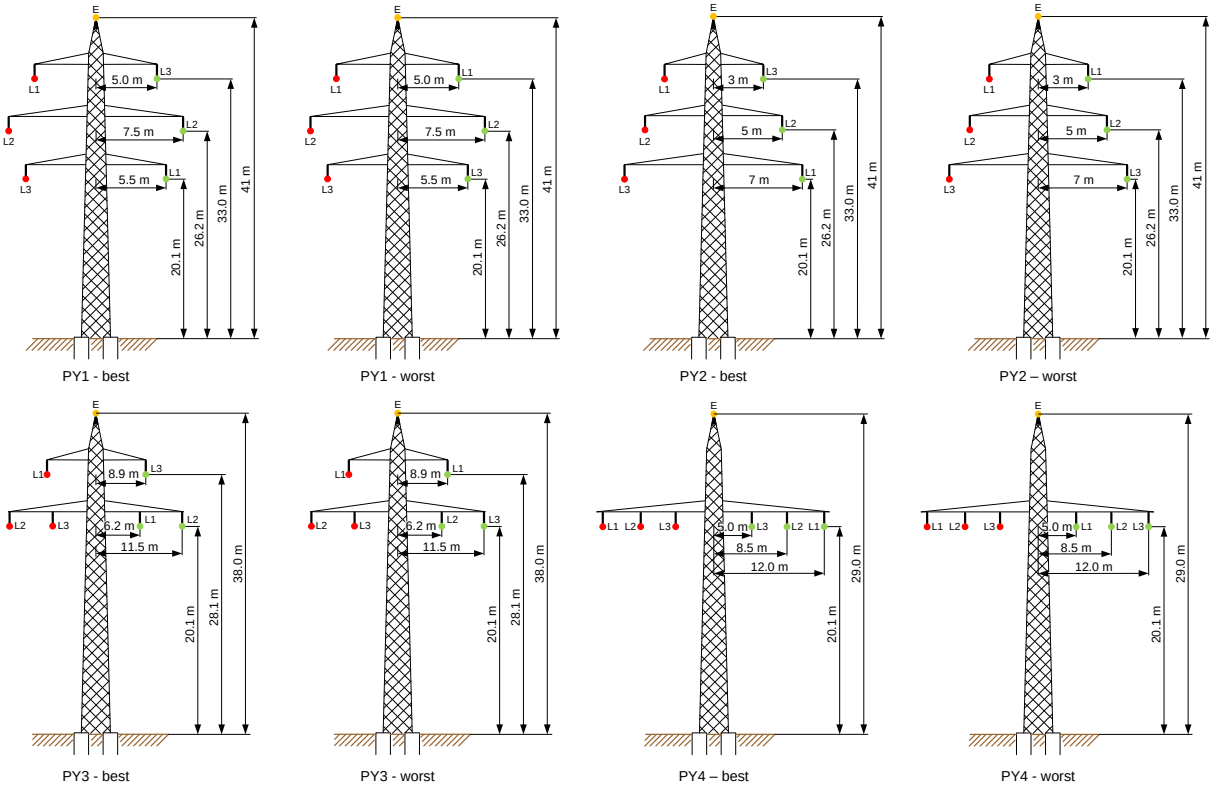

Figure 4-23: Dimensions of pylon types "ton" (PY1), "tan" (PY2), "Danube" (PY3) and "single-plane" (PY4) with the corresponding best and worst CC

Chapter 4.6.3.1 describes in detail, how the following figures in this chapter can be interpreted and, therefore, this chapter focuses solely on the results. The curve progressions for the worst CCs in Figure 4-24 show interesting results because the values for PY3 and PY4 are very different than the results from PY1 and PY2, especially in close proximity to the pipeline. Also, the worst CC for PY4 shows a PIV which is not much higher than for the other pylons for the best CC and not much higher than for the best CC for the same pylon. This means that for PY4, the CC is not very relevant. PY3 lies between PY1 and PY4 and is advantageous when compact pylon dimensions are needed. All pylons with the worst CC show results which are quite close together for distances over 100 m. When comparing the data for the best CC, PY1 is almost always the best choice, especially for distances with high influence (0 to 200 m). A closer look at the right side of Figure 4-24 shows that PY1 is outperformed by PY4 on close approach (5 to 45 m).

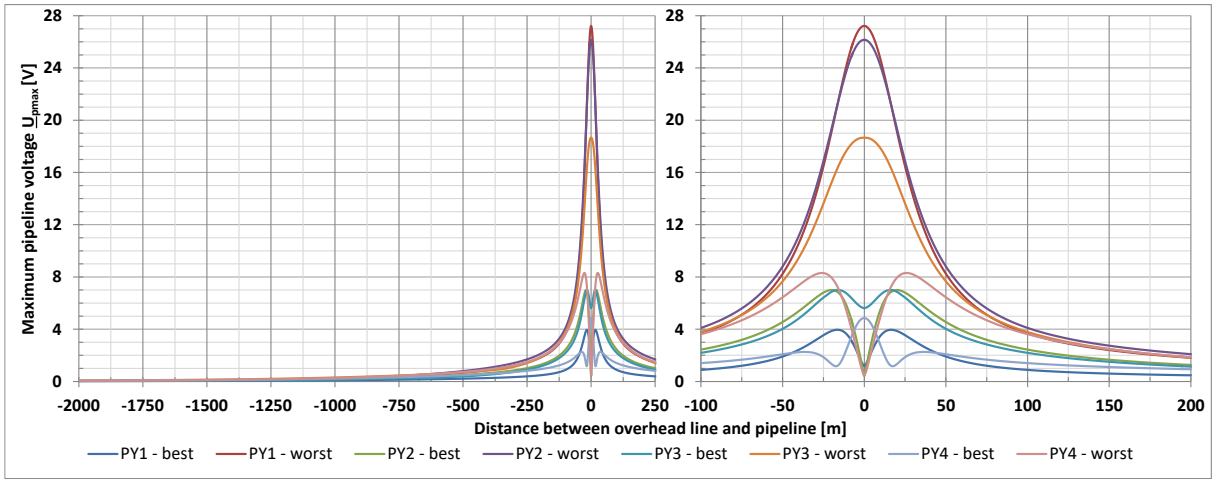

Figure 4-24: Maximum PIV for the pylons PY1, PY2, PY3 and PY4 with the best and worst CC

The very good performance of PY1 over the whole distance can be best seen by the ratio in Figure 4-25. The ratio of PY1 is again fixed to 1 and all other pylons are compared to this type of pylon. The ratio often shows higher values than for the other pylon types. This leads to the conclusion that in case of pipeline interference, PY1 should be used. Surprisingly, PY3 shows also an overall good performance with relatively low PIVs.

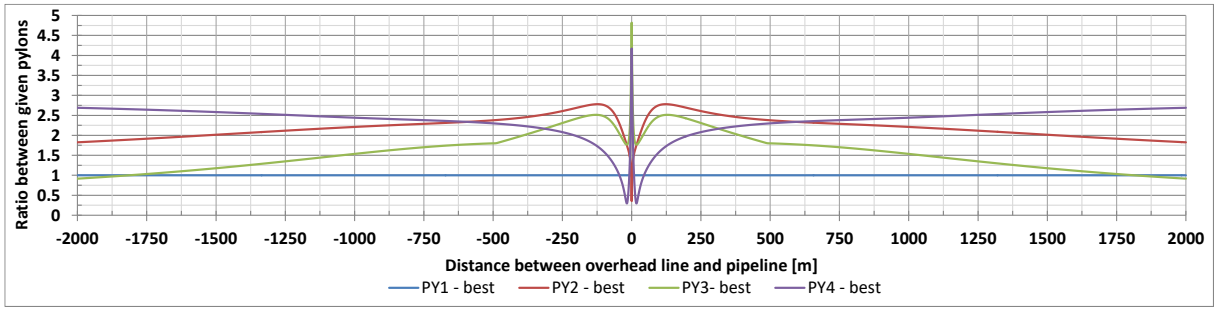

Figure 4-25: Ratio between PY1, PY2, PY3 and PY4 for the best CC; Ratio is related to the PIV values of PY1

In this figure, PY4 shows another interesting effect: The ratio has a kink at a distance of almost 500 meters which stems from always using the maximum PIV, as shown in chapter 4.6.2 with Figure 4-19. This means that for a close approach of pipeline and overhead line (OHL), on the right side of the graph, for distances between zero and 2000 m, the conductor configuration (CC) on the right-hand side has higher values than the same but mirror-inverted left CC. For distances over around 500 m, the opposite is the case and the left CC has higher values than the right CC. For the left side of the graph, for distances between zero and -2000 m, exactly the same happens but right and left CCs are reversed. This shows that the influence of CCs is a complex issue and must be determined in a precise manner.

4.6.3.3 “Ton” versus four quadruple circuit pylon for a voltage level of 380 kV

It is generally assumed that overhead lines (OHLs) with multiple circuit lines have a stronger electromagnetic field with a higher inductive coupling which should lead to higher pipeline interference voltages (PIVs). This chapter shows that this assumption is not always true. Figure 4-26 shows the pylons PY5 and PY6 to compare the maximum PIVs at a voltage level of 380 kV.

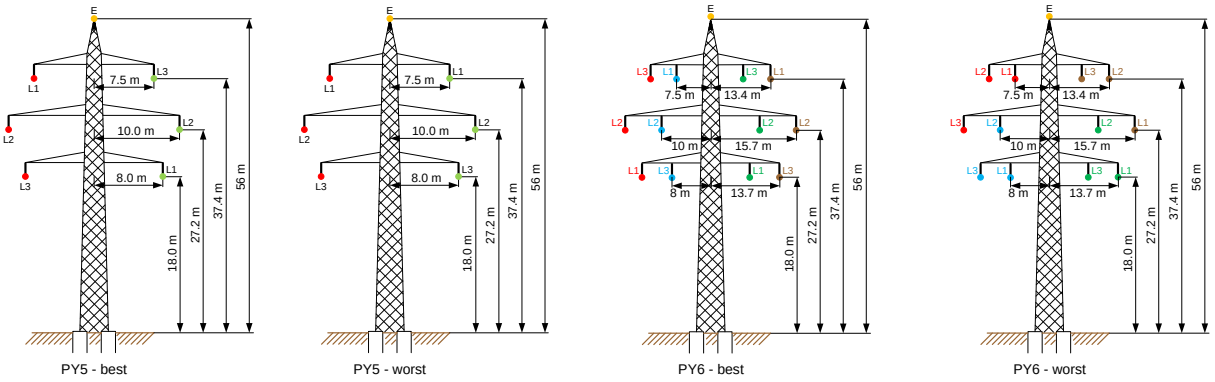

Figure 4-26: Dimensions of pylon types "ton" (PY5) and "quadruple" (PY6) with the corresponding best and worst CC

Chapter 4.6.3.1 describes in detail, how the figures in this chapter can be read out and therefore, this chapter focuses on the results. Figure 4-27 shows interesting results because the assumption that a “heavy” OHL leads to higher PIVs is only valid for the worst conductor configuration (CC). The worst CC also shows that when the pipeline is directly underneath the OHL, even a “heavy” OHL can produce a lower PIV. On the other hand, the best CC for double and quadruple circuit OHLs shows, they can induce similar voltages into a pipeline and lead to similar PIVs. This result is only valid because for both OHLs, the same phase conductor current of 1000 A is used. In reality, however, "heavy" OHLs have higher maximum currents and load currents, which results in a higher PIV, than OHLs with voltage levels of 110 kV or 220 kV.

On close approach with high induced voltages, PY6 surprisingly shows a lower PIV, which will be explained below.

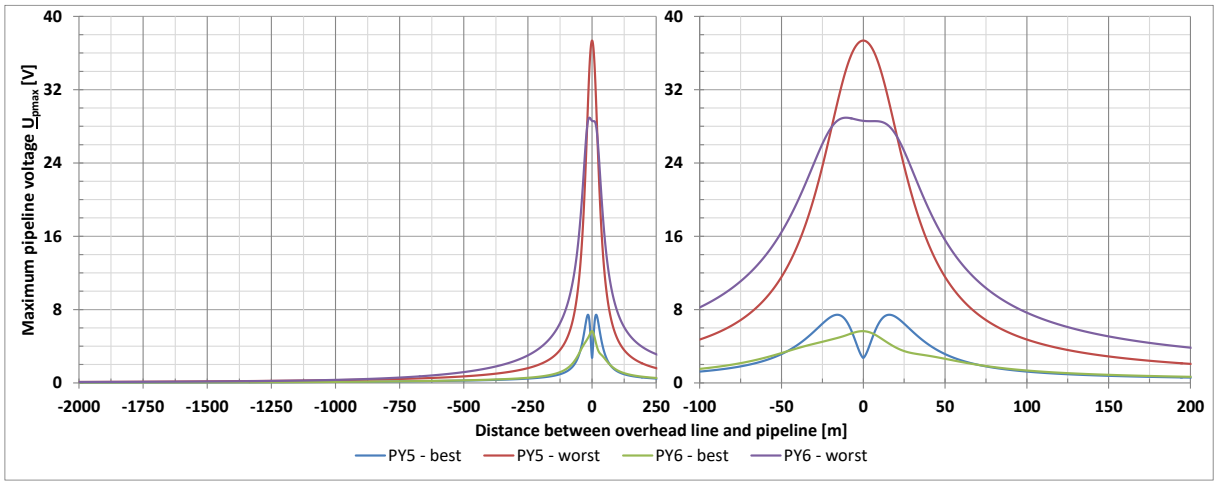

Figure 4-27: Maximum PIV for the pylon PY5 and PY6 with the best and worst CC

Figure 4-28 shows the ratio between PY5 and PY6 for the best CC. The PIV of PY6 lies almost always around 1, which means that both pylons have the same interference on the pipeline. An exception lies in the very close approach, where the induced voltages of PY6 cancel each other out and the earthing conductors (ECs) have a lesser effect on the PIV. Figure 4-27 shows an asymmetrical PIV along the distance between pipeline and OHL for PY6. Finding the symmetrical optimal curve progressions, as described in chapter 4.6.2, is very extensive because for a quadruple circuit OHL, 1296 CCs are possible. This leads to an early conclusion, that finding the optimal solution is extensive, especially in more complicated situations with many other conductors.

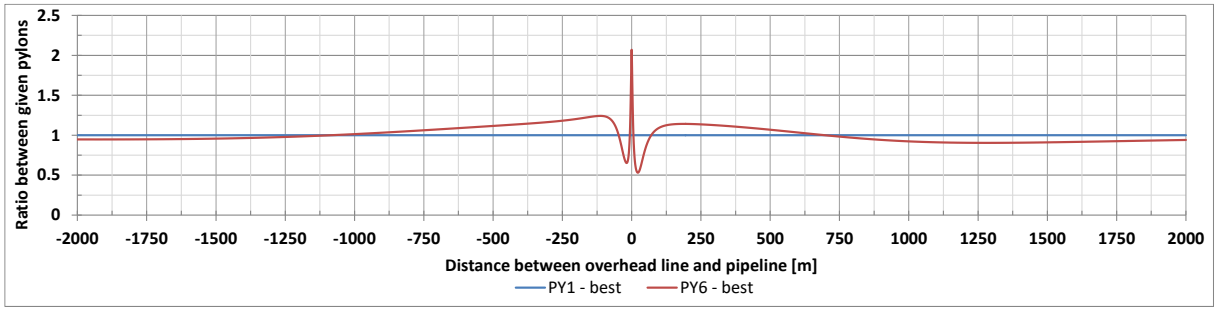

Figure 4-28: Ratio between PY5 and PY6 for the best CC; Ratio is related to the PIV values of PY5

4.6.3.4 "Ton" pylon 220 kV version versus "ton" pylon 110 kV version

In this chapter, PY1 and PY7 are compared because they are of the same pylon type with different dimensions due to different voltage levels. In Figure 4-29, PY1 and PY7 are displayed with their corresponding dimensions.

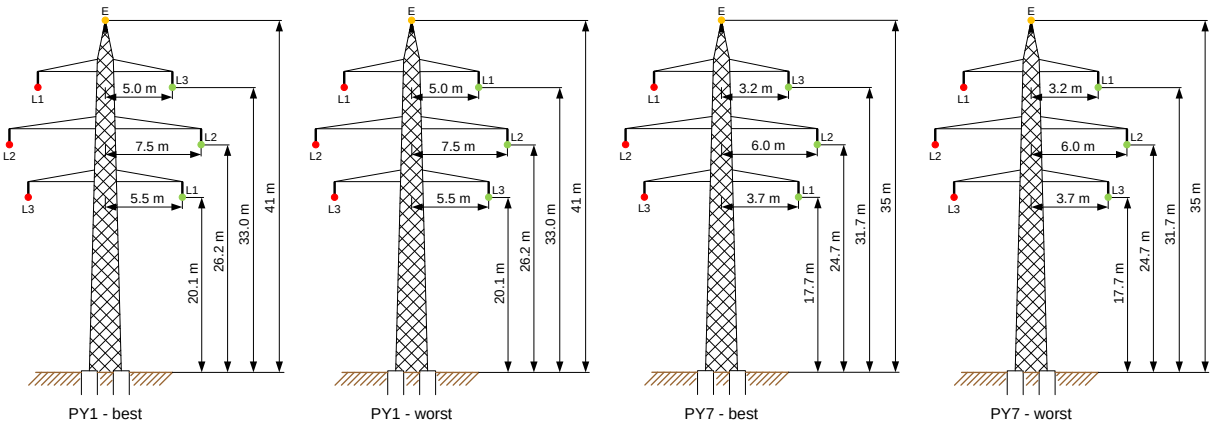

Figure 4-29: Dimensions of pylon types "ton" (PY1, 220 kV) and "ton" (PY7, 110 kV) with the corresponding best and worst CC

Figure 4-30 shows that especially for the worst conductor configuration (CC), the pipeline interference voltage (PIV) differs. This stems mostly from the fact that PY7 is smaller and lower. Two effects appear: One is that the mutual coupling to the earthing conductor (EC) is higher and the phase conductor can induce a higher voltage. The other effect is that the EC lies closer to the pipeline due to lower dimensions which leads to higher PIVs. Again, this result is only valid for equal currents, but in practice, higher currents flow in OHLs with a voltage level of 220 kV and this normally leads to much higher PIVs. For the best CC, the PIV from both pylons shows similar values in Figure 4-30 but, at closer look, Figure 4-31 shows significant differences.

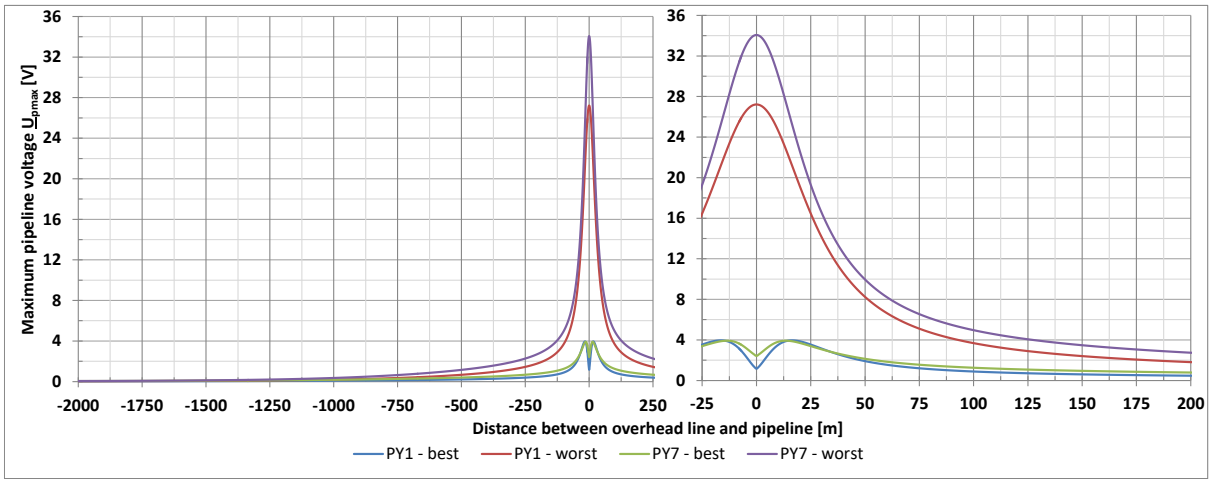

Figure 4-30: Maximum for the pylon PY1 and PY7 with the best and worst CC PIV

When comparing the values as a ratio between PY1 and PY7 in Figure 4-31, the PIV of PY7 doubles for distances greater than 1000 m. For closer distances, the difference decreases slowly and in the case of a close approach between overhead line (OHL) and pipeline, both pylons show comparable results. The difference between PY1 and PY7 for the best CC is caused by the higher current in the EC for PY7, which has a higher impact on greater distances.

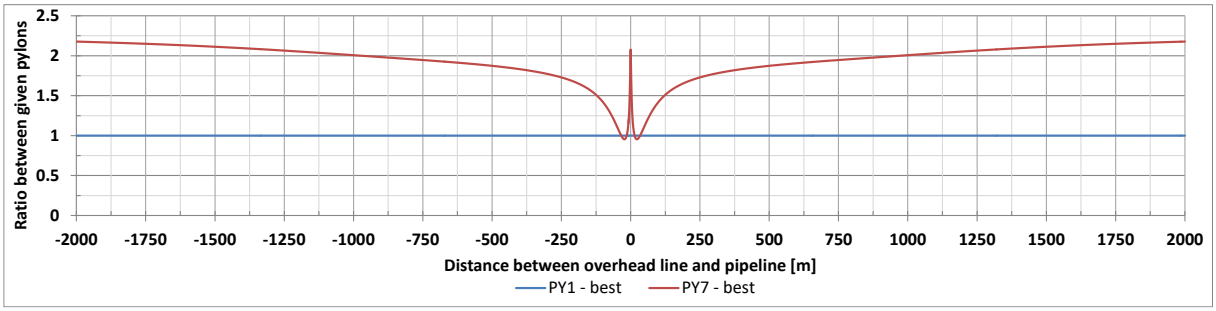

Figure 4-31: Ratio between PY1 and PY7 for the best CC; Ratio is related to the PIV values of PY1

4.6.3.5 Several pylon types for a voltage level of 110 kV

In Austria, for transmission OHLs, the most used voltage level is 110 kV. Therefore, a comparison is crucial between PY7 and PY10, which have the right dimensions. PY3 and PY4 are used for 220 kV lines and with the help of Table 4-3, the dimensions are converted to fit the requirements of the 110 kV voltage level. These pylons are designated PY8 and PY9. The dimensions of the pylons used in this comparison are shown in Figure 4-32.

It can be assumed that the results for the pylons PY7, PY8 and PY9 are similar to the results from chapter 4.6.3.2. This assumption is however only partially correct because the changed dimensions have an effect on the induced voltage of the pylon types.

Comparing Figure 4-24 to Figure 4-33 shows different results: PY7 has already been compared to PY1 and shows higher values for the worst CC. Comparing PY3 (220 kV) with PY8 (110 kV) shows a reduction of 30% of the PIV for PY8. However, PY9 shows an increase of between 20 and 30 % of the maximum PIV, when compared to PY4. This discrepancy is the reason why converting the pylon dimensions to match the regarding voltage level is crucial.

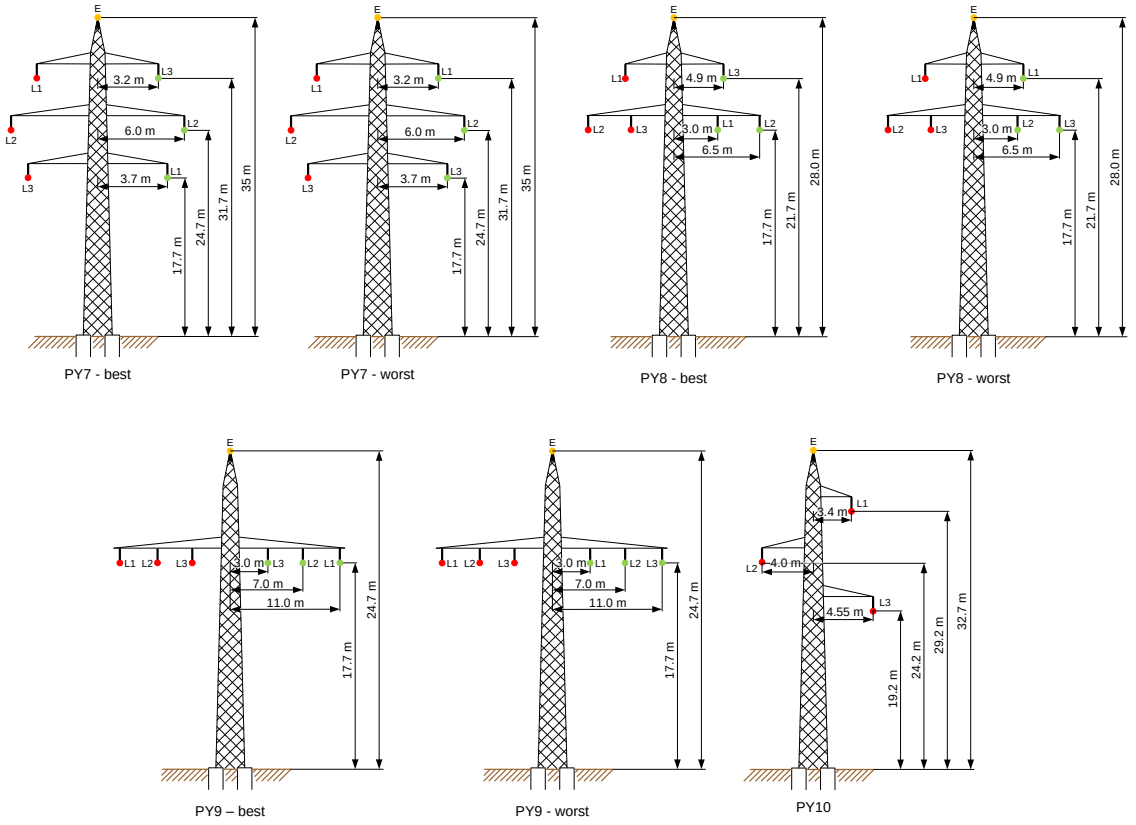

Figure 4-32: Dimensions of pylon types "ton" (PY7), "Danube" (PY8) and "single-plane" (PY9) with the corresponding best and worst CC as well as "single-circuit" (PY10) with the used CC

Comparing the results in Figure 4-33 shows that the "ton"-pylon (PY7) has much higher values for the worst CC, but mostly the best results for the best CC. For the voltage level of 110 kV, PY8 and PY9 have almost always comparable results, especially for the best CC. PY10 is the perfect example for a single circuit overhead line (OHL) and shows that also a "light" system with only a single circuit line has a significant inductive coupling because the CC of the OHL is not symmetrical. Therefore, the curve progression for the PIV in Figure 4-33 is significantly higher than for all other pylon types with the best CC. In the case of the worst CC, it lies in the middle of the observed pylon types.

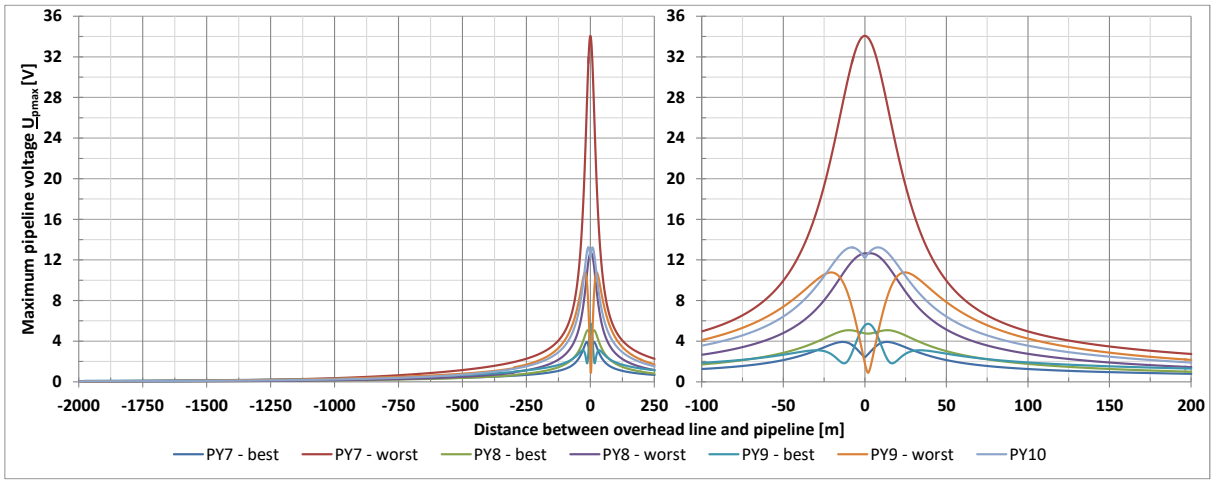

Figure 4-33: Maximum PIV for the pylon PY7, PY8 and PY9 with the best and worst CC as well as PY10 with the used CC

When the ratios between the reference value of PY7 and the other pylons in Figure 4-34 are considered, it can be seen that PY7 has the best values for highly influenced areas between 30 and 500 meters. In the other areas, PY8 and PY9 are the better choices but have their weak points too, e.g. PY8 in the close approach and PY9, which is only the best pylon for a very narrow range. PY10 shows a bad ratio in this chart and should not be used, also in cases with low load currents.

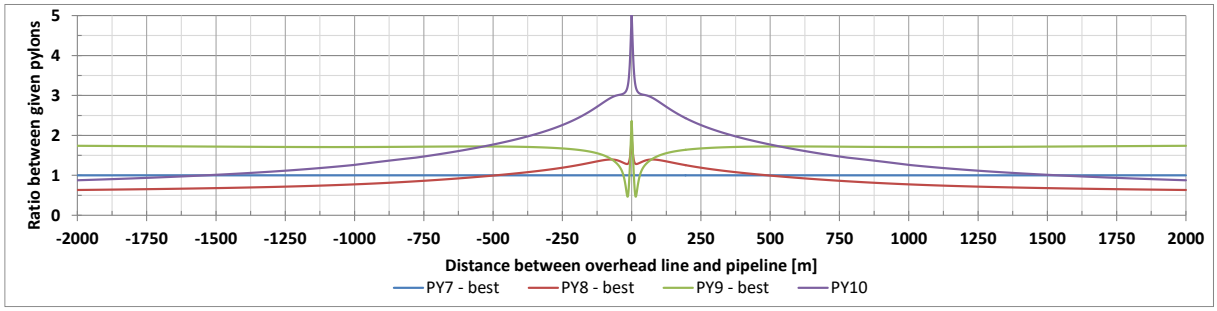

Figure 4-34: Ratio between PY7, PY8 and PY9 for the best CC; PY10 with the used CC; Ratio is related to the PIV values of PY7

4.6.3.6 Conclusion of the pylon comparison

Under the assumption that best practice is always using the best conductor configuration (CC), the following summarized Figure 4-35 can be generated. This chart shows the most relevant range with the highest induced voltage for distances between -200 and +500 meters. In Table 4-4, for selected distances between overhead line (OHL) and pipeline, the maximum pipeline interference voltage (PIV) is listed for all above described pylon types. Generally it can be said that Austria's most used pylon type "ton" is the best choice in almost every case when using the best conductor configuration (CC). This is also shown in Table 4-4, where this pylon type, which has a green background colour, shows an overall good performance.

This chapter described that the number of circuits can be an amplifying factor for the PIV (see PY10) but also showed that with a good CC, "heavy" OHLs (PY6) can have the same influence on the pipeline as OHLs with double circuit lines.

The voltage level is very important for the dimensioning of pylons and has a direct impact on the PIV. This is shown by a direct comparison in Figure 4-35 and Table 4-4, where the same pylon types (in Table 4-4 marked with the same non-white background colour) can have a completely different impact on the results. In some cases, the PIV increases with smaller pylons, in other cases, the PIV is reduced. All of the charts presented can be used to estimate the expected impact of OHLs on the PIV in consideration of the CC, pylon type and the distance between both metallic structures.

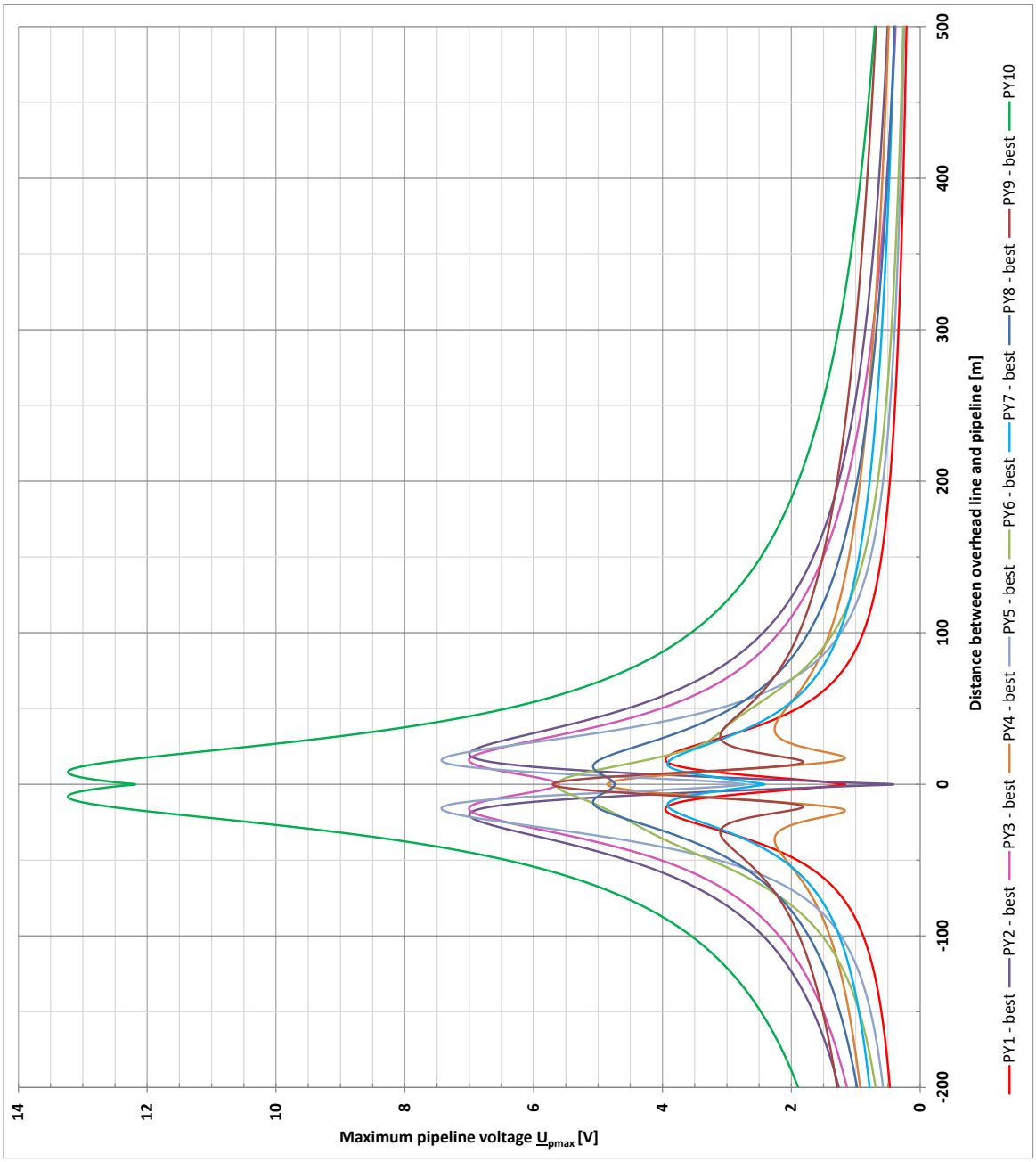

Figure 4-35: Maximum PIV for all above described pylon types with the best CC

		Pylon type									
		PY1	PY2	PY3	PY4	PY5	PY6	PY7	PY8	PY9	PY10
		$\underline{PIV}_{max}$ [V/km]									
Distance x_{ik}	0 m	1.16	**0.41**	5.61	4.86	2.72	5.64	2.42	4.74	5.71	12.19
	100 m	**0.88**	2.43	2.19	1.40	1.23	1.34	1.26	1.73	1.88	3.55
	200 m	**0.47**	1.26	1.14	0.93	0.58	0.65	0.78	0.98	1.29	1.89
	500 m	**0.21**	0.50	0.38	0.49	0.25	0.26	0.40	0.40	0.68	0.70

Table 4-4: Maximum PIV from selected distances for all above described pylon types; bold face indicates the best PIV for the relative distance of 0, 100, 200 and 500 meters; same non-white colour indicates the same pylon type

4.7 Influence of the earthing conductor of overhead lines

4.7.1 Number of earthing conductors

The number of earthing conductors (ECs) has an influence on the pipeline interference voltage (PIV) and has to be investigated. For this purpose, the two most used pylon types “ton” (PY1) and “tan” (PY2) are looked at with either zero, one or two ECs and are analysed for the best and worst conductor configuration (CC). First, the “ton”-pylon (PY1) is compared to PY13 (“ton” without EC) and PY11 (“ton” with two ECs). Figure 4-36 below shows the geometry of these pylons. The conductor positions P1, P2 and P3 are relevant for the best and worst CC (see chapter 4.6.3, PY1 and PY2).

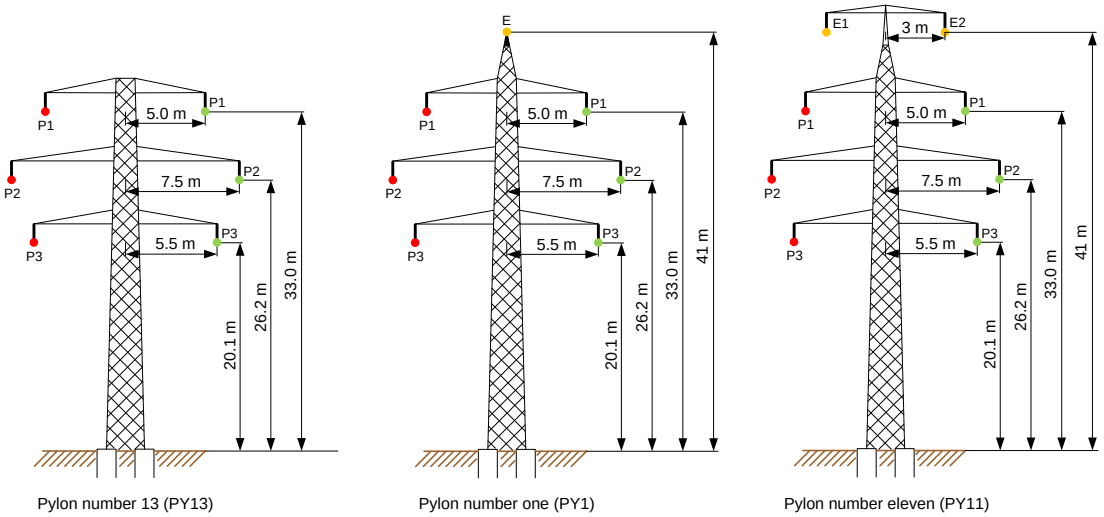

Figure 4-36: "Ton"-pylon with zero, one and two ECs to compare the effect on the PIV

Figure 4-37 shows the results of the calculation for the best case and points out that ECs are an important factor in the case of PIV calculations. The only location where the ECs reduce the maximum PIV is where the overhead lines (OHLs) are directly above or in the direct vicinity of the pipeline.

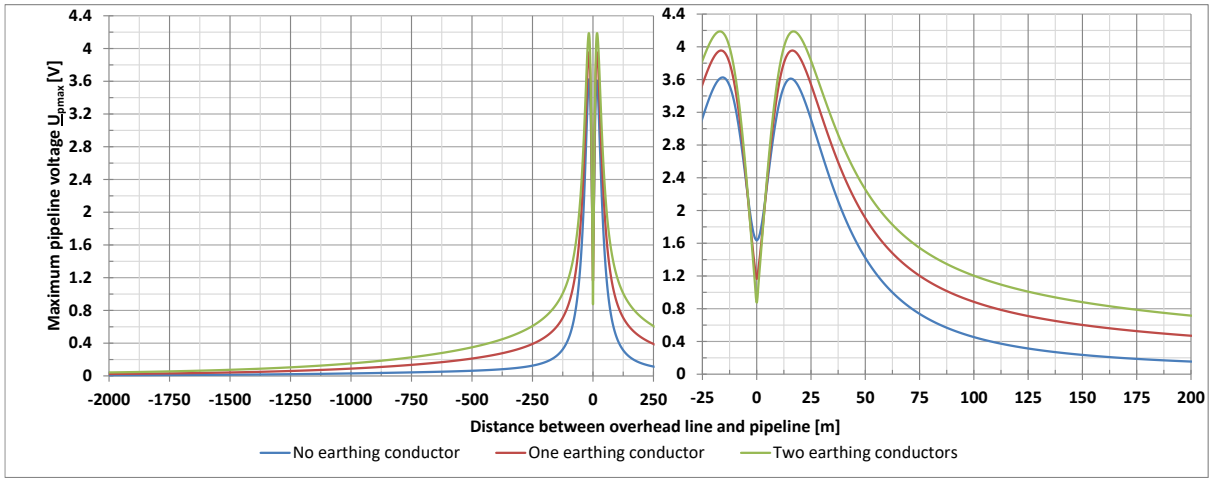

Figure 4-37: Maximum PIV for the "ton"-pylon with the best CC and zero, one and two ECs

In Figure 4-38 shows that the calculations have similar results, also in case of the worst CC. A small change can be noticed for distances over 500 meters, where the three calculations slowly converge. The reason lies therein, that the EC has a smaller impact on the PIV for farther distances in the case of asymmetrical CCs.

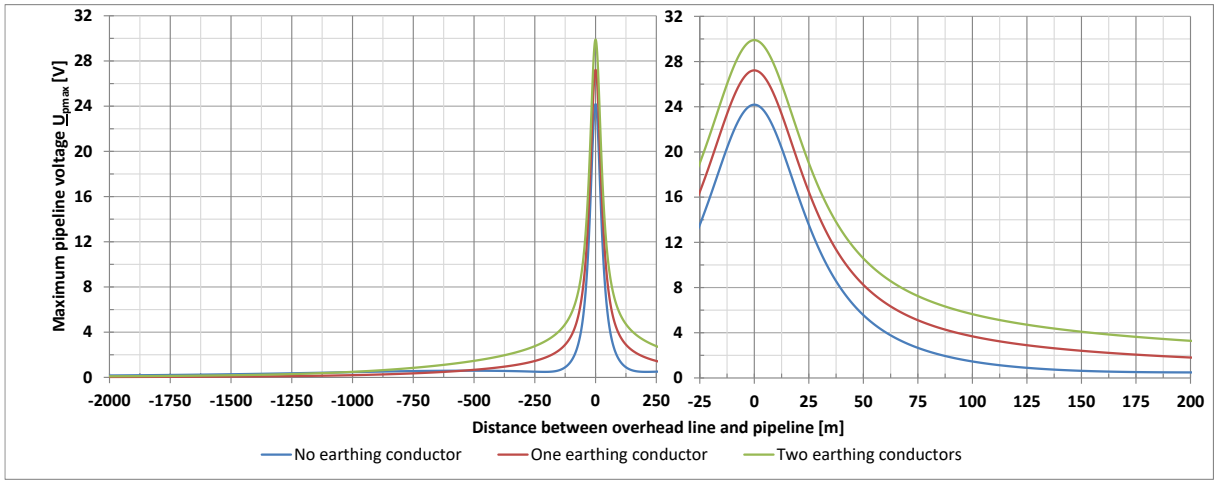

Figure 4-38: Maximum PIV for the "ton"-pylon with the worst CC and zero, one and two ECs

The second example is the “tan” pylon (PY2), as shown below in Figure 4-39. Again, zero (PY14), one (PY2) and two (PY12) ECs are used with the best and worst CCs, as has already been shown in chapter 4.6.2.

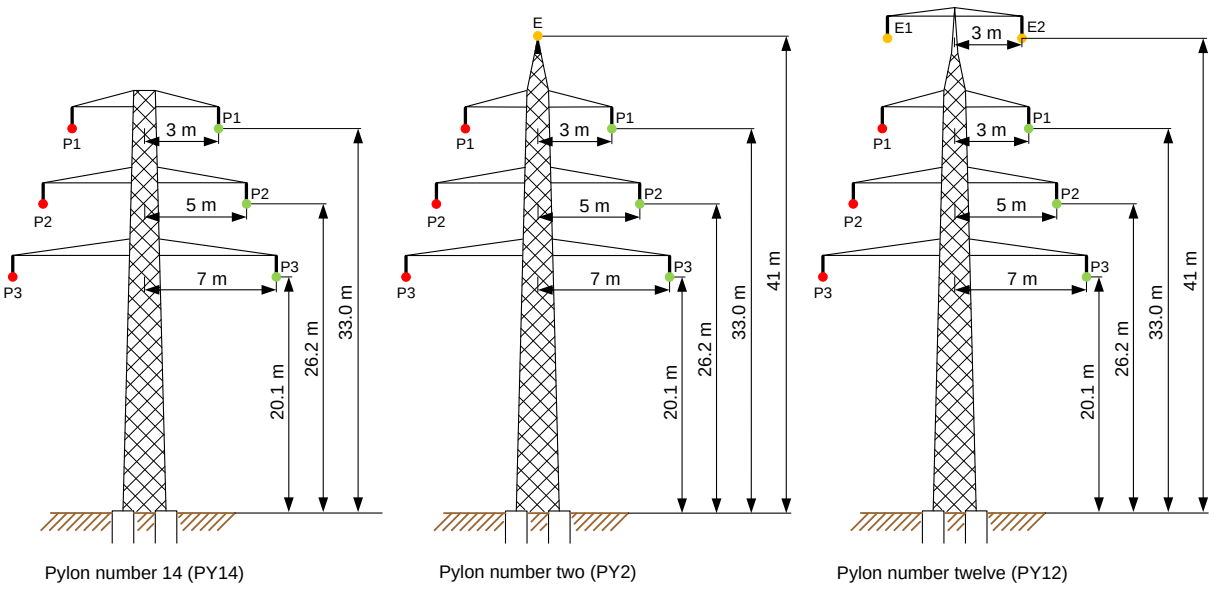

Figure 4-39: "Tan"-pylon with zero, one and two ECs to compare the effect on the PIV

Figure 4-40 shows a rising PIV for the best CC with increasing ECs. However, the difference between the calculations is smaller than for the “ton”-pylon.

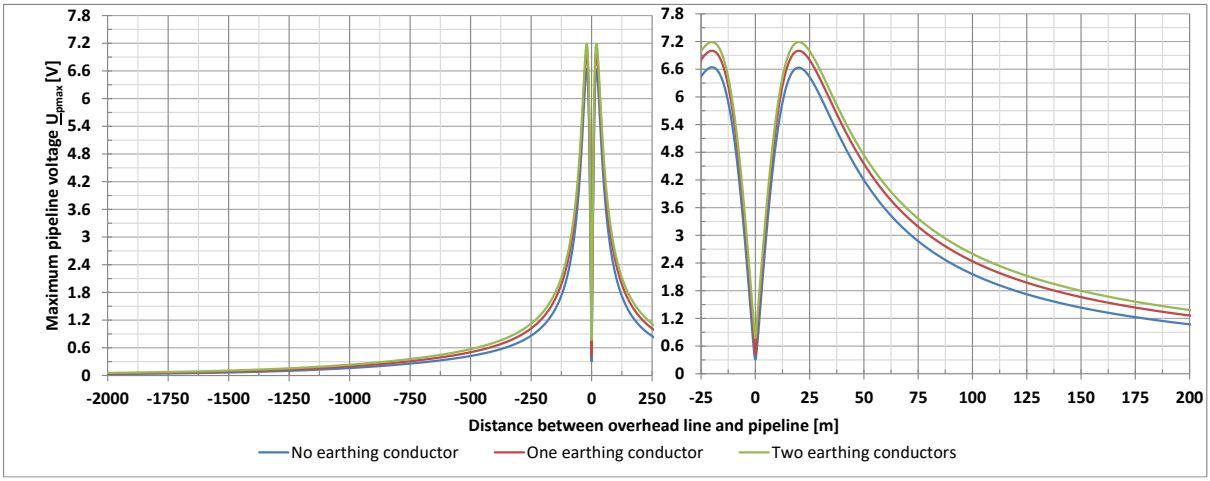

Figure 4-40: Maximum PIV for the "tan"-pylon with the best CC and zero, one and two ECs

With the worst CC, the results in Figure 4-41 for the “tan” pylons are very similar to the calculations for the “ton”-pylons in Figure 4-38. This leads to the conclusion that for standardized pylon types, the EC increases the PIVs and, therefore, widely used EC reduction factors for normal operation modes of overhead lines (OHLs) should be questioned when calculating the PIVs.

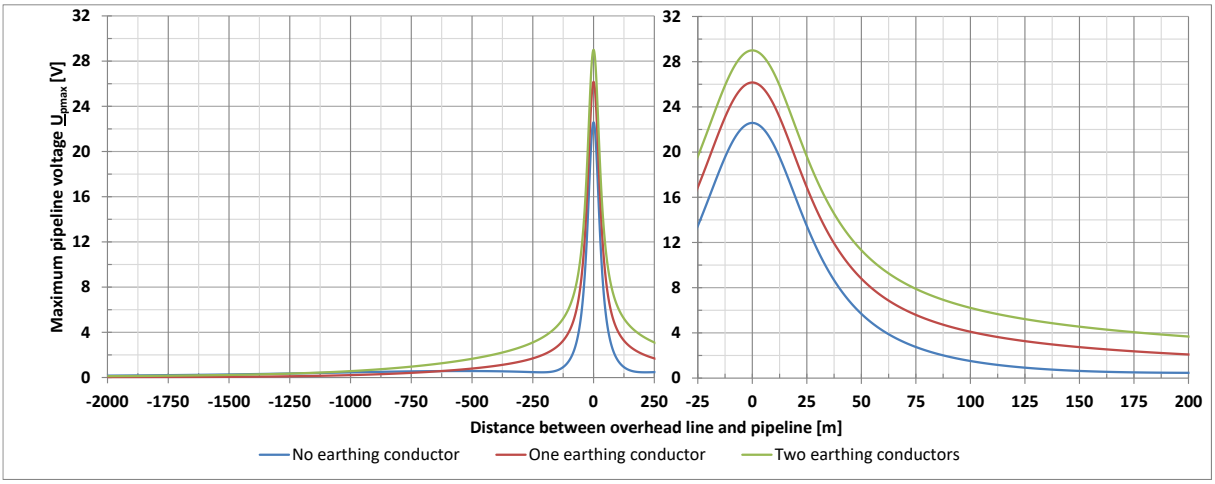

Figure 4-41: Maximum PIV for the "tan"-pylon with the worst CC and zero, one and two ECs

4.7.2 Height of earthing conductors

The chapter above showed that the influence of earthing conductors (ECs) must always be considered. Unfortunately, not only is the number of ECs important, also the height above the surface and the relative distance to the phase conductors has an influence on the pipeline interference voltage (PIV). In addition, the impact of an EC on the PIV depends on the pylon type and the arrangement of the conductors on the pylon.

In this chapter, these effects are looked at in order to be able to assess their influence on PIVs. The calculations are similar to the calculations in chapters 4.1 and 4.6.3, which means that a 1000 meter parallel route between pipeline and overhead line (OHL) is used. For a calculation cycle, the distance between both systems is again varied between -2000 and +2000 meters. Additionally, for each cycle, the height of the EC is varied with specific values between -2 and 65 m and the maximum PIV is recorded for each calculation.

Adding in the calculation cycle without an EC, a total of 25 values for the height are taken into account. This means that approximately 100,000 calculations were performed for each diagram. The values for the height of the EC can be found in the key below the curve and are usually the same for each calculation.

This thesis includes calculations for the following pylon types:

- "Ton"-pylon 220 kV (PY1) in chapter 4.7.2.1
- "Tan"-pylon 220 kV (PY2) in chapter 4.7.2.2
- "Danube"-pylon 220 kV (PY3) in Appendix C.4 and C.5
- "Single-plane"-pylon 220 kV (PY4) in Appendix C.6 and C.7
- "Quadruple"-pylon 380 kV (PY6) in Appendix C.8 and C.9
- "Single-Circuit"-pylon 110 kV (PY10) in Appendix C.10
- "Ton"-pylon with two earthing conductors 220 kV (PY11) in Appendix C.11and C.12
- "Tan"-pylon with two earthing conductors 220 kV (PY12) in Appendix C.13 and C.14

4.7.2.1 "Ton" pylon 220 kV (PY1)

4.7.2.1.1 Best conductor configuration (CC)

First, the standardized example with the "ton"-pylon (PY1) and the best conductor configuration (CC) is considered. Usually, a height of 41 m is used for the EC, resulting in a maximum PIV of 0.88 Volt/km for a distance of 100 m between both systems. Figure 4-42 below shows that the height of the EC of 41 m is not the best choice for this pylon configuration due to high PIVs (green line). For a distance of 100 m between both systems, the best case is without an EC (red line) with a PIV of 0.45 Volt/km, but this case is not possible due to safety regulations. Because of the large number of calculations, it is not possible to spot any details in this figure. Therefore, as an enlarged view of Figure 4-42, Figure 4-43 shows distances between -500 and +500 m.

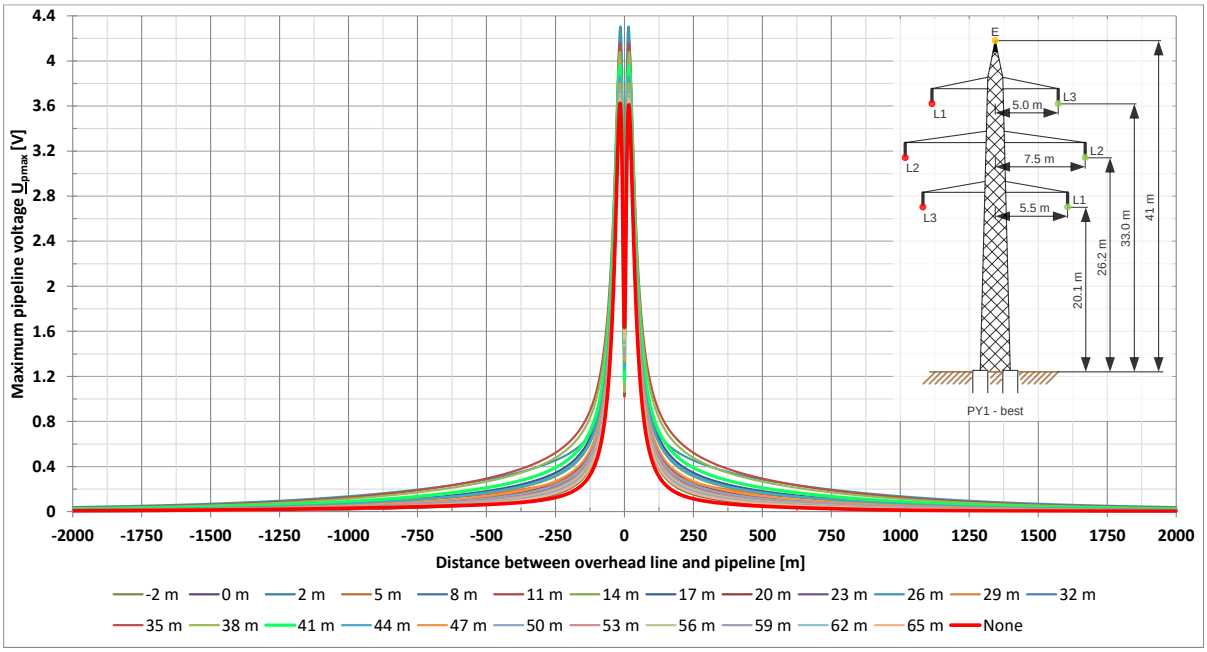

Figure 4-42: Maximum PIVs for the "ton"-pylon with the best CC at different heights of ECs

Figure 4-43 provides better insights for distances between +/-50 m, where pipeline and OHL lie quite close together. In addition, the chart also gives a better overview of the other closer distances within +/- 500 m. The red line, which illustrates the case without an EC, again shows the best overall performance except for distances around 0 m. However, the graph also shows that it is possible to achieve almost the same results with an EC. To get a more detailed understanding of the impact of the different heights of the EC, a different graphic analysis is necessary.

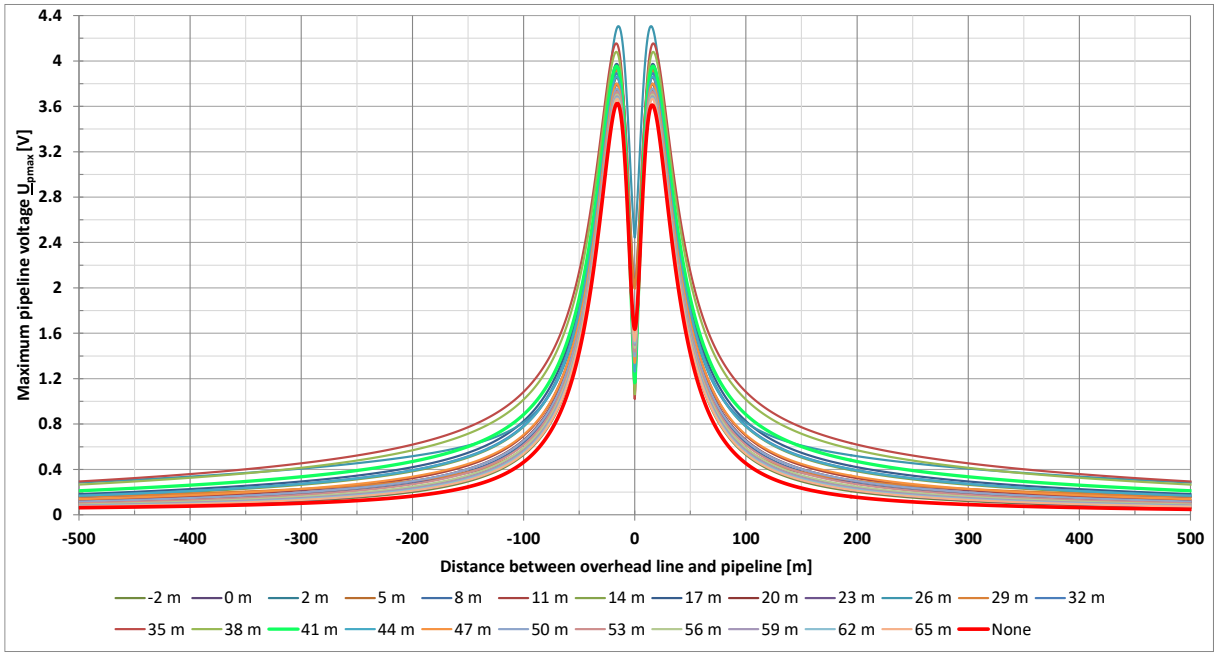

Figure 4-43: Maximum PIVs for the "ton"-pylon with the best CC at different heights of EC; enlarged view

It is preferable to create a vertical profile for specific distances between pipeline and OHL. For this, Figure 4-42 and Figure 4-43 show vertical profiles for distances of 0-25-50-100-200-500-1000 meters between pipeline and OHL to cover the most relevant areas. For each distance, the PIVs for the different values of the EC as well as without an EC are read out to form one single line in the chart. Repeating this process for all seven specific distances leads to Figure 4-44. The values for the height above soil can be seen on the x-axis and the specific distances can be found in the key below the chart.

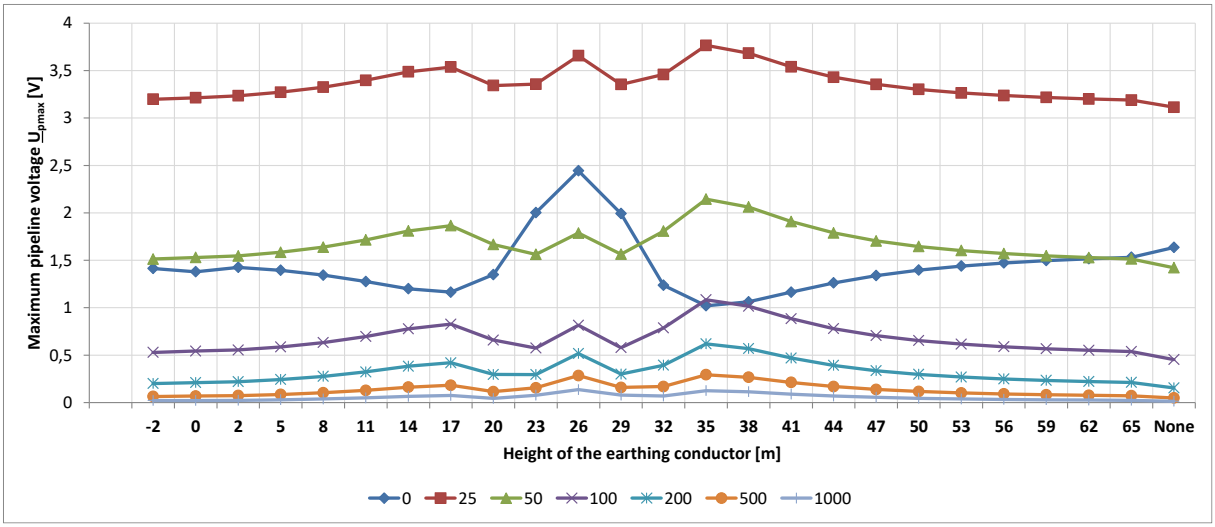

Figure 4-44: Maximum PIVs for the "ton"-pylon at different heights of EC for specific distances (m)

Basically, with an increasing distance between pipeline and overhead line (OHL), the maximum pipeline interference voltage (PIV) decreases, except where both systems are directly on top of each other (distance between both systems = 0 m). This pylon configuration shows that the impact of the height of the earthing conductor (EC) for all distances is not very significant except for the distance of 0 m.

Peak values are always reached when the EC is at the same height as a phasing conductor. Outside of this height range, the impact of the EC on the PIV decreases due to less induced voltage in the EC. All discussed distances show that the PIV is generally lower when the EC lies between the pipeline and the phase conductor. Nevertheless, the PIV with an EC is always higher than without an EC.

As already indicated, the behaviour is completely different when the OHL is directly above the pipeline (distance = 0 m). The highest PIVs exist for EC heights between the lowest and the highest phase conductor and are much more pronounced than at other distances.

On the other hand, a reduction factor of the EC can also be clearly seen when the EC is located directly above or below the phase conductors. This means that, in this case, the EC is a screening conductor and an EC reduction factor can be used. However, this case will hardly be relevant in

practice, since a certain distance is prescribed between the pipeline and OHL in the case of parallel running.

The different PIVs for varying distances with and without an EC can be best seen by looking at the ratio between them. For this, the maximum PIV is taken from the case without an EC and is set to a fixed ratio of 1 which is then used as the reference value. All other heights are then calculated as a ratio between the value of the PIV from the respective height and the value of the PIV in the case without an EC.

When the ratio is higher than 1, the pylon with a specific height of the EC influences the pipeline more than without an EC. This step is then repeated for all heights of the EC for each set distance and is repeated again for all distances between the pipeline and the OHL. With this calculation method it is possible to compare the impact of different heights of the EC on the PIV. In addition, it shows how the ratio changes over the different distances between pipeline and OHL. The calculation of all ratios is shown in Figure 4-45.

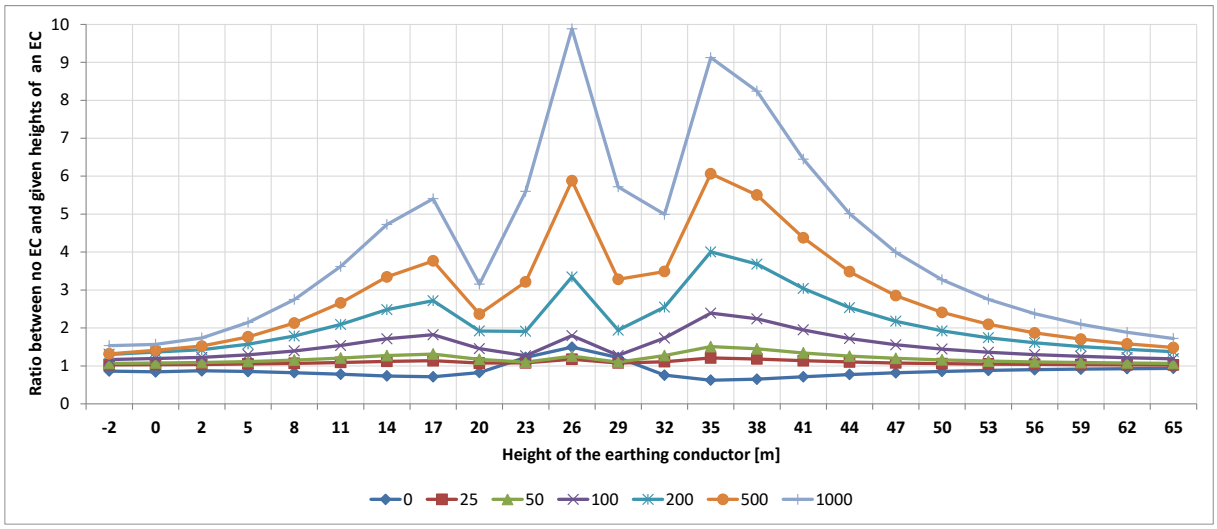

Figure 4-45: Ratio for the "ton"-pylon with the best CC for different heights of the EC for specific distances, where the reference value (value = 1) means using no EC for these specific distances

It can be seen that the influence of the height of the EC increases with an increasing distance between pipeline and OHL. In close vicinity, however, the height of the EC plays a rather subordinate role and is not as relevant as expected. Since the influence is at its maximum within the first 100 meters, these distances are the most relevant. When the distance increases, the impact of the height of the EC is greater, but the basic interference on the PIV and therefore the PIV is lower due to the larger distance. For this pylon type with the given CC, the height of the EC has a minor impact on the PIV.

Further calculations with the same pylon type and the same CC but two ECs can be found in Appendix C.11 and show similar results.

4.7.2.1.2 Worst conductor configuration (CC)

The voltage curves in Figure C- 1 and Figure C- 2 in Appendix C.1 serve as a starting point for the voltages in Figure 4-46 and the ratios in Figure 4-47. For this purpose, the calculation method from chapter 4.7.2.1.1 for the vertical profile is used.

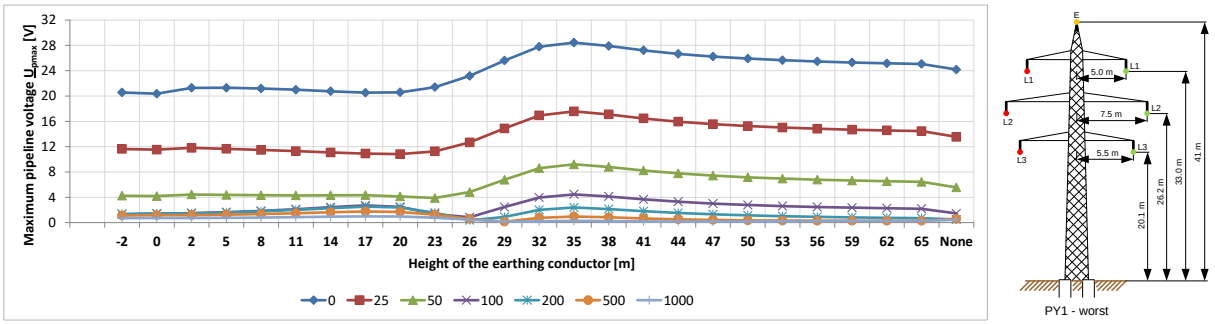

Figure 4-46: Maximum PIVs for the "ton"-pylon at different heights of EC for certain distances (m)

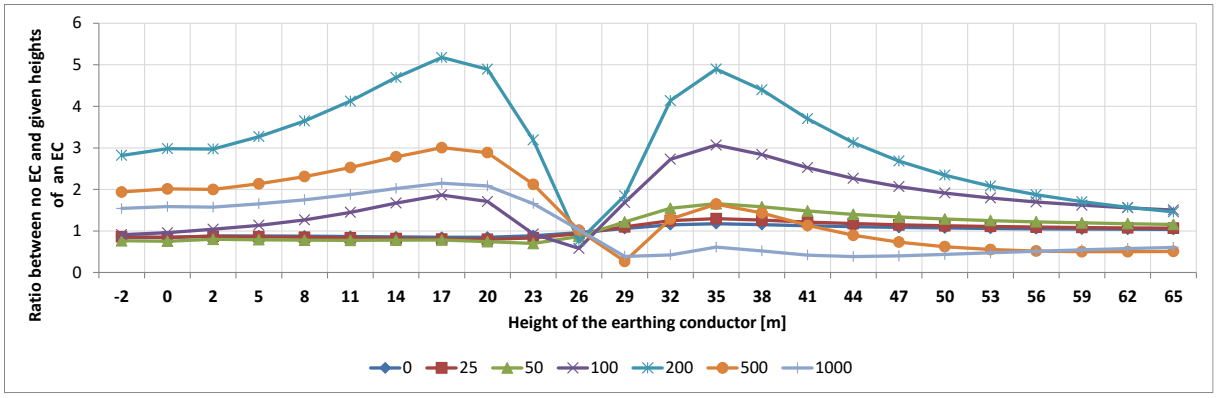

Figure 4-47: Ratio for the "ton"-pylon with the worst CC for different heights of the EC for specific distances (m), where the reference value (value = 1) means using no EC for specific distances

The case of the "ton"-pylon with the worst CC shows that the height of the EC is only relevant for distances greater than 100 m between pipeline and OHL. In areas with higher influence and therefore higher PIV, there is only an increased PIV in cases where the EC lies above the middle level of the phase conductor.

More calculations with the same pylon type and the same CC but two ECs can be found in Appendix C.12 and show similar results.

4.7.2.2 "Tan" pylon 220 kV (PY2)

4.7.2.2.1 Best conductor configuration (CC)

The voltage curves in Figure C- 3 and Figure C- 4 in Appendix C.2 serve as a starting point for the voltages in Figure 4-48 and the ratios in Figure 4-49. For this purpose, the calculation method from chapter 4.7.2.1.1 for the vertical profile is used.

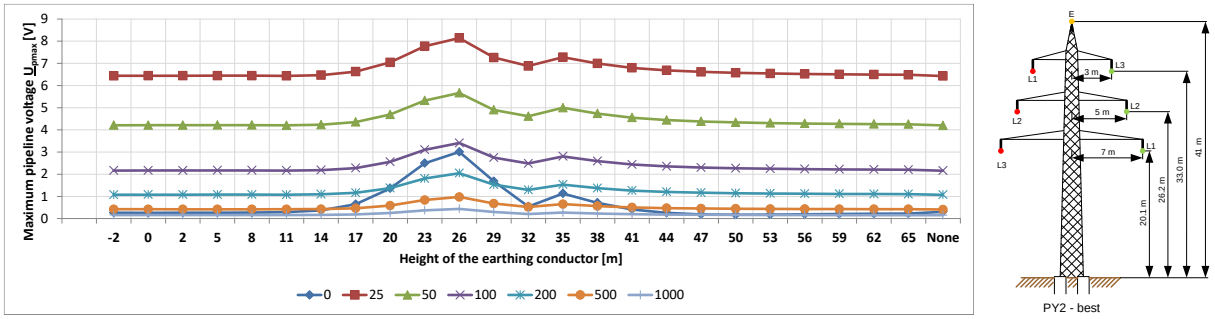

Figure 4-48: Maximum PIVs for the "tan"-pylon at different heights of ECs for specific distances (m)

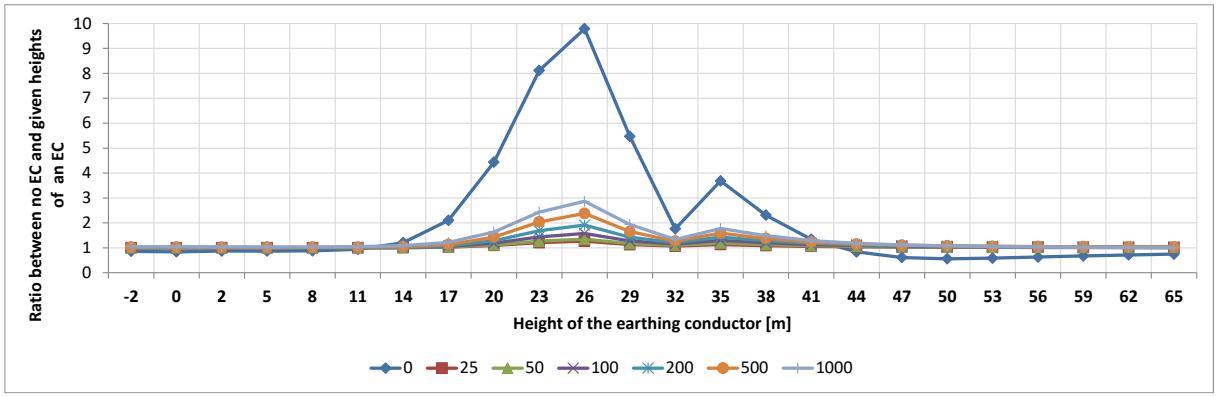

Figure 4-49: Ratio for the "tan"-pylon with the best CC for different heights of the EC for specific distances, where the reference value (value = 1) means using no EC for specific distances (m)

Surprisingly, the pipeline interference voltage (PIV) on the "tan"-pylon with the best CC does not change very much when the height of the earthing conductor (EC) is varied. This means that the PIV between a pipeline and this configuration of the pylon depends only on the distance between both systems and the length of the influenced area because of the electrical symmetry of the phase arrangement.

More calculations with the same pylon type and the same CC but two ECs can be found in Appendix C.13 and show similar results.

4.7.2.2.2 Worst conductor configuration (CC)

The voltage curves in Figure C- 5 and Figure C- 6 in Appendix C.3 serve as a starting point for the voltages in Figure 4-50 and the ratios in Figure 4-51. For this purpose, the calculation method from chapter 4.7.2.1.1 for the vertical profile is used.

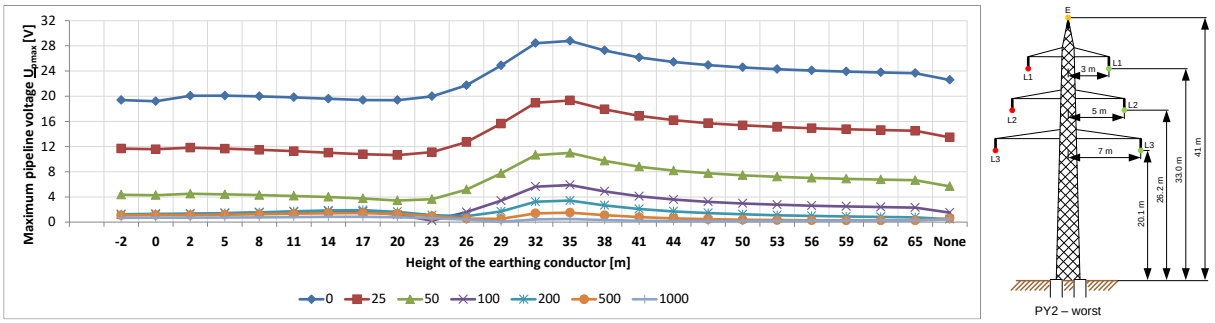

Figure 4-50: Maximum PIVs for the "tan"-pylon at different heights of EC for specific distances

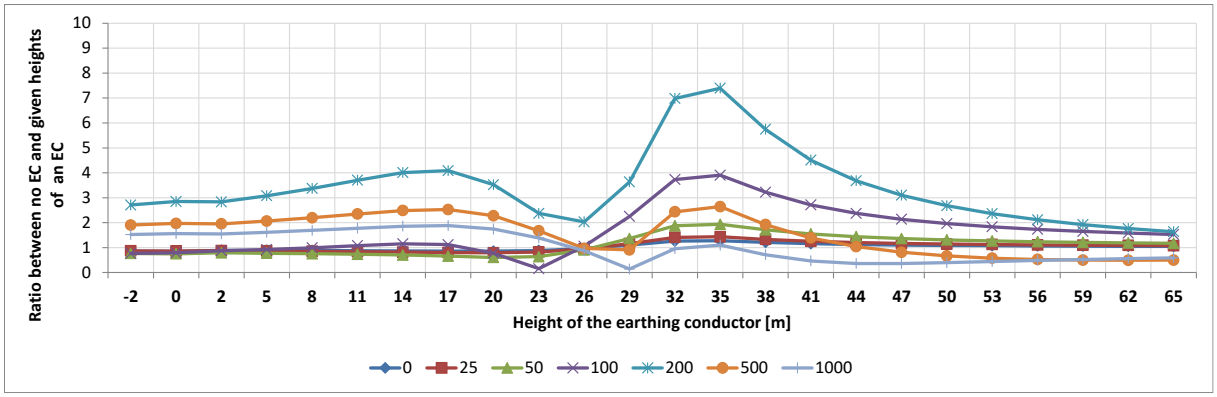

Figure 4-51: Ratio for the "tan"-pylon with the worst CC for different heights of the EC for specific distances, where the reference value (value = 1) means using no EC for specific distances

The case of the "tan" pylon with the worst CC is very similar to the "ton"-pylon with the worst CC. This similarity has already been shown in the comparison of the PIV in chapter 4.6.3.1 and therefore this result is not very surprising. Both examples thus show that the height of the EC in this CC can be neglected, while the configuration of the CC has a significant influence on both pylon types. More calculations with the same pylon type and the same CC but two ECs can be found in Appendix C.14 and show similar results.

4.7.3 Conductor diameter of earthing conductors

Another aspect which should be looked at is the conductivity of earthing conductors (ECs). This value depends on the material used and the diameter of the conductor. This chapter considers the second parameter, the diameter of the EC.

Again, the standardized example from chapter 4.1 is used, which is the "ton" pylon with the best conductor configuration (CC). The impact of different diameters for the EC is shown in Figure 4-52, where six different diameters from 5 mm to 30 mm are compared. It can be clearly seen that the maximum pipeline interference voltage (PIV) rises with an increasing diameter of the EC. The reason for this is the increased conductivity of the EC due to an increased diameter.

Because of this, the phasing conductor can induce a current into the EC more easily. As already mentioned above, currents in an EC deform the symmetrical magnetic flux and therefore, higher currents in the EC have a stronger impact on the magnetic flux which leads to a higher PIV.

Various calculations on other pylon types and CC configurations show that a rising conductivity always leads to the same result and therefore further examples are not shown in this thesis.

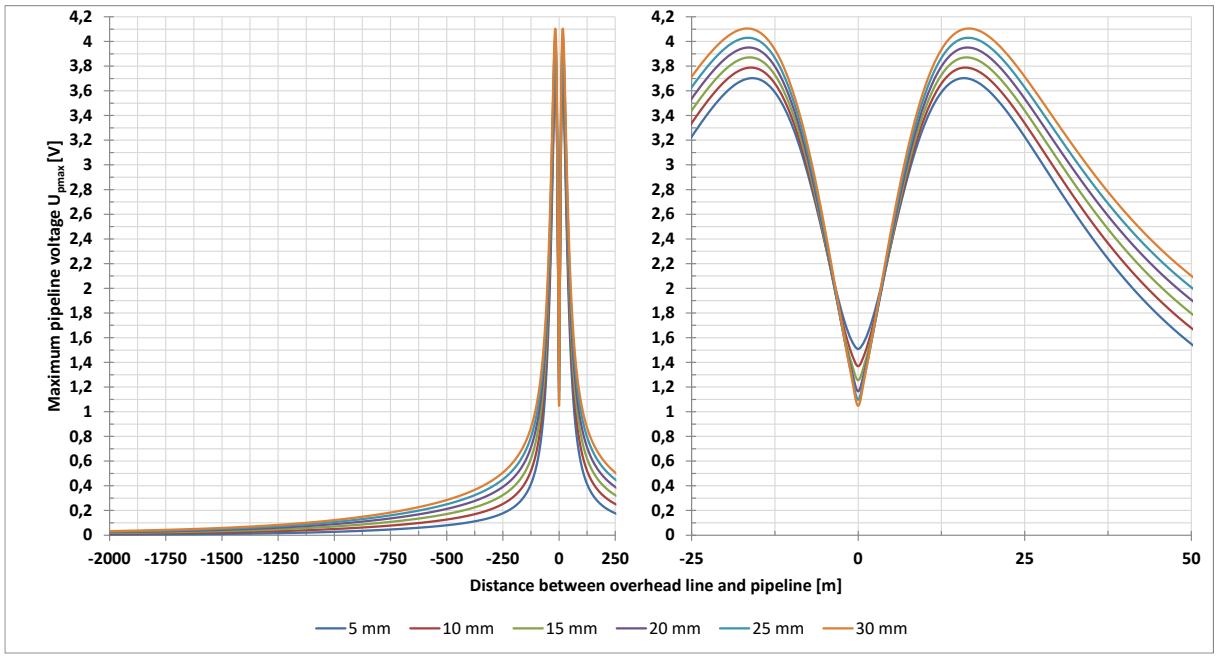

Figure 4-52: Maximum PIVs for the "ton"-pylon with the best CC for different conductor diameters of the EC

Another question is whether there is a linear interrelationship between an increasing diameter of the EC and a rising PIV. This question is answered in Figure 4-53, with vertical profiles for specific distances. The calculation of the vertical profiles is identical to the one described in chapter 4.7.2, on page 93. This figure uses the same specific distances. Apart from the distance of 0 m, all other distances show an almost perfectly increasing straight correlation. This suggests that poor conductivity is desirable for ECs in the case of pipeline interference since it reduces the PIV. However, a high conductivity of the EC is important for other aspects of the OHL (e.g. in the case of a lightning strike or in the event of a fault), as it increases the reliability of the OHL. However, a slightly different aspect is shown at a distance of 0 m, where the correlation shows a decreasing

value. This shows that under ideal conditions, an enlarged diameter can lead to a reduction of the PIV.

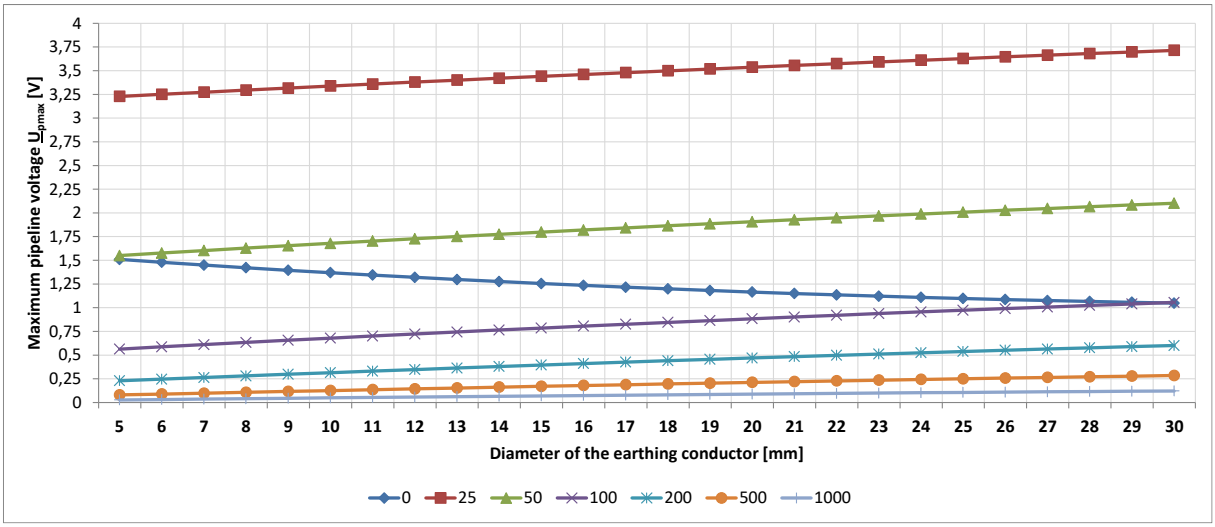

Figure 4-53: Maximum PIVs for the "ton"-pylon at different conductor diameters of ECs for specific distances

There is also a complex interrelationship between an increasing diameter of the EC, the percentage change of the PIV and the distance between the pylon and the pipeline. This is shown in Figure 4-54, where the maximum PIV for a diameter of 5 mm is set as the ratio of 1 for each specific distance. All other EC diameters are calculated as the ratio to the diameter of 5 mm, which means that except for at a distance of 0 m, the ratio is always greater than one because of the above mentioned increasing characteristic of the PIV. The most notable part of this figure is that with an increasing diameter and distance, the influence of the EC on the PIV rises.

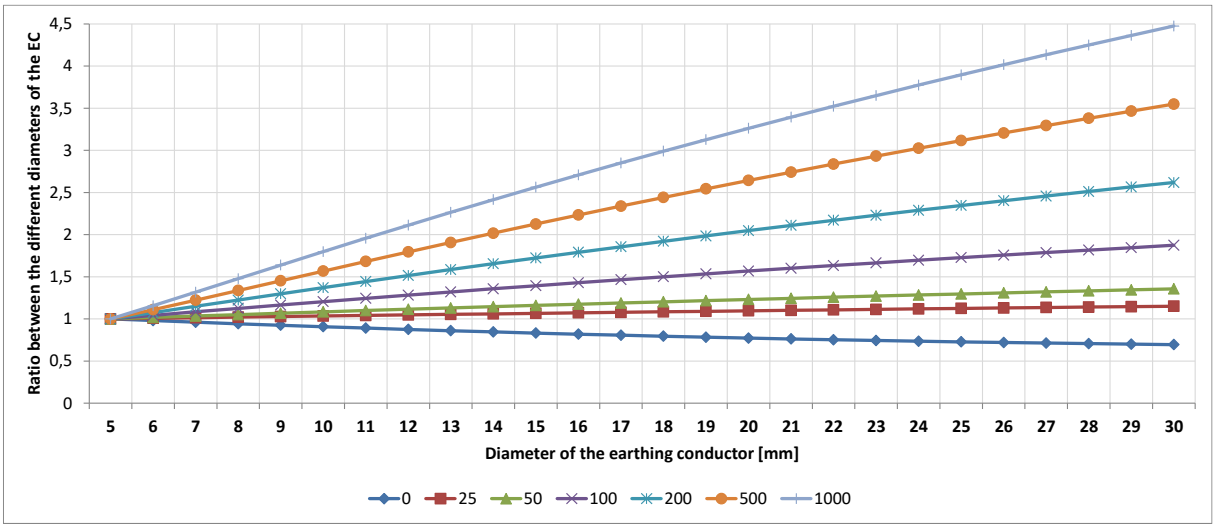

Figure 4-54: Ratio for the "ton"-pylon for the best CC for different conductor diameters of the EC for specific distances, where the reference value (value = 1) is 5 mm for the conductor diameters for specific distances (m)

5 Impact of multiple configurations of metallic structures

There often exist several influencing systems within a pipeline section which may influence each other. In addition, there are always passive metallic structures in the vicinity, which also can have an influence on the pipeline interference voltage (PIV) with increasing or decreasing effects.

Basically, these interactions can be calculated according to chapter 5.1, however, the manual calculations of the screening factor help illustrate its complexity.

Unfortunately, there are countless possible combinations of metallic structures and therefore, only some specific combinations can be examined in this chapter. The purpose of this chapter is to use these combinations to show how the structures interact and how they influence the PIV.

5.1 The screening factor

5.1.1 General calculation of the screening factor

A simplified case for calculating earthing conductor (EC) currents and screening factors was already a topic in chapter 2.4. The general calculation of screening factors and their impacts needs significantly more effort, particularly for cases with more than one screening conductor. Therefore, two examples are chosen to illustrate the rapidly increasing complexity with the rising number of conductors.

5.1.2 Single screening conductor

The first example in Figure 5-1 describes a current-carrying-conductor with a parallel pipeline and a parallel double-sided earthed screening conductor.

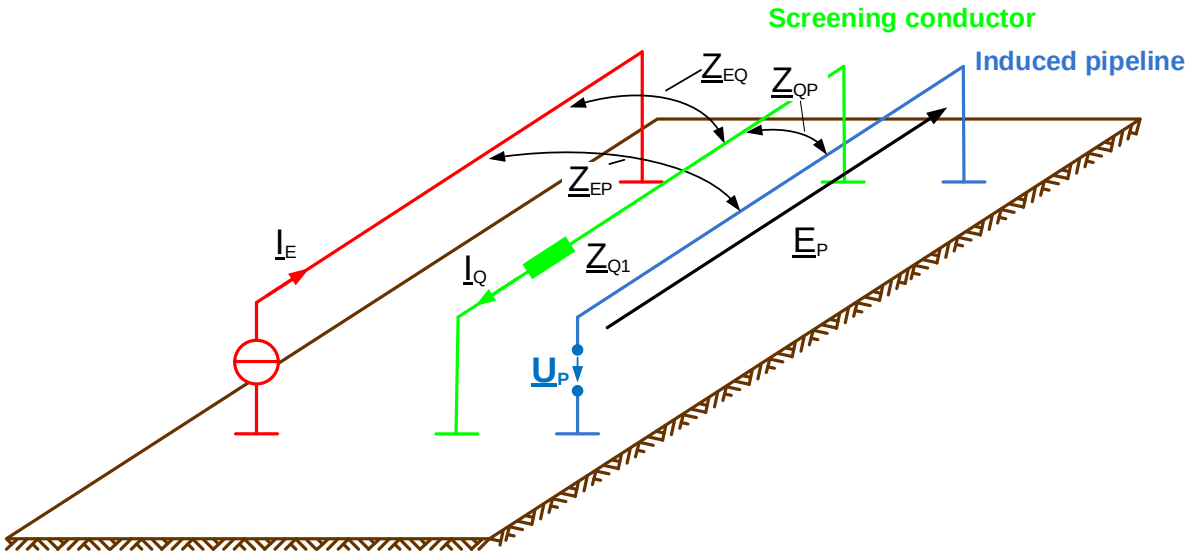

Figure 5-1: Example with a single screening conductor, to calculate the induced voltage into the pipeline

When the self impedance and mutual impedances (MI)s are known, the equations for the induced and screening conductors are the following:

$$E_P = Z_{EP} \cdot I_E + Z_{QP} \cdot I_Q \quad (5\text{-}1)$$

$$0 = Z_{EQ} \cdot I_E + Z_Q \cdot I_Q \quad (5\text{-}2)$$

$\underline{E}_P$:	Electromotive force [Vm]
$\underline{U}_P$:	PIV [V]
$\underline{Z}_Q$	Self-impedances from the EC [Ω/m]
$\underline{Z}_{EP}$, $\underline{Z}_{EQ}$, $\underline{Z}_{QP}$:	MIs respectively [Ω/m]
$\underline{I}_E$:	Inducing current [A]
$\underline{I}_Q$:	Current in the EC [A]

With formula (5-2), the screening conductor current equals:

$$\mathrm{I}_Q = -\frac{Z_{EQ}}{Z_Q} \cdot I_Q \quad (5\text{-}3)$$

Inserting formula (5-4) into formula (5-1) leads to:

$$\mathrm{E}_P = Z_{EP} \cdot I_E \cdot \left(1 - \frac{Z_{EQ} \cdot Z_{QP}}{Z_{EP} \cdot Z_Q}\right) \quad (5\text{-}4)$$

When no screening conductor exists (see Figure 2-1), the induced voltage equals:

$$E'_P = Z_{EP} \cdot I_E \quad (5\text{-}5)$$

The screening factor $\boldsymbol{k}$ equals:

$$k = \frac{\mathrm{E}_P}{E'_P} = 1 - \frac{Z_{EQ} \cdot Z_{QP}}{Z_{EP} \cdot Z_Q} \quad (5\text{-}6)$$

Formula (5-6) shows that the screening (or also reduction) factor can be calculated easily for simple cases. A requirement is that all parameters are homogenous within a segment. This means that in cases with non-parallel-arrangements, segmenting is necessary which increases the effort needed for calculations.

5.1.3 Two screening conductors

To illustrate how fast the effort needed for these calculations rises with increasing screening conductors, the second example in Figure 5-2 includes an extra screening conductor.

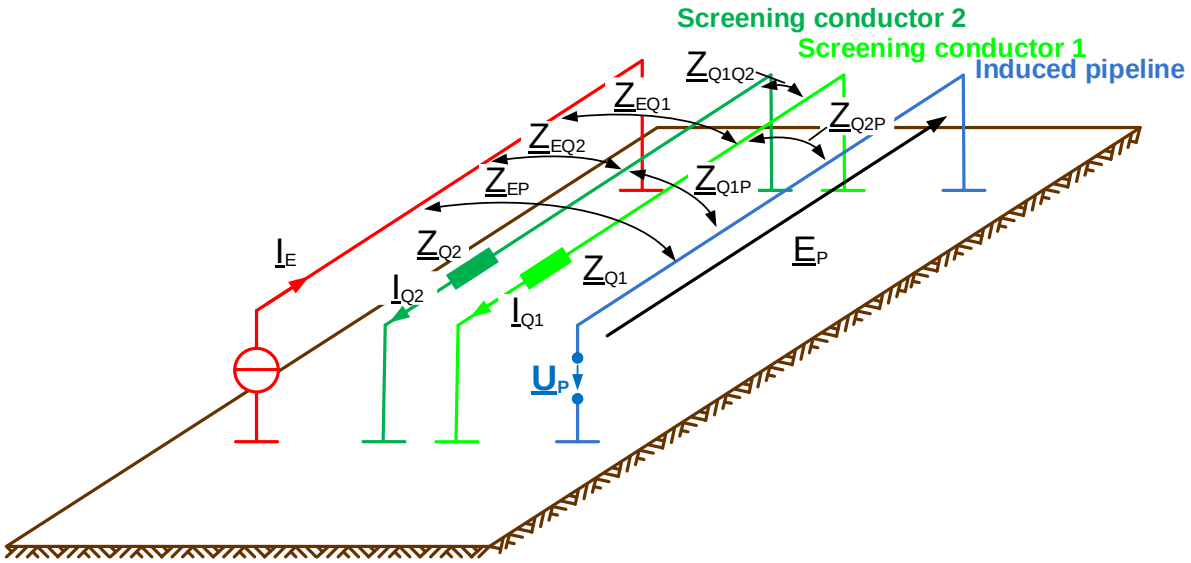

Figure 5-2: Example with two screening conductors to calculate the induced voltage into the pipeline

The calculation procedure is the same is in chapter 5.1.2 above. Thus, the equations (5-1) and (5-2) have to be extended with a second screening conductor equation:

$$\underline{E}_P = \underline{Z}_{EP} \cdot \underline{I}_E + \underline{Z}_{Q1P} \cdot \underline{I}_{Q1} + \underline{Z}_{Q2P} \cdot \underline{I}_{Q2} \quad (5\text{-}7)$$

$$0 = \underline{Z}_{EQ1} \cdot \underline{I}_E + \underline{Z}_{Q1} \cdot \underline{I}_{Q1} + \underline{Z}_{Q1Q2} \cdot \underline{I}_{Q2} \quad (5\text{-}8)$$

$$0 = \underline{Z}_{EQ2} \cdot \underline{I}_E + \underline{Z}_{Q1Q2} \cdot \underline{I}_{Q1} + \underline{Z}_{Q2} \cdot \underline{I}_{Q2} \quad (5\text{-}9)$$

$\underline{E}_P$:	Electromotive force [Vm]
$\underline{U}_P$:	PIV [V]
$\underline{Z}_{Q1}$, $\underline{Z}_{Q2}$	Self-impedances from the EC [Ω/m]
Other $\underline{Z}_{xx}$:	MIs respectively [Ω/m]
$\underline{I}_E$:	Inducing current [A]
$\underline{I}_{Q1}$, $\underline{I}_{Q2}$:	Current in the EC [A]

With formulas (5-8) and (5-9), the screening conductor currents $\underline{I}_{Q1}$ and $\underline{I}_{Q2}$ equal:

$$\underline{I}_{Q1} = \frac{\underline{Z}_{EQ2} \cdot \underline{Z}_{Q1Q2} - \underline{Z}_{Q2} \cdot \underline{Z}_{EQ1}}{\underline{Z}_{Q2} \cdot \underline{Z}_{Q1} - \underline{Z}_{Q1Q2}^{\,2}} \cdot \underline{I}_E \quad (5\text{-}10)$$

$$\underline{I}_{Q2} = \frac{\underline{Z}_{EQ1} \cdot \underline{Z}_{Q1Q2} - \underline{Z}_{Q1} \cdot \underline{Z}_{EQ2}}{\underline{Z}_{Q2} \cdot \underline{Z}_{Q1} - \underline{Z}_{Q1Q2}^{\,2}} \cdot \underline{I}_E \quad (5\text{-}11)$$

Inserting formulas (5-10) and (5-11) into equation (5-7) and summarizing leads to:

$$\begin{aligned} &\mathrm{E}_P \\ &= Z_{EP} \cdot I_E \\ &\cdot \left(1 - \frac{Z_{Q1P} \cdot \left(Z_{Q2} \cdot Z_{EQ1} - Z_{EQ2} \cdot Z_{Q1Q2}\right) + Z_{Q2P} \cdot \left(Z_{Q1} \cdot Z_{EQ2} - Z_{EQ1} \cdot Z_{Q1Q2}\right)}{Z_{EP} \cdot \left(Z_{Q2} \cdot Z_{Q1} - {Z_{Q1Q2}}^2\right)}\right) \end{aligned} \tag{5-12}$$

Using again:

$$E_P' = Z_{EP} \cdot I_E \tag{5-13}$$

The screening factor $\boldsymbol{k}$ is equals:

$$\begin{aligned} k &= \frac{\mathrm{E}_P}{E_P'} \\ &= \left(1 - \frac{Z_{Q1P} \cdot \left(Z_{Q2} \cdot Z_{EQ1} - Z_{EQ2} \cdot Z_{Q1Q2}\right) + Z_{Q2P} \cdot \left(Z_{Q1} \cdot Z_{EQ2} - Z_{EQ1} \cdot Z_{Q1Q2}\right)}{Z_{EP} \cdot \left(Z_{Q2} \cdot Z_{Q1} - {Z_{Q1Q2}}^2\right)}\right) \end{aligned} \tag{5-14}$$

Formula (5-14) shows that the effort needed for these calculations rises rapidly with an increasing number of screening conductors.

Thus, simplifications or other calculation methods are necessary when calculating more than two earthing conductors:

- Screening conductor currents and factors can be calculated beforehand and act as active current-carrying-conductors. This applies mainly to ECs from OHLs but not exclusively.
- Different screening conductors can be merged into a single conductor; the distance to influencing and influenced conductors can be averaged and the conductors are handled as a single, bigger conductor. Unfortunately, this can lead to a significant deviation in calculation results.
- When screening conductors can be attributed directly to the inducing and/or induced conductors, impedances can be equated, e.g. $\underline{Z}_{EP}$ with $\underline{Z}_{EQ2}$ if screening conductor 2 lies directly next to the pipeline. Other examples can be found in [39].

- Using the conductance addition method [48]. The single reduction factors can be converted into conductance values and added. The summarized conductance value is then changed to a single reduction factor.
  - Converting a known reduction factor k_1 into G_1: $G_1 = \frac{\sqrt{1-k^2}}{k \cdot \omega \cdot L_L}$
  - Summarizing different G's: $G_g = G_1 + G_2$
  - Changing into a single reduction factor: $k_g = \frac{1}{\sqrt{(\omega \cdot L_L)^2 \cdot G_g^2}}$

  There are other ways to do this, but they have restrictions, e.g. the single reduction factor should not exceed 0.3 for the reciprocal addition method.

If these methods are not applicable, numeric analysis are recommended because calculations with the above given formulas are quite complex, time-consuming and error-prone due to calculation errors. For this reason, the numerical method from chapter 3 is used and the screening factor is no longer calculated separately.

5.2 Two parallel overhead lines next to one pipeline

This chapter examines the case where two overhead lines (OHLs) and one pipeline are located next to each other. Figure 5-3 shows an example with two OHLs with a "ton"- pylon and a "tan"-pylon and their phase conductor currents $\underline{I}_1$ and $\underline{I}_2$ as well as their earth conductor currents $\underline{I}_{Q1}$ and $\underline{I}_{Q2}$. Two coupling impedances $\underline{Z}_{O1P}$ and $\underline{Z}_{O2P}$ lie between the pipeline and both OHLs, which induce a voltage into the pipeline.

With the earlier mentioned pipeline equivalent network, this leads to the current $\underline{I}_P$ in the pipeline. In addition, there is a mutual coupling with the impedance $\underline{Z}_{O1O2}$ between the two OHLs, which means that the two OHLs also influence each other.

In this figure, OHL1 and OHL2 have a full parallel route, which does not occur very often. Usually OHLs and pipelines are in the same energy corridor and intersect or at least do not have a complete parallel route, as shown in the figure by the route of the pipeline.

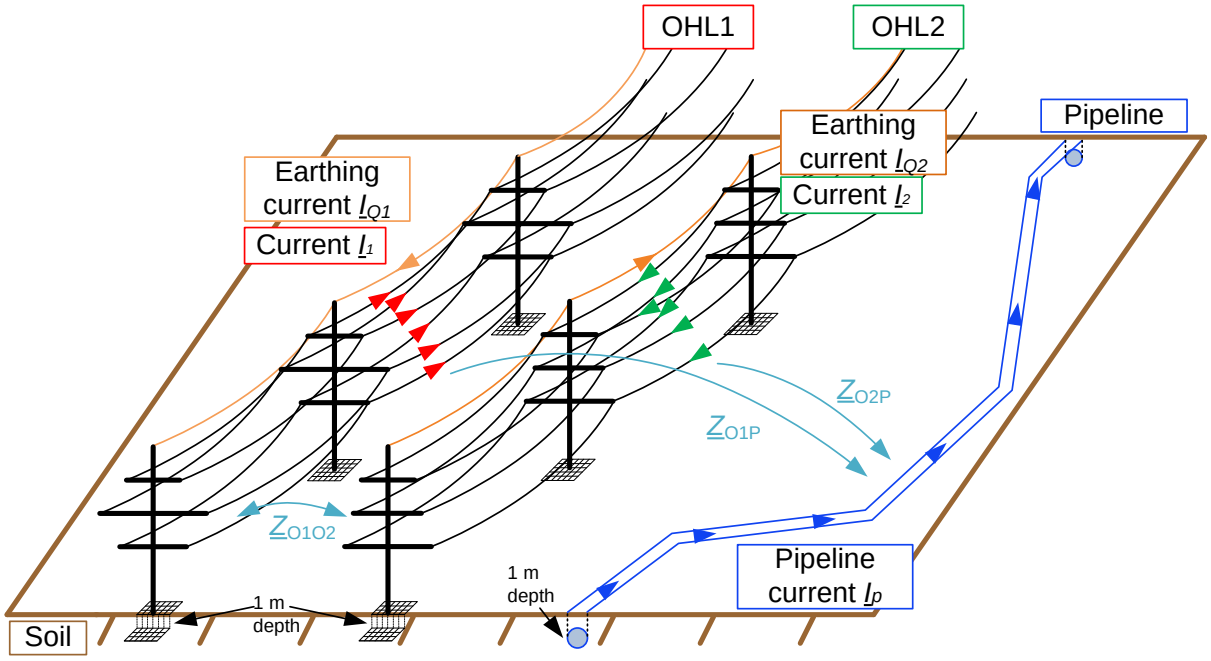

OHL1/OHL2: Overhead lines; setup and material the same as in chapter 4.1 but different pylon types are used
$\underline{I}_1$/$\underline{I}_2$: Phase conductor currents in OHL1 and OHL2
$\underline{I}_{Q1}$/$\underline{I}_{Q2}$: Earth conductor currents in OHL1 and OHL2
$\underline{I}_p$: Induced current flowing along the pipeline
$\underline{Z}_{O1P}$: MI between pipeline and OHL1
$\underline{Z}_{O2P}$: MI between pipeline and OHL2
$\underline{Z}_{O1O2}$: MI between OHL1 and OHL2

Figure 5-3: Two parallel OHLs with a "ton"-pylon next to one not parallel pipeline

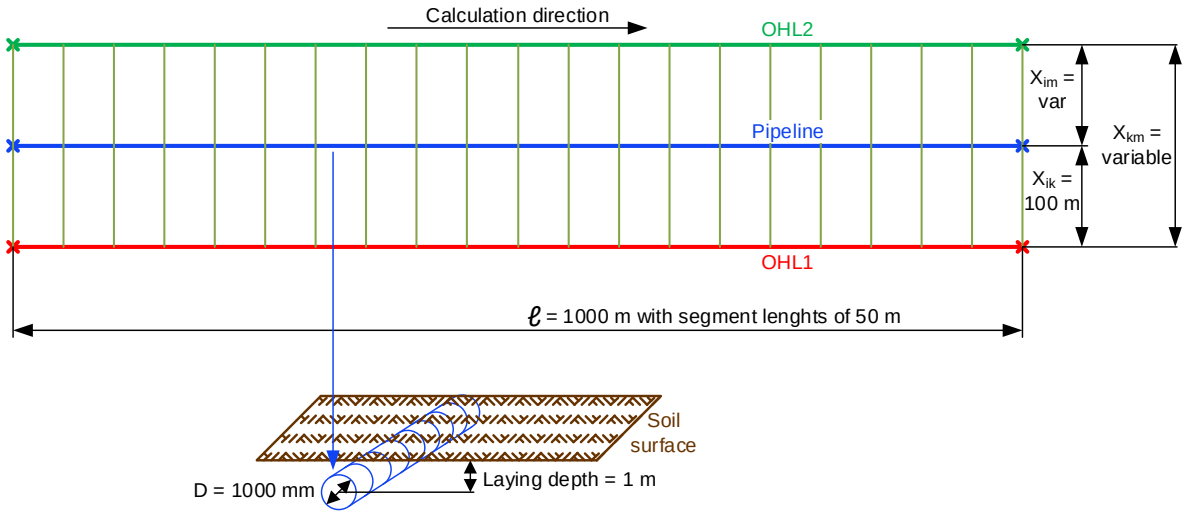

x_{ik}: Distance between pipeline and OHL1; this distance is fixed
x_{im}: Distance between pipeline and OHL2; this distance is variable
x_{km}: Distance between OHL1 and OHL2; this distance is variable

Figure 5-4: Geometrical parameters for examples with two OHLs and one pipeline

To simplify the case in the following example, all three systems are assumed to be fully parallel to each other, as shown in Figure 5-4. Also, the materials used in chapter 4.1 for the standardized example are reused, but the pylon type is varied according to the case. In addition, the phase current direction $\underline{I_2}$ from OHL2 is reversed in some cases. The distance x_{Ik} from the standardized example for the pipeline and OHL1 with 100 m is used, but the distance x_{Im} of OHL2 varies between -2000 and +2000 m to investigate the influence of parallel OHLs on the PIV.

For the first example, two "ton"-pylons with the best conductor configuration (CC) are used for OHL1 and OHL2. They are identical to the "ton"-pylon in chapter 4.6.3.1 ("PY1-best"). Calculating the maximum pipeline interference voltage (PIV) for the distance range of -2000 to +2000 meters leads to Figure 5-5:

The blue line shows the value, when only OHL1 influences the pipeline at a distance of 100 m and the value of the PIV is the same as in the standardized example. For the green curve, both OHLs are calculated separately without the mutual impedance (MI) between both OHLs. The maximum PIV of both calculations is summarized, which is indicated in the legend with "**… without MI**". The phasing current direction in this example is the same for both systems, which is indicated in the key with a **plus sign** ("+") between both pylon type descriptions. The red curve shows the dependence of the two parallel OHLs. The phasing currents flow in the same direction ("+") and the MI between both OHLs is indicated in the key with "**… with MI**".

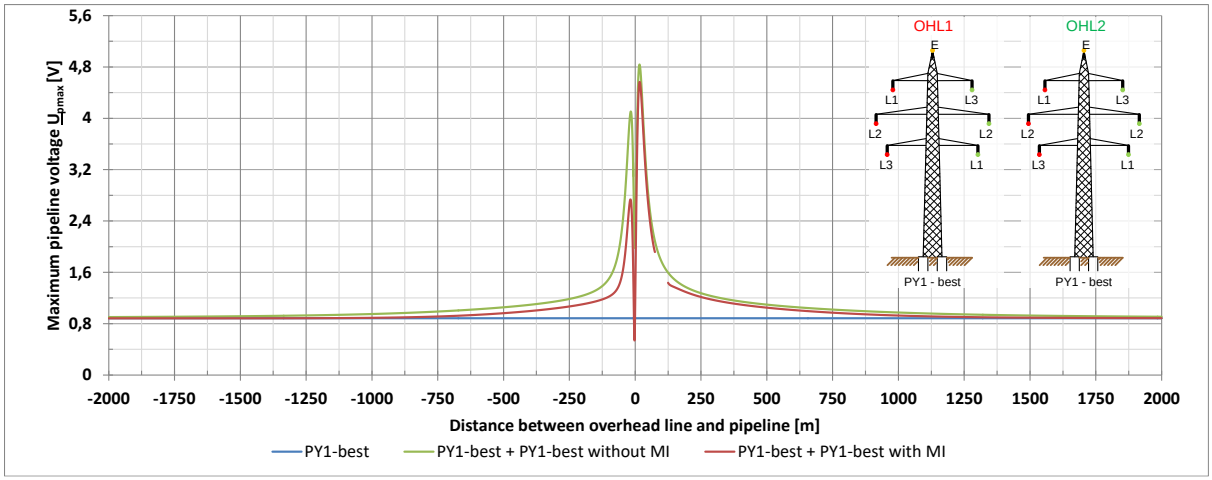

Figure 5-5: Maximum PIVs for the combination of PY1-best and PY1-best for the same current direction

Figure 5-5 shows the calculation of two parallel OHLs next to a pipeline. The calculation of the case with mutual impedances ("with MI") shows lower maximum PIVs than the calculation without consideration of the coupling ("without MI"). Since the maximum PIV varies strongly in the close approach of pipeline and OHL2, an enlarged view of the distances of +/- 300 m is necessary.

This range is shown in Figure 5-6 including a gap between 75 and 125 m because of the presence of OHL1 in this area. When taking into account the MI, the maximum PIV is overall slightly lower

than without the MI. This can be attributed to a more homogenous field with the combination of both OHLs because the influences of each phase conductor partially cancel each other out. For the combination of the "ton"-pylon (PY1) with the best conductor configuration (CC) it is best if there is an OHL on the left and right side of the pipeline because the influence cancels each other out more, e.g. for OHL2 it is at a distance x_{ik} of -50 m.

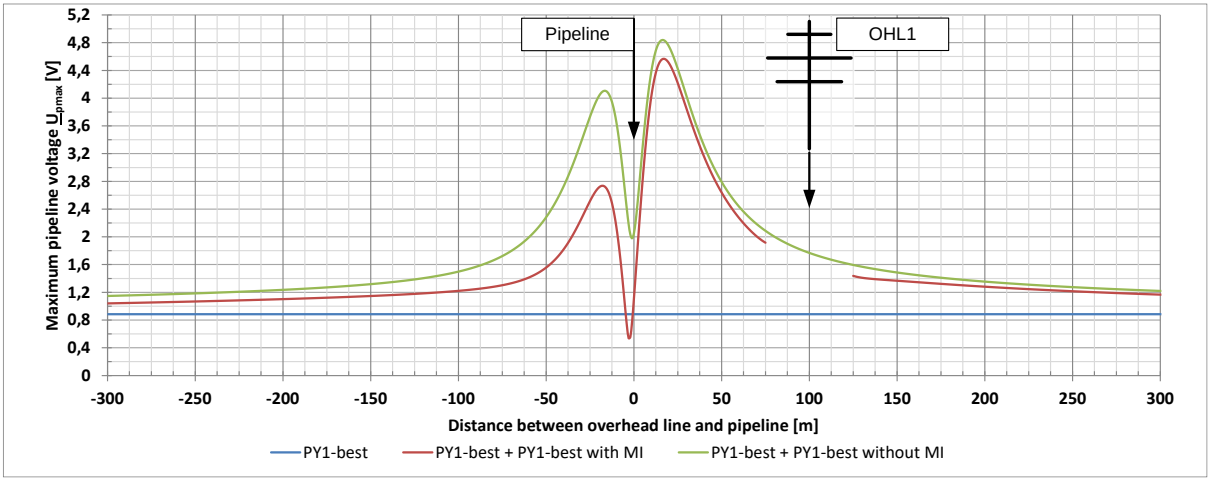

Figure 5-6: Maximum PIVs for the combination of PY1-best with PY1-best for the same current direction; enlarged view

Figure 5-7 shows the PIV for distances of +/- 500 m, when the phase current direction of OHL2 is reversed. This case is indicated in the legend with a **minus sign** ("-") between both pylon type descriptions. The full chart can be found in Appendix D.1, Figure D-1.

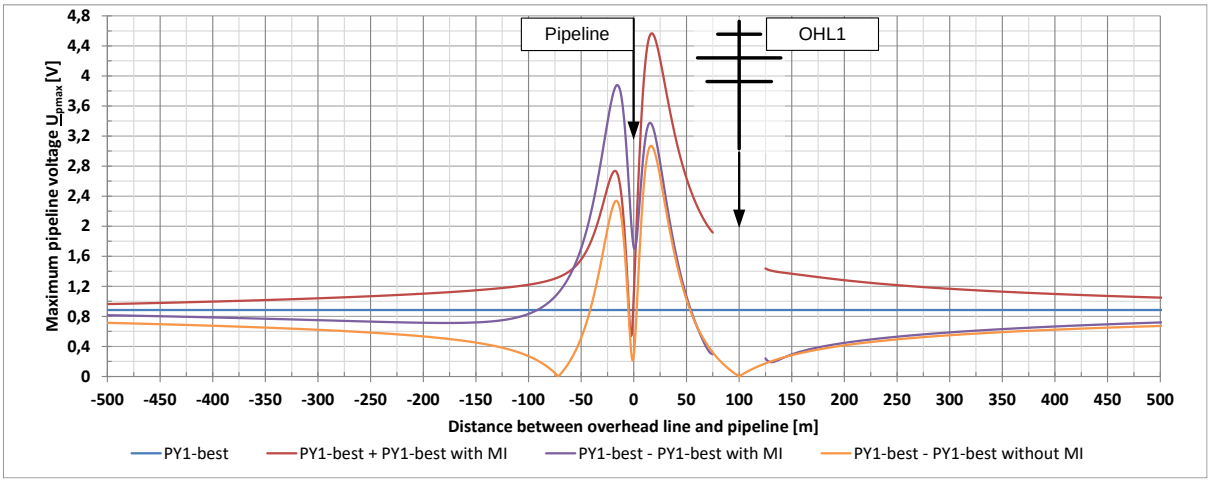

Figure 5-7: Maximum PIVs for the combination of PY1-best with PY1-best for the reversed current direction

As expected, the maximum pipeline interference voltage (PIV) for the reversed current direction of OHL2 is mostly lower because the influences partially cancel each other out. However, the focus in this graph lies in the comparison between not taking into account ("without MI") and taking into

account ("with MI") the inductive coupling between both OHLs. On the one hand, there is almost no cancelling each other out between both OHLs when OHL2 is near or to the right of OHL1. On the other hand, when OHL2 lies left of both other systems (distances smaller than -50 m), the added rotating fields of both OHLs are advantageous (violet line).

Figure 5-7 also shows the difficulty of the comparison between measurements in the field and calculations. Calculations have to always consider the worst-case scenario and therefore, the red line in this graph must always be calculated. For measurements, however, the actual phase current directions can be used, depending on the flow situation in two OHLs, which leads to either the red line or the violet line. For long-term-measurements both options are valid due to time-dependent current flow situations.

Assuming that OHL1 is +100 m and OHL2 is +50 m away from the pipeline, the maximum PIV can be calculated to either 2.6 Volt/km for the same current direction or 0.9 Volt/km for the reversed current direction. This case illustrates why PIV calculations can be three times higher than conducted measurements. At farther distances from OHL2, the difference between these two PIVs decreases but the maximum PIV also decreases due to lower interference. Therefore, the difference in the PIV due to the current direction is more important when OHLs and pipeline are situated in close proximity to each other.

Calculating the worst conductor configuration (CC) leads to completely different results than the calculation for the best CC above. Figure 5-8 shows the calculation for the worst CC for distances between +/-500 m, the full chart can be found in Appendix D.1, Figure D-2. Surprisingly, independent from the current direction of OHL2, both OHLs have no significant influence on each other because the curve progressions for "with MI" and "without MI" are almost identical.

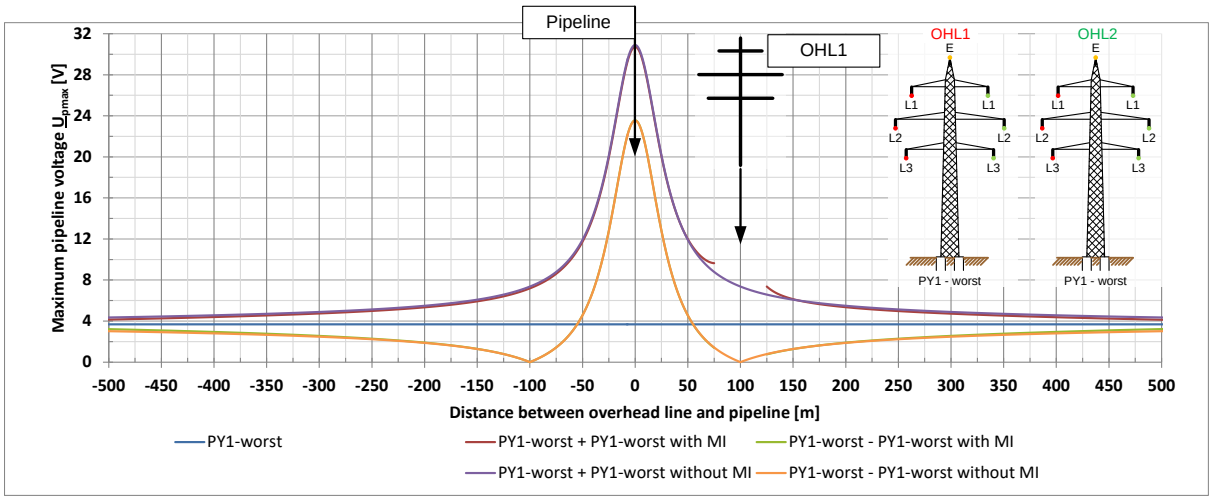

Figure 5-8: Maximum PIVs for the combination of PY1-worst with PY1-worst for the same and the reversed current direction

It is also interesting, how a “heavy” four-circuit-system affects an interference situation of an OHL with a “ton”-pylon and a parallel pipeline. For this case, pylon type PY6 is used for OHL2. The result of this calculation can be seen in Figure 5-9.

Such a high number of conductors and systems create a complex interference situation, which is best seen by looking at the red line which varies stronger in the close approach of OHL1 and OHL2. If both current directions of both OHLs are equal, taking into account the mutual coupling (“with MI”), the maximum PIV is reduced compared to the case “without MI”. This reduction is relatively constant but not very high. Nevertheless, a reduction effect is noticeable.

Reversing the current for OHL2 leads to a reduced PIV for all distances between OHL2 and the pipeline. Unfortunately, taking into account the mutual coupling (MI) leads to a higher PIV than without MI. Generally it can be said that both OHLs influence each other but to a lesser extent than could be expected.

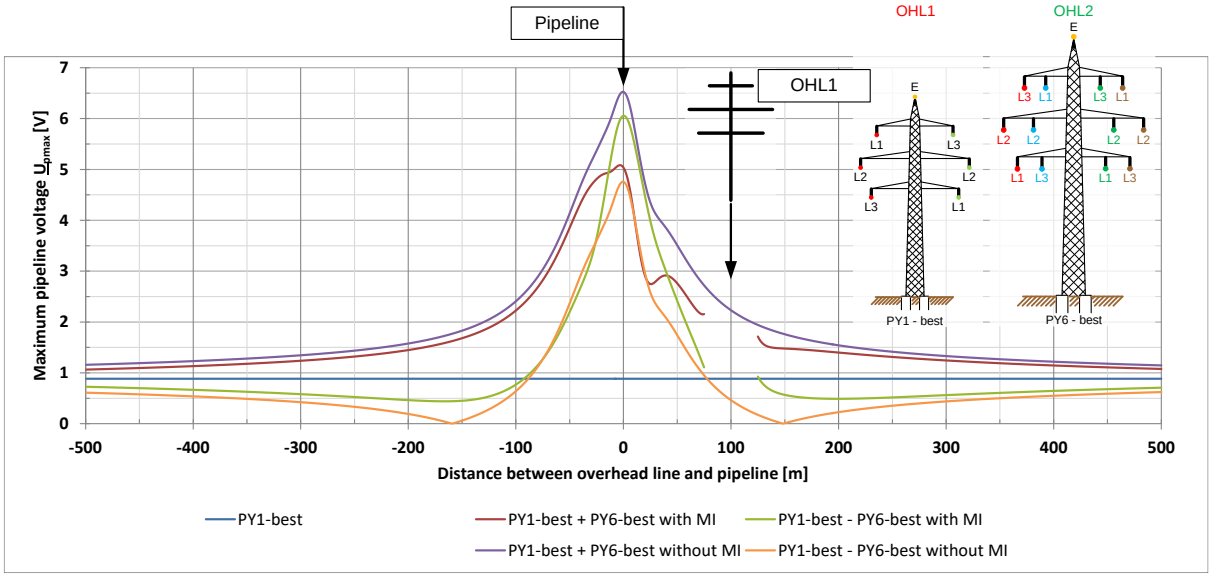

Figure 5-9: Maximum PIVs for the combination of PY1-best with PY6-best for the same and the reversed current direction

As mentioned above, there are countless possible combinations of parallel OHLs next to a pipeline and therefore very few can be described in this thesis. Additional examples in Appendix D.1 show that the PIVs are usually quite similar for different pylon types.

In summary, surprisingly, taking into account the mutual coupling with the MIs between OHLs leads to equal or marginally lower PIVs. Depending on the pylon type and phase current direction, the difference between with and without MI can be very large for the maximum PIV and can be a main reason, why it is so difficult to compare measurements in the field to calculations.

5.3 One overhead line next to one pipeline and several metallic structures

This chapter discusses the case in which one overhead line (OHL), one pipeline and metallic structures are located next to each other. Countless possibilities of combinations are possible and thus, only some typical combinations can be reviewed in this chapter. In these calculation examples, the buried metallic structures consist of steel but in reality, several other metals are possible. Figure 5-10 shows an example with one OHL in the "ton"-pylon configuration next to a non-parallel pipeline and a complex buried metallic structure. Again, all structures are coupled together with the mutual couplings $\underline{Z}_{xxx}$.

The buried metallic structures are called screening conductors (SCs) because they can have a good or bad screening factor and can amplify or reduce pipeline interference voltages (PIVs). When such a buried metallic structure is large enough, it is named as a global earthing system, as is the case in (sub-)urban areas. In this thesis, such large metallic structures cannot be investigated methodically because they have different shapes, dimensions, materials, metallic structure density and so on and therefore, simplifications are needed.

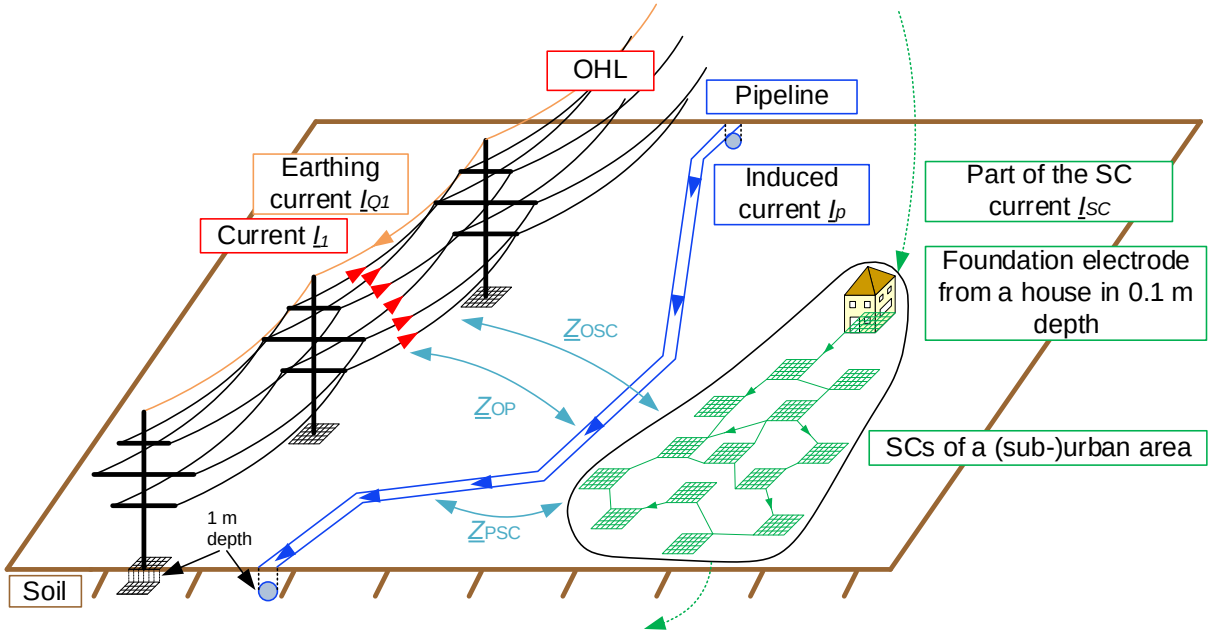

OHL:	Overhead line; setup and material the same as in chapter 4.1 but different pylon types are used
SC:	Screening conductors are secondary metallic structures which influence the PIV
$\underline{I}_1$:	Phase conductor currents in the OHL
$\underline{I}_{Q1}$:	Earth conductor current in the OHL
$\underline{I}_P$:	Induced current which flows along the pipeline
$\underline{I}_{SC}$:	Induced current which flows along the screening conductor
$\underline{Z}_{OP}$:	MI between pipeline and OHL
$\underline{Z}_{PSC}$:	MI between pipeline and screening conductor
$\underline{Z}_{OSC}$:	MI between OHL and screening conductor

Figure 5-10: One parallel OHL with a "ton"-pylon next to one non-parallel pipeline and a metallic structure in the soil

For easier comparison of the impact of different sized metallic structures, it is necessary that all systems are parallel to each other, as shown in Figure 5-11. The OHL and pipeline configuration from the standardized example in chapter 4.1 are used, which means that the distance x_{ik} is again fixed to 100 m and the pylon type PY1 with the best CC is used.

The additional screening conductors (SCs) consist of steel and are buried in a depth of 0.1 m and each conductor has a diameter D_{sc} of 50 mm. In order to analyse the influence of the dimensions of the SCs on the PIV, both the length ℓ_{sc} and width X_{sc} must be varied. The width of SCs can be simulated by placing several conductors parallel to each other with a distance d_{sc} of 2 m between them. The figure below, for example, includes four conductors plotted which leads to a SC with a width of 6 m.

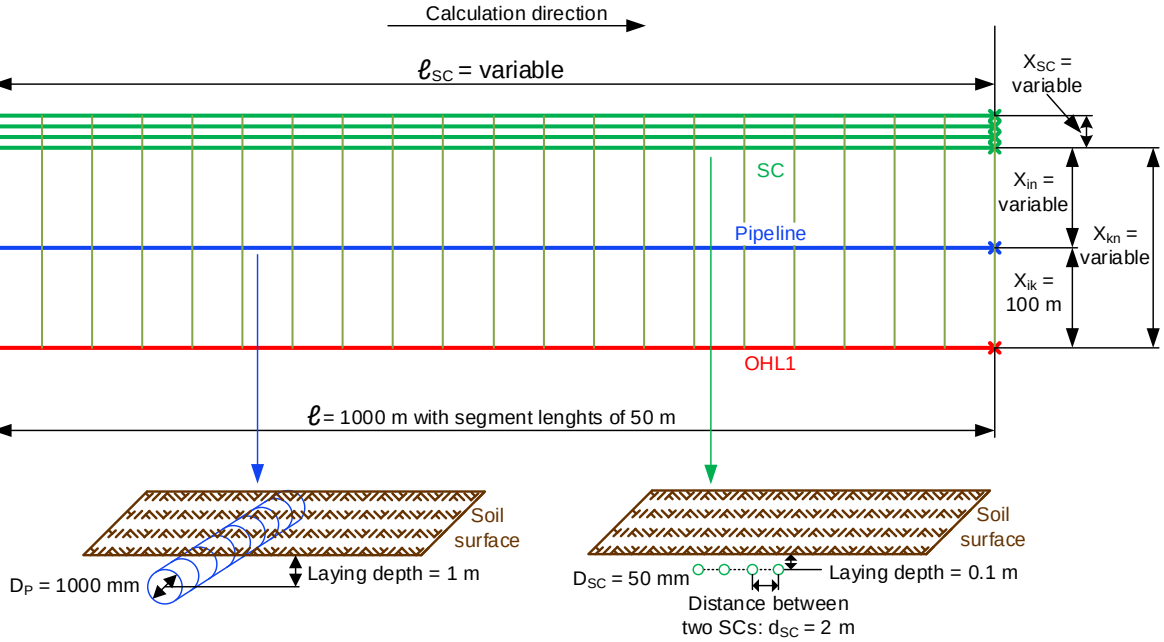

x_{ik}:	Distance between pipeline and OHL; this distance is fixed
x_{in}:	Distance between pipeline and screening conductor; the distance is variable
x_{kn}:	Distance between OHL and screening conductor; this distance is variable
x_{SC}:	Width of the screening conductor; the width is variable
ℓ_{SC}:	Length of the screening conductor; the length is variable
d_{SC}:	Distance between two single screening conductors

Figure 5-11: Geometrical parameters for examples with OHL, pipeline and screening conductor

Calculating the maximum PIV for this combination with a varying SC length ℓ_{sc} between 10 and 1000 m leads to Figure 5-12. The different calculated SC lengths are displayed in the key. In addition, a case without the SC is considered. It can be clearly seen that the influence of a screening conductor is mostly limited to distances x_{km} of approximately +/- 500 m. Therefore, it makes sense to give an enlarged view of this area.

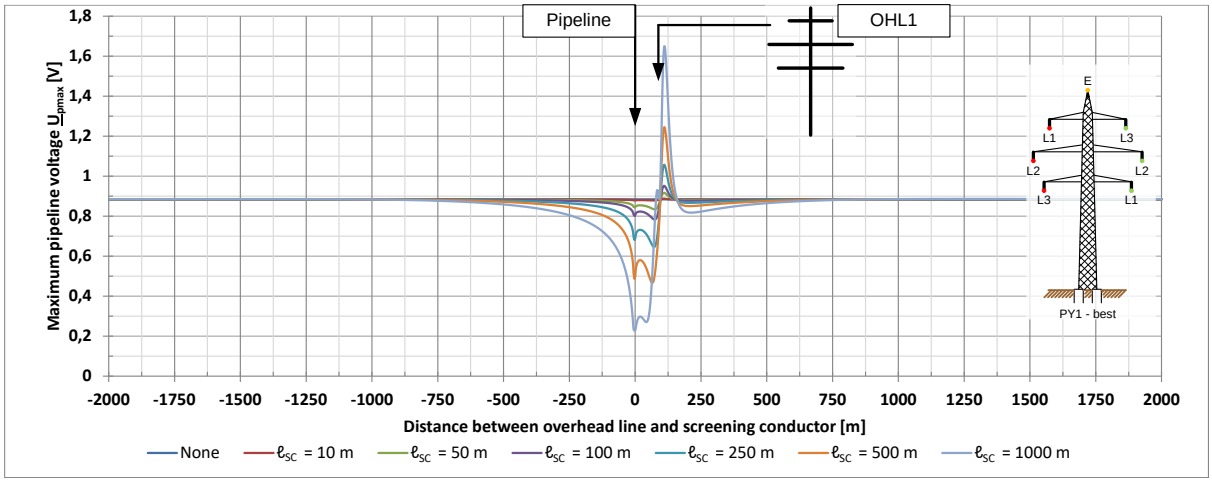

Figure 5-12: Maximum PIVs for the combination of OHL (PY1-best) and a SC with a width of 6 m (4 conductors) for different SC lengths ℓ_{SC}

Figure 5-13 shows the same calculation for distances of +/- 500 m and now, more details can be seen. The length of the screening conductor has a direct influence on the PIV which increases with a rising length. In order to obtain a relatively high influence, the SC length must have a certain size which in this example is longer than 100 m.

When a SC with a width of 6 m lies directly above the pipeline (distance = 0 m) and has a length of 1000 m, then the PIV is massively reduced from 0.88 Volt to 0.23 Volt. Near the OHL, the SC can either amplify (distance = 110 m) or reduce (distance = 70 m) the PIV. Therefore, the best solution is to bury the SC near the pipeline at a distance of between +70 and -200 meters. In some cases, it is possible to bury screening conductors next to a pipeline during the construction phase because a later installation is too cost-intensive. In most cases, however, this is not possible because screening conductors belong to buildings and other structures and hence, their locations are fixed. These "unwanted" SCs must therefore still be considered regardless of their position and size.

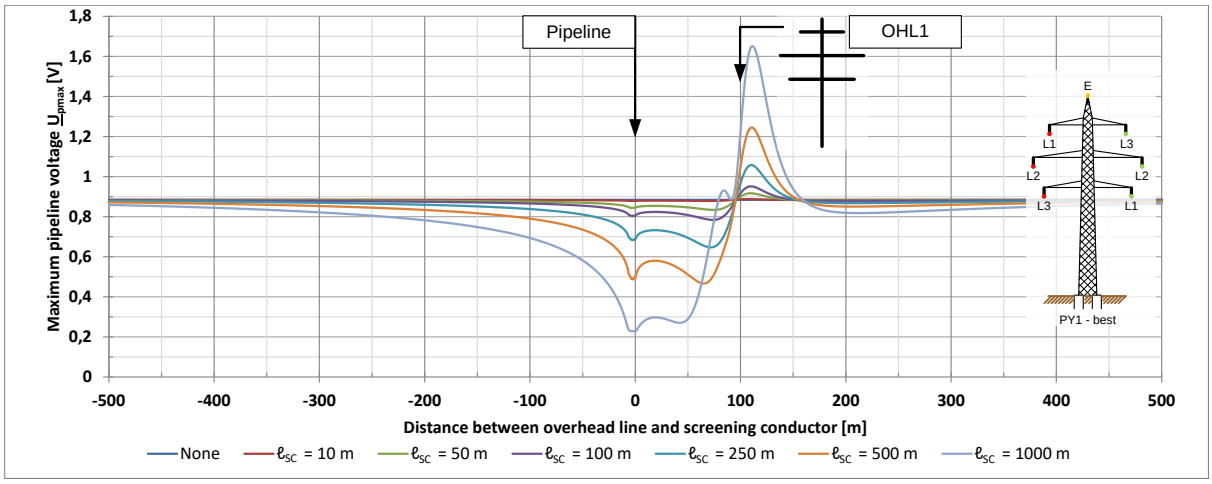

Figure 5-13: Maximum PIVs for the combination of OHL (PY1-best) and a SC with a width of 6 m (4 conductors) for different SC lengths; enlarged view for distances between +/- 500 m

The length of the screening conductor is not the only key parameter. Figure 5-14 shows that a better reduction effect can be achieved, in particular in the area of the pipeline, with a larger width of the SC. Unfortunately, this is not fully correct because, as the figure shows, a SC with a width of 58 m (30 conductors) does not further reduce the PIV with a rising number of conductors.

Such a larger screening conductor simulates a smaller village with a global earthing system, which can often be found in practice. The reason is quite simple. Each SC is influenced by the OHL and thus, a SC becomes to a current-carrying-conductor which is also an active conductor, similar to an OHL. As a result, the SC influences the pipeline in return. When more parallel conductors are placed, increasing the width of the SC, as a consequence, more conductors influence the pipeline with the outcome of a possibly higher PIV.

This effect can be seen in the curve shape of the SC with the width of 58 m, which is different to the other calculation examples. In general, however, even such big screening conductors mostly reduce the PIV, except in especially unfavourable distance configurations, such as distances of around 105 m.

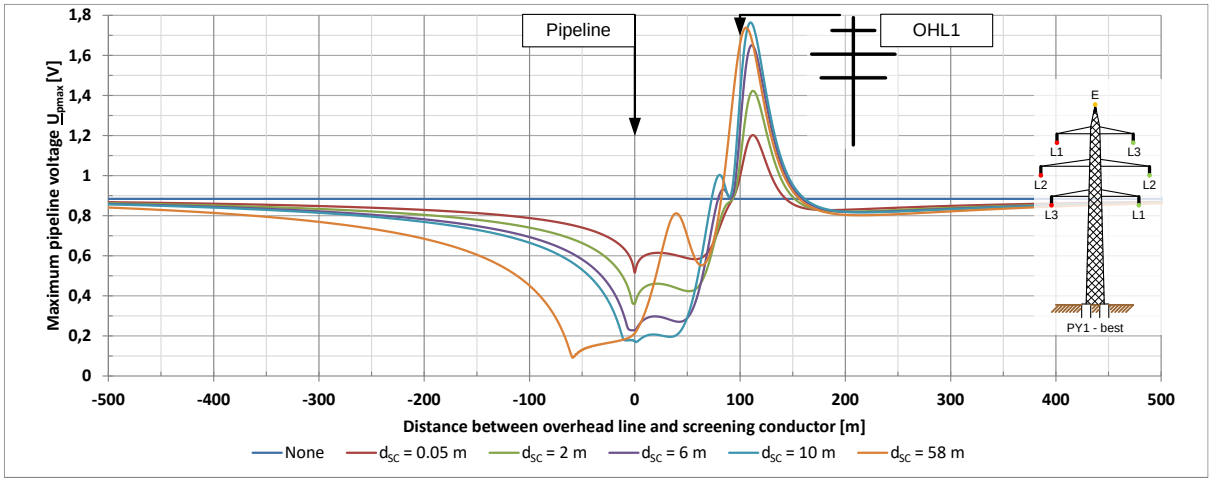

Figure 5-14: Maximum PIVs for the combination of OHL (PY1-best) and a SC with a length of 1000 m for different SC widths

The pylon type PY1 with the worst CC with a SC shows surprising results. Figure 5-15 shows that the SC can always greatly reduce the PIV, with one exception. If the length of the SC is long enough and lies next to the OHL, then an amplifying effect appears. A possible reason is the ratio of the size of the metal surface between the pipeline and the SC.

When the size of the surface of the SC compared to the surface of the pipeline is large enough when the SC lies at the right distance to the OHL, the SC is influenced stronger. This may lead to a higher PIV than without the SC. This figure shows that even the smallest metal structures nearby can influence the PIV in the case of unfavourable CCs.

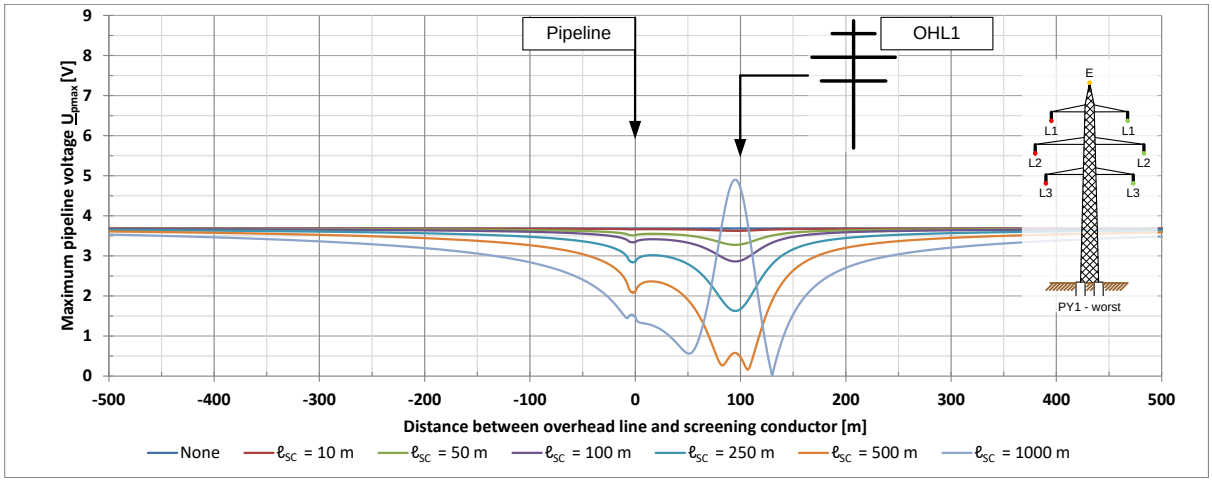

Figure 5-15: Maximum PIVs for the combination of OHL (PY1-worst) and a SC with a width of 6 m (4 conductors) for different SC lengths; enlarged view for distances between +/- 500 m

When the width of the SC is varied for the pylon PY1-worst, the results resemble the results for PY1-best. Figure 5-16 shows differences only in the close vicinity of the OHL and for larger widths of the SC (d_{SC} = 58 m) with a higher amplifying factor on the PIV of the pipeline.

This distinct difference shows the effect on the PIV due to the ratio between the size of the surfaces of the pipeline and the SC because especially the large SC has a greatly enlarged surface. However, in principle, this result shows that the reduction or amplifying factor of a SC is nearly independent of the conductor configuration (CC) of this pylon.

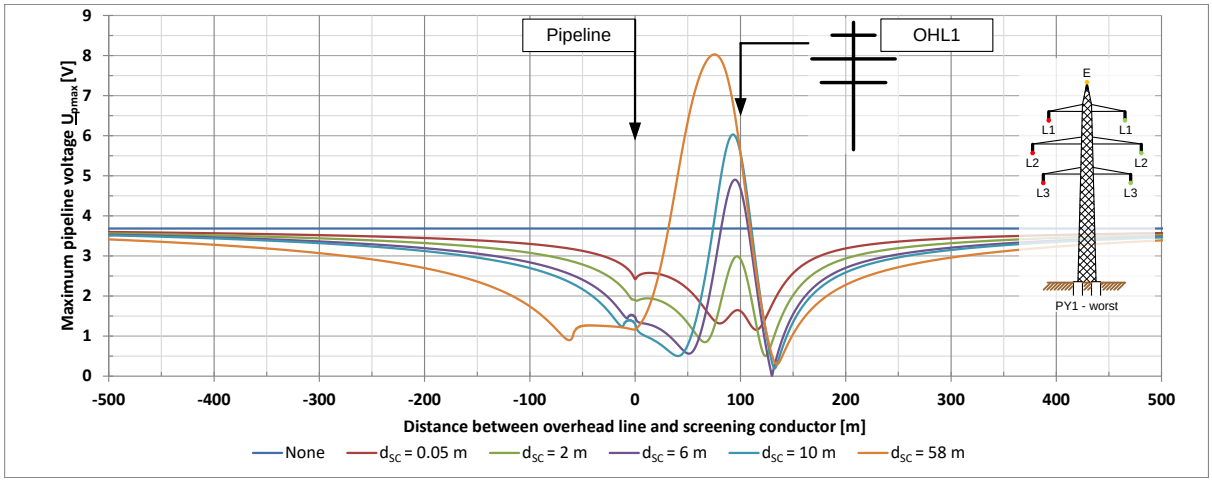

Figure 5-16: Maximum PIVs for the combination of OHL (PY1-worst) and a SC with a length of 1000 m for different SC widths

5.4 Two overhead lines next to one pipeline and several metallic structures

This chapter will discuss complex interference situations, a combination of chapters 5.2 and 5.3. The crucial problem for this thesis is that unlimited combinations of pylon types, current direction, conductor configurations, pipeline parameters, metallic structure dimensions and a variety of other parameters are possible.

Especially when considering the many coupling impedances, it becomes clear that the complexity and thus also the computational effort increases sharply. Therefore, this chapter will narrow down the possibilities to show the impact of to the different parameters on the pipeline interference voltage (PIV). Figure 5-17 shows a combined example, where a pipeline is situated next two overhead lines (OHLs) with "ton"-pylons and a buried metallic structure, which is used as a screening conductor (SC). All the symbols (currents, mutual coupling impedances) used in the previous two chapters remain the same. Because all mutual interferences (MIs) between all systems are considered and calculated, the figure shows a strongly increasing number of couplings.

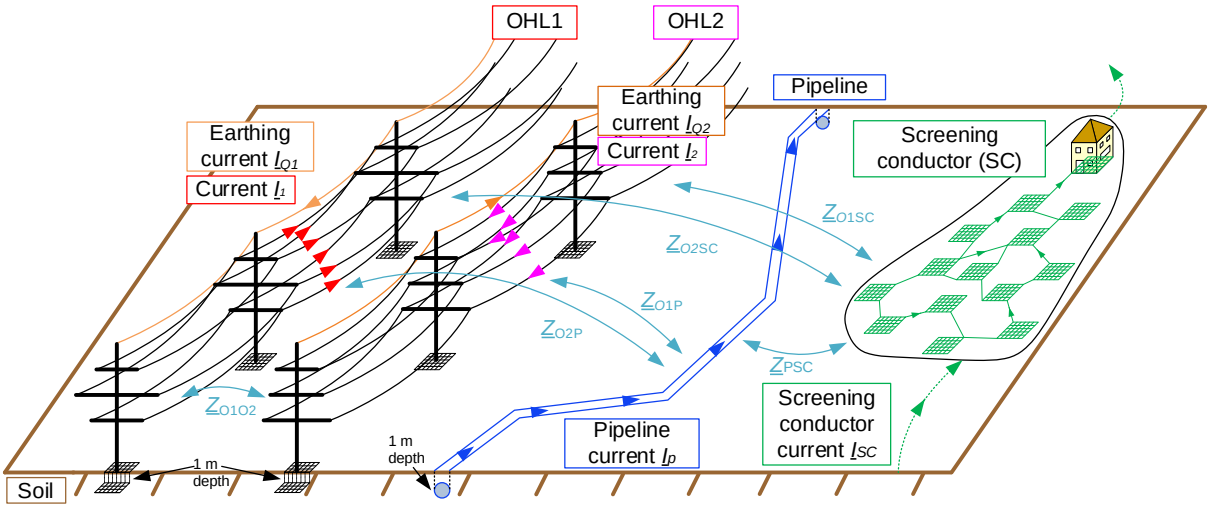

OHL1/OHL2:	Overhead lines; setup and material the same as in chapter 4.1 but different pylon types are used
SC:	Screening conductors are secondary metallic structures which influence the PIV
I_1/I_2:	Phase conductor currents in the OHL1/OHL2
I_{Q1}/I_{Q2}:	Earth conductor currents in the OHL/OHL2
I_P:	Induced current which flows along the pipeline
I_{SC}:	Induced current which flows along the screening conductor
Z_{O1P}:	MI between pipeline and OHL1
Z_{O2P}:	MI between pipeline and OHL2
Z_{PSC}:	MI between pipeline and screening conductor
Z_{O1O2}:	MI between OHL1 and OHL2
Z_{O1SC}:	MI between OHL1 and screening conductor
Z_{O2SC}:	MI between OHL2 and screening conductor

Figure 5-17: Two parallel OHLs next to one non-parallel pipeline and a metallic structure in the soil

5.4.1 Variable distance for the secondary overhead line

To compare the impact of the complex interference situation, all systems are considered to be parallel to each other. This standardized example from chapter 4.1 assumes that the distance x_{ik} between the pipeline and OHL1 is fixed to 100 m and that the pylon type PY1 ("ton"-pylon) is used. Additionally, a second OHL2 with a full parallel route is used and the distance to pipeline (x_{im}), OHL1 (x_{km}) and SC (x_{mn}) is varied in this example.

The last element is the same SC from chapter 5.3 with a length of 1000 m. The distance x_{in} to the pipeline is fixed to 2.5 m and thus, the distance to the OHL1 is also fixed. The width X_{sc} of the SC can be simulated by placing several conductors parallel to each other with a distance d_{sc} of 2 m each. For example, the figure below shows four conductors which results in a SC with a width of 6 m. The width of the SC is calculated for 1 conductor (X_{sc} = 0.05 m) and 4 conductors (X_{sc} = 2 m).

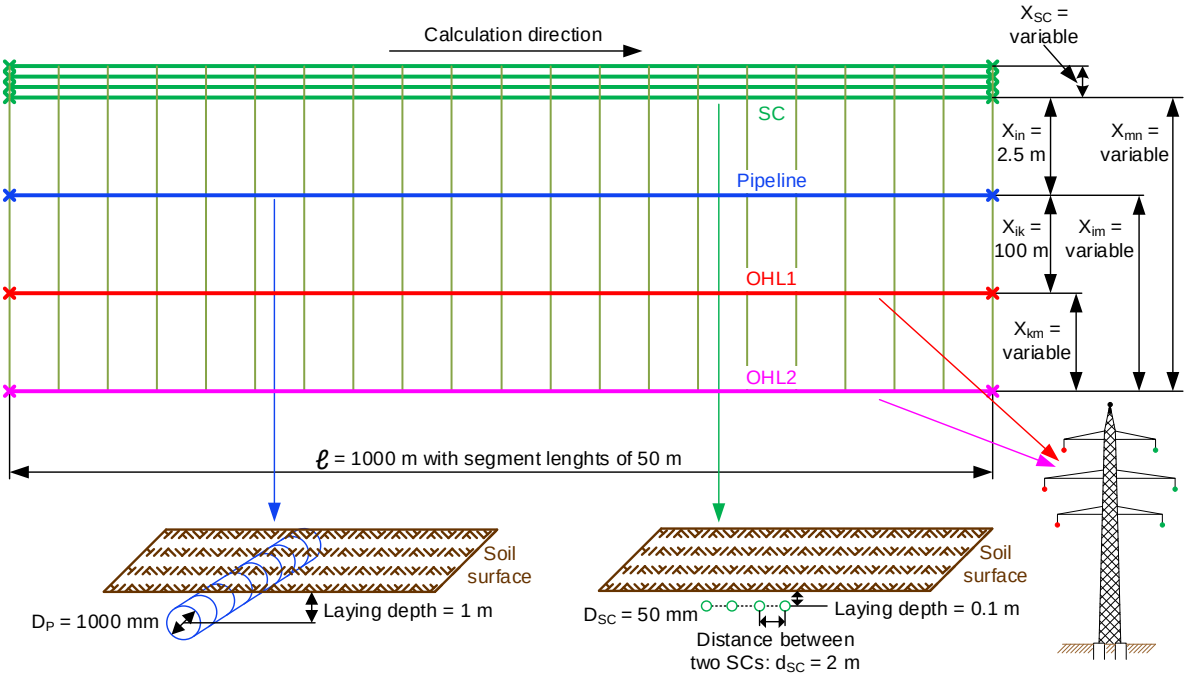

x_{ik}:	Distance between pipeline and OHL1; this distance is fixed
x_{in}:	Distance between pipeline and screening conductor; the distance is fixed
x_{km}:	Distance between OHL1 and OHL2; this distance is variable
x_{kn}:	Distance between OHL1 and screening conductor; this distance is variable
x_{mn}:	Distance between OHL2 and screening conductor; this distance is variable
x_{sc}:	Width of the screening conductor; the width is variable
d_{SC}:	Distance between two single screening conductors

Figure 5-18: Geometrical parameters for an example with two OHLs, a pipeline and a screening conductor when varying the distance of OHL2

For the first example, two "ton"-pylons with the best conductor configuration (CC) are used for OHL1 and OHL2 and are identical to the pylon in chapter 4.6.3.1 ("PY1-best"). As usual, the maximum PIV is calculated for a distance of -2000 to +2000 m between OHL2 and pipeline.

Figure 5-19 only shows the interesting part of this calculation: The blue line ("PY1-best") shows the value, when only OHL1 influences the pipeline in a distance of 100 m and the value of the PIV is identical to the standardized example of chapter 4.1. The red line ("PY1-best + PY1-best) is the same red line (PY1-best + PY1-best with MI") as in Figure 5-6 because it is the same calculation.

The more interesting curve progression of the PIV takes into consideration the screening conductors. Comparing the red (none SC), green (1 SC) and yellow line (4 SC), the PIV is reduced constantly by using more and more SCs over the entire calculation range. This means that the selected distance of the SC of 2.5 m distance to the pipeline is very well chosen because the PIV is almost always reduced regardless of the distance from OHL2 to the pipeline.

The calculations also show that the increasing effect on the PIVs from OHL2 takes place within 300 meters and slowly decreases to constant values. These constant values are the same as calculated in chapter 5.3 for Figure 5-14 for the distance of 2.5 m between pipeline and a SC length d_{SC} of 0.05 m (red curve) and 2 m (green curve).

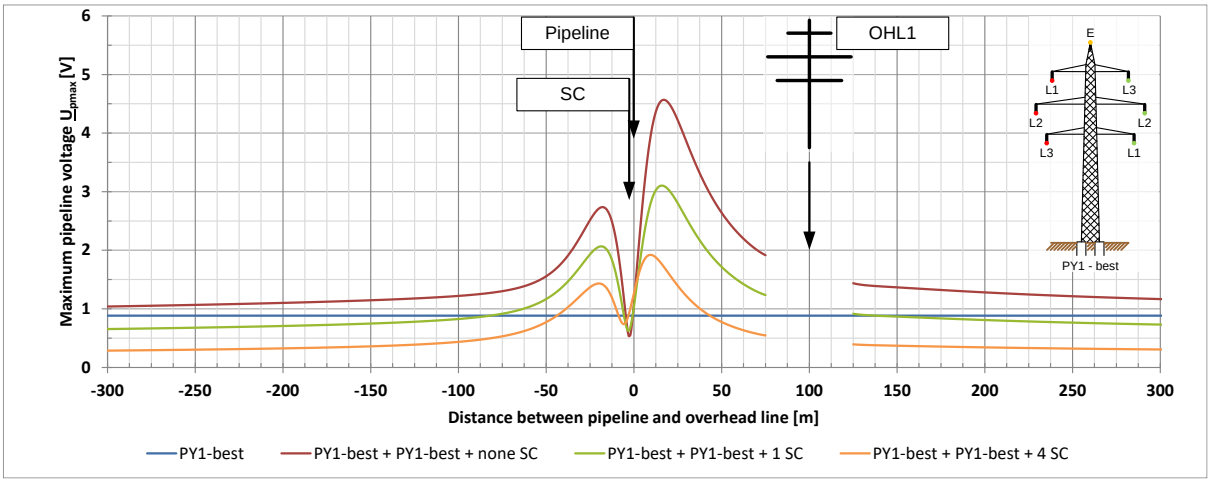

Figure 5-19: Maximum PIVs for the combination of two OHLs with the pylon-type PY1-best and with or without differently sized SC when the distance to OHL2 is varied

Figure 5-20 shows a similar example but for the worst CC of PY1 ("PY1-worst"). This has already been described in detail in chapter 4.6.3.1: The blue line shows the maximum PIV for the OHL in in a distance of 100 m to the pipeline. The red line ("PY1-worst + PY1-worst") is the same red line ("PY1-worst + PY1-worst with MI") as in Figure 5-8. Again, the position of the SC is chosen well because the PIV decreases with an increasing number of SCs (none – one – four). Furthermore, both curves with SC (green and orange lines) reach a constant value at a distance of more than 300 m, which is the same as in Figure 5-16 for the distance of 2.5 m between pipeline and the corresponding SC length.

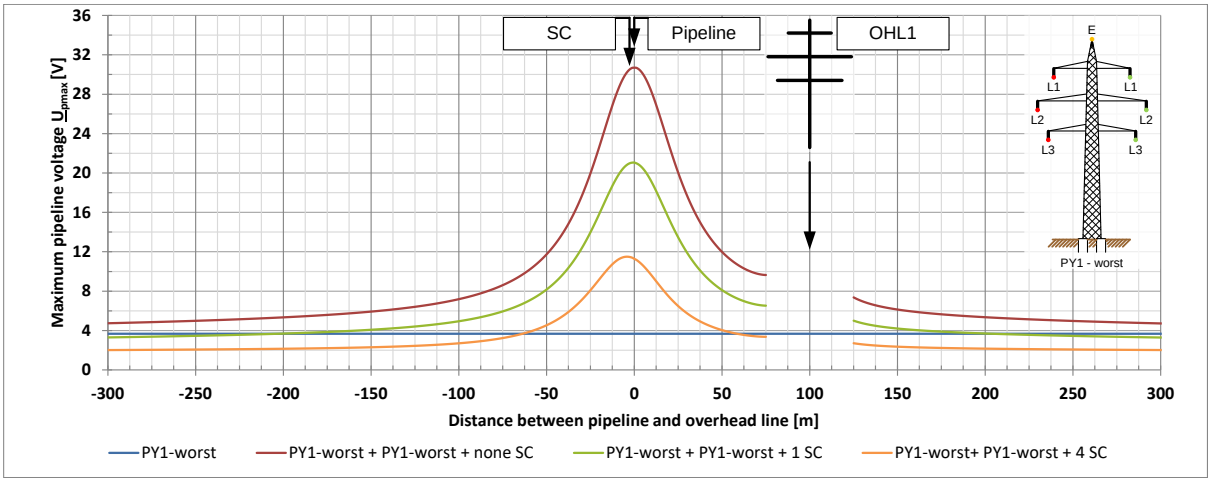

Figure 5-20: Maximum PIVs for the combination of two OHLs with the pylon-type PY1-worst and with or without differently sized SC when the distance of OHL2 is varied

It seems that the ratio of the PIV when using none, one, and four SCs remains roughly the same over the entire calculation range and individual results from these calculations confirm the results of other chapters. These finding mean that it may be possible to split the calculations into two halves according to the following method: One calculation can be used to find the amplifying or reducing screening factor of the SC on the PIV. This result can be used for the second calculation of the combination of PIV and OHLs. The screening factor can be integrated later. This reduces the calculation effort.

To verify this, taking a ratio for all above discussed curve progressions from Figure 5-19 and Figure 5-20 is crucial. According to the following formula (5-15), each distance step between pipeline and OHL2 is calculated, which leads to Figure 5-21.

$$Ratio1 = \frac{"PY1-best\ +\ PY1-best\ +\ 1\,SC"}{"PY1-best\ +\ PY1-best\ +\ none\,SC"} \qquad Ratio2 = \frac{"PY1-best\ +\ PY1-best\ +\ 4\,SC"}{"PY1-best\ +\ PY1-best\ +\ none\,SC"}$$

$$Ratio3 = \frac{"PY1-worst\ +\ PY1-worst\ +\ 1\,SC"}{"PY1-worst\ +\ PY1-worst\ +\ none\,SC"} \qquad Ratio4 = \frac{"PY1-worst\ +\ PY1-worst\ +\ 4\,SC"}{"PY1-worst\ +\ PY1-worst\ +\ none\,SC"} \qquad (5\text{-}15)$$

The result shows that for a rough calculation, this simple way is possible. It cannot, however, be recommended for exact calculations because the ratio is not constant over the full calculation range. Regardless of whether two parallel OHLs with PY1-best or PY-worst influence the pipeline, the ratio is always lower than 1 except for one short range when using SCs on the correct position. It also shows that regardless of the conductor configuration in the same pylon type, the reduction effect is roughly similar with the same number of SCs.

In summary, it can be said that a screening conductor in the right position always reduces the PIV but the reduction effect is not constant when a secondary OHL influences the pipeline. It is thus shown that the result of the calculation can no longer be exactly predicted in more complex situations.

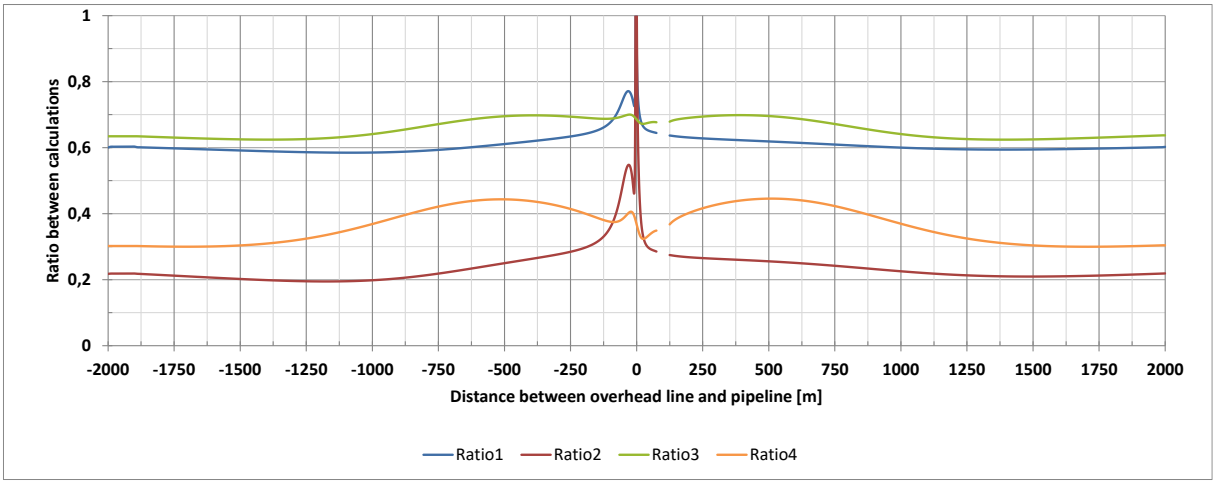

Figure 5-21: Ratio for the PY1-best and PY1-worst between none, one and four SCs

5.4.2 Variable distance for the screening conductor

For these calculations, the second overhead line (OHL) is now fixed to a distance of x_{km} =100 m to OHL1 and $x_{ik} + x_{km}$ = 200 m to the pipeline. All other distances are variable because the distance x_{in} of the SC to the pipeline is varied. Both OHLs are type PY1 (“ton”-pylon) and all other parameters of the pipeline and the screening conductor (SC) remain unchanged. Again, in this calculation, the width of the SC is 1 conductor (X_{SC} = 0.05 m) and 4 conductors (X_{SC} = 2 m).

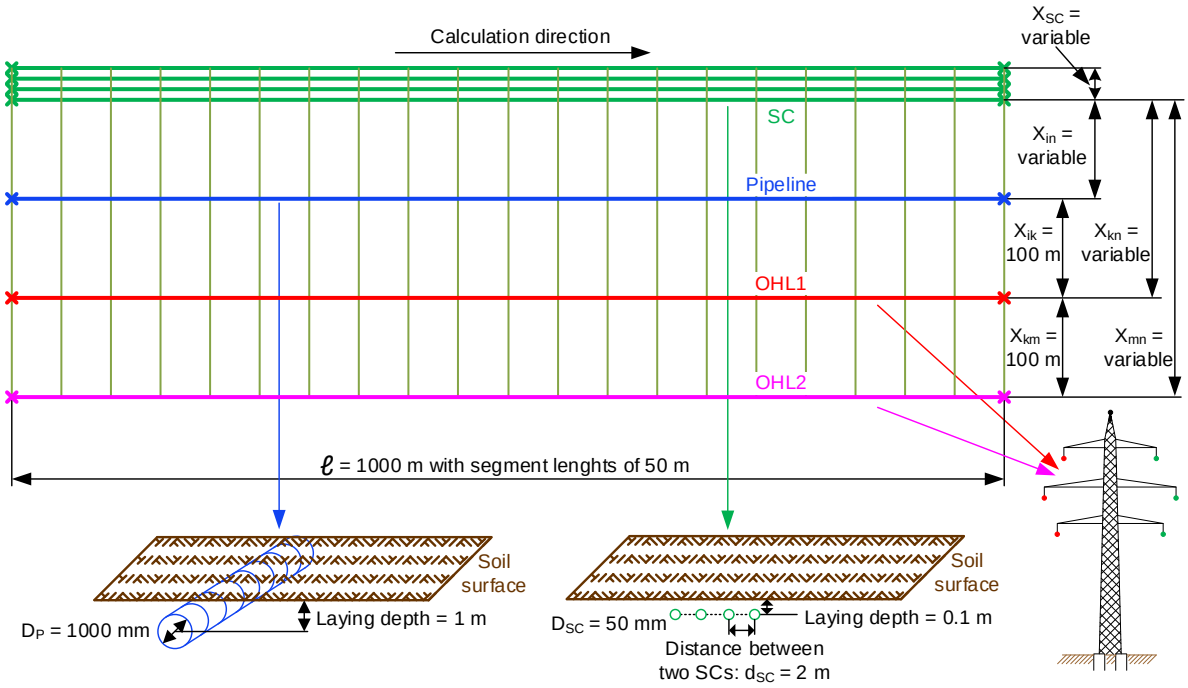

x_{ik}:	Distance between pipeline and OHL1; this distance is fixed
x_{in}:	Distance between pipeline and screening conductor; the distance is variable
x_{km}:	Distance between OHL1 and OHL2; this distance is fixed
x_{kn}:	Distance between OHL1 and screening conductor; this distance is variable
x_{mn}:	Distance between OHL2 and screening conductor; this distance is variable
x_{sc}:	Width of the screening conductor; the width is variable
d_{SC}:	Distance between two single screening conductors

Figure 5-22: Geometrical parameters for an example with two OHLs, a pipeline and a screening conductor when varying the distance of the screening conductor

For the calculation with the above defined parameters, the best conductor configuration (CC) for the "ton"-pylon ("PY1-best") is used first. This leads to Figure 5-23 where the maximum pipeline interference voltages (PIVs) for the varying distance between pipeline and screening conductor (SC) of -100 m to 300 m are shown.

As usual, calculations are done for distances of +/- 2000 m but this figure shows an enlarged view of the most interesting results. The blue line is the reference value when calculating the maximum PIV without SC and gives same result as the red curve in Figure 5-6 for a distance of 200 m between pipeline and overhead line (OHL). The red and green lines in the figure below approach this value at a distance of around +/- 750 m.

When comparing these curves to Figure 5-14, it turns out that despite the second OHL, there is little change in the voltage curve except for near OHL2. Therefore, it can be concluded that in this example, the SCs have a similar reduction effect on the PIV except for in the vicinity of the OHLs despite the increasing number of OHLs. This opens up the possibility of performing the calculations separately. However, the additional influence of OHL2 must still be taken into account and thus it is less difficult to calculate all conductors in one go than performing separate calculations.

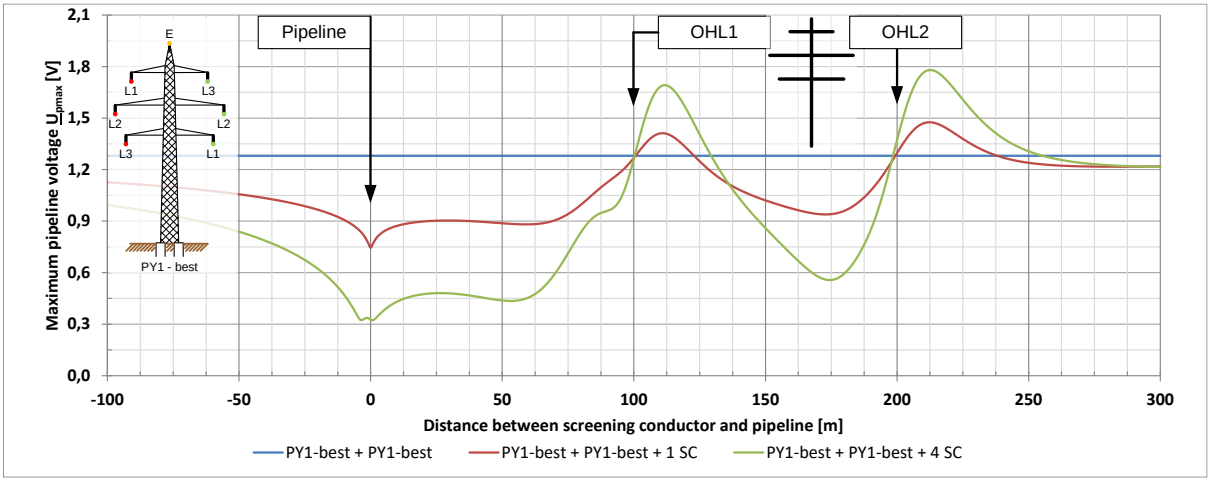

Figure 5-23: Maximum PIV for the combination of two OHLs (PY1-best) on the same side of the pipeline and a SC for different SC widths

Moving the second OHL (OHL2) to the other side of the pipeline, at a distance of 100 m, the overall reduction effect of the SC does not change significantly, except for near OHL2. This can be seen when comparing Figure 5-23 and Figure 5-24, especially in the vicinity of the pipeline but also across the full range of the calculation.

Both figures also show that increasing the number of SCs and thus, adding bigger metallic structures, generally leads to a stronger reduction effect on the PIV. It can also have a stronger amplifying effect if the metal structures are close the OHLs.

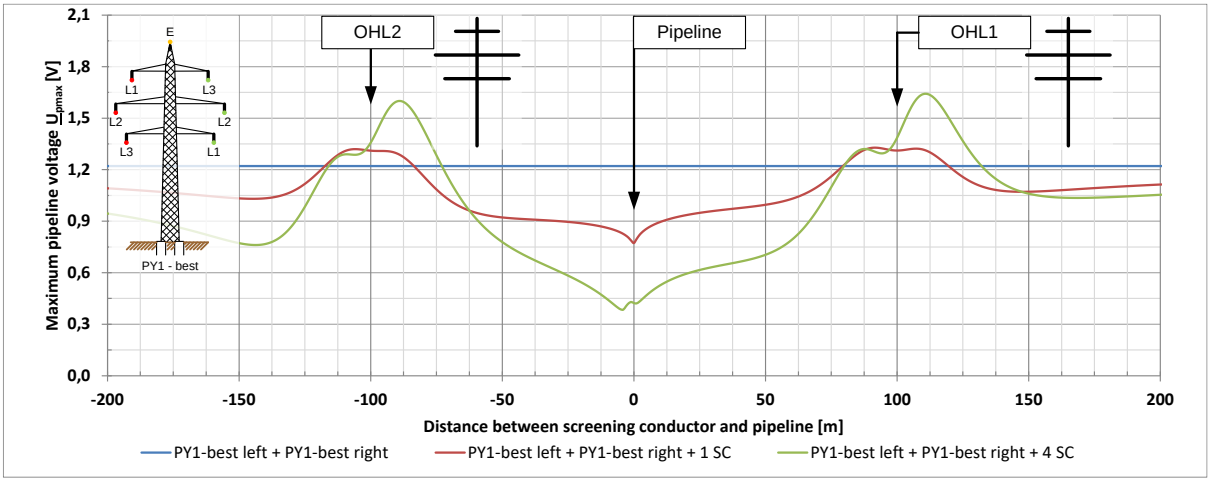

Figure 5-24: Maximum PIV for the combination of two OHLs (PY1-best) on each side of the pipeline and a SC for different SC widths

Using the initial calculation model from Figure 5-22 with two overhead lines (OHLs) on the same side but including the worst conductor configuration (CC) of the “ton”-pylon (“PY1-worst”), leads to Figure 5-25. The blue line indicates the pipeline interference voltage (PIV) when no screening

conductor (SC) is nearby. This offers the same result as the red curve in Figure 5-8 for a distance of 200 m between pipeline and OHL. Again, the calculated red and green line in the figure approach this value in a distance of around +/- 750 m.

When comparing these voltage curves to those of Figure 5-16, it turns out that despite the second OHL, there is little change in the voltage curve except for in the vicinity of OHL2. A minor difference can be seen next to the pipeline because in Figure 5-16, when using 4 conductors (X_{SC} = 2 m), the PIV decreases while in Figure 5-25, the PIV is shaped like a dome.

This result corresponds to the calculation in Figure 5-16 when more conductors (X_{SC} = 6 m and more) are used. This can be explained by the fact that more current flows in the SC due to the higher interference and thus the additional influence of the SC is higher than the reduction effect of the SC. To completely cancel out the reduction effect, an even greater interference of high voltage power systems (HVPSs) is necessary. It turns out that it may be possible that an SC near a pipeline increases the PIV.

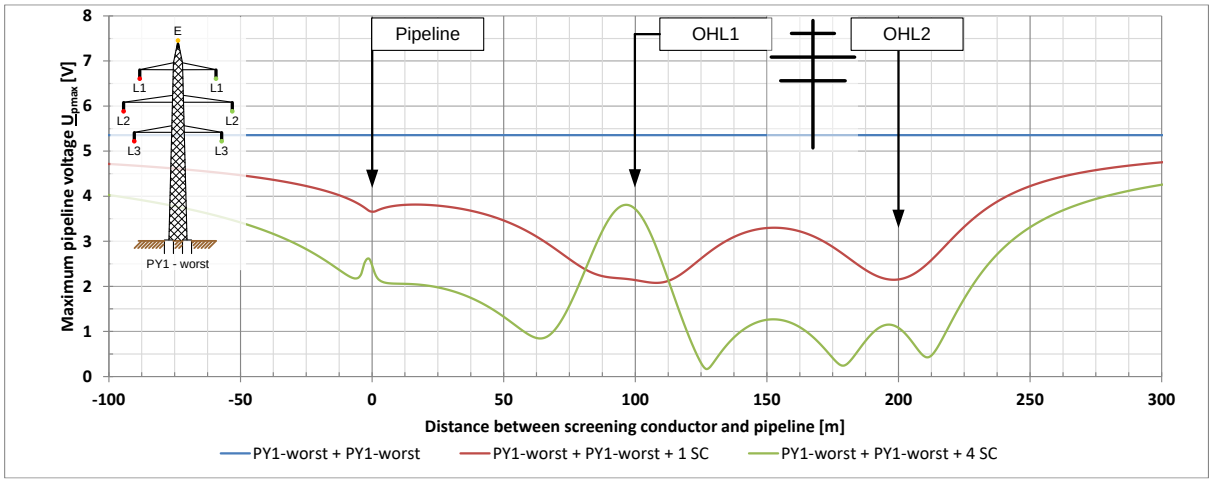

Figure 5-25: Maximum PIV for the combination of two OHLs (PY1-worst) on the same side of the pipeline and a SC for different SC widths

In summary, moving the SC nearer to the pipeline has a stronger effect on the pipeline than the position or the number of OHLs, as can be seen in chapter 5.3 and this chapter. It has been shown that the surrounding metallic structures have a significant effect on the PIV and that they can be an underlying reason why calculations are higher than measurements. Often, SCs reduce the PIV especially when the SC lies near the pipeline. However, under certain conditions, SCs can also have an amplifying effect, especially when SCs are located near an OHL. This conclusion is completely independent of the number of influencing sources. Unfortunately, it is very difficult to determine the geography and structure of the metallic structures and to insert them in the calculations. It has also been shown that it is theoretically possible to split the calculations up for many parallel conductors, but the effort is much less to calculate them in one go.

5.5 One overhead line next to two pipelines

This small subchapter is necessary because energy routes have already been bundled in the past for various reasons and this bundling of energy routes is about to be intensified in the present and future. As a result, it often happens that several pipelines are buried parallel to each other. This has its advantages, but, with regard to the electrical characteristics of a pipeline, it can lead to disadvantages. One of these disadvantages is the dependence on each other in case of inductive interference. This effect has never been considered or scientifically studied.

As the previous chapters show with the calculation of the influence of SCs on the PIV, similar dependencies can occur with pipelines. This chapter looks at two pipelines that are located next to an overhead line (OHL), as shown in Figure 5-26. Overall, the calculations are the same as in the chapters above and therefore all mutual couplings $\underline{Z}_{xxx}$ can again be used. In contrast to the directly grounded metallic structures in the previous chapters, the second pipeline has a pipeline coating and therefore the pipeline is isolated from the soil. In addition, pipelines usually have larger diameters and rarely more than two of them are located parallel to each other.

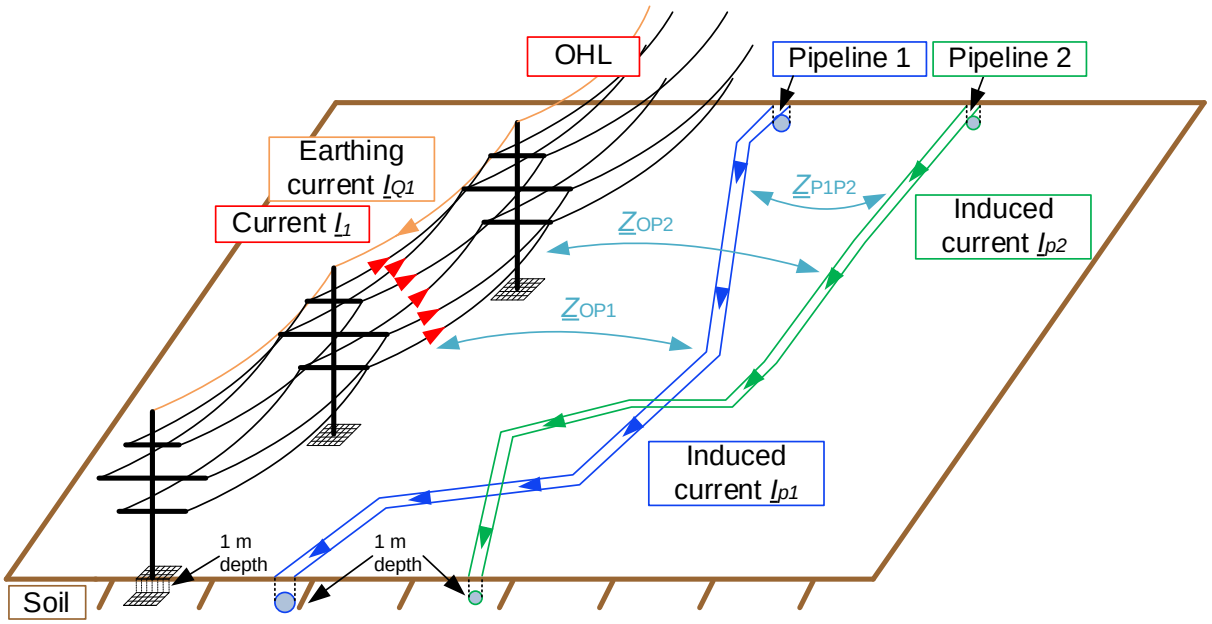

OHL:	Overhead line; setup and material the same as in chapter 4.1; different pylon types are used
$\underline{I}_1$:	Phase conductor currents in the OHL
$\underline{I}_{Q1}$:	Earth conductor current in the OHL
$\underline{I}_{p1}$/ $\underline{I}_{p2}$:	Induced current which flows along pipeline 1 and pipeline 2
$\underline{Z}_{OP1}$:	MI between pipeline 1 and OHL
$\underline{Z}_{OP2}$:	MI between pipeline 2 and OHL
$\underline{Z}_{P1P2}$:	MI between pipeline 1 and pipeline 2

Figure 5-26: One parallel OHL with a "ton"-pylon next to two non-parallel pipelines

All systems have to be parallel to each other for easier comparison. This leads to Figure 5-27, where the distance x_{ik} between pipeline 1 and the OHL is set at 100 m and the second distance x_{km} between both pipelines is variable.

For this case, the standardized example with the pylon type PY1 with the best conductor configuration is used. Only this pylon is calculated in detail due to varying parameters of both pipelines.

The second pipeline is made of steel. All other parameters are noted in Figure 5-27. At the beginning, the pipeline diameter D_{P2} and the specific pipeline coating resistance r_{u2} from the second pipeline are varied.

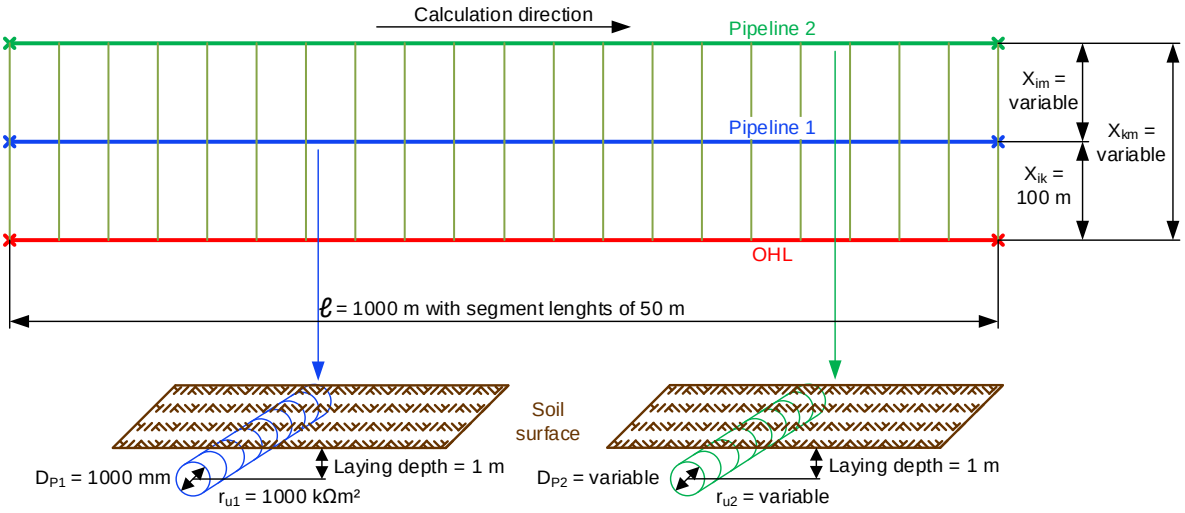

xik:	Distance between pipeline 1 and OHL; this distance is fixed
xim:	Distance between pipeline 1 and pipeline 2; this distance is variable
xkm:	Distance between pipeline 2 and OHL; this distance is variable

Figure 5-27: Geometrical parameters for examples with an OHL and two pipelines

In the first calculation example, the coating resistance of the second pipeline is fixed to 0.1 kΩm² and the pipeline diameter is varied between 10 and 1000 mm. When varying the distance between both pipelines, Figure 5-28 shows that the diameter of pipeline 2 has a significant influence on the maximum pipeline interference voltage (PIV) from pipeline 1. Smaller diameters of up to 100 mm lead mostly to a reduction of the PIV of pipeline 1 and have a similar curve characteristic to a narrow screening conductor with widths of 2 m. Because the pipeline coating has a certain resistance against ground, pipelines have a smaller reduction effect than comparable directly grounded screening conductors.

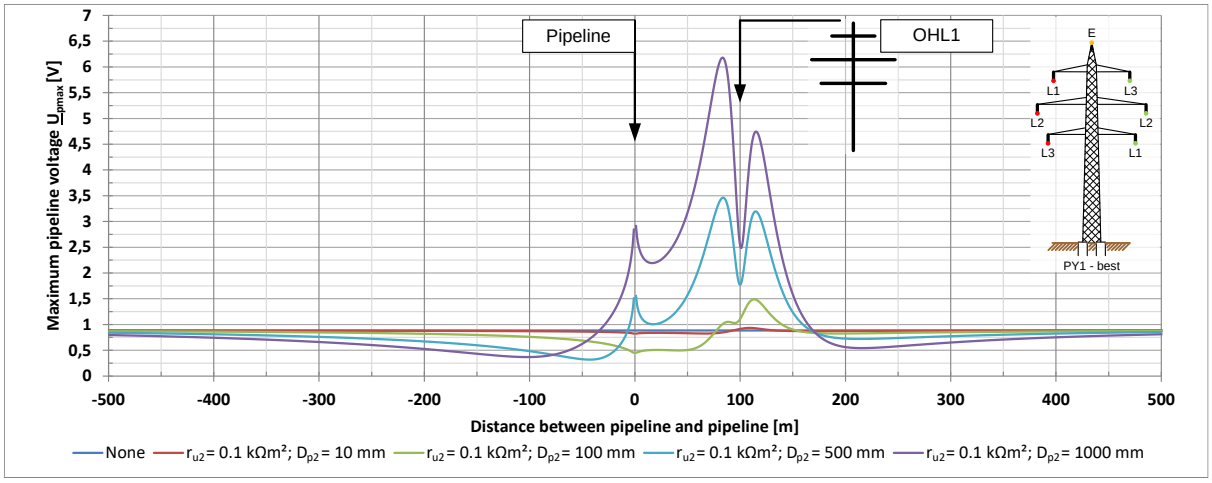

Figure 5-28: Maximum PIVs for the combination of OHL (PY1-best) and a second pipeline with a r_{u2} = 0.1 kΩ for different diameters D_{P2}

Larger diameters show a completely different behaviour because they amplify the pipeline interference voltage (PIV) from pipeline 1 over a wider range, especially when pipeline 2 is in the vicinity of pipeline 1 or the overhead line (OHL). This is due to a complex reaction between pipeline 2 and the earthing conductor of the OHL and the ratio between their surface sizes, similar to the effect of large screening conductors. This means that an increased diameter of pipeline 2 leads to higher induced currents and a higher impact on the PIV of pipeline 1.

Increasing the coating resistance of the second pipeline to a fixed value of 10 kΩm² leads to a similar result, but the influence of the second pipeline is lower.

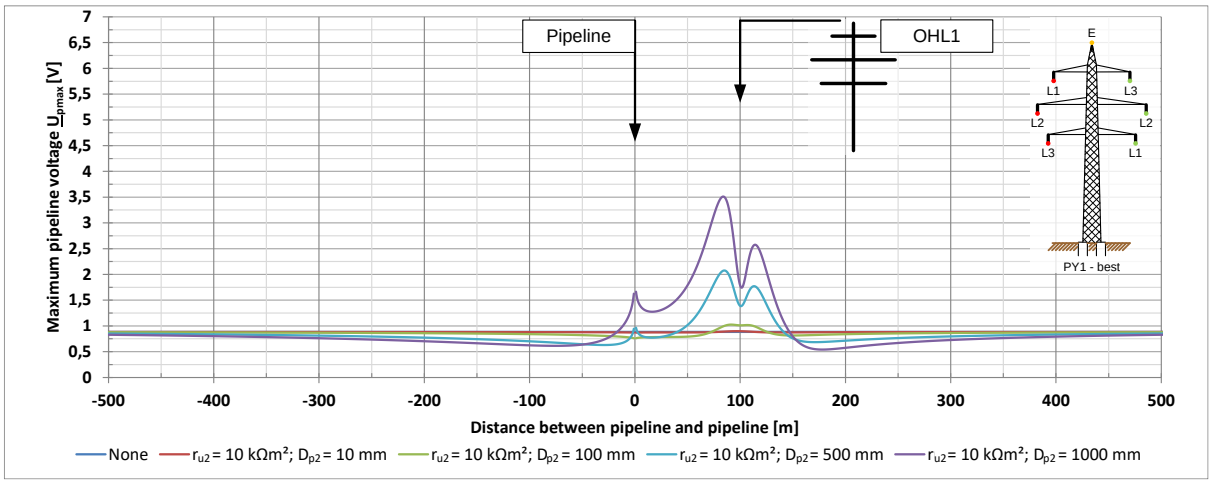

Figure 5-29: Maximum PIVs for the combination of OHL (PY1-best) and a second pipeline with a r_{u2} = 10 kΩ for different diameters D_{P2}

Figure 5-30 shows that further increasing the coating resistance to a value of 1000 kΩm² leads to a much smaller impact on the PIV of pipeline 1. The small enlarged area shows the influence of the different pipeline diameters. In general, pipelines with high coating resistances do not affect other pipelines.

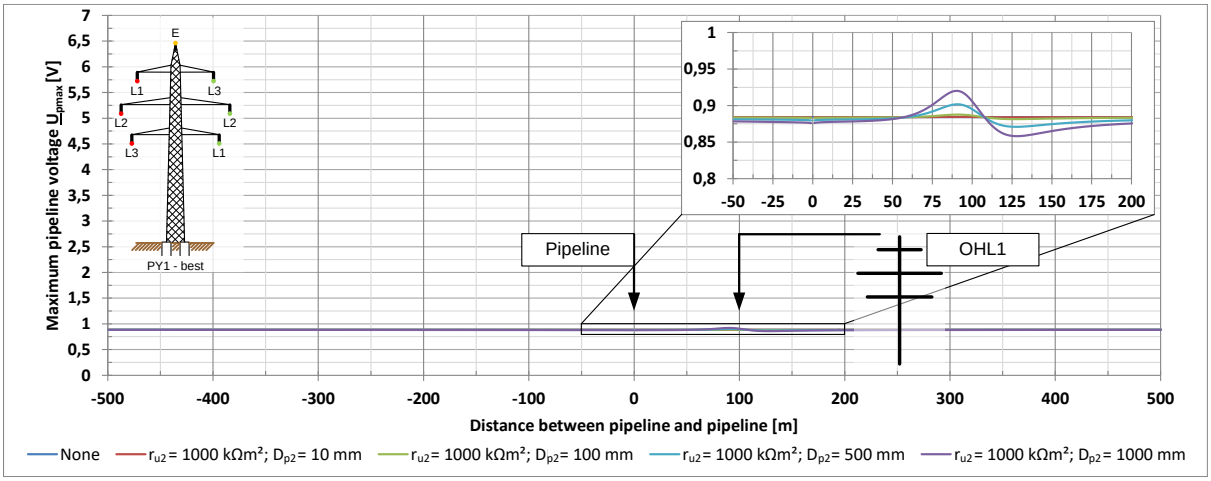

Figure 5-30: Maximum PIVs for the combination of OHL (PY1-best) and a second pipeline with a r_{u2} = 1000 kΩ for different diameters D_{P2}

Based on these calculations, it can be shown that the influence of pipeline 2 on the PIV of pipeline 1 depends on both, the diameter, the coating resistance and the distance between both pipelines. These two parameters can reduce or amplify the PIV of pipeline 1.

To investigate this, further calculations are needed in which it is necessary to set a fixed distance between all affected pipelines and OHL. In general, both pipelines are buried in the same corridor and therefore, the distance between both pipelines is fixed to a small value of 10 m, which means that pipeline 2 lies between pipeline 1 and the influencing OHL. In order to investigate the influence of the parameters of pipeline 1 on the calculation, the diameter and coating resistance are varied.

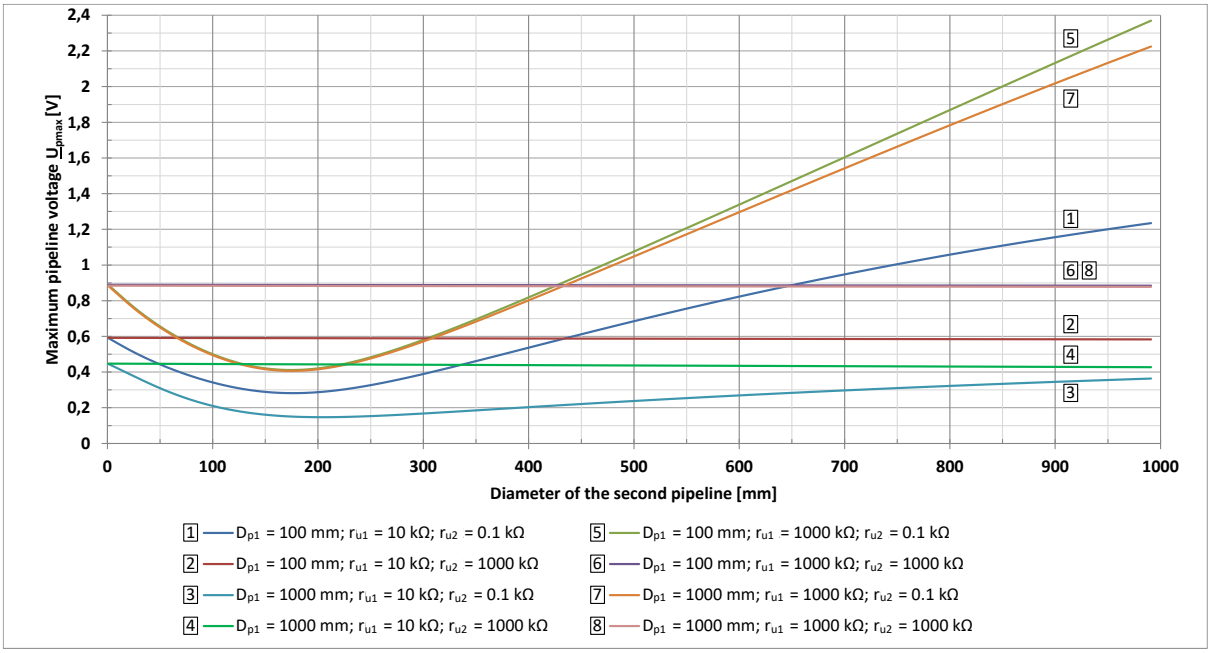

Figure 5-31: Maximum PIVs for the combination of OHL (PY1-best) and a second pipeline for varying parameters of both pipelines for a fixed distance of 10 m between both pipelines

Figure 5-31 shows that with a very high coating resistance of pipeline 2, the diameter of pipeline 2 has almost no influence on the maximum pipeline interference voltage (PIV) of pipeline 1. This result does not depend on the diameter and coating resistance of pipeline 1 and can be seen in the curves 2, 4, 6 and 8 for different parameters of pipeline 1. Therefore, this calculation coincides with the results shown in Figure 5-30.

The curve progression for the curves 1, 3, 5 and 7 shows the case where the coating resistance of pipeline 2 is very low. When the diameter of pipeline 2 is lower than around 200 mm, a reduction effect of the PIV of pipeline 1 can be seen.

Further increasing the diameter of pipeline 2 leads to a higher PIV. This effect is much stronger for a small diameter of pipeline 1, which clearly shows that the ratio between the surface sizes of conductors can be a key parameter. This coincides with the results in this chapter and is also the case for the size of the screening conductor in chapter 5.3.

Distributed conductor systems such as global earthing systems, as already discussed with large screening conductors in chapter 5.3, have a similar but weaker effect because they distribute the interference over a larger area.

6 Measurements on pipelines

6.1 Measurement of pipeline interference voltages

6.1.1 Measurement equipment

Basically, measurement of the AC pipeline interference voltage (PIV) is nothing else than a simple voltage measurement. Measurements of the AC PIVs are conducted by pipeline operators daily and, mostly, the values are below the limit of the standardisation and technical specifications (see chapter 2.1). In these cases, operators may tend to ignore them because they may assume that the measured values do not harm the pipeline, their personnel or other people.

However, in fact, measurements are only a snap shot, especially when they are conducted over only a short period of time. Longer measurements are unfortunately only conducted when the quick measurements show a high value or when someone conducting calculations instructs the operator to do so.

In Central Europe, these longer measurements are often conducted with the measurement device "Minilog2", produced by the company "Weilekes Elektronik GmbH" [49] (see Figure 6-1). With this measurement device, long measurements of the PIV up to one-week can be conducted directly on the pipeline until the internal memory is full or the storage battery is empty.

Figure 6-1: Weilekes Minilog2 device [49]

The following graph shows the subsequent reporting of the measurement results after copying the measurement results from the device to a computer.

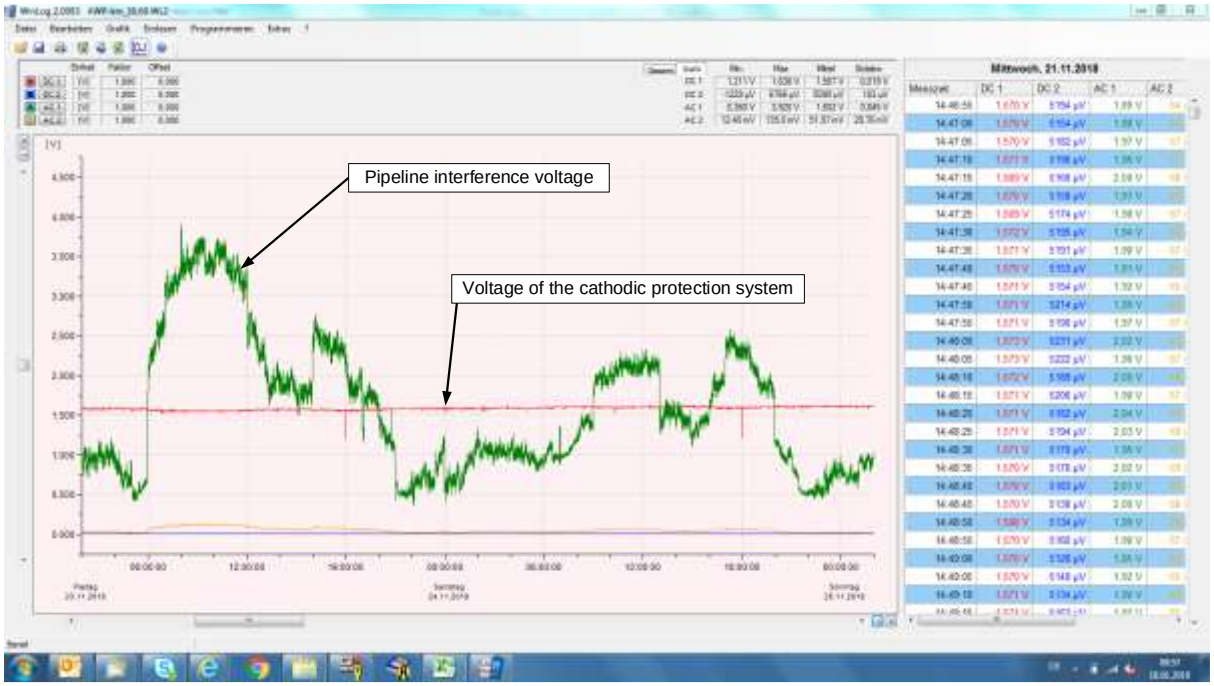

Figure 6-2: Software with PIV measurement results from the measurement device "Minilog2"

If a very long measurement with real-time data view is required, a remote-control system is very useful since measurements are done automatically, stored safely and a live view from any computer is possible. Such systems are available e.g. from the company “TPA KKS GmbH” [50] and an example of their user interface with real time data is shown in Figure 6-3.

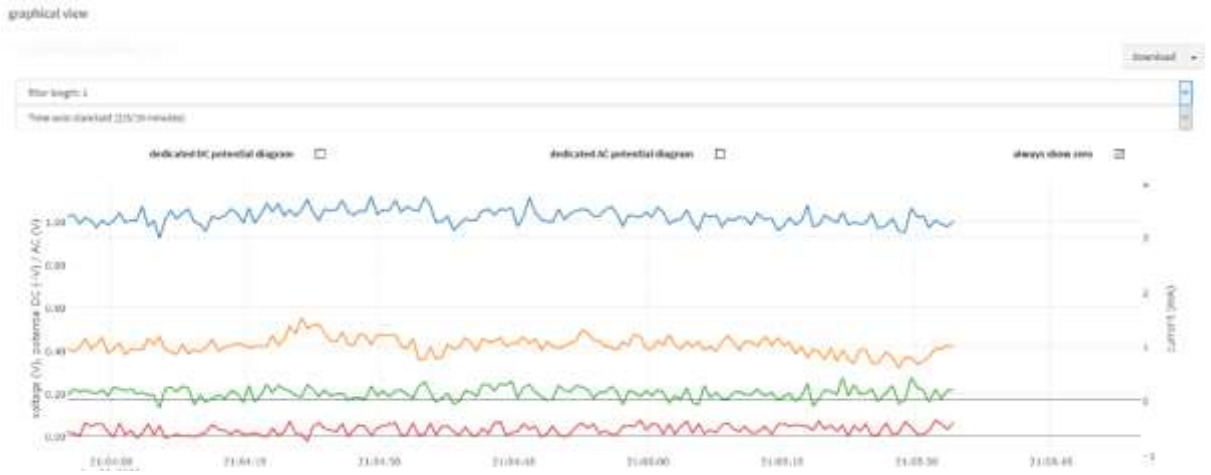

Figure 6-3: Real-time data from a measurement station

6.1.2 Interpretation of measurements

No matter which system is used, the interpretation of the results is important. It can, for example, determine the source of an influence, whether there are any abnormal states on the source of the influence or if the measured voltages can be harmful to people and equipment in unfavourable situations. The following two examples show fully analysed measurements of the influence of an overhead line (OHL) and a railroad on the pipeline interference voltage (PIV).

Figure 6-4 shows a measurement which was conducted for a measurement period of 168 hours (1 week) at a specific pipeline location. The figure shows that the measured PIV is mainly influenced by an overhead line (OHL). For a better understanding, the load current of the OHL with the highest influence, which is very similar to the measured PIV, has also been added to this graph. This example shows that there must be other influencing high voltage power systems (HVPSs), as the curves differ in some areas. Both curves show a typical curve progression of an OHL, because the values of both curves do not change abruptly and because it shows a weekday/weekend as well as a day/night rhythm. The same effect has been described for the load currents in chapter 4.5.

Unfortunately, these rhythms do not always appear because of the production of renewable energy. This energy must be transported to other locations or countries, where it is needed or where it can be stored (e.g. in pumped storage hydro power stations). Then, the shape of the load current and also the PIV looks very different.

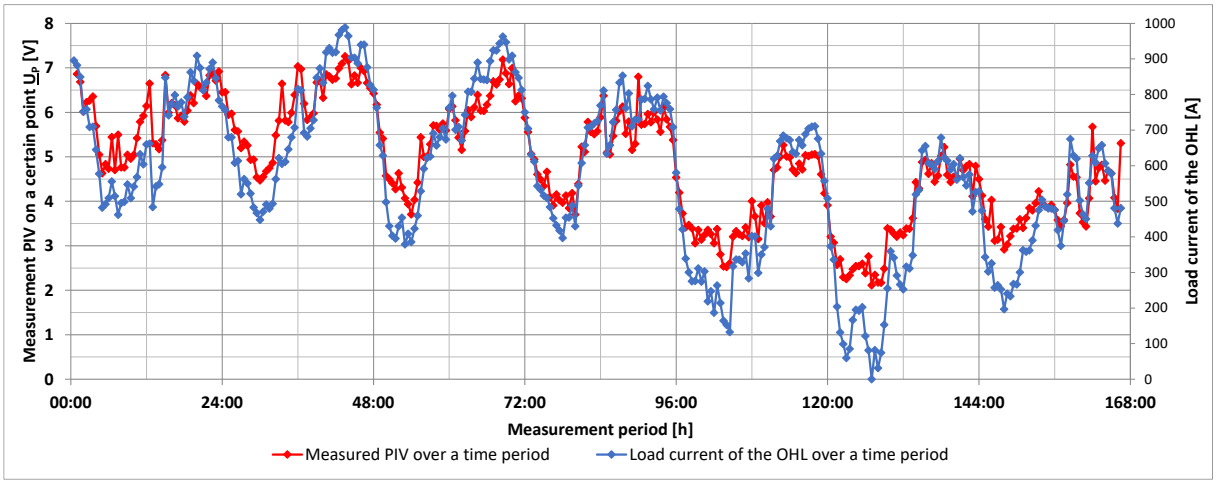

Figure 6-4: Measured PIV at a specific location over a period of time; main influencer is an overhead line

Figure 6-5 shows a scatter plot which investigates the correlation between the PIV and the load current of the OHL. It turns out that the PIV is strongly dependent on the load current of the considered OHL because all data points show a low scattering and lie near the rising trend line.

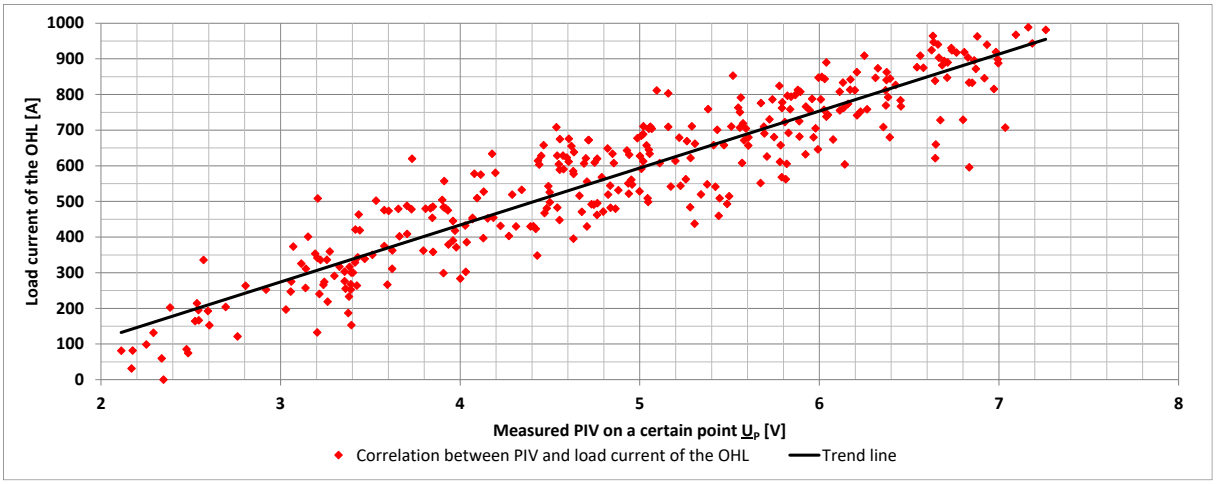

Figure 6-5: Scatter plot of Figure 6-4

Another picture of a one-week-measurement is shown in Figure 6-6, where the PIV barely shows any patterns. A light day / night rhythm can sometimes be detected, but basically the PIV jumps between higher and lower values. In this case, the main source for the interference is clearly a railroad. To illustrate this, the curve progression of the railroad load current has been added to the figure. Here, it is obvious that both curves are very similar and that there are no other strong sources of influence. The reason for the strong fluctuation in the curve progression is that an electric locomotive needs a high current for acceleration and, in addition, the current flow direction can be reversed because during braking, the kinetic energy is recuperated into a current. Also, the currents and therefore the interference is not only time-dependent, it is also position-dependent due to the movement of the car. The same effect has already described for load currents in Figure 4-13 in chapter 4.5.

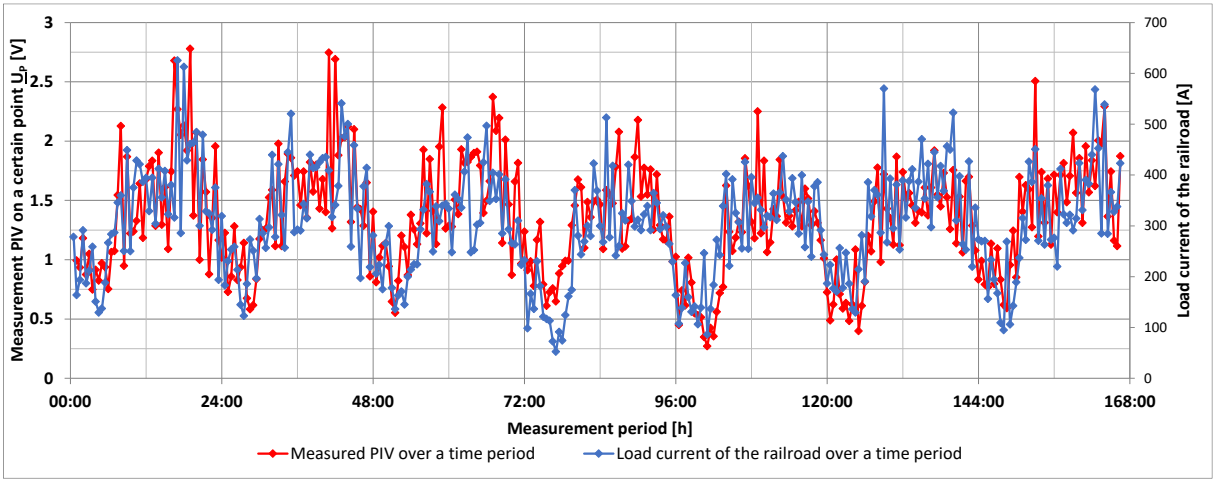

Figure 6-6: Measured PIV on a specific location over a period of time; main influencer is a railroad

Figure 6-7 shows another scatter plot where it is obvious that the data points scatter more widely than in the previous scatter plot. This is, on the one hand, due to the above mentioned characteristics

of the current flow in railroads. On the other hand, it is caused by the fact that both, the measurement at the pipeline and the measurement at the operator of the railway line, do not always measure the exact same strongly changing values. Nevertheless, a strong correlation can be seen between the influence of the railroad and the PIV.

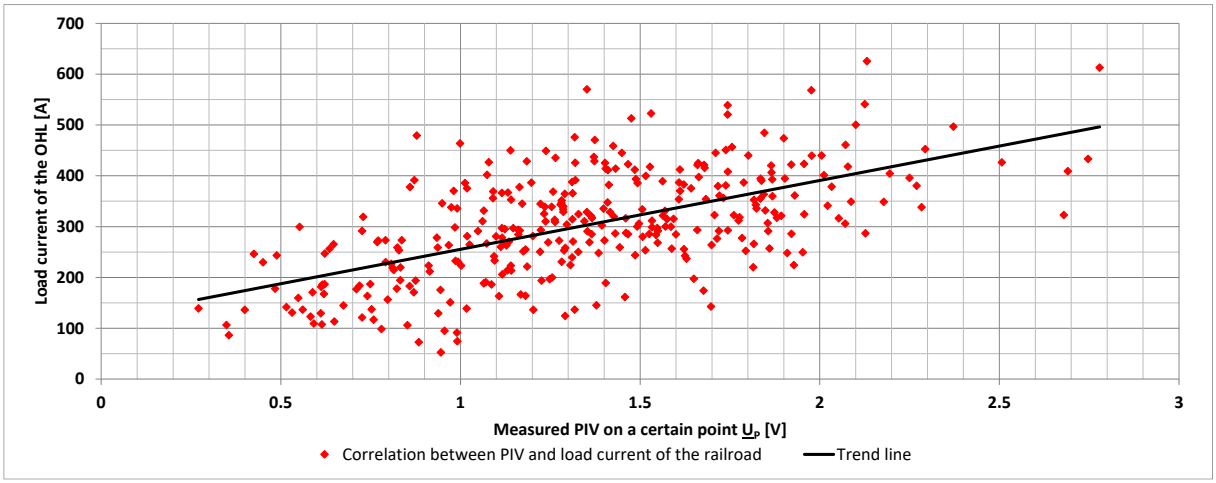

Figure 6-7: Scatter plot of Figure 6-6

There are many cases where more than one source of high voltage power systems (HVPS) influences the pipeline interference voltage (PIV). In the previous chapter 5.4 the case of two parallel overhead lines (OHLs) was discussed and in fact such cases occur frequently. Due to focussed energy routes, there are often several OHLs in the vicinity of pipelines and often also railway lines. This last case is displayed in Figure 6-8, where a one-week-measurement was conducted.

Without knowing the load currents of the influencing HVPSs, the PIV (red line) in Figure 6-8 looks like a combination of the two figures 6-4 and 6-6, as both day / night and weekday / weekend rhythms are visible and also, the value of the PIV shows sudden changes. For such cases, it can be challenging to determine the influence factor of the OHL and the railway lines on the PIV and to find the correct ratio between them. The complexity increases when trying to determine how many sources of HVPS actually have a relevant impact on the PIV at this location over the time of the measurement.

The problem becomes particularly apparent when the load currents of the influencing HVPSs are added to Figure 6-8. Several sources must now be taken into account, which have different load current characteristics. In an accurate comparison of the PIV and the load currents, it can be seen that the railroad has a significant influence on the PIV. However, this is no longer true for the three influencing OHLs, as a correlation is difficult to detect.

The scatter plot in Figure 6-9 shows a similar picture. It can be seen from the trend line (blue line), for the correlation between PIV and railroad, that there is a strong correlation. Furthermore, the violet and green trend lines also show a correlation between PIV and the respective load currents, but these correlations are much weaker. This example shows that in complex influencing situations,

without in-depth analysis, it becomes relatively difficult to identify the main influencing source for the PIV.

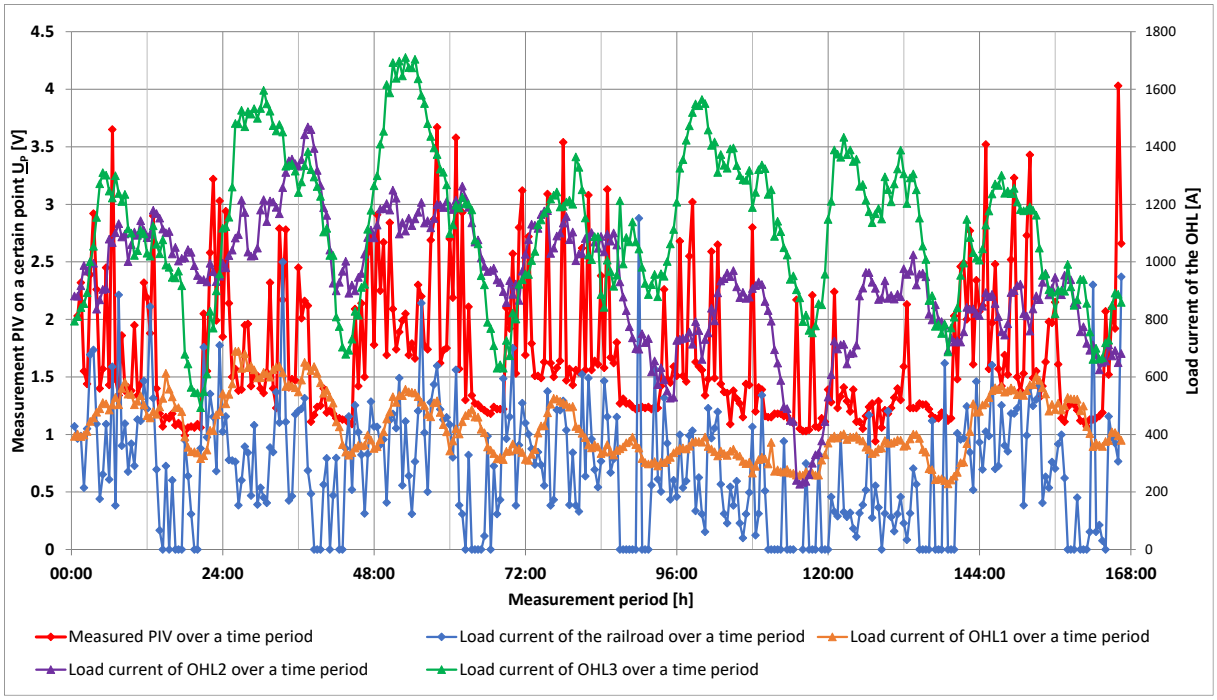

Figure 6-8: Measured PIV at a specific location over a period of time; no determined main influencer

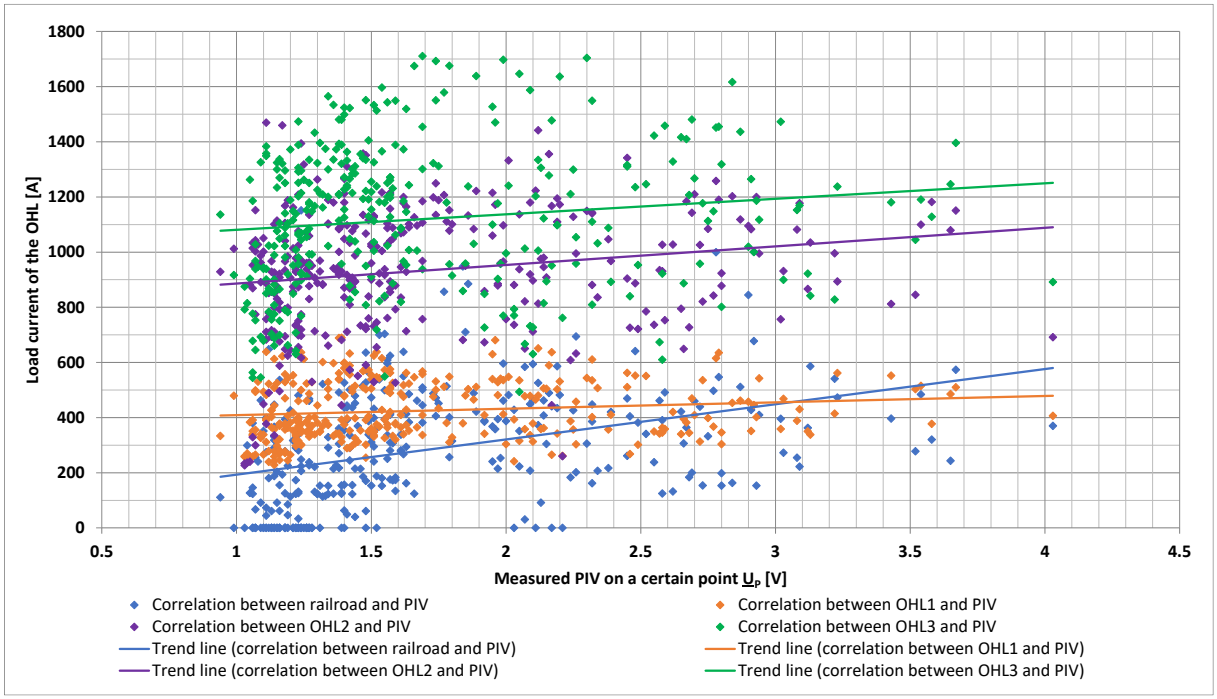

Figure 6-9: Scatter plot of Figure 6-8

Therefore, accompanying calculations of the inductive influence are recommended, as only with this combination of measures, the correct conclusions can be drawn.

6.1.3 Influence of external ohmic potential gradients in measurements

Another aspect that may be overlooked in praxis during measurements is the interference by an ohmic potential gradient in the earth. For pipeline measuring locations, it is often the case that the (permanent) reference electrode of the measurement is close to the pipeline as can be seen in Figure 6-10. It is assumed that this reference point has a potential value similar to the ground. This is usually the case, except for when the reference point lies in an external ohmic AC potential gradient.

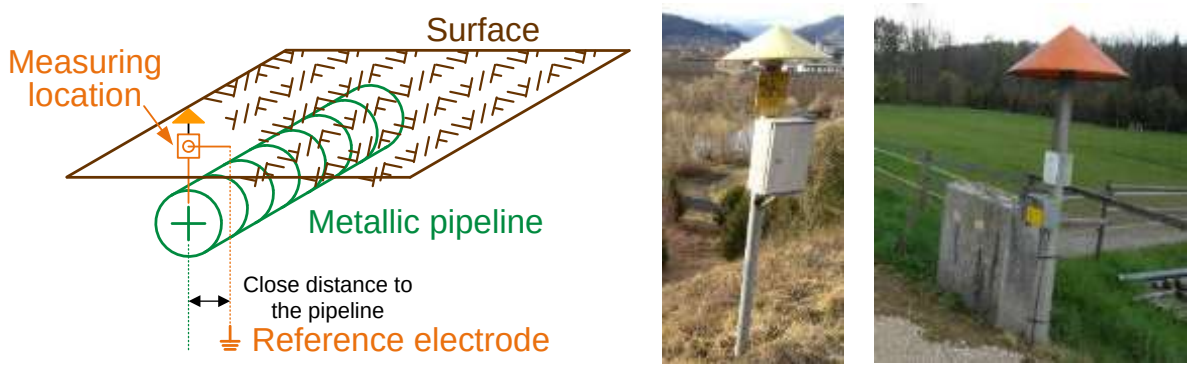

Figure 6-10: Measuring locations with their reference electrode as the reference point

An ohmic potential gradient appears when a current flows into the soil from the earthing system or a bigger pipeline coating holiday. If the reference electrode of this measurement is in this gradient, the reference electrode is no longer the reference ground but a measuring location with a specific value. Due to this fact, the measured voltage value is false. Figure 6-11 shows this example.

The current I_{earth} flows from a pylon, a substation or another earthing system over their underground earthing system into the soil. This leads to the ohmic potential gradient (EPS, earth potential rise) with a maximum value $U_{earth;max}$. When the underground earthing system ends, the potential decreases with distance. After a certain distance, the value reaches a value around zero and thus, it is equal to the reference ground.

In this figure, the pipeline lies at a distance x_P from the underground earthing system. Next to the pipeline is an underground constant reference electrode, which is normally used for measuring the PIV and/or the cathodic protection potential. The reference electrode has the distance x_{ref} to the external earthing system. A conducted measurement between pipeline and reference electrode is supposed to be correct and should show the PIV U_P. Unfortunately, in this case, the reference electrode lies in the external ohmic potential gradient and is therefore not connected to the reference ground.

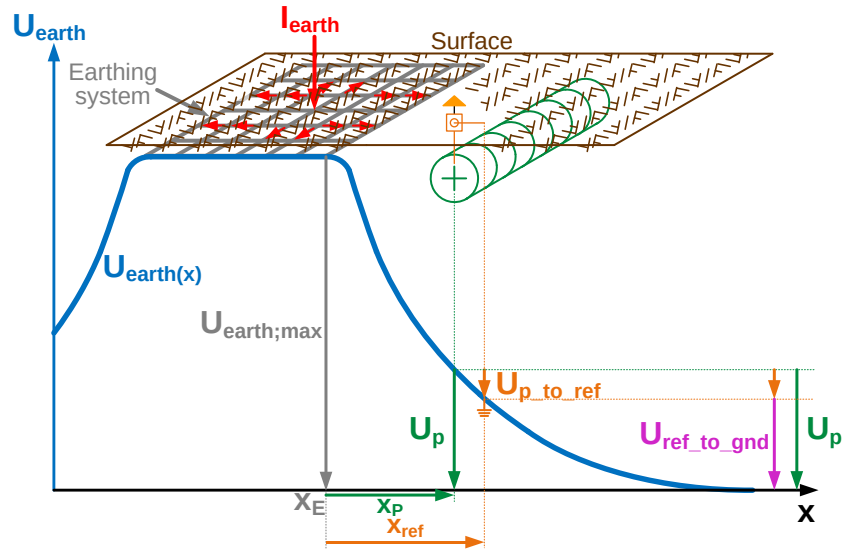

$U_{earth(x)}$:	Ohmic potential gradient[V]
$U_{earth;max}$:	Maximal value of the ohmic potential gradient[V]
I_{earth}:	HVPS current flowing into the earthing system [A]
U_P:	PIV [V]
$U_{P\_to\_ref}$:	Measured PIV against the permanent reference electrode
$U_{ref\_to\_gnd}$:	Potential difference between the reference ground and the reference ground
x_P:	Minimal distance between pipeline and the earthing system
x_{ref}:	Minimal distance between reference electrode and the earthing system
x_E:	Outer end of the earthing system

Figure 6-11: Example of the impact of an external ohmic potential gradient on a measurement by using the reference electrode inside the external ohmic potential gradient

The outcome of this is a measurement of only the PIV $U_{P\_to\_ref}$, which is measured too low. The potential difference between U_P and $U_{P\_to\_ref}$ is $U_{ref\_to\_gnd}$ which is the potential difference of the reference electrode to the reference ground and therefore, the measuring error.

This measuring error can be removed either by deactivating the source of the external AC ohmic potential gradient or, if this is not possible, by moving the measuring location out of the gradient. In order to verify the correctness of the assumption of the external potential gradient, a temporary measuring location can be set up, as shown in Figure 6-12. The distance x_{tmp} of the temporary measuring location is now far enough from the potential gradient so that its residual voltage $U_{tmp\_to\_gnd}$ corresponds to that of the reference ground. The result of this is that the measured PIV $U_{P\_to\_tmp}$ corresponds exactly to the real PIV U_P.

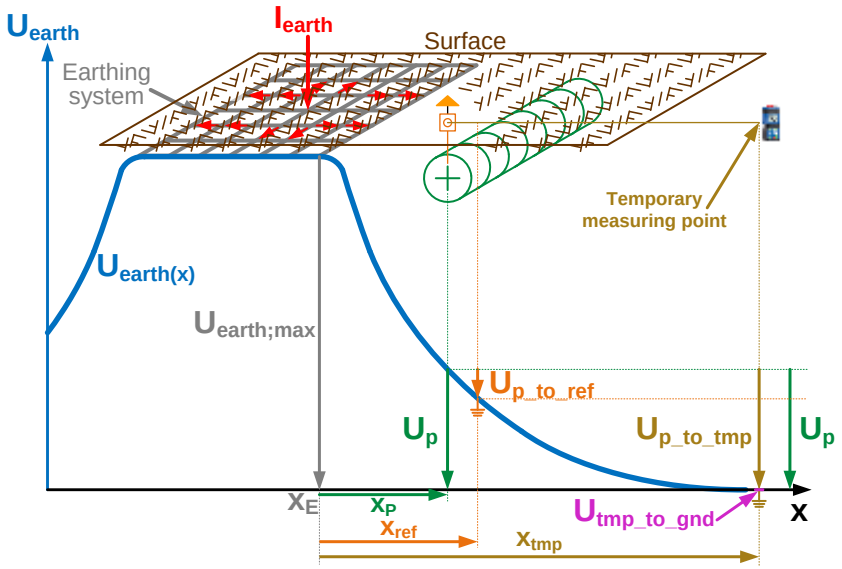

$U_{earth(x)}$:	Ohmic potential gradient[V]
$U_{earth;max}$:	Maximal value of the ohmic potential gradient[V]
I_{earth}:	HVPS current flowing into the earthing system [A]
U_P:	PIV [V]
$U_{p\_to\_ref}$:	Measured PIV against the permanent reference electrode
$U_{p\_to\_tmp}$:	Measured PIV against the temporary measuring point
$U_{tmp\_to\_gnd}$:	Potential difference between temporary measuring point and reference ground
x_P:	Minimal distance between pipeline and the earthing system
x_{ref}:	Minimal distance between reference electrode and the earthing system
x_E:	Outer end of the earthing system
x_{tmp}:	Minimal distance between temporary measuring point and the earthing system

Figure 6-12: Example of the impact of an external ohmic potential gradient on a measurement – temporary measuring point

The problem is depicted in the following numeric example: The conducted measurement of the pipeline interference voltage (PIV) $U_{p\_to\_ref}$ results in a value of 40 volt and thus it is assumed that there is no danger at this location. However, the external ohmic potential gradient $U_{tmp\_to\_gnd}$ in this location already has a value of 35 volts which means that the real PIV has a value of 75 volt. This correctly measured value $U_{p\_to\_tmp}$ can be measured using a temporary earthing system at the location x_{tmp}, which would immediately indicate that the touch voltage limit has been exceeded. In addition to this problem, longer measurements can be false when the reference electrode is within the ohmic potential gradient. These incorrect measurements make it difficult to interpret the PIV profile along the pipeline, as well as comparing PIV measurements to calculations.

6.2 Measurement of pipeline parameters

Over the years, many calculations have led to doubts about whether the calculation formulas from chapter 2.3 are correct. Also, the value of the specific pipeline coating resistance has been questioned because known resistance values were given from measurements with DC currents by pipeline

manufactures or operators. However, there are assumptions about a frequency depending behaviour of the coating resistance or, in this case, the coating impedance. All these questions and assumptions were investigated in a master thesis [33]. This thesis gives a summary of the measurement setup as well as the results.

6.2.1 Experimental measurement on a test pipeline

In a first step, measurements were conducted under controlled laboratory conditions. Measurements were done on a 2-meter-long pipeline with a pipeline coating (see Figure 6-13 a)) to observe the dependence from interference current and interference frequency. As a result, the longitudinal impedance was measured to obtain the information as to whether the theoretical results are comparable with the measured results in the laboratory. A part of the experimental setup is shown in Figure 6-13 b). In addition, it provided an outlook on possible results for the measurement on an active buried pipeline.

a) b)

Figure 6-13: a) Pipeline for the measurement in the laboratory [33]; b) Experimental setup for the measurement of the pipeline parameters [33]

The measurement of the longitudinal impedance shows interesting behaviour because with rising pipeline currents, the impedances rise. Figure 6-14 shows this behaviour for an interference frequency of 50 Hz. In addition, the phase angle slowly decreases. This can be explained by the experimental setup: On every step, a current was flowing into the pipeline for a limited time. After a short break, another higher current was used. Each time, electrical work was also inserted into the pipeline, which caused the metal to heat up. Heated iron has the property that the impedance increases with rising temperature.

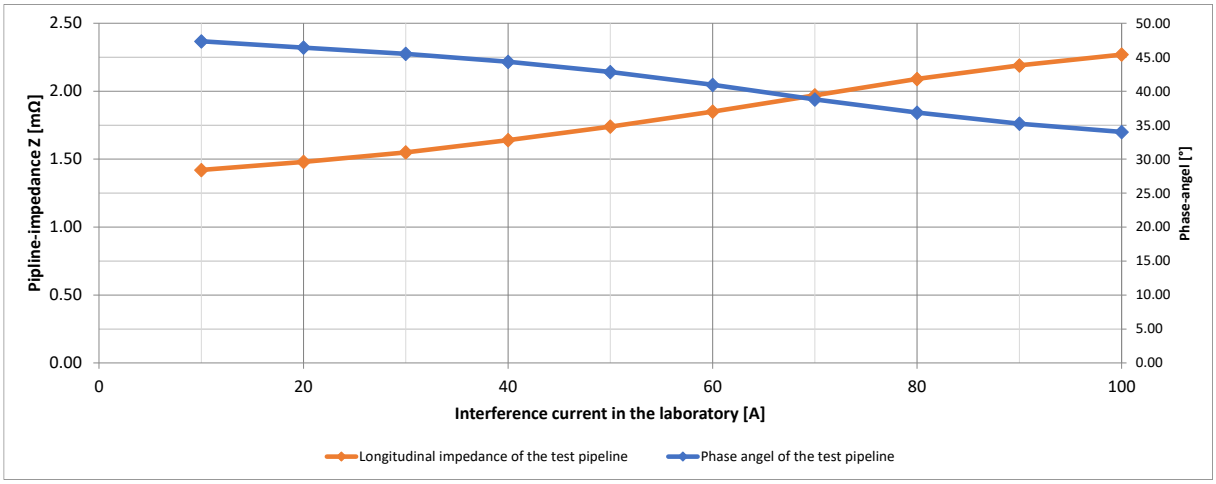

Figure 6-14: The dependence of the longitudinal impedance and the phase angle of the test pipeline from an interference current by an interference frequency of 50 Hz

Another measurement shows the dependence of the interference frequency when using a constant pipeline current of 100 A. As is already known, the longitudinal impedance rises with a rising frequency.

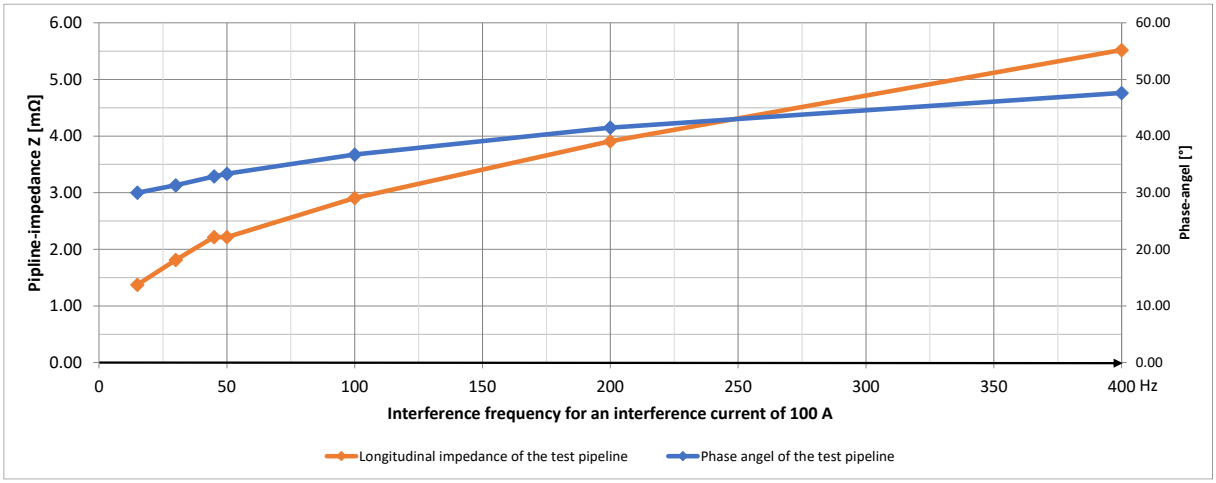

Figure 6-15: The dependence of the longitudinal impedance and the phase angle of the test pipeline from an interference frequency by an interference current of 100 A

Calculations were also done in the master thesis ([33], chapter 4). In ([33], chapter 4.4), the theoretical formulas are used to calculate the test pipeline. ([33], chapter 4.4.1) shows the parameters used for calculating the parameters of the test pipeline and the results are shown in ([33], chapter 4.4.5, page 41). Table 6-1 shows the summarized results:

Type of result	Formula used / Pipeline current	Longitudinal impedance
Calculation	([33], chapter 4.4.2), AFK3 (this work: "Formula C")	1,27 mΩ
Calculation	([33], chapter 4.4.3), Theorie Vollleiter (this work: "Formula S")	2,03 mΩ
Calculation	([33], chapter 4.4.4), Theorie Hohlleiter (this work: no equivalent)	0,90 mΩ
Measurement	([33], figure 5-16), Pipeline current: 100 A	2,22 mΩ
Measurement	([33], figure 5-16), Pipeline current: 50 A	1,75 mΩ

Table 6-1: Comparison of the calculated and measurement results of the test pipeline

It can be seen from this table that the "Formula S" fits best on the test pipeline. However, this does not necessarily mean that this result is still valid for the measurement on a real pipeline. In addition, there is the problem that the shunt admittance could not be measured on this laboratory model. This is clearly possible only if the pipeline is buried. In short, further measurements on a real buried pipeline are necessary.

6.2.2 Measurement on a real buried pipeline

The next step was to conduct the measurement on a real buried pipeline. In addition, some requirements were absolutely necessary, otherwise the measurement would have become too complex or the measurement would have been influenced by external sources. This means, that the pipeline should not be too long, should have no electrical connections to other pipelines and it should not be affected by interference currents from HVPSs. Fulfilling these requirements, with the support of a pipeline operator, a small transmission pipeline with a length of 606 m was found. All other specifications are described in [33] in chapter 4.5.1, page 42. Figure 6-16 shows the geographical overview of the measurement, where the feeding point of the interference current, the pipeline itself and the return cable are shown. More details about the measurement itself, the measurement setup, used equipment and other specifics are discussed in [33], chapter 6.

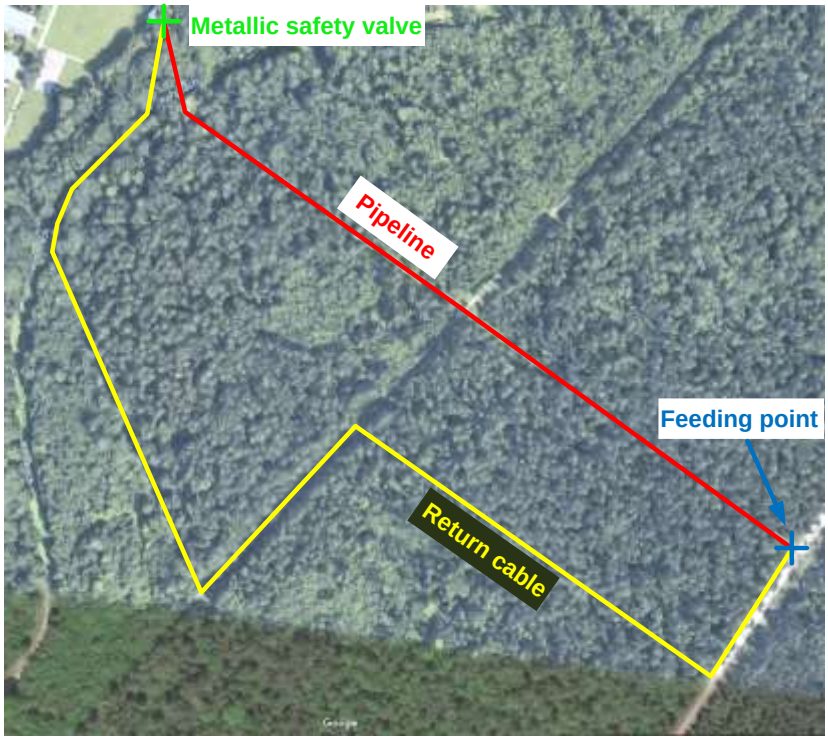

Figure 6-16: Geographical overview of the measurement

6.2.2.1 Measurement of the longitudinal impedance

The first measurement determined the longitudinal impedance. The measurement setup is described in [33] in chapter 6.5.1, figure 6-14. For this, different interference frequencies and a current of 1 A ([33], chapter 6.5.2, table 6-5), respectively the maximum power generator current of 14 A, were used because the power generator was limited. Table 6-2 shows a summary of ([33], chapter 6.5.2, table 6-6).

Frequency	Current	$\underline{Z}_{meas}$
15	14.23	1.91 Ω | 13.49°
30	14.70	2.09 Ω | 22.91°
50	14.75	2.36 Ω | 32.30°
100	14.77	3.16 Ω | 47.37°
200	9.78	5.00 Ω | 60.69°
400	3.94	8.93 Ω | 69.55°

$\underline{Z}_{meas}$: Measured longitudinal impedance of the complete measurement distance (pipeline plus return cable) from Figure 6-16 [Ω]
Frequency: Simulated interference frequency, fed directly into the pipeline [Hz]
Current: Maximum interference current from the power generator [A]

Table 6-2: Results for the longitudinal impedance for different interference frequencies with the maximum power generator current of 14 A or less

The results show that the longitudinal impedance of the pipeline rises with higher frequencies - the same result as the test pipeline in the laboratory. This same result is also shown by the phase angle, when comparing the results for 10 or 20 A in ([33], table 5-1 and table 5-2). The higher simulated interference current in ([33], table 6-6) was compared to ([33], table 6-5) and is preferable for the real-world-measurement because it shows more reliable measurement results.

6.2.2.2 Measurement of the shunt admittance

The second measurement determines the shunt admittance which can only be measured on a buried pipeline. The measurement setup is described in [33] in chapter 6.6.3, figure 6-19. The main difference between this measurement setup and the longitudinal impedance setup is that the return cable is no longer used because the current of the power generator has to find a different way back to the power generator. The measurement showed that the correct shunt admittance is difficult to determine. A problem arose because, at the end of the pipeline, a metallic safety valve had been installed (see Figure 6-16) which unfortunately had a slight connection to the ground. Therefore, this factor had to be taken into account in the evaluation. The following Table 6-3 shows a summary of ([33], table 6-9):

Frequency	Current	$\underline{Z}_{meas}$
15	329	749.0 Ω | -1.15°
30	550	719.0 Ω | -4.40°
50	771	704.9 Ω | -7.70°
100	882	670.0 Ω | -12.5°
200	868	599.0 Ω | -21.0°
400	764	460.3 Ω | -26.4°

$\underline{Z}_{meas}$: Measured impedance of the complete measurement distance (pipeline plus return cable) from Figure 6-16 [Ω]
Frequency: Simulated interference frequency, fed directly into the pipeline [Hz]
Current: Maximum interference current from the power generator [mA]

Table 6-3: Results of the measurement of the shunt admittance for different frequencies

The result shows that, because of the missing return cable, the pipeline now has a much higher measured impedance because the simulated current must flow back through the soil and the pipeline coating.

6.2.3 Evaluation of the measurements

6.2.3.1 Longitudinal impedance

To get correct pipeline parameter results of real-world-measurements, certain additional elements have to also be considered. For the measurement and calculation of the correct longitudinal impedance, these elements are the return cable and the contact resistance of all the cable

connections. For a simulated interference frequency of 50 Hz, the following results were measured and calculated:

$\underline{Z}_{meas}$	R_{meas}	R_{wire}	R_{conn}	**R_{pipe}**	**R_{theo}**	**R_{afk}**
2.39 Ω | 31.90°	2.03 Ω	1.21 Ω	0.4 Ω	**0.42 Ω**	**0.44 Ω**	**0.43 Ω**

$\underline{Z}_{meas}$:	Measured longitudinal impedance of the complete measurement distance from Figure 6-16 for 50 Hz
R_{meas}:	Ohmic part of the longitudinal impedance (**$R_{meas} = Z_{meas} \cdot \cos(\varphi)$**)
R_{wire}:	Ohmic resistance of the return cable (measured in the laboratory)
R_{conn}:	Contact resistance between all cable connections (measured in the laboratory)
R_{pipe}:	Correct ohmic part of the longitudinal impedance for the pipeline (**$R_{pipe} = R_{meas}-R_{wire}-R_{conn}$**)
R_{theo}:	Calculated ohmic part of the resistance (this thesis: "Formula S"; [33]: Theorie Vollleiter
R_{afk}:	Calculated ohmic part of the resistance (this thesis: "Formula C"; [33]: AFK3

Table 6-4: Measurement and calculation of the ohmic part of the longitudinal impedance of the pipeline

$\underline{Z}_{meas}$	X_{meas}	X_{wire}	X_{conn}	**X_{pipe}**	**X_{theo}**	**X_{afk}**
2.39 Ω | 31.90°	1.26 Ω	0.46 Ω	0 Ω	**0.80 Ω**	**0.85 Ω**	**0.58 Ω**

$\underline{Z}_{meas}$:	Measured longitudinal impedance of the complete measurement distance from Figure 6-16 for 50 Hz
X_{meas}:	Inductive part of the longitudinal impedance (**$X_{meas} = Z_{meas} \cdot \sin(\varphi)$**)
X_{wire}:	Inductive resistance of the return cable (measured in the laboratory)
X_{conn}:	Inductive resistance between all cable connections (measured in the laboratory)
X_{pipe}:	Inductive part of the longitudinal impedance for the pipeline (**$X_{pipe} = X_{meas}-X_{wire}-X_{conn}$**)
X_{theo}:	Inductive part of the resistance (this thesis: "Formula S"; [33]: Theorie Vollleiter
X_{afk}:	Inductive part of the resistance (this thesis: "Formula C"; [33]: AFK3

Table 6-5: Measurement and calculation of the indutice part of the longitudinal impedance of the pipeline

After measurements and calculations were conducted on a buried pipeline, the longitudinal impedance shows that theory and praxis lie quite close together. Only the inductive part X_{afk} for the AFK3-formula ([33], chapter 4.3.1), which in this work corresponds to the CIGRE-formula (chapter 2.3.1), points to a slightly increased difference between calculation and measurement. But the mathematical comparison of the "Formula S" and "Formula C" in chapter 2.3.1.2 and 4.2 shows that both formulas have similar results. Such small differences can stem from different presuppositions on the material constants, because material constants have a certain range of valid values.

This conclusion is also valid for a wide range of interference frequencies, as can be seen in Figure 6-17 for the ohmic part and in Figure 6-18 for the inductive part of the longitudinal impedance.

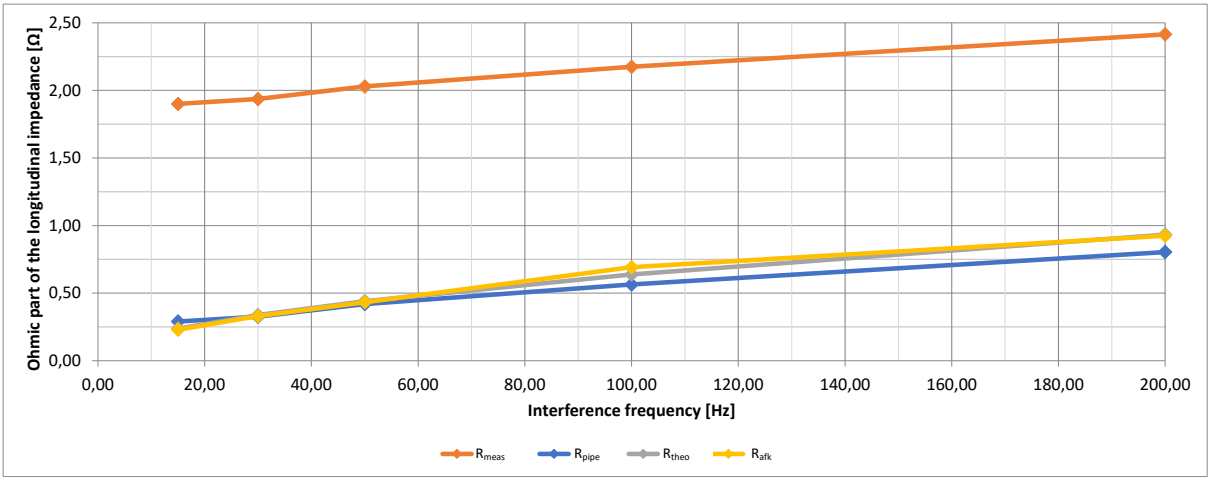

Figure 6-17: Results for the ohmic part of the comparison for different interference frequencies

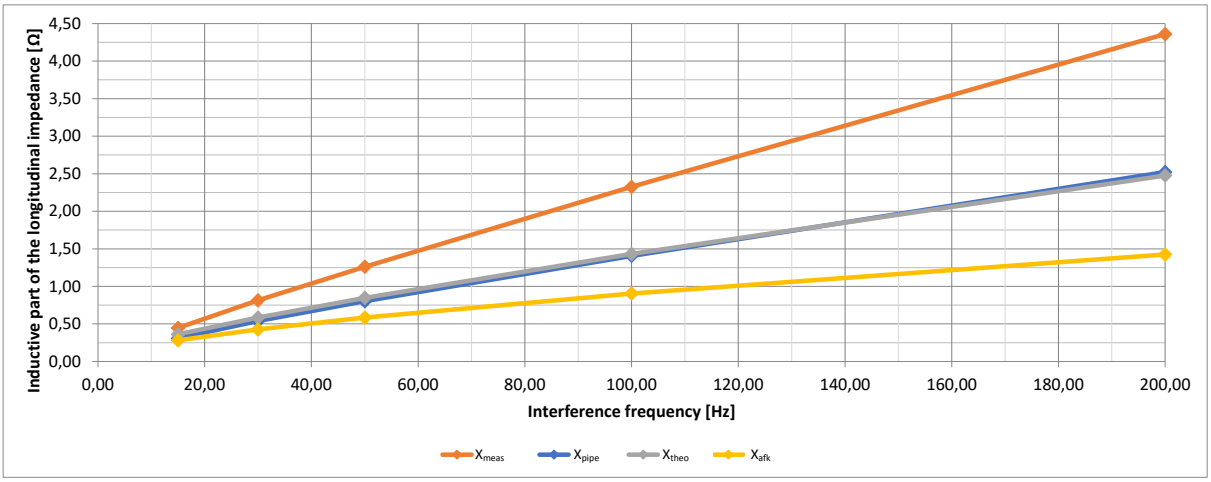

Figure 6-18: Results for the inductive part of the comparison for different interference frequencies

6.2.3.2 Shunt admittance and the specific pipeline coating resistance

To get correct pipeline parameter results of real-world-measurements, certain additional elements must be considered. For the measurement and calculation of the correct shunt admittance, this is the above mentioned metallic safety valve which was slightly connected to the ground. For a range of simulated interference frequencies, the following results were measurement and calculated:

Interference frequency	$\underline{Z}_{meas}$	Z_{corr}	Z_q	**R_q**
15	749.00 Ω | -1.15°	463.43 -j 9.30 Ω	1915.3-j163.3 Ω	**1915.3 Ω**
30	719.00 Ω | -4.40°	450.49 -j 34.66 Ω	1613.2-j486.2 Ω	**1613.2 Ω**
50	704.90 Ω | -7.70°	426.73 -j 57.70 Ω	1232.8-j582.4 Ω	**1232.8 Ω**
100	670.00 Ω | -12.50°	412.88 -j 91.53 Ω	937.1-j720.4 Ω	**937.1 Ω**
200	599.00 Ω | -21.04°	322.58 -j 124.09 Ω	477.6-j486.7 Ω	**477.6 Ω**

$\underline{Z}_{meas}$: Measured shunt admittance for the complete measurement for 50 Hz

Z_{corr}: Correct impedance without considering the simulated earthing system for the power supply; calculated with the supplied current from the power generator into the pipeline and the measured voltage between reference ground and the impedance equivalent network of the pipeline, safety valve and return cable (see [33], page 77 to 79)

Z_q: Calculated Shunt admittance ($Z_q = \frac{Z_{corr} \cdot (Z_{pipe} + R_{safety\_valve})}{(Z_{pipe} + R_{safety\_valve}) - Z_{corr}}$) with R_{safety_valve} = 610 Ω and Z_{pipe} = 0.42+j0.80 Ω

R_{safety_valve}: Earthing resistance of the safety valve

R_q: Resistive part of the shunt admittance

Table 6-6: Measurement and calculation of the shunt admittance of the pipeline

Details about the calculation steps and the equivalent circuit used can be found in ([33], pages 77 to 85). Apparently, the resistive part of the shunt admittance decreases while the capacitive part of the admittance rises. More interesting, however, is the next step, where the galvanic conductance g_Q' is calculated. With the galvanic conductance, the specific pipeline coating resistance can be calculated.

Interference frequency	R_q	g_Q'	g_{Qcalc}'	r_u
15	1915.3 Ω	0,00086 mS/m		218,840 Ωm²
30	1613.2 Ω	0,00102 mS/m		184,300 Ωm²
50	1232.8 Ω	**0,00134 mS/m**	**0,00189 mS/m**	140,842 Ωm²
100	937.1 Ω	0,00176 mS/m		107,059 Ωm²
200	477.6 Ω	0,00345 mS/m		54,563 Ωm²

$\underline{R}_q$: Resistive part of the shunt admittance [Ω]

g_Q': Galvanic conductance per meter ($g_Q' = \frac{1}{R_q \cdot l_{pipeline}}$) [mS/m]

g_{Qcalc}': Calculated galvanic conductance per meter ([33], page 46; this thesis: both used formula of chapter 2.3.2.1)

r_u: Specific pipeline coating resistance ($r_u = \frac{d \cdot \pi}{g_Q'}$) [Ωm²]

Table 6-7: Measurement and calculation of the galvanic conductance and coating resistance

The measurements and the final calculations of the galvanic conductance and the specific pipeline coating resistance show very interesting results: First of all, the calculations which are made with the formula from chapter 2.3.2.1 of this thesis and also used in [33] on page 46 show similar results

as the measurement. This is particularly important because the measurement was challenging due to the circumstances and there are natural factors that cannot be considered in the calculations. Both results can be found in bold in Table 6-7.

In short, calculations with the “Formula S” and the “Formula C” are correct and can be used despite some minor differences in the theoretic calculations in chapter 2.3.1.2 which have no effect on calculating the pipeline interference voltage (PIV) in chapter 4.2.

The second result was the confirmation of a hypothesis. At the beginning of this chapter, it is stated that one of the goals of the master thesis was to find out, whether the assumption about the frequency depending behaviour of the coating resistance is correct. After measurements and calculations, a strong correlation could be found, which can best be shown in the following Figure 6-19.

The reason for this behaviour is still unclear. Possible explanations are that the coating material itself has a capacitive element or that an interaction between the coating and the surrounding soil exists which is not taken into account in the formulas. It is also possible that this measurement setup is simply not suitable for measuring the SPCR or that other reasons apply. In this case, this means that further research is required, especially since manufacturers of coating material also have no information about the frequency dependence and continue to specify only the DC resistance.

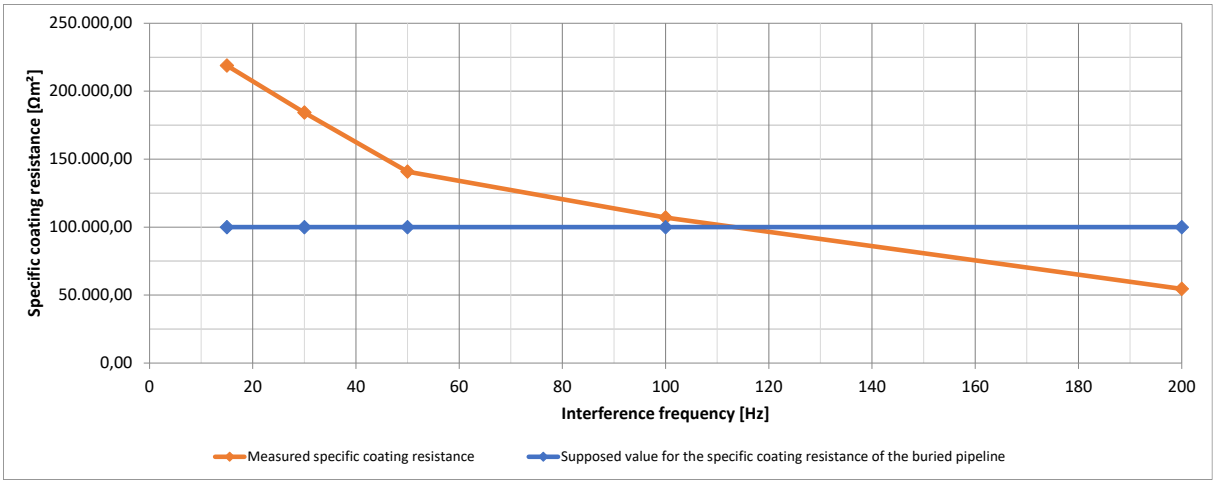

Figure 6-19: The frequency depending behaviour of the specific coating resistance

7 Comparison of measurements and calculations on the pipeline interference voltage in specific locations

In the following chapter it must be noted that only selected anonymised data and calculations are shown and only a few important geographical circumstances can be included in the discussion for reasons of protection of the companies' data.

7.1 Methods for handling the data and the calculation

Calculations are based on the worst-case scenario, therefore the maximum possible current of a high voltage power system (HVPS) is used to assess whether the personal safety can always be guaranteed. To estimate the level of risk for AC corrosion, a sufficiently large current is used, e.g. a 24-hour average current, the maximum allowed continuous current according to the (n-1)-criterion or the 95 % quantile of the continuous load current. For an analysis of the measured PIV, it is necessary to set the calculation in the context of the already performed measurement. Since the calculations and the measurements are based on different current levels of HVPSs (see chapter 4.5), the load currents of HVPSs during the measurement period must be considered in the calculations. The calculations can then be adjusted and a correct correlation between calculation and measurement can be established.

7.1.1 Top-down method

The top-down method is based on the standardized method for calculating the PIV with subsequent measurement. Subsequently, the next step is the consolidation of the measured data. For this purpose, the load currents are queried, and the calculations of the PIV made to include modified and plausible current data. In the last step, these adapted calculations are compared to the measured data. Figure 7-1 shows the sequence of steps. The conventional calculation path for determining the pipe tension is surrounded by a red frame. A detailed description of the individual steps can be found below the figure.

Based on the worst-case calculations, the calculations are modified with the load currents of HVPSs to compare the modified results with the measurement to determine whether the worst-case calculations are plausible or not.

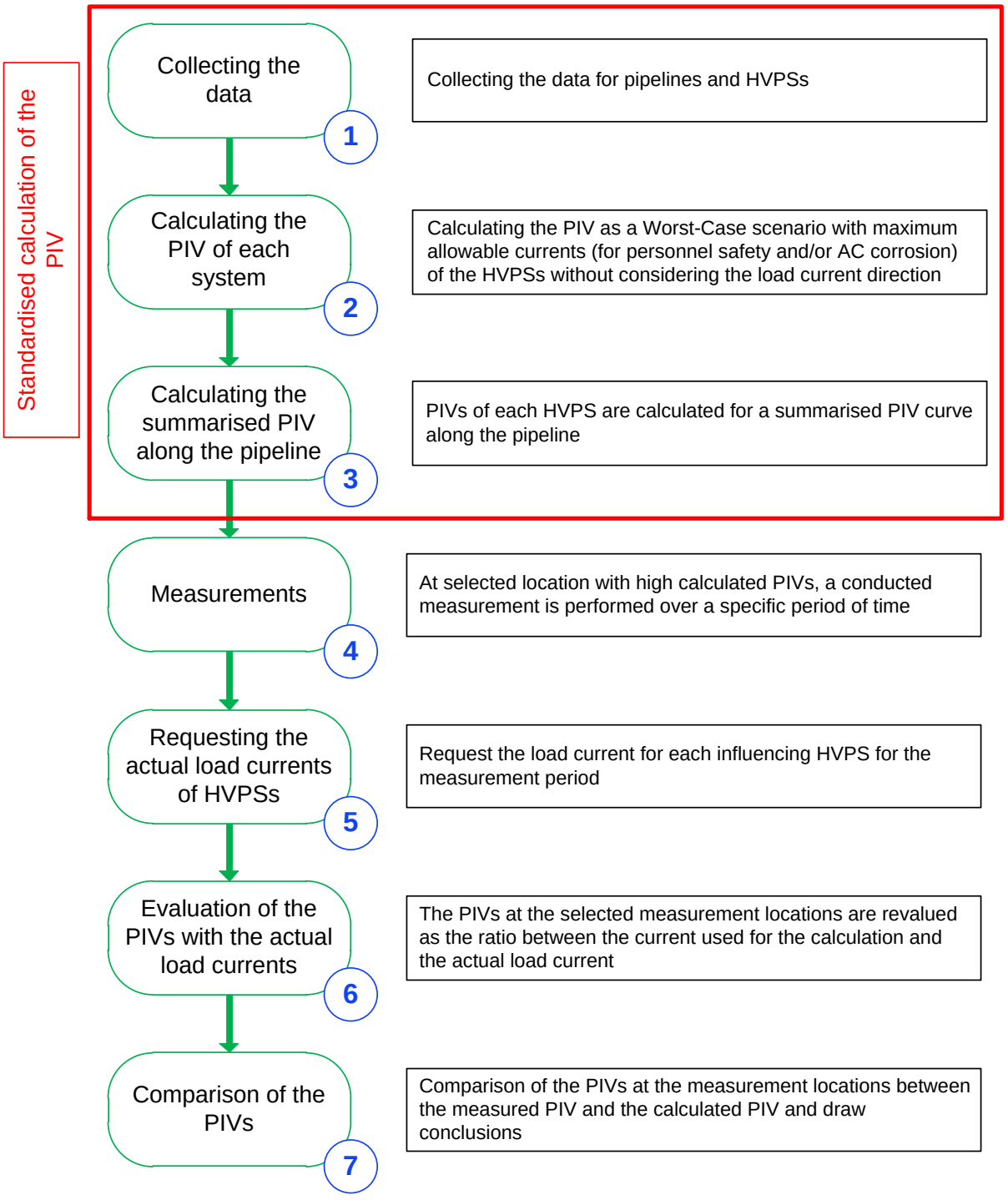

Figure 7-1: Top-down method for analysing the PIV

(1) Collecting the data

The data of pipelines and HVPSs are collected and checked for correctness and completeness.

(2) Calculating the PIV of each system

The PIV is calculated according to the current technical calculation methods. As mentioned above, on page 146, the calculations must always be assumed to be a worst-case scenario. If several HVPSs influence a pipeline, the currents of the different HVPSs are assumed to flow in the same direction (worst-case). The gain or reduction effect of metallic installations (underground metallic structures, parallel HVPSs and so on) may also be considered. Especially size, structure and/or material of metallic structures are mostly unknown and the effects of parallel HVPSs have to been sufficiently investigated previous to this thesis and therefore, the effects of these components on the PIV can only be estimated based on experience.

(3) Calculation of the summarised PIV along the pipeline

The calculations lead to the PIV U_{p_Imax} along the pipeline. Depending on a standard or guideline, either the peak value method or a summation method must be used. In the first method, the highest influenced PIV of a HVPS is used on a specific location along the pipeline, regardless of how many HVPS influence a location. This must be done for each location along a pipeline. In the second method, a summation of the PIV along the pipeline must be done when more than one HVPS influences the pipeline. This summation of the influencing potential U_{HVPS_Imax} for each HVPS is done by RMS-value addition (see formula (7-1)) of the individual PIVs and leads to a total PIV along the pipeline.

$$U_{p\_Imax} = \sqrt{\sum_{k=1}^{n} \left| U_{MHPVS\_Imax(k)} \right|^2} \qquad (7\text{-}1)$$

(4) Measurements

At selected locations with a high calculated (summarized) PIV U_{p_Imax}, measurements U_{meas} are conducted which last at least one day, ideally one week or longer.

(5) Requesting the actual load currents of HVPSs

On each selected location, each HVPS with a high influencing potential U_{HVPS_Imax} must be identified because these power systems have a higher impact on the summarized PIV U_{p_Imax}. This can be very different for each selected measurement location and requires a thorough analysis. Subsequently, the load currents for the relevant HVPSs must be requested for the measurement period.

(6) Evaluation of the PIVs with the actual load currents

The influencing potential U_{HVPS_Imax} of each HVPS is always calculated separately with their maximum current I_{max}. These calculations must be adapted with the actual load current I_{load} over the whole duration of a measurement and lead to a newly calculated influencing potential U_{HVPS_Iload}.

$$U_{HVPS\_Iload} = U_{HVPS\_Imax} \cdot \frac{I_{load}}{I_{max}} \tag{7-2}$$

Therefore, the adapted influencing potential U_{HVPS_Iload} of each HVPS is calculated and visualised over the whole measurement period. This potential U_{HVPS_Iload} is lower because of using the lower load currents and not the rated currents, and fluctuates with the load currents over the duration of the measurement.

In the case of a single interference, the new PIV U_{p_Iload} is the same as the adapted influencing potential U_{HVPS_Iload}. In the case of a multiple interference, each influencing potential U_{HVPS_Iload} is calculated to a summarized PIV U_{p_Iload}. For this, a simple summation can be used (see formula (7-3)) or again the RMS-value addition (see formula (7-4)).

$$U_{p\_Iload} = \sum_{k=1}^{n} U_{HPVS\_Iload(\boldsymbol{k})} \tag{7-3}$$

$$U_{p\_Iload} = \sqrt{\sum_{k=1}^{n} \left| U_{MHPVS\_Iload(\boldsymbol{k})} \right|^2} \tag{7-4}$$

With both methods, an evaluation of the PIV at the respective measurement location and measurement period can be executed. As will be shown later in chapter 7.2, the RMS-value summation shows better results because it takes into account the simultaneity of the different influencing HVPSs and is therefore state of the art.

(7) Comparison of the PIVs

In the last step, the originally calculated PIV U_{p_Imax}, the adapted calculated PIV U_{p_Iload} and the measurement PIV U_{meas} along the pipeline are compared. It makes sense to draw the measured and adjusted PIV of each measurement location in a graph on the correct pipeline path kilometre. For this, two different methods of comparison can be used.

With the first method, the time-comparison-method, it is possible to make a comparison of the PIVs U_{p_Imax}, U_{p_Iload} and U_{meas} for each measurement location over the complete measurement period. This method shows the chronological sequence of calculations as well as the measurement and can be also compared to the load current of high influencing

HVPSs. With time synchronising, also U_{p_Imax}, U_{p_Iload} and/or U_{meas} of different measurement locations can be compared to get a long snapshot of how high influencing potential of HVPSs is distributed along the pipeline. This means, the time-comparison-method is a useful tool to get detailed information about specific locations, but it is not very useful do get a clear information about the comparison of U_{p_Imax}, U_{p_Iload} and U_{meas} along the pipeline.

The second method is the peak-value-comparison-method. For this purpose, the maximum PIV over the entire duration of the measurement is determined for each measuring location and then the 95 % of the maximum value or the 95 %-quantile is formed to filter any measuring errors or other individual phenomena at the newly PIV U_{meas_max}. In addition, the peak value of U_{p_Imax} and U_{p_Iload} for the duration of measurement must also be calculated for each measurement location. In the next step, the beforehand calculated PIV along the pipeline is drawn in a graph with the pipeline path kilometre. Finally, all the peak values for each measurement location are inserted into the graph at the corresponding pipeline path kilometre and then, a comparison of all values is possible.

7.1.2 Down-top method

The basic idea behind the down-top method is to avoid calculations and work only with conducted measurements. Since measurement data are absolutely necessary, this method can only be used for an already built pipeline. An estimation of the maximum expected PIV is calculated with the help of the load current(s) of HVPS(s) or with additional measurements of the rotating magnetic field of HVPS(s) [41] to get the induced voltage $\underline{E}_P$ (see chapter 2.2). This direct method is feasible for simple problems but it is only a punctual method because the estimation is based on only a few measurement locations. This method is not very useful in most cases and therefore, this method has to be extended. With additional calculations, the method is similar to the Top-down method but the calculation of the results is different and also leads to different results because conducted measurements on the pipeline are done before calculations and afterwards, a comparison of the result and the estimation of the maximum expected PIV is made. Figure 7-2 shows the sequence of steps. A detailed description of the individual steps can be found below the figure.

Based on measurements and the load currents of HVPSs, finding the worst-case scenario of the PIV should be possible by extrapolating the measurement results with a comparison between the maximum allowed currents and the load currents of HVPSs.

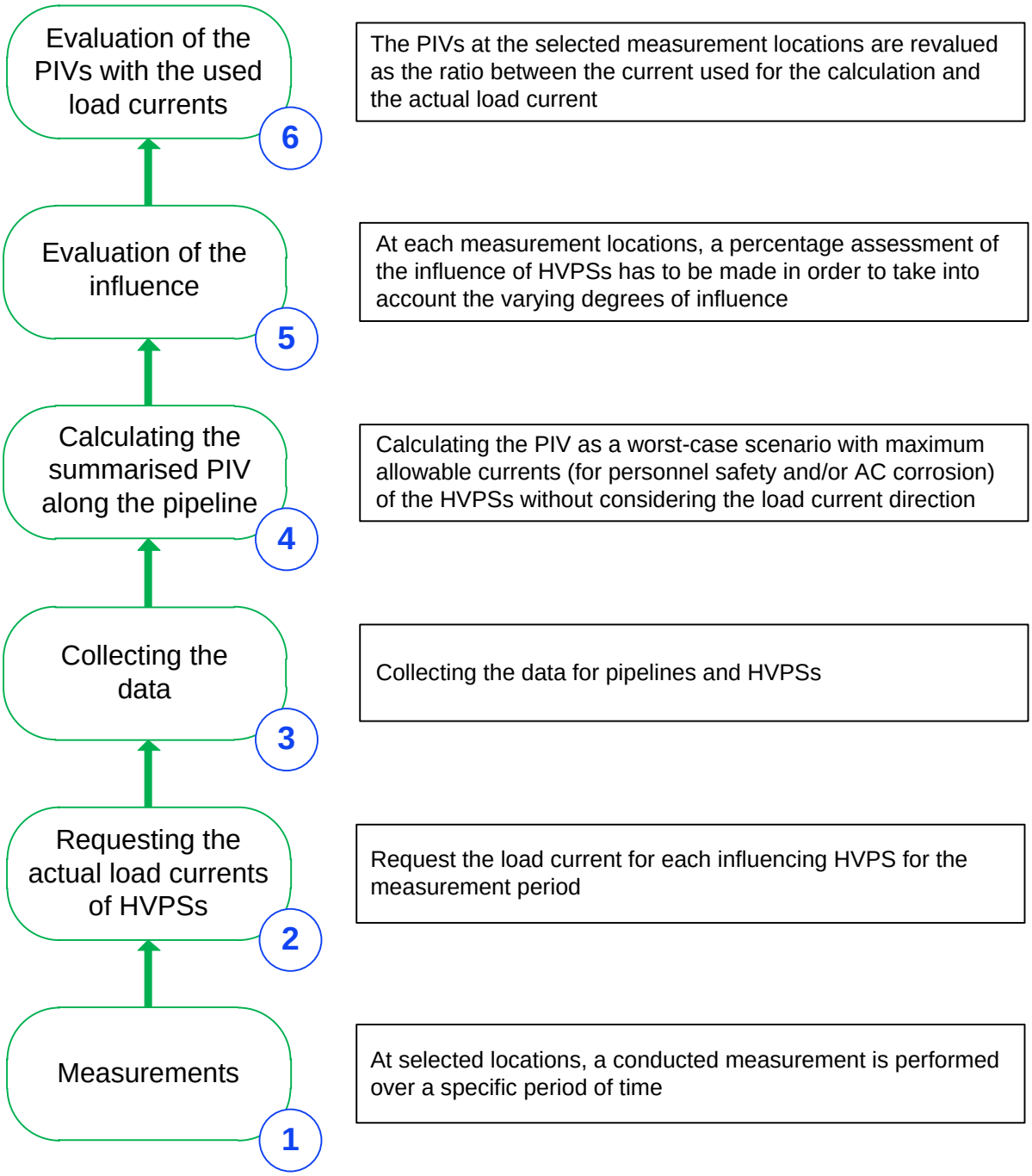

Figure 7-2: Down-top method for analysing the PIV

(1) Measurements

It is similar to the top-down method, point (4). The difference lies in the fact that without calculations, measurement locations must be estimated taking into account the interference situation or previous measurements on specific locations that already showed higher PIVs. Due to the situation that no precise data are available, the data collection becomes much more complex as much more measurements are needed.

(2) Requesting the actual load currents of HVPSs

This point is the same as in the top-down method, point (5).

(3) Collecting the data

This point is the same as in the top-down method, point (1).

(4) Calculating the summarised PIV along the pipeline

As mentioned before, in complex interference situations it is necessary to calculate the PIV U_{p_Imax} along the pipeline. An estimation of the maximum expected PIV with only measurements is not possible or too inaccurate. In addition, for each measurement location, the induced potential U_{HVPS_Imax} for each HVPS is required. In the other aspects, the calculation corresponds to the top-down method, points (2) and (3).

(5) Evaluation of the influence

After calculations corresponding to point (4), the PIV U_{p_Imax} and the induced potential U_{HVPS_Imax} for each measuring location is noted and can be used to weigh the influence for each HVPS on the PIV on each measuring location. For this, all interference potentials of all HVPSs are summarized which leads to a temporary PIV U_{p_temp}, which has a rating of 100 %.

$$U_{p\_temp} = \sum_{k=1}^{n} U_{HPVS\_Imax(\boldsymbol{k})} \tag{7-5}$$

After that, the weighting of each HVPS on the PIV U_{p_temp} is determined, e.g. a HVPS has an interference potential of 5 V on the summarized U_{p_temp} of 20 V, which means that the HVPS has a percentage rating of 25 % of the calculated PIV U_{p_temp}.

$$rating\ in\ \% = \frac{U_{HVPS\_Imax}}{U_{p\_temp}} \tag{7-6}$$

This rating can be mirrored to the beforehand calculated U_{p_Imax} and is also valid for the measured PIV U_{meas} because a similar ratio can be assumed. Another segmentation of the influence of different HVPSs on the measured PIV is not possible.

(6) Evaluation of the PIVs with the used load currents

With the calculated rating of each HVPS on the measured PIV U_{meas}, the adapted influencing potential U_{HVPS_Iload} can be calculated. In contrast to the top-down method, point (6), the measured PIV U_{meas} is the product of the inductive coupling with the actual load currents I_{load} that appear over the whole duration of a measurement. However, in order to obtain the

maximum PIV, the load currents have to be extrapolated to the maximum current I_{max}. The combination of all factors leads to formula (7-7).

$$U_{HVPS\_Imax\_recalculated} = \frac{rating\ in\ \%}{100} \cdot U_{meas} \cdot \frac{I_{max}}{I_{load}} \tag{7-7}$$

This also means that the adapted influencing potential $U_{HVPS\_Imax\_recalculated}$ must be calculated for as long as the measurement lasts. In addition, the rating varies for each measuring location and thus, the $U_{HVPS\_Imax\_recalculated}$ must be determined anew for each location. After this, the summarized PIV $U_{p\_Imax\_recalculated}$ for each measuring location can be calculated and is of course higher than the U_{meas} because of using the maximum currents I_{max} instead of the load currents I_{load}. The rest of the calculation of $U_{p\_Imax\_recalculated}$ is already specified as the calculation of the U_{p_Iload} in the top-down method, point (6).

The comparison as well as the evaluation of the different PIVs has already been described in the top-down method, point (7). The usage of the 95 % of the maximum value or the 95 %-quantile of the influencing rated currents of the power lines should be noted.

7.1.3 Top-down-top method

The final method is an enhancement of the top-down method with an additional feedback loop, as shown in Figure 7-3. Calculating and looking through the comparison between the PIVs U_{p_Imax}, U_{p_Iload} and U_{meas} for a specific measuring location or the complete pipeline length may lead to satisfying results. However, if this is not the case, further investigations and a feedback loop are necessary. This includes an analysis of the calculation parameter, measurement errors, a detailed analysis of the comparison and furthermore, considering other effects such as surrounding parameters. All of these topics have already been described in this thesis. It must also be mentioned that this method can only be applied to existing pipelines, as exact measurement data are required.

The top-down-top method is the most exact method of calculating the PIV but it takes a lot of time to take into account all of these factors. After are all factors are considered, further calculations lead to a new comparison as well as the feedback loop until the results between calculation and measurement are comparable. Of course, this method only considers individual locations on a pipeline. The calculation can be adjusted, however, so that the results roughly correspond to the real PIV even outside the measuring locations. Figure 7-3 shows the sequence of steps. A detailed description of the individual steps can be found below the figure.

Based on the worst-case calculations and conducted measurements on the pipeline, the calculations are modified with the load currents of HVPSs to compare the modified results with the measurement. This shows whether the worst-case calculations are practicable or not. If not, the calculations are repeated, by modifying parameters, to find a reasonable worst-case scenario.

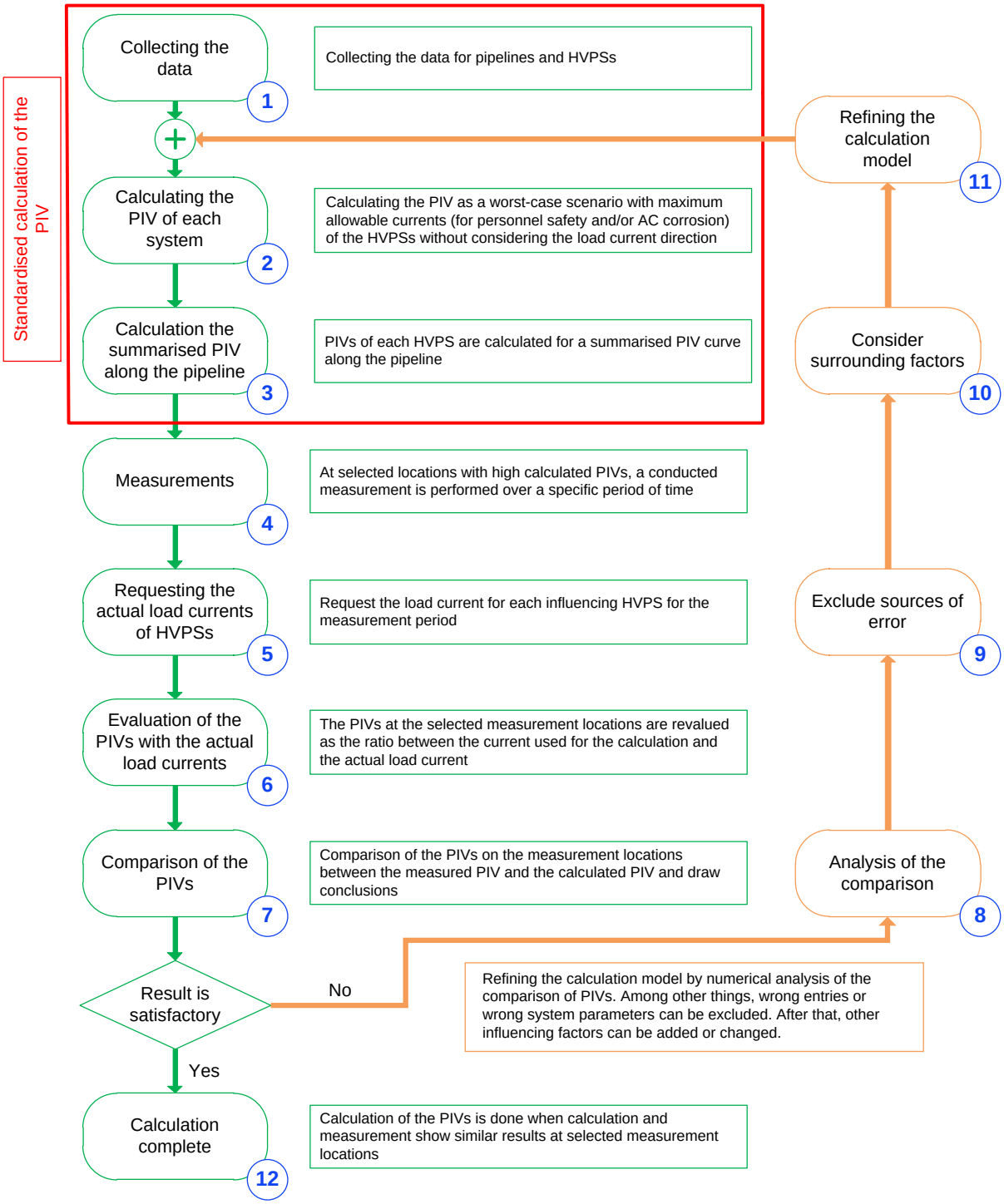

Figure 7-3: Top-down-top method for analysing the PIV

(1) Collecting the data

See top-down method, point (1).

(2) Calculating the PIV of each system

See top-down method, point (2).

(3) Calculation of the summarised PIV along the pipeline

See top-down method, point (3).

(4) Measurements

See top-down method, point (4).

(5) Requesting the actual load currents of HVPSs

See top-down method, point (5).

(6) Evaluation of the PIVs with the actual load currents

See top-down method, point (6).

(7) Comparison of the PIVs

See top-down method, point (7). Calculating and looking through the comparison between the PIVs U_{p_Imax}, U_{p_Iload} and U_{meas} for a specific measuring location or the complete pipeline length may lead to satisfying results. However, if this is not the case, further investigations and a feedback loop are necessary.

(8) Analysis of the comparison

Further investigations begin with a more exact analysis of each comparison of measuring locations and of the calculations over the full pipeline length. For this purpose, it must first be examined which HVPS is the main source of interference. This can be done for each measuring location by analysing and overlapping the load currents of each overhead line and railway line with the measured PIV. It is also necessary to estimate whether the pipeline parameters and soil resistance have been correctly selected or correctly specified by the operator by considering how the influencing potential of each HVPS develops along the pipeline.

(9) Exclude sources of error

Calculation parameters can be wrongly selected or specified by the operators of pipelines and HVPSs. Chapters 4.2, 4.3, 0 and 6.2 already showed that the calculation model is correct with the proper parameters. The formula of the inductive coupling was also verified in chapters 2.3.3, 0 and 4.1 as well as in the thesis [24].With wrong parameters given by operators, incorrect PIVs can be calculated. Furthermore, correct information about overhead lines (OHL) is necessary, as shown in chapters 4.6 and 4.7, otherwise the wrong interference potential of the OHLs is considered. As shown by [25], the same is true for railroads.

(10) Consider surrounding factors

When all calculation parameters are correct, then surrounding factors such as the soil resistivity (layer model, unsteady values) and other metallic structures can play a key role, as shown in various examples in chapters 0 and 5. Getting detailed information about these factors is difficult and sometimes very time-consuming; therefore, an estimation of the reduction or amplifying factors is required.

The factors must be estimated to a somewhat realistic and not exaggerated value for the specific measuring locations. The surrounding factors, however, can influence the PIV outside of these locations as well. Outside of these measuring locations, estimations are possible but the factors must be properly estimated, which is difficult. This illustrates the limitations of the calculation model.

(11) Refining the calculation model

At this point, all pipeline and HVPS parameters should be correctly considered and now surrounding factors like soil resistivity or surrounding metallic structures can be optimized in each calculation step. Adding other metallic structures in the calculation model of chapter 3 is quite simple but as already mentioned there, more structures in the model lead to a higher calculation complexity and the computing time as well as the memory usage rises exponentially.

(12) Calculation completed

After all factors and parameters are considered and verified and the calculation results are similar to the data from specific measuring locations, the top-down-top method is completed. If this is not the case, it is possible to extend the calculation model to the full pipeline to get more realistic results for the worst-case scenarios.

7.2 Comparison on selected measuring locations for analysing the calculated and measured pipeline interference voltage

This chapter discusses the main idea of this thesis. As already stated, calculations usually consider worst-case scenarios but conducted measurements show much lower values than the calculations suggest. To get comparable results, the top-down method was created. The research into the literature showed that such comparisons are very rare ([26], [27]) and they are only for a specific project. There, surprisingly, the differences between calculations and measurements are almost very small. Also, these works do not discuss formulas, the calculation method or other elements, chapter 5 showed that there exist many surrounding effects which cannot all be considered in calculations, leading to calculation errors.

7.2.1 Overview

For research and also for customer orders, a variety of different locations on some pipelines have been calculated, including comparisons of calculated and measured PIVs. The following selected examples show different results of comparisons on specific measuring locations. It must be said that the illustrations for the measurement locations do not correspond to specific existing locations and show only exemplarily the problem of the comparison between measurement and calculation. These figures also show the calculation with the maximum allowed current of the HVPSs. The calculations were done beforehand and because it is the worst-case scenario, the value of the PIV remains constant over the complete measurement duration, as can be seen in the figures as a straight line. The calculated worst-case PIV is labelled “calculation”. In these examples, the conducted measurements are labelled “measurement”.

For analysing the examples, the top-down method is used with both calculation formulas. Method 1 describes the RMS-value addition (see formula (7-4)), method 2 the simple summarising (see formula (7-3)). As mentioned above, it can be said in advance that the RMS-value method shows better results than the simple summarising because it takes into account the simultaneity of the different influencing HVPSs. Therefore, the following examples show that it is state of the art and that the RMS-value method is a good choice for comparisons between measurement and calculation. This method is also described in the ÖVE/ÖNORM EN 50443 [12] as well as in the ÖVE/ÖNORM EN 15280 [13] / ÖNORM EN ISO 18086 [14].

The following seven examples show different problems that can occur when comparing calculation and measurement. The first example shows a simple problem. The complexity then increases in the other examples, where more factors have to be taken into account, which make a comparison increasingly difficult. The following table lists the influencing factors that are relevant for the respective example:

Example number	Simple influence	Mixed influence	Surrounding effects	Wrong calculation parameter	Measurement problem
1; page 159	✔				
2; page 160		✔		✔	
3; page 161		✔	✔		
4; page 162		✔	✔		
5; page 162		✔	✔	✔	
6; page 164	✔				✔
7; page 166	✔		✔		✔

Table 7-1: Influencing factors for the respective examples

The legend of the table is described as follows:

- **Simple influence:** Describes a simple influence between pipeline and HVPS. In this case, a single HVPS at the measurement location is largely responsible for the PIV.
- **Mixed influence:** Describes multiple influences of HVPSs on the pipeline. Without a more detailed analysis, it is not immediately clear, which HVPS is the main cause of the PIV.
- **Surrounding effects:** Describes whether surrounding factors such as metallic structures have a significant influence on the calculation of the PIV.
- **Wrong calculation parameters:** Describes whether parameters such as soil resistivity were incorrectly taken into account in the calculations, which then led to incorrect results in the calculation of the PIV.
- **Measurement problem:** Describes the occurrence of an error in the measurements of the PIV.

7.2.2 First example: Influence of an overhead line with a similar result of measurement and calculation

Figure 7-4 shows the first simple example with an overhead line next to a pipeline and the measurement location.

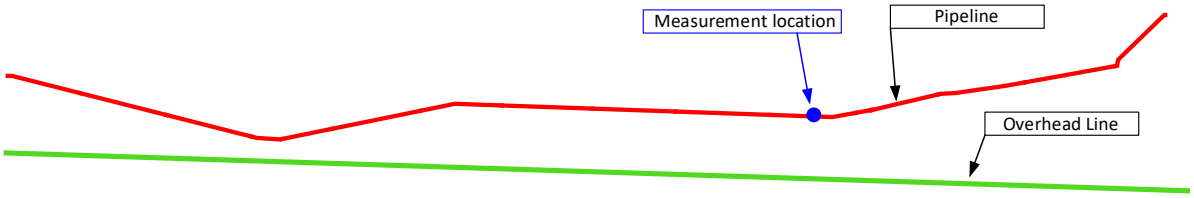

Figure 7-4: Measurement location of the first example

Figure 7-5 shows the first example of this comparison method. At this measuring location, only a low PIV is calculated. Interestingly, the calculated worst-case value with around 1.7 Volt is correct. This finding is shown after adding the load currents, because the red and green calculated and the blue measured voltage curve have an almost identical progression and the voltage values of the calculation are around the same level as the measured values.

In addition, the curve progression clearly shows that an overhead line (OHL) with their day/night and weekday/weekend rhythm influences the pipeline due to the shape of the graph, as already illustrated in chapter 6.1.2.

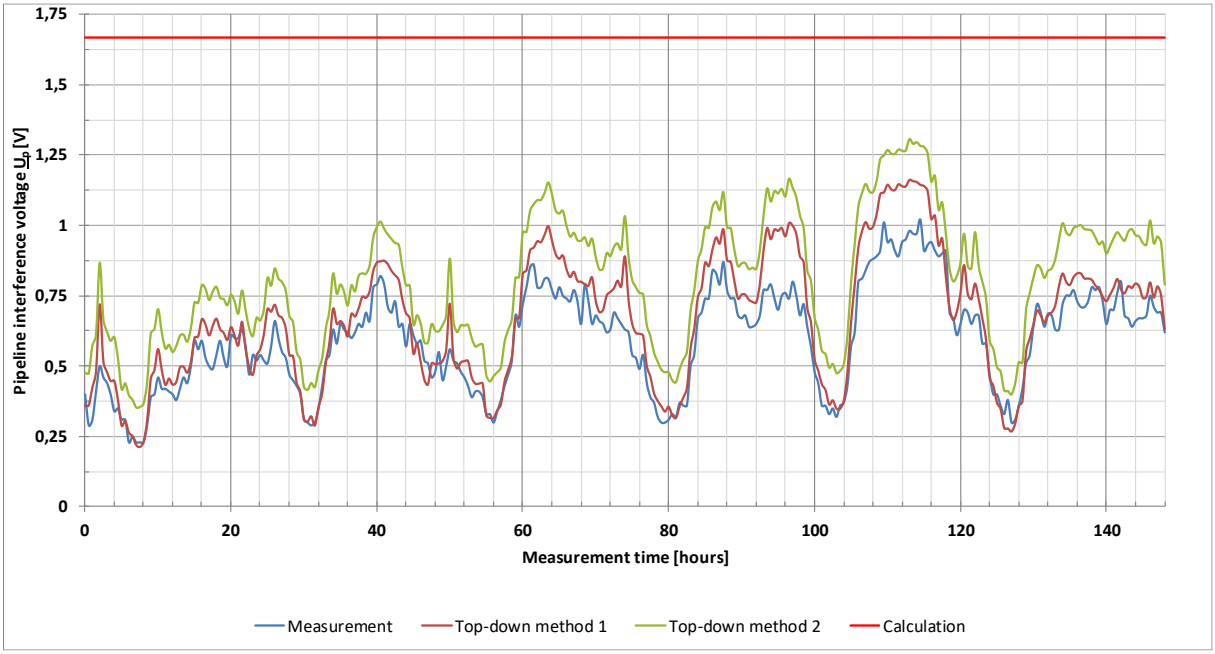

Figure 7-5: Top-down method; similar results of calculation and measurement, example with only an OHL

7.2.3 Second example: Influence of two railroad systems with a similar result of measurement and calculation

The interference of railroads on the PIV is very different than from OHLs, as already explained in chapter 6.1.2. Figure 7-6 shows the measurement location next to a pipeline mostly influenced by two railroads.

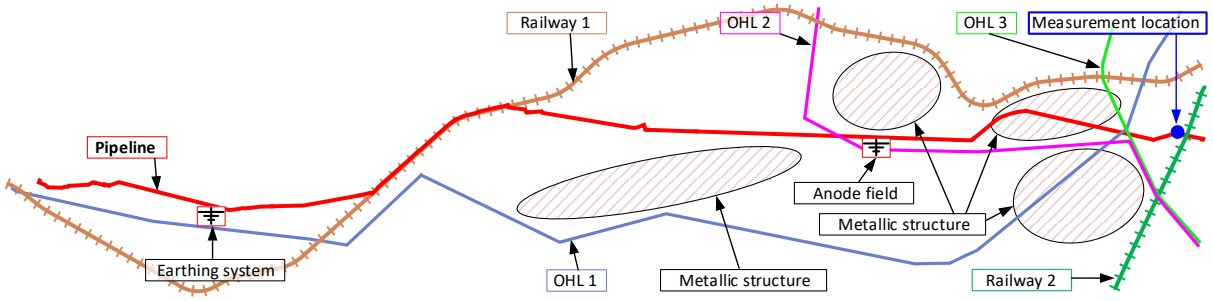

Figure 7-6: Measurement location of the second example

Figure 7-7 shows that the correct calculation of the influence is possible despite the sometimes complex electrical systems of railway lines. The figure shows that the calculated worst-case scenario is only a little too high because, after applying the top-down method 1, the voltage curve is almost identical to the curve of the measurement, but the voltage value is somewhat too high. A possible reason might be a too high specific pipeline coating resistance (SPCR).

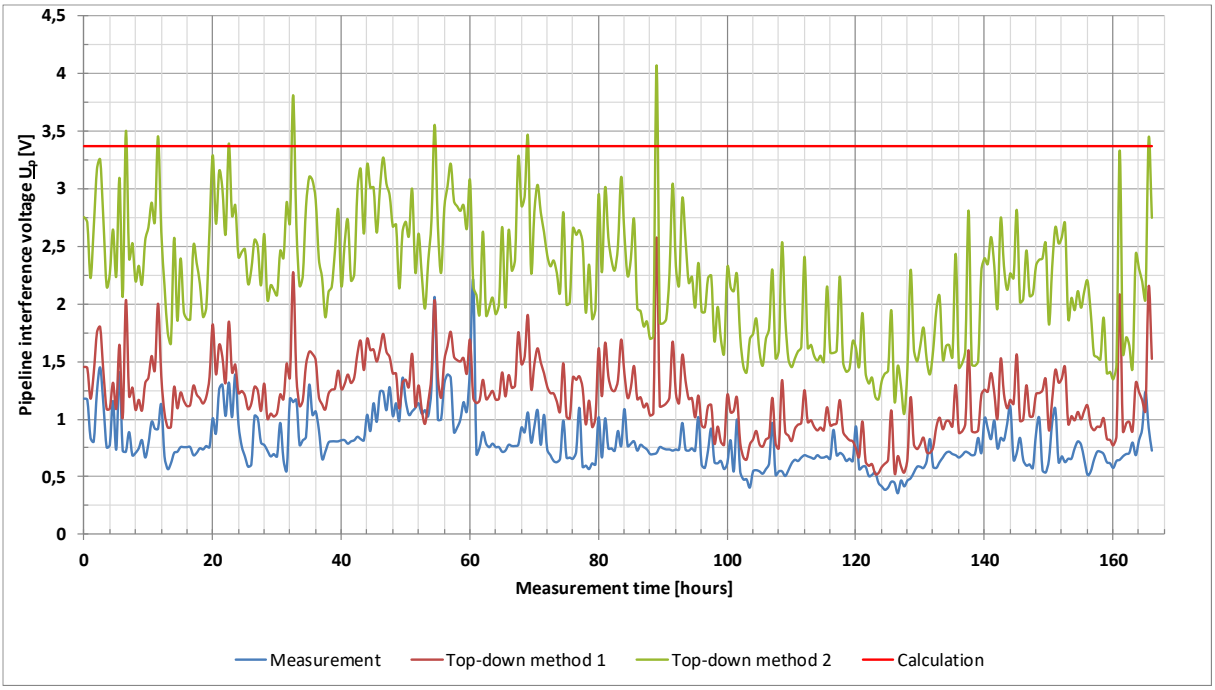

Figure 7-7: Top-down method; similar results of calculation and measurement for method 1

Here, the positive impact of taking into account the simultaneity of two or more sources of influence comes into effect and clearly shows that the RMS-value addition is well-suited for the calculation of the PIV. From this it can be concluded that the top-down method 2 calculates a voltage level which is too high, as shown in the figure below.

7.2.4 Third example: Mixed influence of overhead line and railroad system with a similar result of measurement and calculation

Figure 7-8 illustrates the measurement location next to a mixed influence of an OHL and a railroad system.

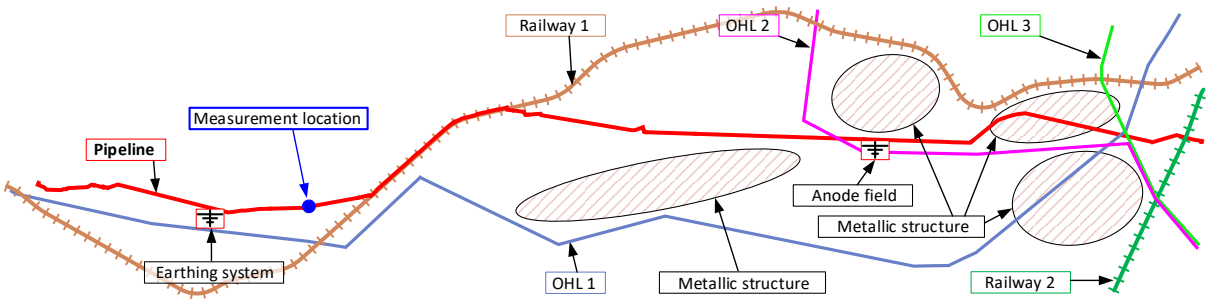

Figure 7-8: Measurement location of the third example

Figure 7-9 shows a similar result with some bigger differences. First of all, the measured voltage curve still shows a day/night and weekday/weekend rhythm but after taking a closer look, the curve appears more jagged and has some strong upturn movements. As explained in chapter 6.1.2, it is clear that an OHL as well a railroad system must influence the pipeline but the OHL has a bigger impact. Also, the top-down method 1 (RMS-value addition, see formula (7-4)) yields a much better result than the simple summarising method (top-down method 2). This finding is important because all other examples in this thesis (as well as not shown examples) show the same result. Since this method is also described in the ÖVE/ÖNORM EN 50443 [12] as well as in the ÖVE/ÖNORM EN 15280 [13]/ÖNORM EN ISO 18086 [14], it must be assumed that this is correct.

In addition to these two main findings, the figure shows a certain decoupling between measurement and calculation in between the measurement time of 50 and 70 hours. In the period of 50 to 60 hours, the measurement values are higher than the calculated ones. This is caused by the railroad system which means that it induced more into the pipeline than calculated.

There can be two assumptions: First, the specific pipeline coating resistance (SPCR) was better than estimated and the influence has spread further, or second, other secondary railroad systems like amplification conductors also influence the pipeline [25].

For the period of 60 to 70 hours, the OHL and railroad may induce their interference currents into the pipeline in different directions which leads to the result that a part of the interference current of both systems is cancelled out, creating a lower PIV.

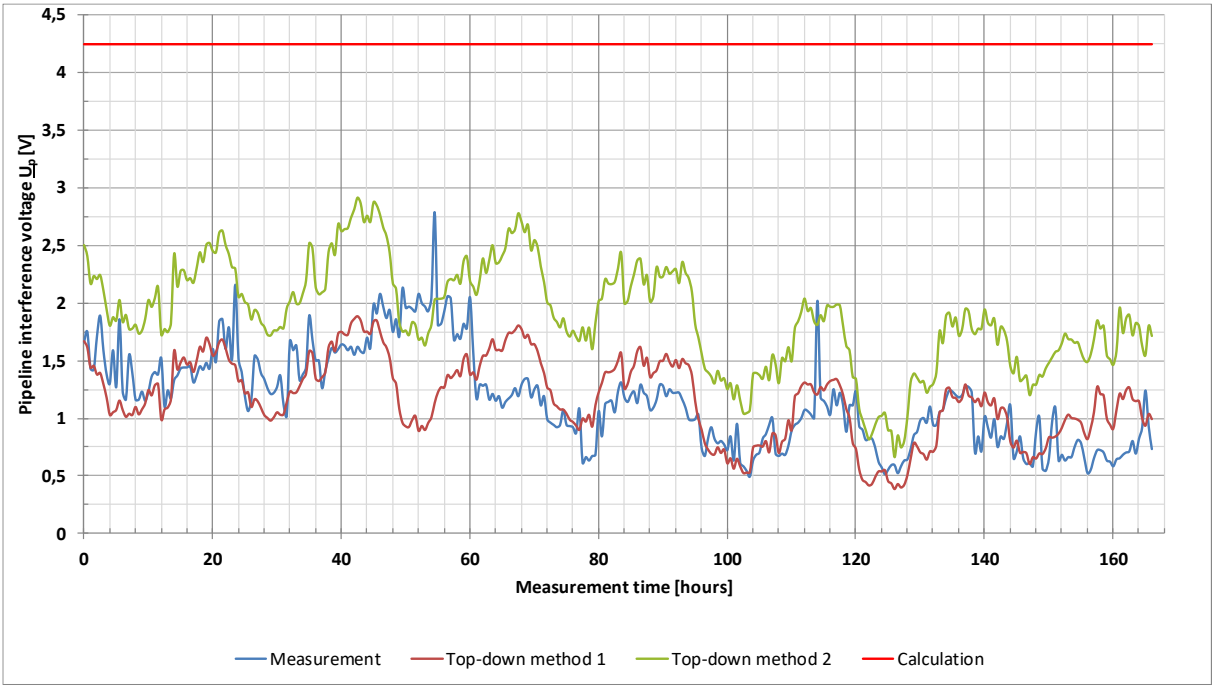

Figure 7-9: Top-down method; similar results of calculation and measurement, example with a combination of OHL and railroad system

7.2.5 Fourth example: Influence of multiple influencing systems with surrounding effects

Without taking into account surrounding effects, such as metallic structures, worst-case calculations as well as adapted calculations cannot be correct.

Figure 7-10 shows the measurement location next to multiple influencing systems as well as unknown metallic structures.

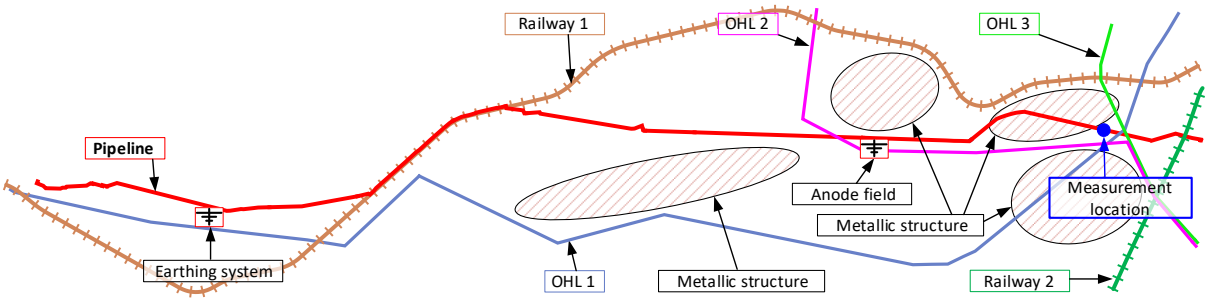

Figure 7-10: Measurement location of the fourth example

Figure 7-11 simply shows that the top-down method 1 with the adapted calculation is too high. It is obvious that the voltage curve of method 1 (and 2) and the measurement are very similar and also have no zero point shift. Possible influencing factors are mainly metallic structures that are located in the vicinity and have a strong influence on the PIV.

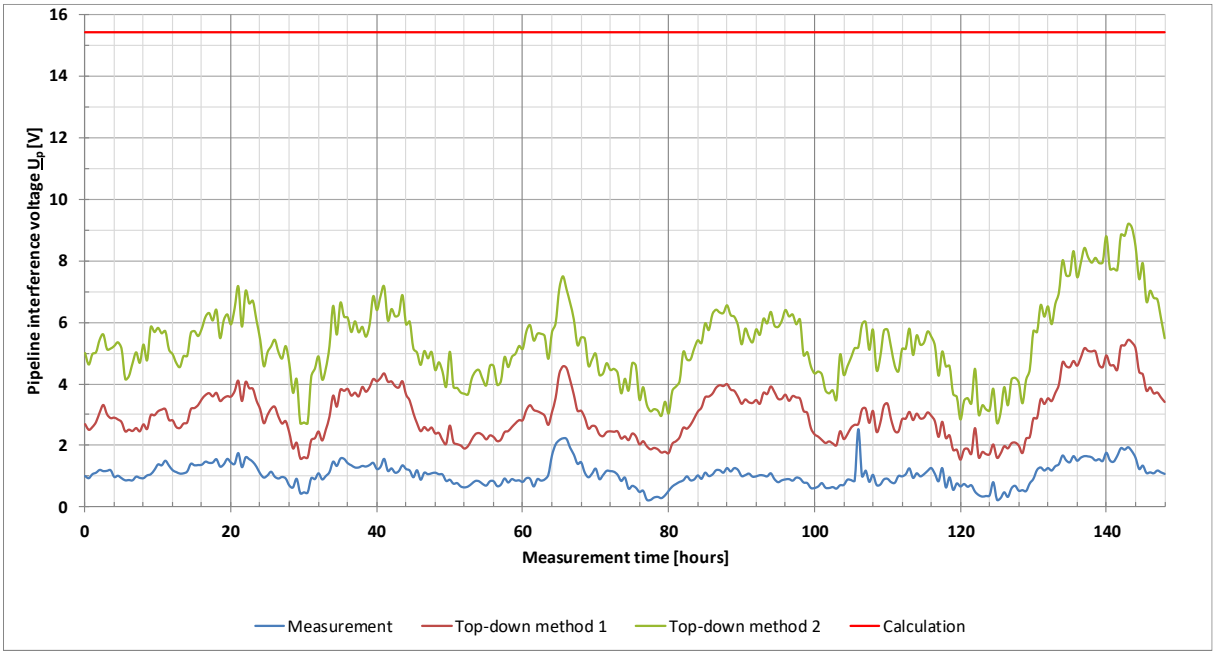

Figure 7-11: Top-down method; results of calculation and measurement are very different because of surrounding effects

7.2.6 Fifth example: Influence of multiple influencing systems with wrong calculation parameters

Figure 7-12 shows a measurement location next to multiple influencing systems. It represents an interesting example and illustrates the problems that often occur.

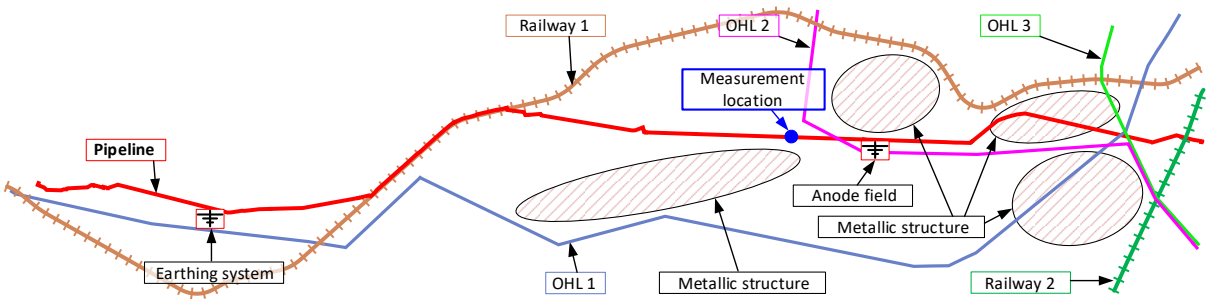

Figure 7-12: Measurement location of the fifth example

Figure 7-13 shows that the red line with the calculated worst-case scenario is considerably higher than the measurement. This indicates that one or more parameters are wrong. The voltage level of the top-down method is too high because surrounding effects like other metallic structures reduce the induced potential from the HVPSs. Another problem can be that an essential parameter for the calculation was assumed wrong or a wrong value was given by the operator. This parameter can be either a too low soil resistivity (see chapter 4.3) or a too low SPCR (see chapter 4.4) because the mean of the top-down method 1 shows a zero point shift compared to the mean of the measurement.

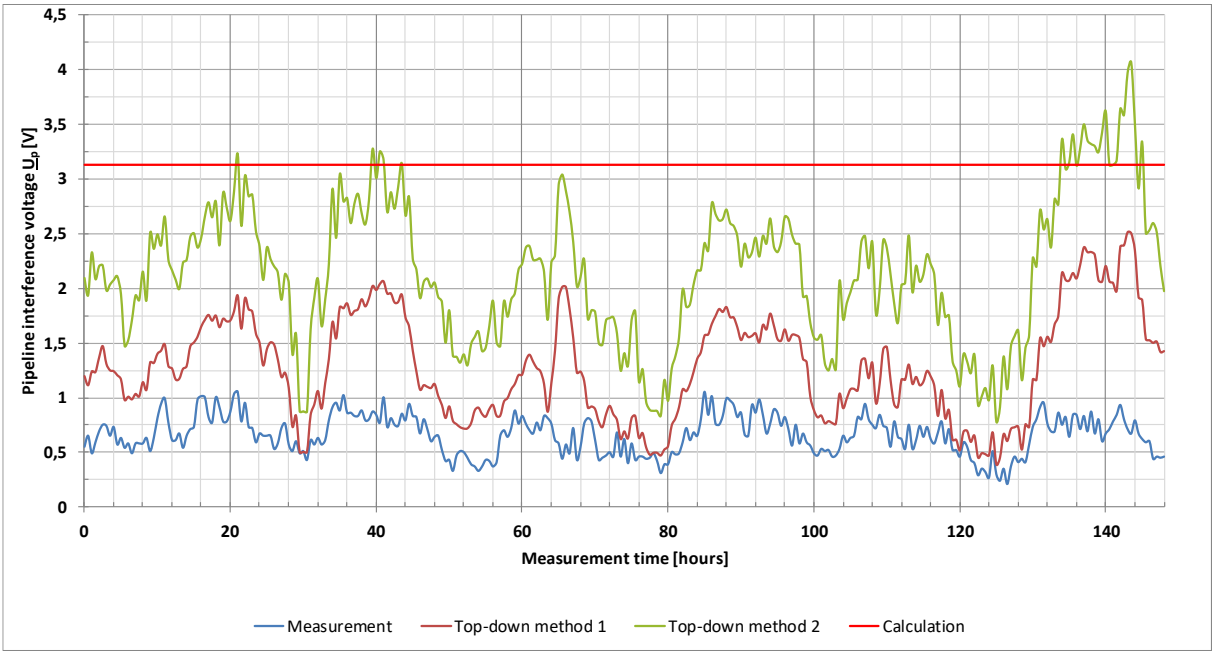

Figure 7-13: Top-down method; results of calculation and measurement with wrong calculation parameters

7.2.7 Sixth example: Measurement problems make comparisons difficult

The Figure 7-14 shows a measurement location with multiple influencing systems but focuses on an additional problem in which calculation and measurement do not match.

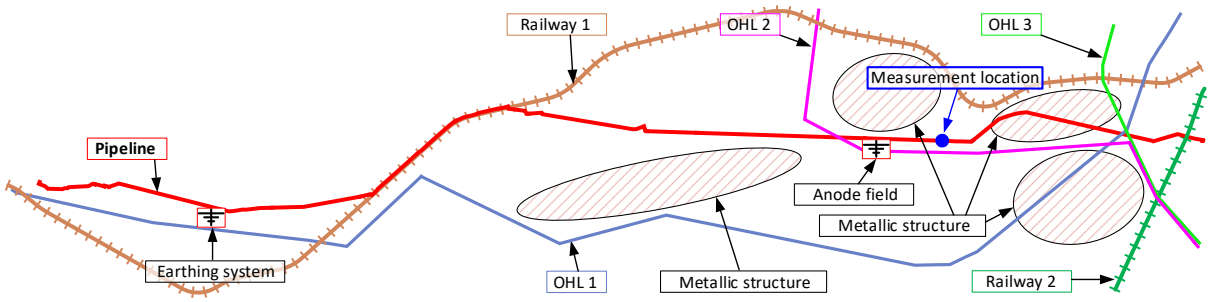

Figure 7-14: Measurement location of the sixth example

Figure 7-15 depicts a frequent problem of missing data or measurement errors. The second half of the voltage curve shows a very good example of how measurement and adapted calculation with the top-down method 1 should look. Conversely, this also means that the worst-case calculation (red line) is correct. However, the first half of the graph shows that the measuring results cannot be correct.

The operators of the pipeline cannot explain why the measurement was wrong in the first half of the measurement period. Possible reasons can be e.g. the reference potential of the measurement does not have good ground contact or the measuring device is poorly connected. However, this measurement is crucial, because the conducted measurement is suddenly correct starting from the middle of the measurement period. Further investigations showed that a temporary reference potential was used for the measurement. It started to rain in the middle of the measurement and thus, the reference potential had a good connection to the ground.

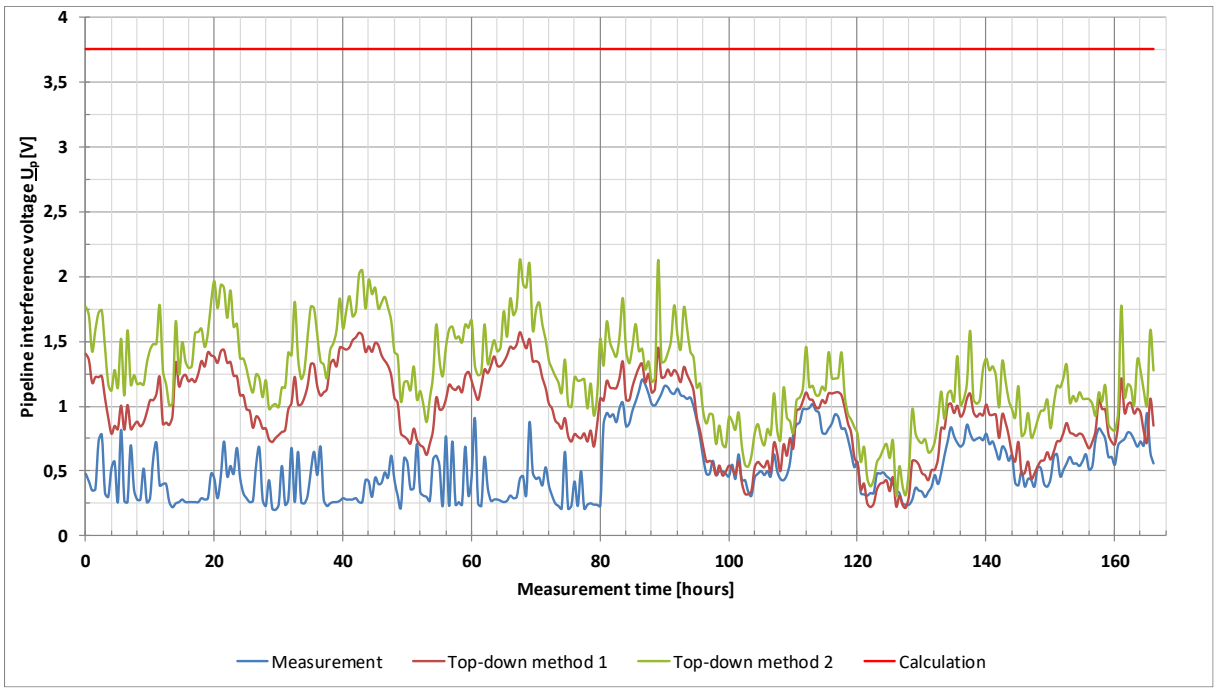

Figure 7-15: Top-down method; results of calculation and measurement; the problem of measurement errors

7.2.8 Seventh example: Influence of an overhead line without curve correlation

The last Figure 7-16 shows a measurement location in which calculation and measurement do not match.

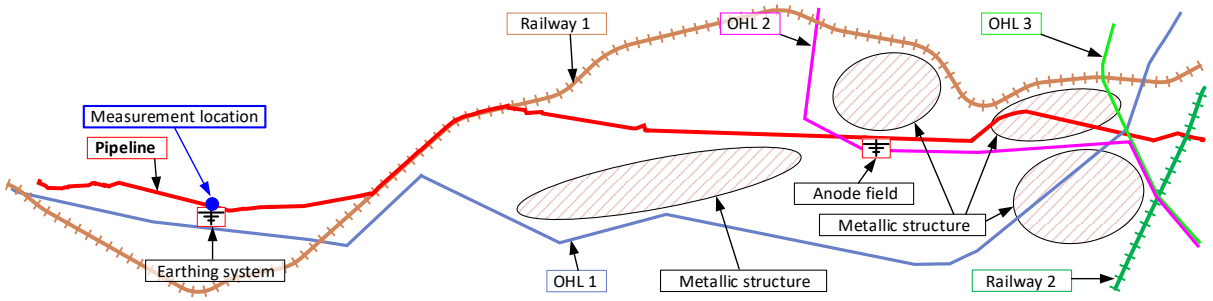

Figure 7-16: Measurement location of the seventh example

The results of the last example of this chapter are shown in Figure 7-17. It shows that in addition to the problem with excessive voltages, another interesting detail can be seen: The exact comparison of the curve shape of the top-down method 1 and the measurement leads to the result that no correlation between the two curves can be found. In the next chapter 7.3, the solution will show a surprising result. This and other comparable cases show that an explanation is difficult to find.

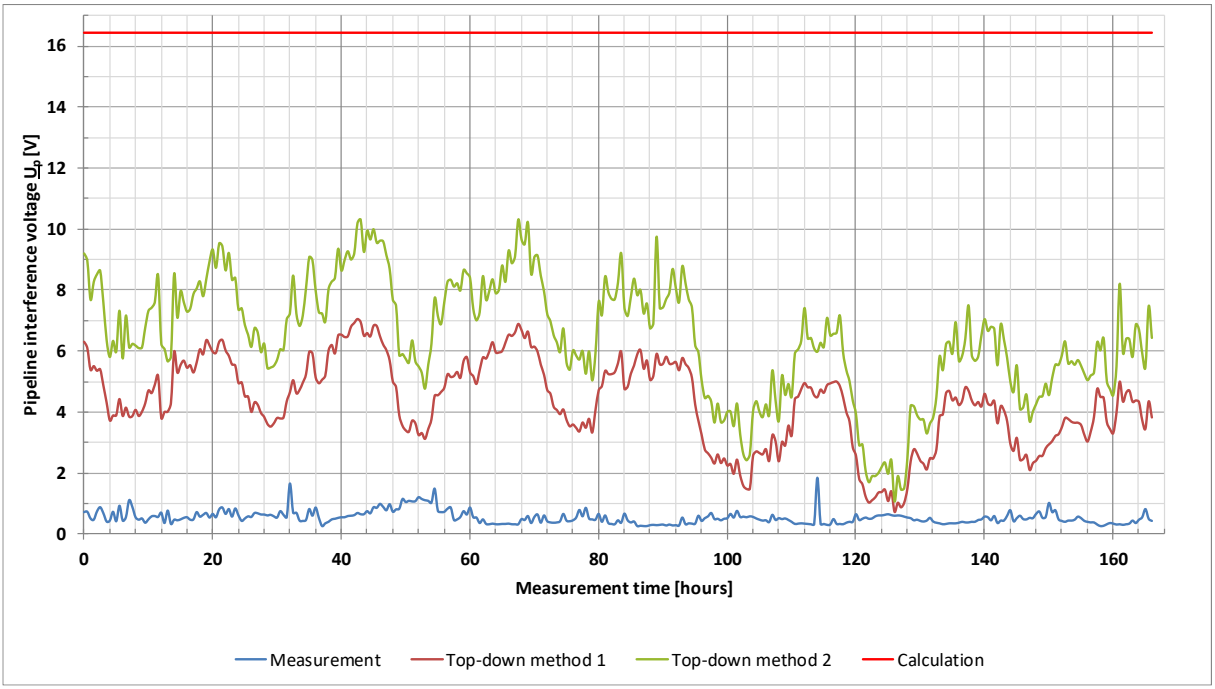

Figure 7-17: Top-down method; results of calculation and measurement shows no curve correlation

7.2.9 Summary

In summary, considering the load currents after the worst-case calculations is a good idea because it can show that the calculations are correct in some cases. For other measuring locations, the worst-case calculations are too high and thus, further analysis is needed to find out which parameter is causing a problem. This method also shows fundamental measurement errors and therefore, the accuracy of measurements can be improved by giving feedback to the pipeline operators about wrong measuring results.

7.3 Considering calculation parameters and surrounding effects for the comparison on measuring locations

7.3.1 Overview

This chapter is based on the previous chapter 7.2 but here the top-down-top method is also used. As described in chapter 7.1.3, a feedback loop is activated in calculations, which takes into account all calculated parameters of chapters 4.2 to 4.7 and all surrounding metallic structures of chapter 5. Considering the surrounding structures leads to a screening factor which can increase or decrease the pipeline interference voltage (PIV), as described in chapter 5. After all calculated parameters have been verified and possibly corrected, the screening conductor (SC) has to be considered. For privacy reasons, selected analysis but no geographical data can be discussed.

Most examples from the chapter before are recalculated considering the feedback loop with the additional SC and the adapted calculation parameters. New interesting examples from other locations are also included. These figures show the calculation with the maximum allowed current of the HVPSs which is now labelled “Worst-case scenario”. Again, conducted measurements are labelled “measurement”. For the analysis, the top-down method as well as the top-down-top method with the RMS-value addition (see formula (7-4)) is used to achieve better results. These calculations are also indicated in the graphic and show the difference between non-consideration and consideration of the feedback loop. Taking this loop into account, the worst-case scenario, labelled “Adapted worst-case scenario”, is recalculated with the help of the calculated reduction factor (or screening factor).

Similar to chapter 7.2, this chapter deals with various problems that may arise when comparing calculation and measurement. It starts with a simple problem and then shows a higher complexity of the comparison. This chapter also in part continues the analyses of the examples discussed in chapter 7.2. The following table lists the influencing factors that are relevant for the respective example:

Example number	Based on example	Simple influence	Mixed influence	Wrong calc. para.	Surrounding effects	Time stamp problem	Earthing system
1; page 169	**2**; p. 160		✔	✔			
2; page 170	**4**; p. 162		✔		✔		
3; page 171	**5**; p. 163		✔	✔	✔		
4; page 172	none		✔				✔
5; page 173	**7**; p. 166	✔				✔	✔
6; page 175	none	✔		✔		✔	

Table 7-2: Influencing factors for the respective examples

The legend of the table is described as follows:

- **Based on example:** Shows whether the selected example has already been discussed in chapter 7.2. If this is the case, then the example and page number are given.
- **Simple influence:** Describes a simple influence between pipeline and HVPS. In this case, a single HVPS at the measurement location is largely responsible for the PIV.
- **Mixed influence:** Describes multiple influences of HVPSs on the pipeline. Without a more detailed analysis, it is not immediately clear, which HVPS is the main cause of the PIV.
- **Wrong calc. para. (wrong calculation parameters):** Describes whether pipeline parameters such as soil resistivity or the specific pipeline coating resistance, or parameters from the influencing systems (HVPSs) were incorrectly taken into account in the calculations, which then led to incorrect results for the calculation of the PIV.
- **Surrounding effects:** Describes whether surrounding factors such as metallic structures have a significant influence on the calculation of the PIV.
- **Time stamp problem:** In the respective example, the problem of incorrect time stamps in measurements as well as in load current data is discussed.
- **Earthing systems:** Based on measurements, we describe the problem of unknown earthing systems that have not been taken into account in the calculations. In addition, it is shown how the earthing systems were correctly implemented in the calculations based on the measurements.

7.3.2 First example: Minor optimisation of the PIV

Again, the measurement location from chapter 7.2.3 is used and shown in Figure 7-18.

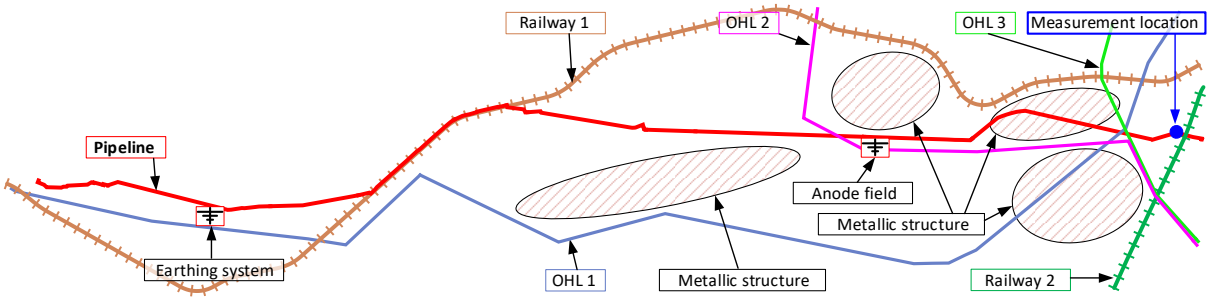

Figure 7-18: Measurement location of the first example

Figure 7-19 is the result of recalculating Figure 7-7 in chapter 7.2.3. There it is mentioned that the result of the top-down method is a little too high but acceptable. Even though the PIV curve was recalculated, the result below shows that optimising is still possible. The curve shape of the measurement and the top-down-top method are quasi identical which means that the adapted worst-case scenario has a lower voltage level (orange line around 2.25 Volt).

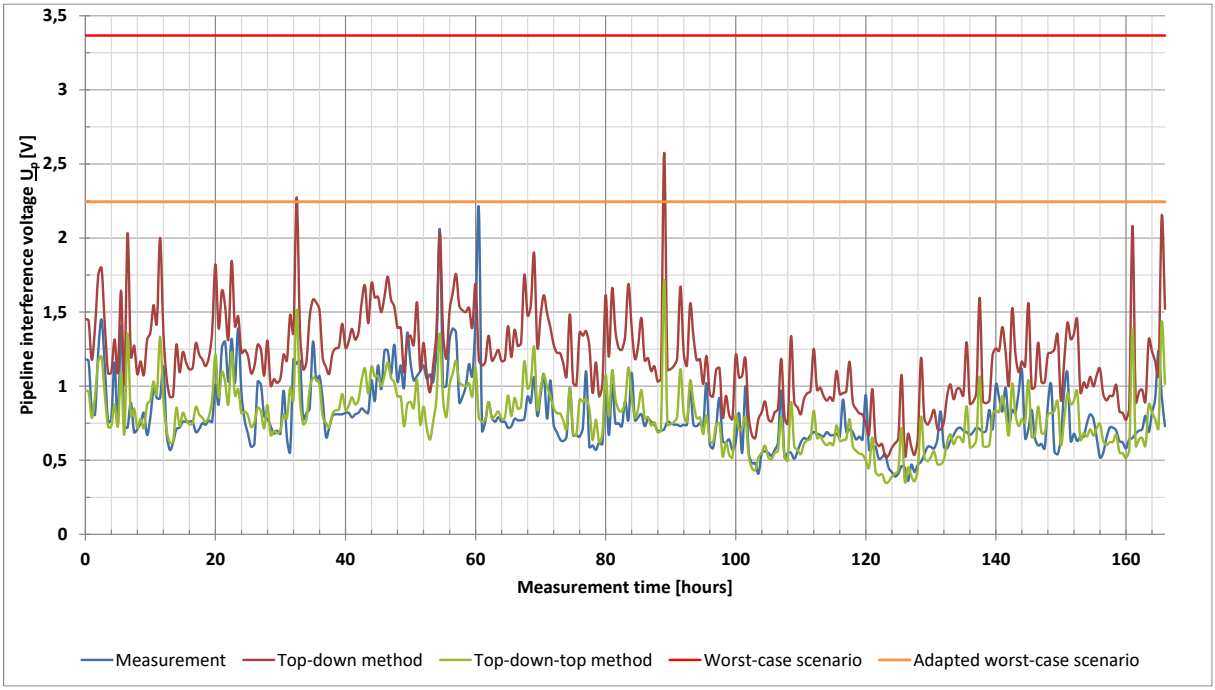

Figure 7-19: Top-down-top method; recalculating Figure 7-7

This example is not significantly affected by surrounding structures and the basic calculation parameters were also by and large correct. However, it turned out that after the SPCR was changed, almost the same results could be achieved. This illustrates how difficult it is to have calculation results that are similar to the measurements, even when considering all parameters carefully,

because some measurable pipeline parameters still differ from the theoretical ones. In short, it shows the limitations of how similar calculation results can be to the real values when there is no exact knowledge of all pipeline parameters.

7.3.3 Second example: Considering larger suburban areas

Again, the measurement location from chapter 7.2.5 is used and shown in Figure 7-20.

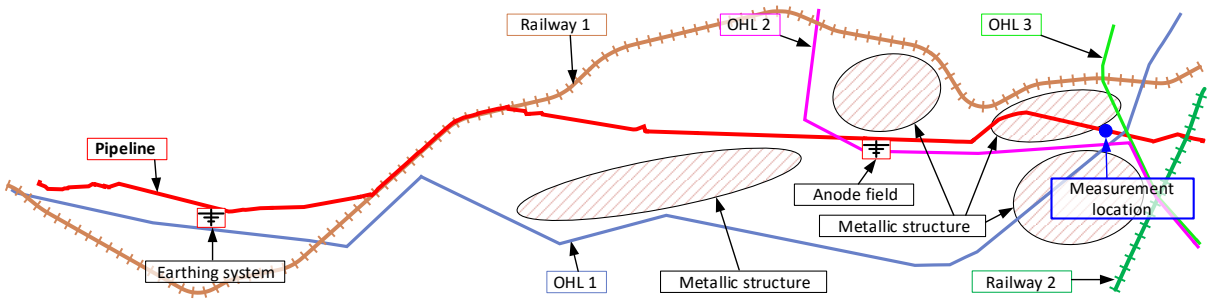

Figure 7-20: Measurement location of the second example

Figure 7-21 shows the recalculated example of Figure 7-11 in chapter 7.2.5. The description of Figure 7-11 is short because it simply shows the calculation of a PIV that is too high. This characterisation is still valid for this figure when using the top-down-top method.

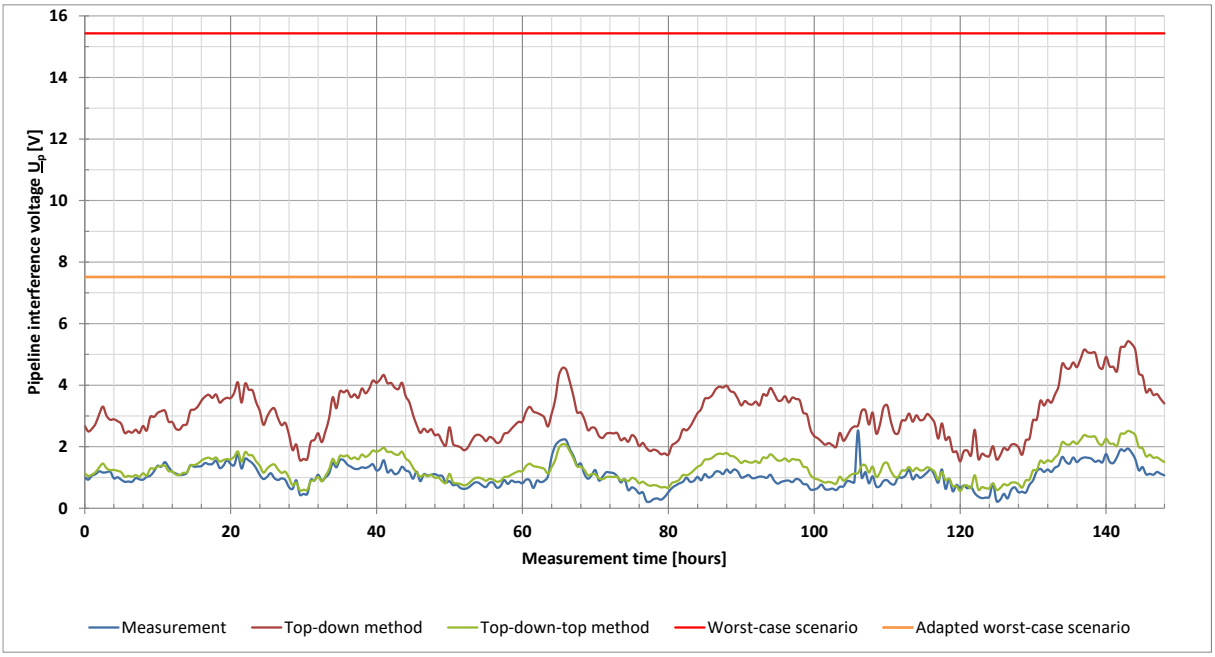

Figure 7-21: Top-down-top method; recalculating Figure 7-11

After recalculating with this method and taking into account larger suburban areas with their metallic structures as screening conductors (SCs), the result shows almost identical voltage curves. Such examples can be frequently found which makes the comparison between calculation and measurement a little easier. It is notable that such examples often occur in simple interference situations and/or in the close vicinity of OHLs.

7.3.4 Third example: Suburban areas and an incorrect specific soil resistivity

Again, the measurement location from chapter 7.2.5 is used and shown in Figure 7-22.

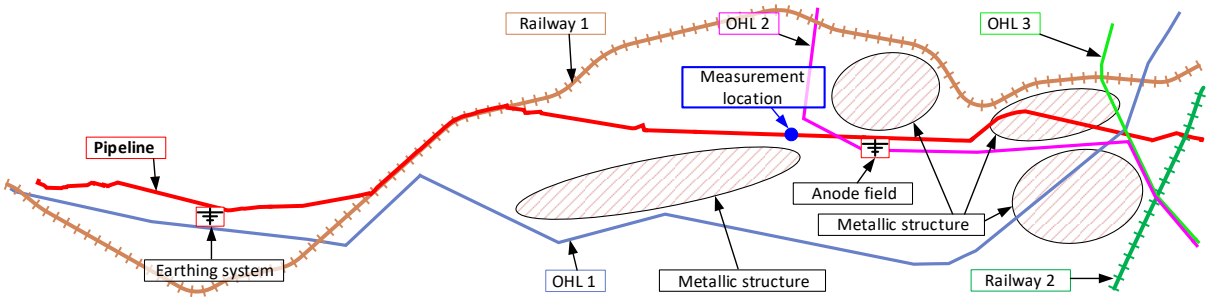

Figure 7-22: Measurement location of the third example

Recalculating Figure 7-13 of chapter 7.2.5 leads to the next Figure 7-23. As already described in Figure 7-13, the top-down method calculated a voltage curve higher than the measurement due to a too high worst-case calculation.

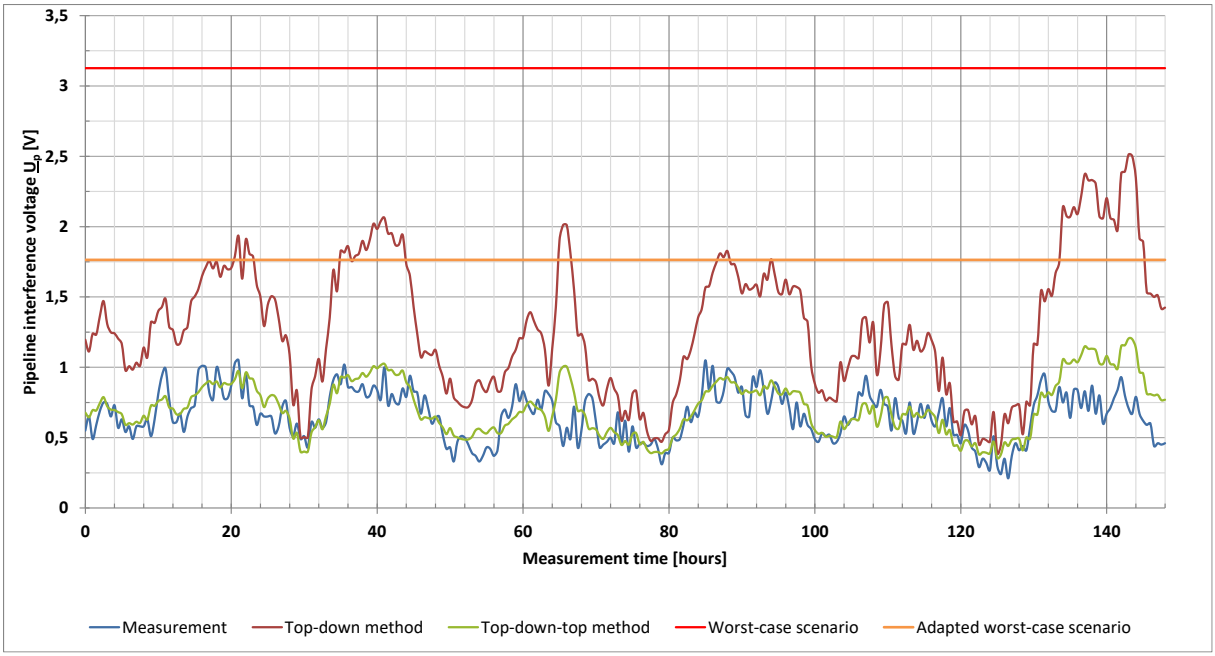

Figure 7-23: Top-down-top method; recalculating Figure 7-13

After recalculating with the top-down-top method and under consideration of the suburban areas with their metallic structures in the vicinity, a very good and realistic result was achieved. However, as previously stated with regards to Figure 7-13, a negative zero-point shift was also found. Further investigations showed that the SPCR was correct but the specific soil resistivity was higher than estimated.

Chapter 4.4 on page 64 shows a theoretical calculation where a higher soil resistivity leads to a higher PIV especially when the SPCR is high. This calculation and measurement was conducted on a well-wrapped pipeline and thus, the SPCR is high enough. The soil resistivity had a strong influence on the voltage curve and because the value of the soil resistivity was estimated at a too low value, there was the negative zero-point shift. Increasing the soil resistivity eliminates the zero-point shift and leads to a good result. After considering all parameters, the values of the adapted worst-case scenario are only half as high as the values suggested by the original worst-case scenario.

7.3.5 Fourth example: Anode field as an earthing system

Figure 7-24 shows a measurement location that lies directly at the feeding point of the cathodic protection system of the pipeline. Such a system always includes an anode field.

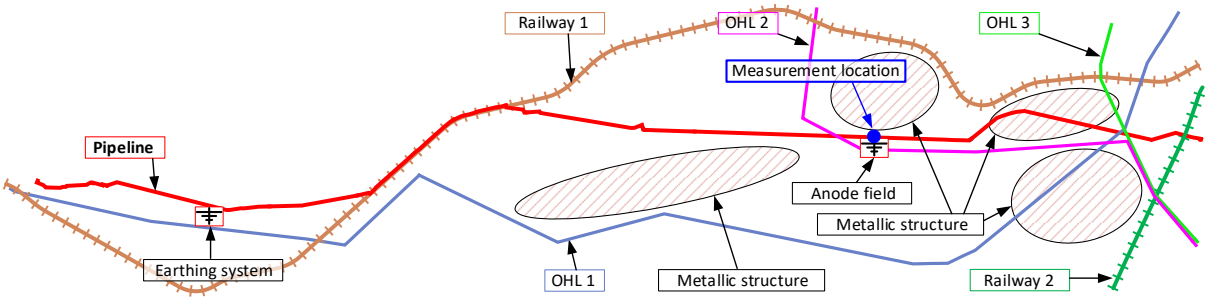

Figure 7-24: Measurement location of the fourth example

Figure 7-25 shows a big voltage difference between the worst-case and the adapted worst-case scenario. Simply put, in the initial calculations no earthing system was included but in reality, an earthing system exists at exactly this position. This earthing system was not built to reduce the PIV but is part of the cathodic protection system of the pipeline. This earthing system is called the anode field and is the negative pole of the supply system for the cathodic protection system and thus, the anode field is not directly connected to the pipeline. Until these measurements, it was unknown that such an anode field is also an effective earthing system for the PIV. After this discovery, anode fields were considered to be earthing systems in the calculations.

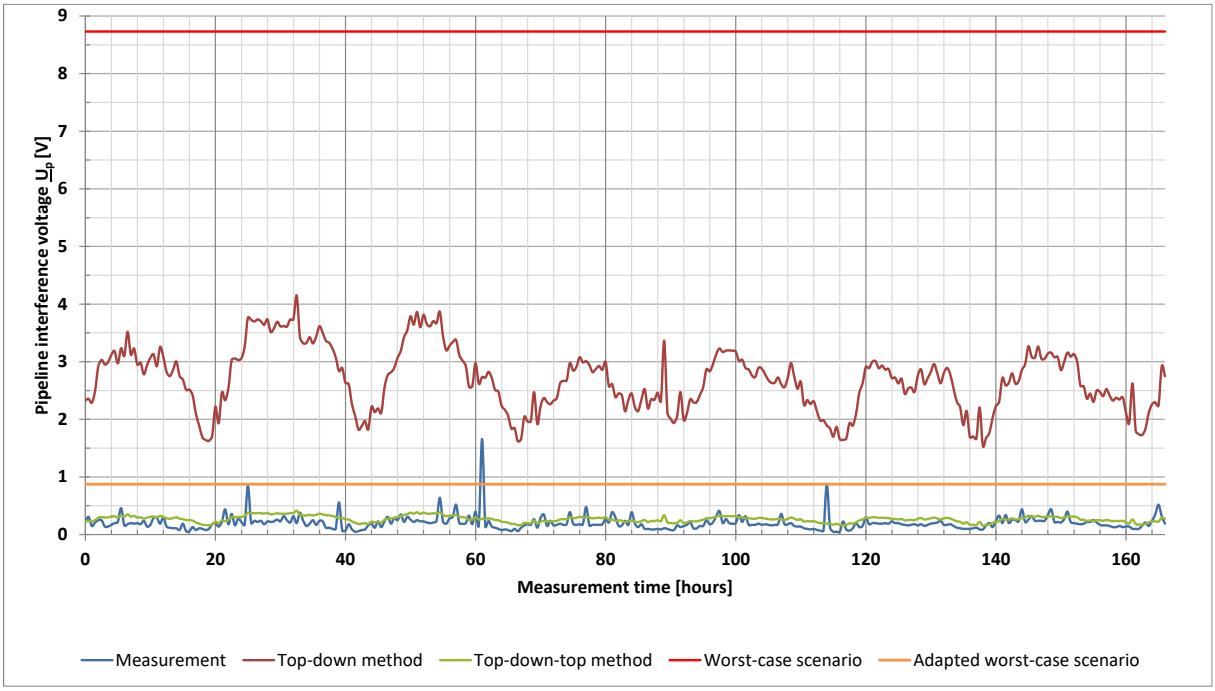

Figure 7-25: Top-down-top method; recalculating of a measurement point with an earthing system

7.3.6 Fifth example: Wrong time stamp and a not properly integrated earthing system

Again, the measurement location from chapter 7.2.8 is used and shown in Figure 7-26.

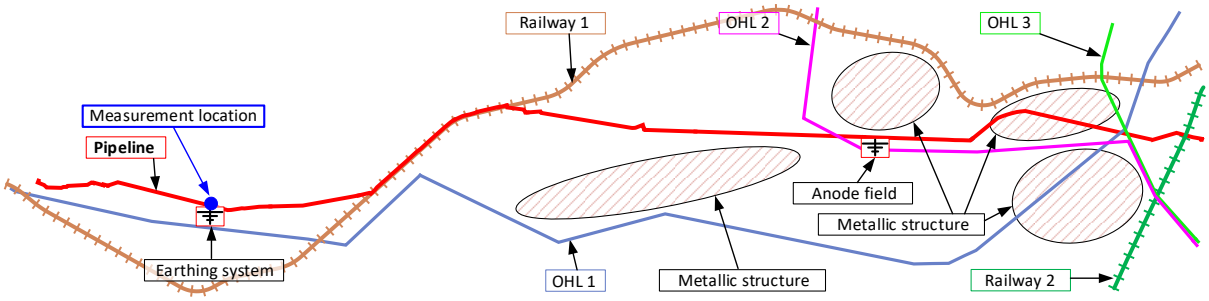

Figure 7-26: Measurement location of the fifth example

As already mentioned in chapter 7.2.8, the voltage curves in Figure 7-17 do not match at all. A closer analysis has shown that there is a time difference between the two curves. In Figure 7-27 this time offset of 12 hours is solved with the top-down-top method and brought into the right context. Examining the time stamp of the load currents and the measurement data was necessary and with the help of other measurement data it quickly became clear that the time stamp in the measuring device at the measuring location was wrong. These measurement devices normally have a GPS

signal for synchronising the time stamp but sometimes the device is set up too quickly in the measuring room and thus, it cannot synchronise.

In addition, the surrounding metallic installations must be taken into account again, which reduce the PIV accordingly. There is also a further reduction effect on the PIV, which has led to the calculation method being improved. Calculations with known earthing systems properly reduced the PIV, but the calculations were inaccurate near these earthing systems. This was due to the fact that the formulas included the earthing systems to a lesser extent than necessary and therefore did not take into account the correct earthing system resistance. This led to a relatively high PIV at these locations. Based on comparisons, the programming could be improved so that the earthing systems are now correctly integrated and the PIV is calculated correctly.

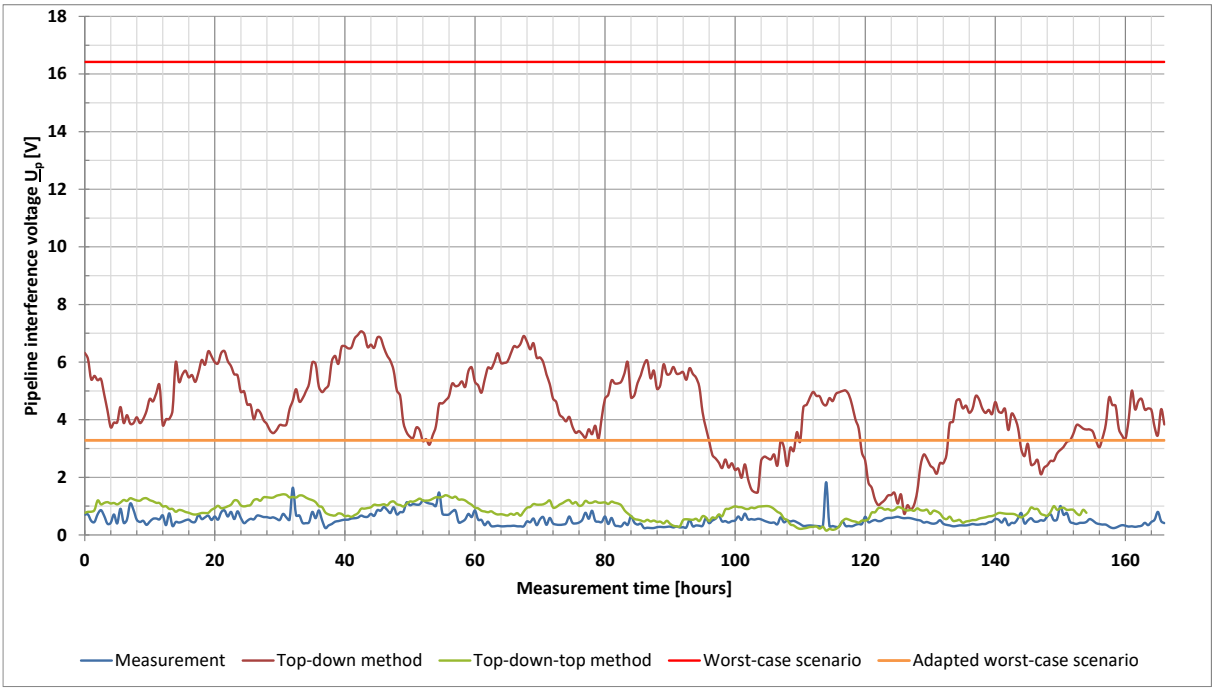

Figure 7-27: Top-down-top method; recalculating Figure 7-17

7.3.7 Sixth example: Wrong time stamp and amplifying conductors of a railway line

The interference of railroads on the PIV is very different than the interference from OHLs, as already explained in chapter 6.1.2. The last example in this chapter, illustrated in Figure 7-28 shows the measurement location next to the routes of a pipeline and a railway line, which run close to each other.

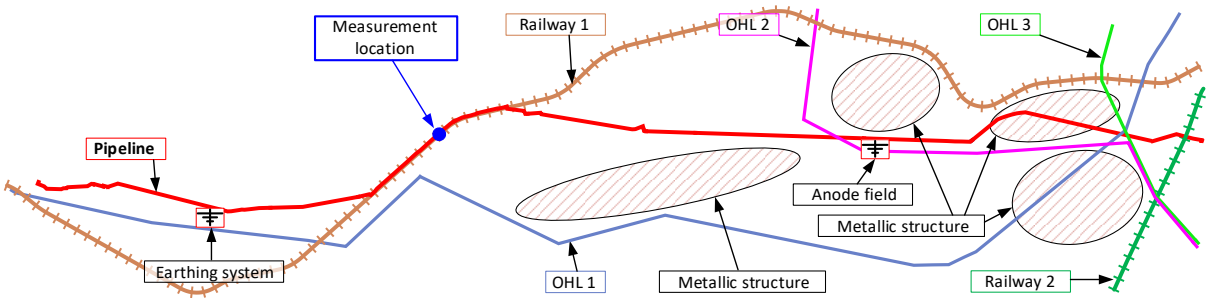

Figure 7-28: Measurement location of the sixth example

The last example in this chapter is shown in Figure 7-29 with another time shift problem, again 12 hours, but in the opposite direction.

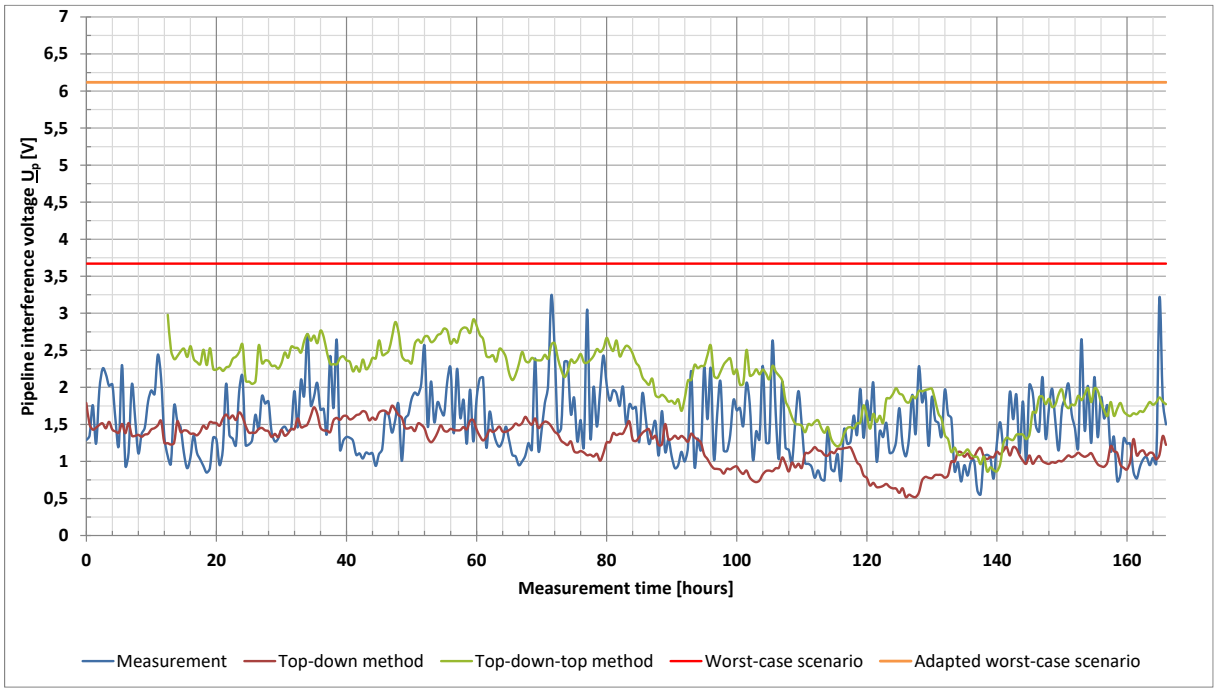

Figure 7-29: Top-down-top method; another wrong time stamp

Another interesting observation is that the calculation of the adapted worst-case scenario is higher than the original calculation of the worst-case scenario. This is caused by the influencing railway line which had some amplifying and reduction conductors. These conductors can have an

amplifying or reducing impact on the PIV but are sometimes difficult to implement in the calculations because the load currents are often unknown and these conductors are used to supply trains farther away.

7.3.8 Summary

In summary, extending the top-down method with the feedback loop to the top-down-top method brings the same advantages, as have already been mentioned in the top-down method. This shown method extends the calculations and more data analysis is needed to get better results which are comparable with the conducted measurements. In addition, with this method, one is forced to take a closer look at the calculations and to question whether they are correct or whether something is missing in the calculation. As shown in the examples, with the top-down-top method it is possible to do adapted worst-case calculations. This increases the reliability of calculations as well as personnel and equipment safety.

7.4 Comparison of the pipeline interference voltage along a complete pipeline

7.4.1 Overview

This part of the chapter represents the core goal of this thesis. These calculations were done over the last years. All investigations and recalculations in this thesis conclude in this chapter.

Sometimes a pipeline operator conducts measurements and determines that the measured values are high and a further investigation should be performed. If these measured values are greater than approximately 30 volts peak or 10 volts average, additional calculations should be done. In the following subchapters, the results of three pipelines will be further examined and analysed in more detail.

7.4.2 Measurement conducted before the calculation

Figure 7-30 shows an example in which the pipeline operator first conducted measurements on his pipeline. The results were evaluated and some of the PIVs were so high, that further analysis was needed. The measurement locations with their measured maximum PIV are shown in the figure as green dots and are connected. Unfortunately, the pipeline operator did not disclose the detailed voltage curve from the measurement, so only the maximum and the average values were known. This also meant that further investigations such as using the top-down-top method were simply not possible due to missing data.

Only a standardized calculation was possible, which is labelled “Calculated without earthing systems”. At the beginning of the calculation, it was not known whether earthing systems were required. However, after finishing the calculation it was clear that they would be needed because the calculated PIV was higher than the maximum permissible voltage for the touch voltage (60 Volt in Austria). In particular, the high level of interference as well as the high specific pipeline coating resistance (SPCR) leads to a high PIV along the pipeline and could hardly be reduced via the shunt admittance (AC earthing systems along the pipeline) see chapters 2.3.1.2 and 4.3). After placing proper earthing systems on the calculated locations, it was possible to reduce the PIV to values below the limit voltage of 60 Volt. This curve progression is labelled “Calculated with earthing systems”.

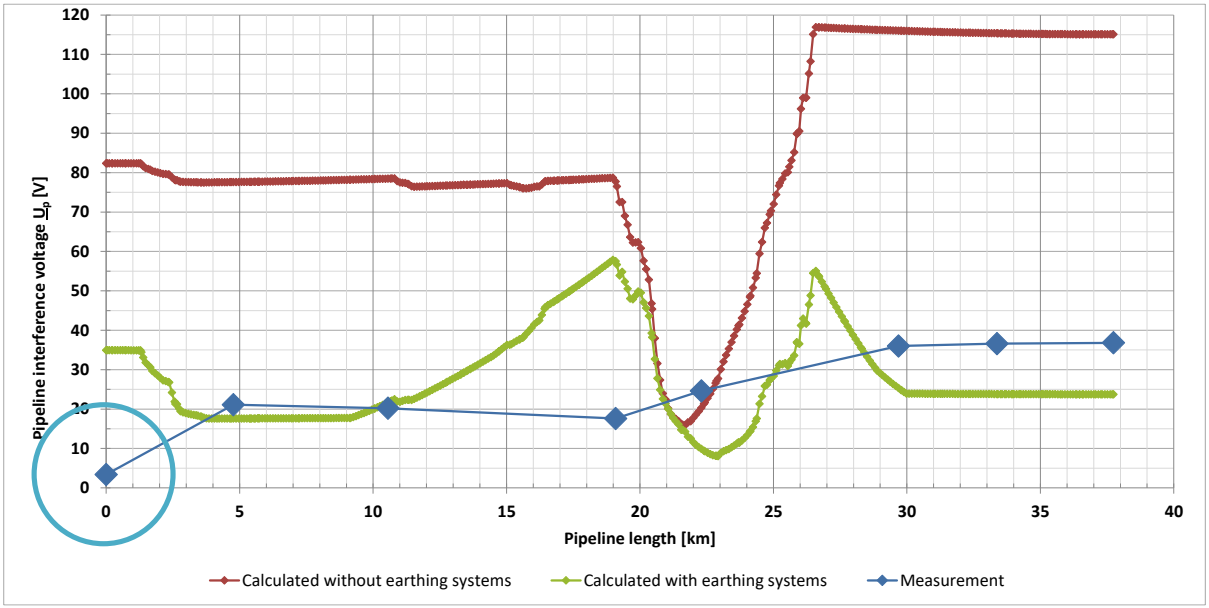

Figure 7-30: Comparison between two calculations and the measurement of a pipeline with a high specific pipeline coating resistance

First, calculations were done without earthing systems and the results show that the PIV exceeds the limits of the standards used. Based on this, further calculations were done to reduce PIV with earthing systems. Both voltage curves are shown in Figure 7-30. However, the measurements on the pipeline were conducted prior to the installation of the earthing systems. This makes the comparison between the measurement and the calculation before the installation of the earthing systems much more interesting.

The principal voltage curve of both curve progressions in Figure 7-30 is similar and the voltage level differences can be explained by the different currents (load current versus maximum current, see chapter 4.5) used. But it also shows that measurements can only represent a very small part of the voltage curve along the pipeline and therefore calculations make sense. Another interesting detail was found when comparing measurement and calculation. At the beginning of the pipeline, the measurements showed a very small value (marked in the figure as a blue circle), but the calculation a high one. It was then discussed with the pipeline operator, whether there was an anode field or something similar at this location. This was soon ruled out, but there is a station of another pipeline right next to the measuring location. It turns out that this foreign station influenced the reference point of the measurement, as described in chapter 6.1.3. After further measurements at this measuring location, it was discovered that measurements had been incorrect over the course of several years and that the calculations were correct. This example shows that calculations can help improve the measurement quality by finding unknown sources of error or influence on pipeline interference voltage.

7.4.3 Calculation and measurements on a long pipeline

Figure 7-31 shows a pipeline with calculation, evaluation and measurements. However, in the special case of this pipeline, the calculations had been done a few years ago and therefore also before the start of this thesis. At that time, an older calculation method was used and the interaction between the PIV and the parameters of the pipeline and HVPSs and the surrounding factors, such as foreign metallic conductors, had not yet been investigated. At that time the calculation was made according to the state of the art. It is too high according to today's knowledge. Measurements and evaluation were done a few years later to verify the calculation results. All data can be found in the following figure.

The green dots show the maximum measuring results as well as the measuring locations. The appropriate evaluations have been done for all the measuring locations and are marked as differently coloured dots. The dots are connected in order to clarify the basic PIV along the pipeline and to make the dots more visible. The "Top-down method" corresponds to the top-down method 1 in chapter 7.1.1 with RMS-value addition (see formula (7-4)). The RMS-value addition is also used for the method "Top-down-top method" from chapter 7.1.3 and the method "Down-top method" from chapter 7.1.2. The calculations were recalculated with the top-down-top method which leads to a new worst-case scenario, labelled "Adapted worst-case scenario" (which is also described and used in chapter 7.3).

What is particularly interesting here is that the results of the "Adapted worst-case scenario" and the "Down-top method" are similar in some parts, despite the fact that, as stated in chapter 7.2, the "Down-top method" does not produce satisfactory results. The results of this method would still roughly correspond to the expected values in some areas of the pipeline which is actually the reason why this method was included in this thesis.

There are possible reasons why both methods show similar results. One of them is that the originally calculated PIV is very high, which means that the "Adapted worst-case scenario" is extrapolated particularly strong despite using the reduction factors from the "Top-down-top method". Another factor is that none of the influencing sources at a measurement location has more than 50% influence on the entire PIV. This distribution helps the "Down-top method" in particular. However, it can be seen in the figure that the "Down-top method" has much stronger outliers than the "Top-down-top method" or the "Top-down method". These outliers make this method not very reliable and therefore the "Down-top method" should only be used if there is no alternative.

The alternative to this is the "Top-down-top method" with recalculating the worst-case scenario, which shows very good results in this calculation. This method is more complex and also costly but can verify points that show a high calculated PIV. Furthermore, the calculations can be refined to optimise the costs for measures to reduce the risk of AC corrosion or dangerous touch voltages. Especially the second hazard is significantly more important because of the lower probability of its appearance. Long term touch voltages can be measured but long-duration measuring periods are

needed. When a high PIV is measured this could be highly risky. Especially problematic are short-term touch voltages, as it is almost impossible to measure them, but they can occur. With the help of the "Top-down-top method", short-term interference calculations can also be optimised and increase personnel safety.

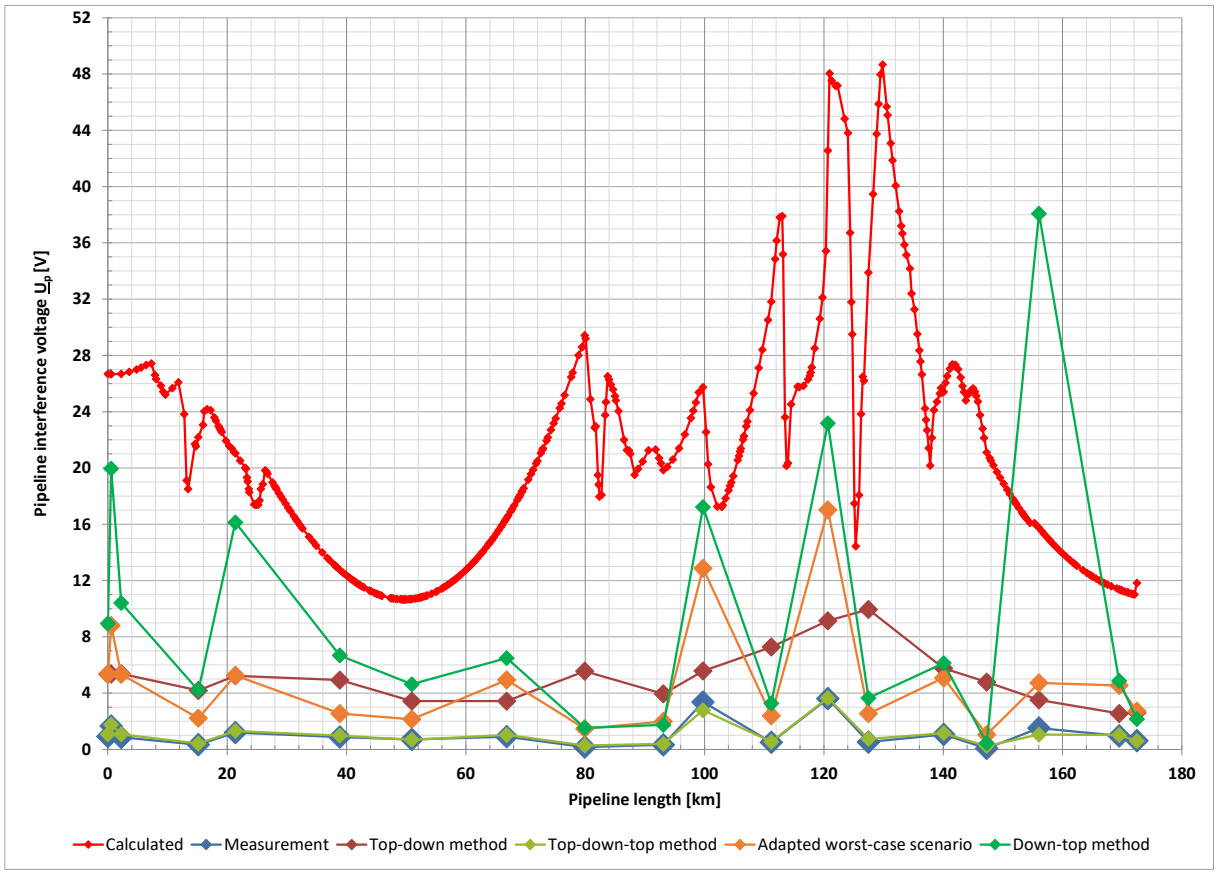

Figure 7-31: Comparison between calculation, evaluation and measurement of a pipeline when calculation results are clearly too high

Figure 7-31 also shows that the measurements are relatively evenly distributed over the entire pipeline. However, it is again evident that a higher number of conducted measurements increase the quality of the PIV calculation and thus, the worst-case calculation can be refined. Such an extension of the measurement would make a lot of sense for pipeline km 130, where a high calculated PIV exists but no measurements were conducted. Overall, it can be seen that a comparison between measurement and calculation is considerably more difficult when only a few measurements are conducted on the pipeline.

7.4.4 Calculation and measurements on a pipeline with an isolation joint and installed earthing systems

The final example in Figure 7-32 shows a newer and better calculation. It has the same legend as Figure 7-31. This pipeline is divided electrically into two parts with an isolation joint at km 30. Such joints are normally used to have better control over the flowing currents in the pipeline cathodic protection system but can also be used for splitting up the PIV, which is not the main reason in this case. Splitting the pipeline into parts can reduce or also amplify the PIV. Also some parts of a pipeline without or with less interference can be isolated [6]. In this example it is interesting that the "Down-top method" shows extremely inconstant results which are often even higher than the results of the initial calculation ("Calculated"). This underscores the conclusion that the "Down-top method" provides calculation results that are too unreliable.

In this example, measurement and initial calculation have a similar curve progression which means that the initial calculations go in the right direction but the results are too high. Using the "Top-down method" (russet line) leads to the same result and a better comparison with the measurement. After using the "Top-down-top method" (lime green line), the difference between the russet and line green line becomes obvious and shows that the initial calculation is mostly too high.

As has been stated in chapters 7.2 and 7.3, surrounding factors such as foreign earthing systems (see chapter 5) can influence and strongly reduce the PIV. This is often the case but not always. Sometimes, the soil resistivity can be estimated wrong or given by the pipeline operator at a wrong value because this value varies a lot along a pipeline and can neither be measured so accurately nor taken into account in the calculations, and therefore an average value for a longer section of a pipeline is presumed (see Figure 7-23). Also, the pipeline operator may not give the exact information about the used earthing systems or anode fields (see Figure 7-25). In some cases, where all the given information is correct and no foreign metallic structure is nearby, measurement and calculation such as in Figure 7-32 are similar (see km 50) or equal (see km 0).

The "adapted worst-case scenario" is usually smaller than the initial calculation because of the factors listed above and increases the safety of personnel and pipeline, as stated in the description to Figure 7-31.

Measuring locations cannot cover the whole pipeline which is illustrated in this example, where calculation peak values on km 34 and km 44 are not part of the measurements. Especially km 34 is critical because measurements were done nearby but always on locations with a much lower calculated PIV. This means that either the measurement must be expanded by a new, cost-intensive evaluation or the calculated worst-case scenario must be used as a prerequisite for possible measures to increase pipeline security.

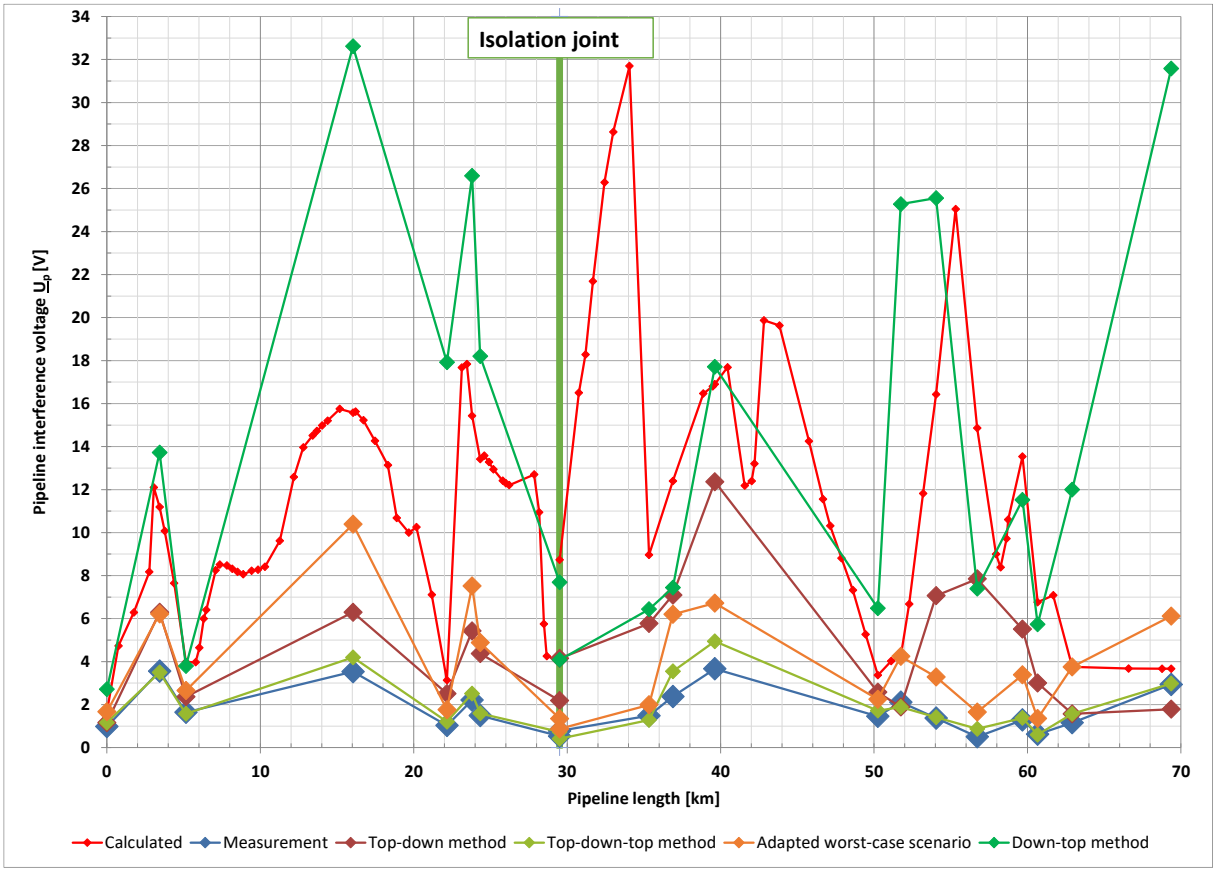

Figure 7-32: Comparison between calculation, evaluation and measurement of a pipeline with acceptable calculation results

7.4.5 Summary

Shortly summarized, this chapter shows impressively how measurement, calculation and evaluations can be meaningfully complement each other and how safety for personnel and material can be increased. It also shows that calculations will always be necessary because worst-case scenarios cannot be covered with measurements. In addition, measurements cannot be performed at many locations along the pipeline because of no access or it being too costly. However, measurements do make sense, since they can improve calculations using the "top-down-top method" with all the advantages (much more accurate) and disadvantages (costs time and money). But this method shows satisfied results and can be used in future for further research. It has also been shown that the "down-top method" is an interesting approach, but, unfortunately, not reliable enough. This method might be improved and become more precise with further research.

8 Conclusion and outlook

8.1 Conclusion

The main focus of thesis is the comparison between calculation and measurement of pipeline interference voltage (PIV) with the goal that the calculations achieve results which better fit the measurements. It presents a program with an efficient mathematical analysis to improve the known calculation model. This is the key element of this thesis, because a “fresh” program can calculate faster, the results are more accurate and it can do more automatic calculations and visualisations without user intervention. With this, a standardized model is created to better evaluate and compare the influence of different parameters on the PIV.

The first part of this thesis reviews the relevant pipeline interference parameters: The equivalent network used for the pipeline consists of longitudinal impedances and shunt admittances. The longitudinal impedances are determined by the diameter of a conductor or pipeline and the soil resistivity, where the conductor diameter is a more potent influencing parameter. In addition, the frequency of the source of influence (high voltage power system) must be taken into account, as higher frequencies lead to a reduced conductivity of the material. In general, the longitudinal impedance can be calculated relatively easily.

The opposite is true for the shunt admittance, since the shunt admittance depends on the known conductor diameter, the varying soil resistivity along the pipeline as well as on the difficult to estimate specific pipeline coating resistance (SPCR). This is crucial because the PIV is highly dependent on shunt admittance. The problem is that manufacturers of pipeline coating only guarantee the resistance value for DC currents under laboratory conditions or on delivery. In practice, however, pipelines lie buried in soil where coating holidays can occur frequently which may reduce the SPCR. In addition, AC currents can lower the value of the SPCR. These unknown variables make it very difficult to determine a realistic value. This poses a significant problem because the value of the SPCR determines how the soil resistivity affects the PIV. To summarize, it can be said that the SPCR is the key parameter.

Another part of this thesis discusses and compares the different calculation formulas for the longitudinal impedance and shunt admittance. It is shown that "formula S" and "formula C" are equivalent and calculate lower maximum PIVs compared to the other formulas. Lower values are preferable because calculations usually show higher values than measurements in the field.

This thesis focuses on interference by overhead lines (OHLs) and not by railway lines or underground cables. OHLs can be built with different pylon types and phase conductor configurations and often also have earthing conductors. As shown by the calculations in this thesis, it is very important that the phase conductor configuration is configured correctly, because otherwise a much higher PIV can be expected.

Calculations show that the specific pylon types cause different levels of interference on pipelines and, therefore, different PIVs under the same technical specifications. Basically, the calculations show that the "ton"-pylon with two circuits gives the best calculation results for the PIV. There are also other pylon types with only slightly worse results. Surprisingly, the results show that also the "quadruple" pylon with four circuits (it could be assumed that more phase conductors lead to a higher interference) with an optimal phase conductor configuration does not significantly increase the PIV. In contrast, asymmetric phase conductor configuration increases the PIV considerably (the "single-circuit" pylon shows a much higher PIV than the "ton"-pylon despite a smaller number of phase conductors).

Another vital parameter in the calculations are earthing conductors (ECs) of overhead lines (OHLs). Calculations with none, one and two ECs show a notable influence on the PIV with the result that OHLs without ECs can have a lower interference on pipelines in normal operation. The height of ECs for OHLs is normally fixed for the respective pylon types. The calculations in this thesis show, however, that the height of the ECs can be optimised for each pylon type with regards to pipeline interference. This finding could be used in the planning of future OHL construction projects, but due to design and safety reasons e.g. lightning protection, only a few alternative mounting heights are possible.

This thesis shows that EC cables with bigger diameters or highly conductive materials have a lower self-impedance and, therefore, a higher EC current can flow, which leads to a higher PIV. This finding is essential because as OHLs are equipped with better and better ECs, PIVs are increasing.

When several metallic structures influence the PIV, calculations become more complex. There are countless possible combinations of pipelines, OHLs, railway lines and other metallic structures and therefore analytical calculations are complex and can only cover a fraction of them. However, these examples help to understand the complex interaction of the different conductors and to adapt and refine the PIV calculations.

The consideration of other metallic structures is difficult because size and material are unknown in the majority of cases. Whether the pipeline is affected by one or two or more OHLs, when metallic structures are nearby, this can either increase or (often) reduce the PIV. It depends on the position, the geographical expansion and also the material used in the metallic structure. This thesis shows that the often used general reduction factors for the environment are not correct. Instead, many variables have to be considered. In summary it can be said that complex interference situations are difficult to calculate and especially unknown metallic structures are difficult to estimate. This is the underlying reason, why often the results of calculations are higher than measurements.

This thesis indirectly also takes into account screening conductors as reduction conductors, which are usually located directly next to or above a pipeline. It is shown that these have a reducing effect, but they are rarely installed during pipeline construction and almost never at a later point due to high costs or because the pipeline is inaccessible.

In this thesis, combinations of two parallel OHLs are considered. When the currents in both OHLs flow in the same direction, the PIV often remains the same or decreases, when taking into account the mutual impedance (MI) as well as when the OHLs are considered individually without MI. When the currents in the two OHLs flow in different directions then, as expected, the PIV is basically lower then when the currents in both OHLs flow in the same direction. However, considering the MI leads to a higher PIV than without MI. The consideration of the current directions also shows that PIV is strongly dependent on them. Reversed current directions cannot be taken into account in the calculations because calculations must always cover the worst-case scenario. In addition, the difference in the PIV due to the current direction is more important when OHLs and pipeline are situated in close proximity to each other.

It is shown that in the case of two parallel pipelines, a high specific pipeline coating resistance (SPCR) of both pipelines does not lead to a noticeable mutual influence. However, if one pipeline has a low SPCR, then there is mutual influence, which depends on the distance and the diameter. This means that information on SPCR must be obtained from nearby pipelines.

In general, measurements on the pipeline are not particularly difficult if certain factors, such as an external ohmic potential gradient caused by earthing systems are taken into account. Only for the comparison between measurement and calculation is it important to interpret measurements to determine the main source of the influence on the PIV. This is not always easy because there may be multiple sources of interference at a specific measurement location.

Experimental measurements to verify the formulas for the lattice network model of the pipeline are very interesting. It turns out that the formulas discussed in chapters 2 and 4 are correct and can be used without restrictions. An essential aspect is the behaviour of the SPCR and the frequency depending behaviour of the coating resistance which decreases with a rising interference frequency, reducing the PIV.

The central chapter of this thesis looks at the comparison between calculation and measurement of pipeline interference voltage (PIV), using different methods. Analysing different measurement locations over a measurement period shows that considering the load currents is a precondition.

At most measurement locations, the results of worst-case calculations are too high and therefore, a “top-down method” is introduced to analyse the adapted calculation results and the measurements. The “down-top method” includes measurements and calculations, but does not produce good estimations of the worst-case scenarios. Therefore, this method may only be applicable in simple influencing cases.

Adding a feedback loop to form the “top-down-top method” brings some advantages. This method extends the calculation by a data analysis to include the surrounding unknown metallic structures. Adapted worst-case calculations can then be performed which increases the reliability of calculations, especially with regards to personnel safety.

These methods are then used to compare and evaluate calculation and measurement at different measurement locations. Various examples describe problems that can occur. These can be, for example, a not adequate soil resistivity or SPCR, but also incorrect measurement data or unknown grounding systems. Once these problems have been analysed and compensated for, these often complex interference situations can be analysed to estimate the reduction factors. The examples show impressively how overall safety can be increased by a combination of measurements, calculations and evaluations.

It becomes clear that calculations are always necessary because worst-case scenarios, which are necessary for the assessment of the risks caused by interference cannot be covered with measurements alone (also, not all locations along a pipeline might be accessible for measurements). But measurements are crucial to improve the calculations by using the "top-down-top method". This method shows satisfying results and can be the subject of further research in the future. Better calculations increase personnel safety and the durability of the pipeline. In many cases, because of more accurate calculations, it is possible to avoid additional earthing systems or other countermeasures against high pipeline interference voltages, thus reducing costs. These costs include, on the one hand, the construction as well as decades of maintenance and renewal of the necessary measures and can affect both the operators of the pipeline and the operators of the high voltage power system.

8.2 Outlook

This thesis extensively discusses the comparison between calculation and measurement of pipeline interference voltage (PIV) and a many calculation factors. With the improved calculation program based on a detailed analysis of different important factors, many questions could be answered. However, some questions remain open and further experiments or comparative calculations are required.

The focus of this thesis is to determine the factors that influence PIV calculations and not their optimisation. For example, the pylon type of overhead lines (OHLs) as well as the exact phase conductor configuration can be chosen taking into consideration PIVs. But based on this and other publications, the influence on the PIV can also be optimised by the geographical position of the pylon conductors or by the position and size of earthing conductors. This thesis considered the influence of OHLs only during normal operation. Therefore, it would be useful to look at the fault operation as well to find out which pylon type causes a stronger influence and how big the influence of the EC is on the PIV.

Furthermore, more combinations of pipeline types, OHL types and other metallic structures can be reviewed to find out if and how the calculations can be optimised. Another interesting topic is the usage of reduction conductors next to a pipeline. This is an interesting and challenging subject because many elements, such as active and passive conductors, can be used (an analysis should include diameter and placement).

All these factors can be included in the calculation and the comparison of the PIV along a pipeline or at specific measurement locations. The methods used in this thesis for the comparison can also be optimised, especially calculation methods of the worst-case scenario which include measurement data. In addition, more comparisons between measurement and calculation on different pipelines would be beneficial to offer additional data for further research.

More experimental measurements are needed. It should be examined, what effect an external ohmic potential gradient has on the pipeline when a coating holiday occurs within the ohmic potential gradient. Here the question is how large such a holiday must be so that enough energy can be transferred to the pipeline and a correspondingly large current flow can occur on the pipeline which can then lead to a dangerous electrical potential between pipeline and soil at greater distances.

And more measurements on pipelines for confirming the value of the longitudinal impedance and shunt admittance are needed, even if the first results are promising. The open question for these parameters is how the value of the SPCR changes with the frequency of the interference and whether environmental parameters also play a role because the SPCR is the most important pipeline parameter.

9 Bibliography

[1] J. Carson, Wave Propagation in Overhead Wires with Ground Retourn, Bell System Technical Journal 5, Page 539 to 554, 1926.

[2] F. Polllaczek, Über das Feld einer unendlich langen wechselstromdurchflossenen Einfachleitung, Elektrische Nachrichtentechnik, Heft 9, Band 3, 1926.

[3] M. Michailow, Z.D. Rasumov, Electrical paramters of metallic pipelines in earth, Èlektričestvo, Journal 5, p. 60-63, 1963.

[4] H. Dommel, Ein digitales Rechenverfahren zur Lösung transienter Vorgänge in ein- und mehrphasigen elektrischen Netzen, Professorial dissertation, 1967.

[5] C. Dubanton, Calcul approche des paramters primaires et secondaires d'une ligne detransport. Valeurs homopolaires, CIGRE, 1970.

[6] R. Braunstein, Technical and economical evaluation of measures deacreasing inductive interference of metallic pipelines, Ph.D. dissertation: Institute of Electrical Power Systems, Graz University of Technology, 2012.

[7] F. M. Starr, Equivalent Circuits-I, Transactions of the American Institute of Electrical Engineers (Volume: 51 , Issue: 2 , June 1932), 1932.

[8] E. Clarke, Circuit Analysis of AC Power Systems, New York: John Wiley & Sons, Inc., 1950.

[9] Technische Empfehlung Nr. 7, Massnahmen bei Bau und Betrieb von Rohrleitungen im Einflussbereich von Hochspannungsanlagen, Schiedsstelle für Beeinflussungsfragen, 1966.

[10] ÖVE-B1/1976 (Österreichische Vorschriften für die Elektrotechnik), Beeinflussung von Fernmeldeanlagen durch Wechselstromanlagen mit Nennspannungen über 1 kV, Wien: Österreichischer Verband für Elektrotechnik, 1976.

[11] TE 30 (Technische Empfehlung 30), Massnahmen bei Errichtung und Betrieb von Rohrleitungen und Starkstromanlagen mit Nennspannungen über 1 kV zur Vermeidung unzulässiger Beeinflussung, 1968: Technisches Komitee für Beeinflussungsfragen (TKB/TKS).

[12] ÖVE/ÖNORM EN 50443, (2012-10-01): Auswirkungen elektromagnetischer Beeinflussungen von Hochspannungswechselstrombahnen und/oder Hochspannungsanlagen auf Rohrleitungen.

[13] ÖVE/ÖNORM EN 15280, (2013-10-01): Beurteilung der Korrosionswahrscheinlichkeit durch Wechselspannung an erdverlegten Rohrleitungen, anwendbar für kathodisch geschützte Rohrleitungen.

[14] ÖNORM EN ISO 18068, (2017-11-15): Korrosion von Metallen und Legierungen - Bestimmung der Wechselstromkorrosion - Schutzkriterien (ISO 18086:2015).

[15] TE 30: Technische Empfehlung Nr. 30, (Ausgabe 2014): Maßnahmen bei Errichtung und Betrieb von Rohrleitungen und Starkstromanlagen mit Nennspannungen über 1 kV zur Vermeidung unzulässiger Beeinflussung, Technisches Komitee für Beeinflussungsfragen, (VEÖ).

[16] R. Muckenhuber, Einflussgrößen bei der Berechnung induktiver und ohmscher Beeinflussungen, Leipzig: Beitrag zur 2. Fachtagung "Starkstrombeeinflussung von Fernmeldeanlagen", 1966.

[17] E. Schmautzer, Ein Beitrag zur Berechnung der induktiven Beeinflussung von Rohrleitungsnetzen, Ph.D. dissertation: Graz University of Technology, 1990.

[18] M. Büchler, C-H. Voùte, H.-G. Schöneich, Die Auswirkungen des kathodischen Schutzniveaus, 3R internat. 47 (2008) Nr. 6, S 344-349.

[19] M. Büchler, C.-H. Voùte, H.-G. Schöneich, Kritische Einflussgrößen auf die Wechselstromkorrosion: Die Bedeutung der Fehlstellengeometrie, 3 R internat. 48 (2009) Nr. 6, S. 324-330.

[20] M. Büchler, S. Collet and U. Angst, The effect of coating defect distribution on buried steel pipelines on the effectiveness of cathodic protection, Luxembourg: CEOCAR, 2017.

[21] U. Bette, C. Dornemann, Ergebnisse von Laboruntersuchungen zur Wechselstromkorrosion, 3R internat. 47, Nr. 11, S. 631-638, 2008.

[22] U. Bette, T. Schulte, Messtechnische Ermittlung von Streustrombeeinflussungen, 3R internat. 45, Nr. 7, S. 363-366, 2006.

[23] C. Wahl, Implementierung von Algorithmen zur optimalen Verortung von Erdungsanlagen entlang induktiv beeinflusster Rohrleitungen, Master thesis: Institute of Electrical Power Systems, Graz University of Technology, 2011.

[24] A. Steinkellner, Der Einfluss der Verdrillung auf die Stromunsymmetrie bei induktiv gekoppelten Hochspannungsfreileitungssysteme, Master thesis: Institute of Electrical Power Systems, Graz University of Technology, 2012.

[25] M. Roßmann, Auswirkungen der metallischen Strukturen von Wechselstrombahnanlagen auf die induktive Beeinflussung von Rohrleitungen, Master thesis: Institute of Electrical Power Systems, Graz University of Technology, 2018.

[26] G.C. Christoforidis, D.P. Labridis, P.S. Dokopoulos, AC Interference on a Gas Pipeline caused by nearby Power Lines in a complex right-of-way - Comparison between Measurements and Calculations, Dresden: CEOCOR Dresden - Sector A, Paper N. 10, 2004.

[27] D. Markovic, Induced currents in gas pipelines due to nearby power lines, Wollongong, Australia: University of Wollongong, 2005.

[28] A.H. Al-Badi, H.M. Al-Rizzo, Simulation of Elektromagnetic Coupling on Pipelines close to Overhead Transmission Lines: A Parametric Study, Journal of Communications Software and Systems, Vol. 1 No. 2, 2005.

[29] C. Wahl, E. Schmautzer, L. Fickert, Auswirkungen des Hochspannungs-Freileitungsausbaues auf Pipelines, 13. Symposium Energieinnovation, Graz/Austria, 2014.

[30] C. Wahl, E. Schmautzer, L. Fickert, Impact of High Voltage Overhead Line Design on Pipeline Security, Berlin: Pipeline Technology Conference 2014.

[31] C. Wahl, E. Schmautzer, Impact of Global Earthing Systems on the Inductive Interference on Buried Isolated Metallic Pipelines, Paper 1058, 23rd International Conference on Electricity Distribuation (CIRED), Lyon, 2015.

[32] C. Wahl, E. Schmautzer, Possible Reasons why Calculations of Inductive Interference Pipeline are higher than Conducted Measurements, Pipeline Technology Conference, Berlin, 2015.

[33] M. Muffat, Modellierung und Messung der elektrischen Paramter von Pipelines, Master thesis: Institute of Electrical Power Systems, Graz University of Technology, 2015.

[34] H.-G. Unger, Elektromagnetische Wellen auf Leitungen, Heidelberg: Hüthig Buch Verlag GmbH, 4. Auflage, ISBN: 3-7785-2390-2, 1996.

[35] D. Oeding and B.R. Oswald, Elektrische Kraftwerke und Netze, 6th ed. Springer, 2004.

[36] W. Klein, Mehrtortheorie, Berlin: Akademie-Verlag, 1961/1976.

[37] International Inquiry CIGRE Working Group 36.02, Guide on the influence of high voltage AC power systems on metallic pipelines, CIGRE, 1995.

[38] U. Bette, M. Büchler, Taschenbuch für den kathodischen Korrosionsschutz 8. Auflage, Vulkan-Verlag GmbH, Essen, ISBN: 978-3-8027-2556-2, 2010.

[39] ITU-T, Directives concerning the protection of telecommunication lines against harmful effects from electric power and electrified railway lines, ITU-T, 1998.

[40] A. Déri, G. Tevan, Mathematical Verification of Dubanton's Simplified Calculation of Overhead Transmission Line Parameters and its Physical Interpretation, Archiv für Elektrotechnik, vol. 63, page 191 to 198, 1981.

[41] K. Friedl, Power Frequency Electric and Magnetic Fields: Worst-Case Calculation and Optimisation Through Optimal Conductor Arrangement, Ph.D. dissertation: Institute of Electrical Power Systems, Graz University of Technology, 2012.

[42] R. Braunstein, E. Schmautzer, M. Ölz, Neue Herausforderungen an die induktive Rohrleitungsbeeinflussung unter Berücksichtigung des aktuellen Forschungsstandes, 11. Symposium Energieinnovation in Graz, Austria, 2010.

[43] H. Schmole, D. Vogt, Potentialausgleich, Fundamenterder, Korrosionsgefährdung, Berlin, Germany: 6. Edition, VDE Verlag GmbH, 2004.

[44] M. Muffat, Der spezifische Erdwiderstand im jahreszeitlichen Verlauf, Bachelor thesis: Institute of Electrical Power Systems, Graz University of Technology, 2012.

[45] J. Backes, Bewertung der Versorgungszuverlässigkeit: Neue Ansätze zur Verwendung probabilistischer Zuverlässigkeitskenngrößen in der Netzplanung und -optimierung, 2nd Edition, Hertbert Utz Verlag, Munich, Germany, ISBN: 978-3-8316-8018-4, 2013.

[46] E. Schmautzer, R. Braunstein, M. Ölz, Simulation and Optimised Reduction of Induced Pipeline Voltages Caused by High-Voltage Lines on inductively interfered Pipelines, Paper 0014, 21rd International Conference on Electricity Distribuation (CIRED), Frankfurt, 2011.

[47] E. Schmautzer, J. Silny, K. Friedl, L. Fickert, M. Aigner, A. Gaun, G. Rechberger and A. Albert, Elektromagnetische Felder im Bereich elektrifizierter Bahnanlagen und ihre gesundheitlichen Risiken, Verlag der Technischen Universität Graz, 2011.

[48] TE 8: Technische Empfehlung Nr. 8, (Ausgabe März 1980): Anleitung zur rechnerischen und meßtechnischen Ermittlung der Reduktionswirkung von Kompensationsleitern, Verlags- und Wirtschaftsgesellschaft der Elektrizitätswerke mbH VWEW, ISBN: 3-8022-0013-6, 1980.

[49] Weilekes Elektronik GmbH, [Online]. Available: https://www.weilekes.de/de/minilog2/allgemeine-informationen.htm. [Zugriff am 14 6 2020].

[50] TPA KKS GmbH, [Online]. Available: https://www.tpa-kks.at/home/. [Zugriff am 14 6 2020].

[51] AfK-Empfehlung Nr. 3, Maßnahmen beim Bau und Betrieb von Rohrleitungen im Einflussbereich von Hochspannungsfreileitungen, Arbeitsgemeinschaft für Korrosionsfragen.

10 Appendix

Contents of the appendix

A Additional charts of chapter 2

A.1 Longitudinal impedance with varying specific soil resistivity

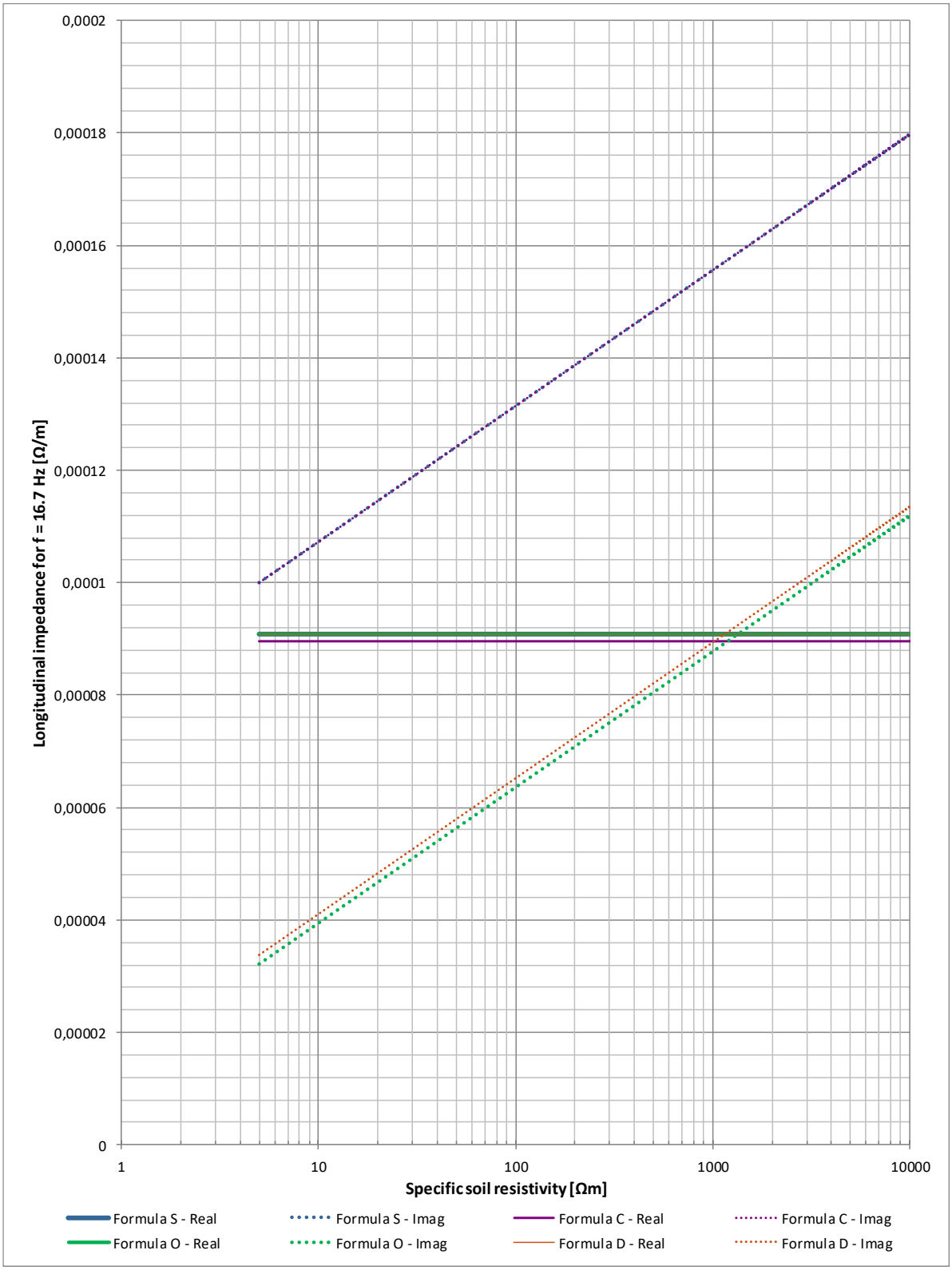

Figure A-1: Comparison of the different formulas for the longitudinal impedance with varying specific soil resistivity for 16.7 Hz, divided up into real and imaginary part

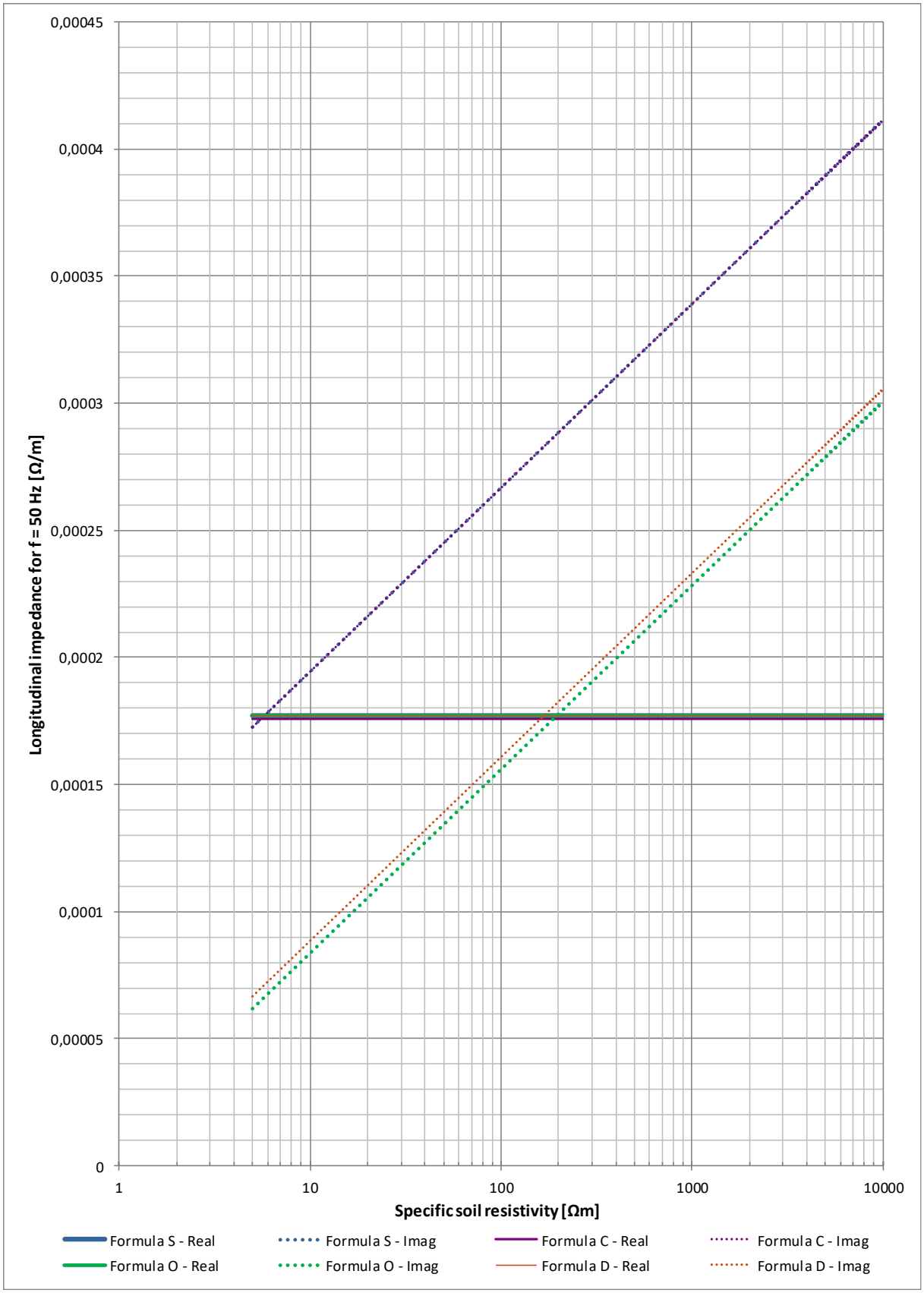

Figure A-2: Comparison of the different formulas for the longitudinal impedance with varying specific soil resistivity for 50 Hz, divided up into real and imaginary part

A.2 Longitudinal impedance with varying conductor diameter

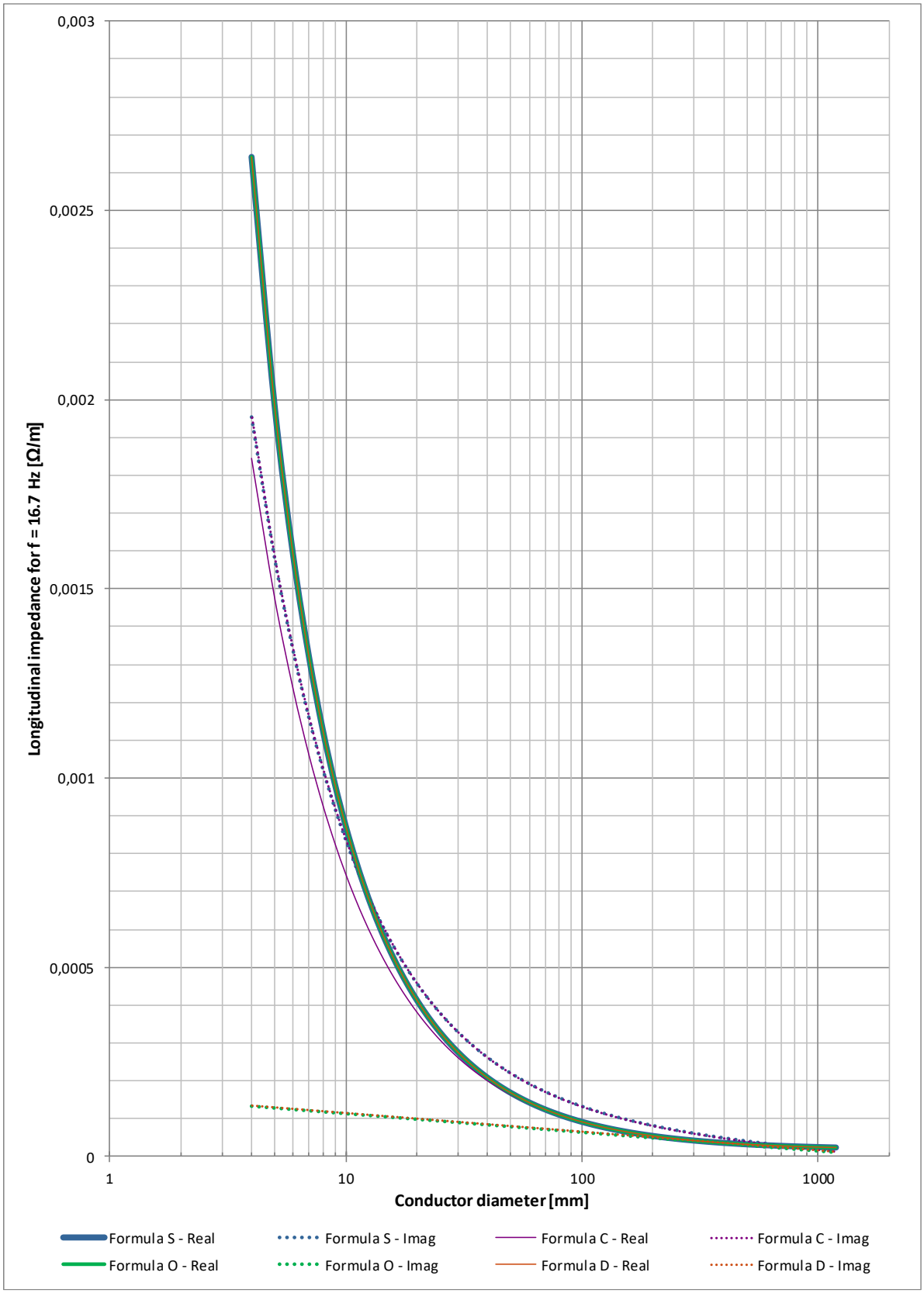

Figure A-3: Comparison of the different formulas for the longitudinal impedance with varying conductor diameter for 16.7 Hz, divided up into real and imaginary part

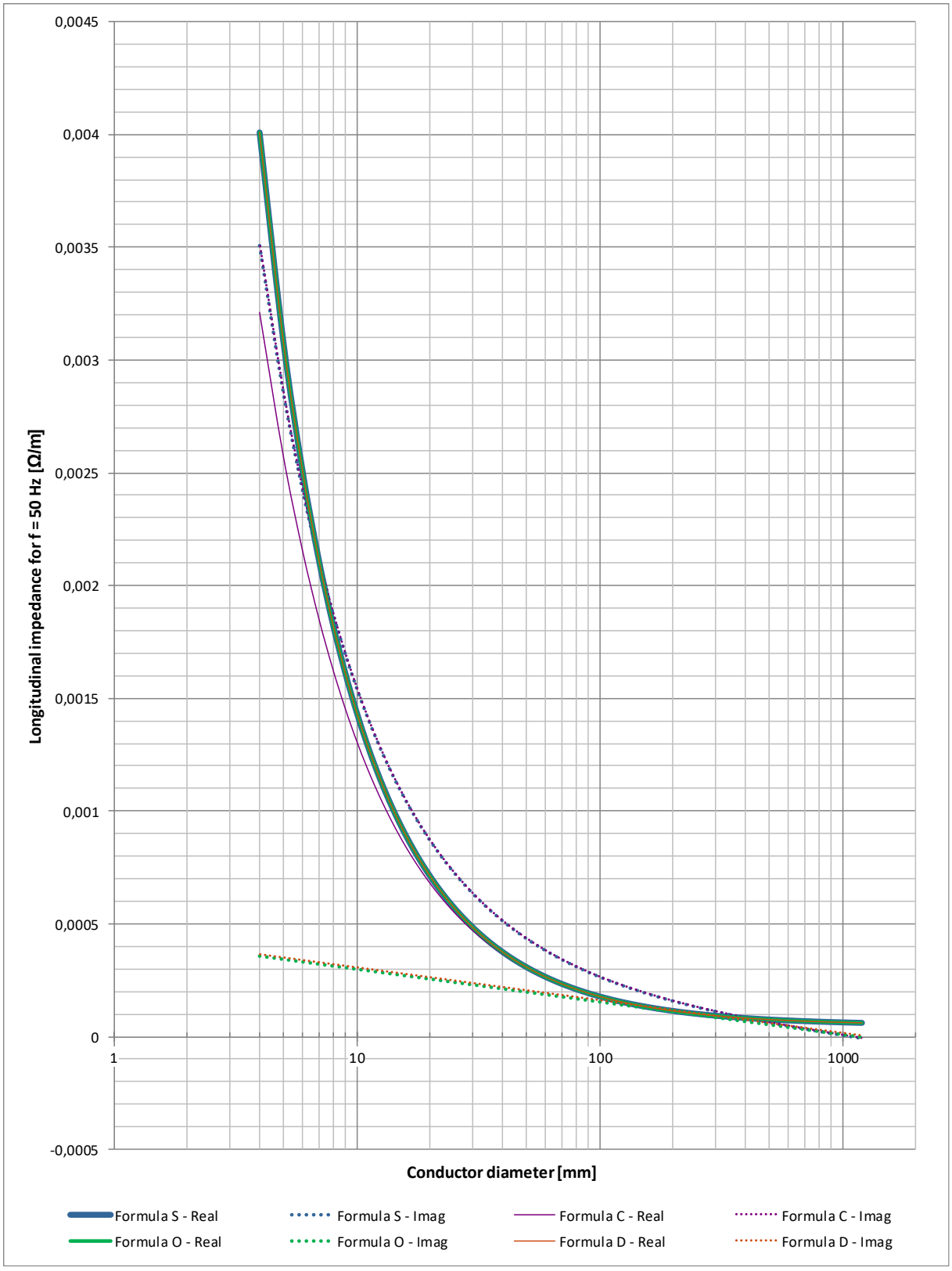

Figure A-4: Comparison of the different formulas for the longitudinal impedance with varying conductor diameter for 50 Hz, divided up into real and imaginary part

A.3 Full chart for the formulas for calculating the mutual impedances

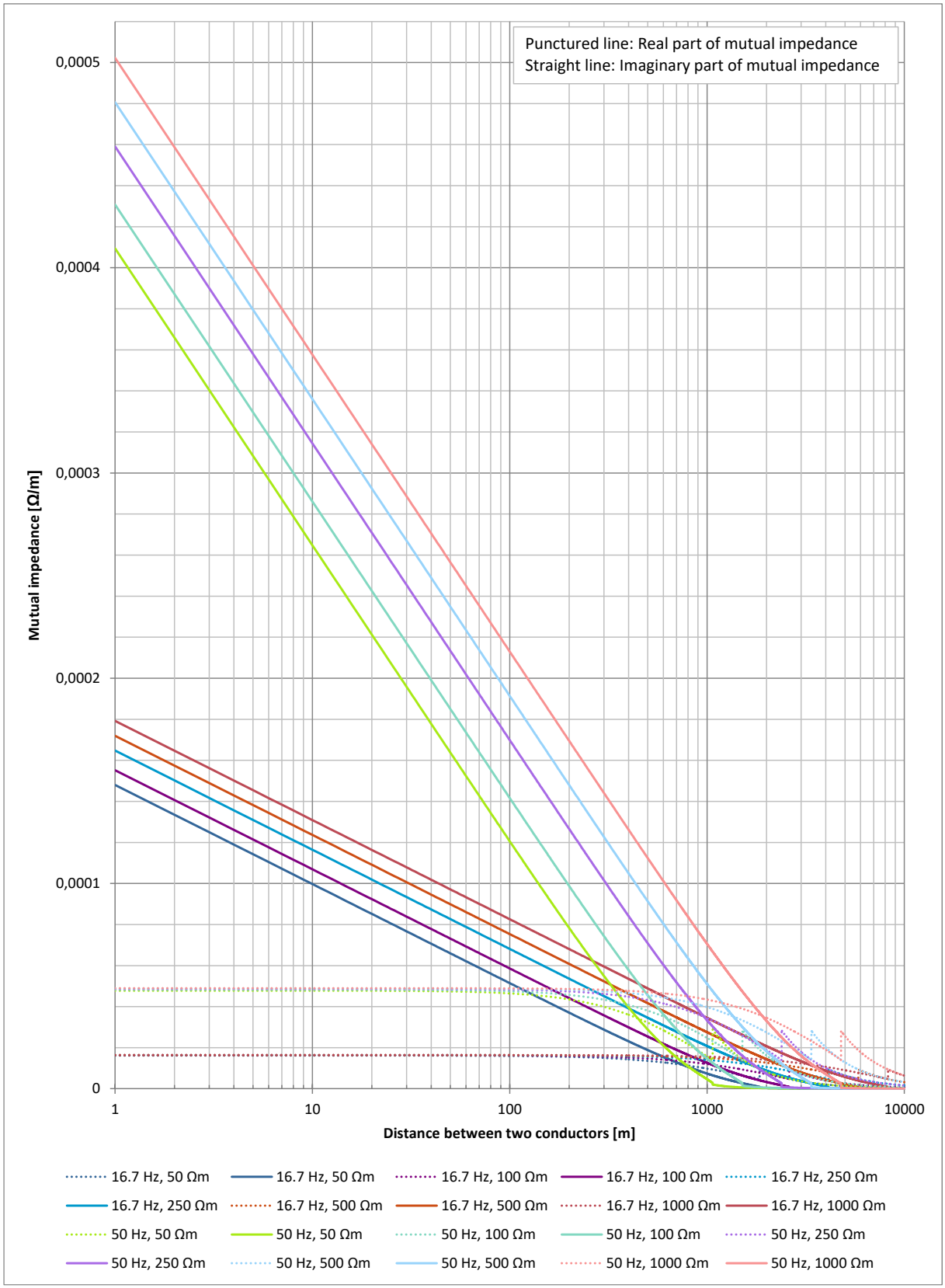

Figure A-5: Full Chart for the Carson-Dommel Formula for 16.7 and 50 Hz for different specific soil resistivities

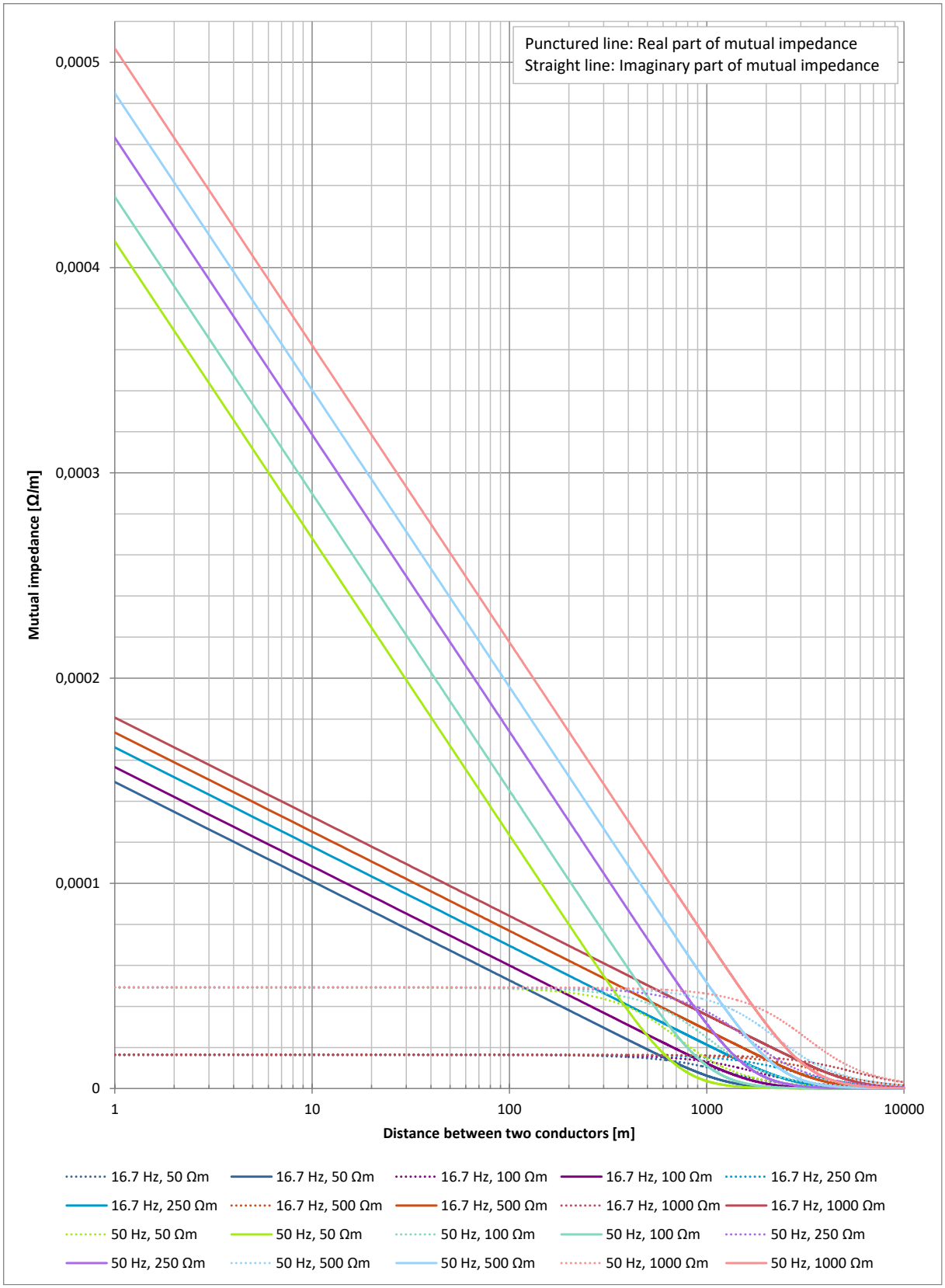

Figure A-6: Full Chart for the Complex Image Formula for 16.7 and 50 Hz for different specific soil resistivities

B Additional graphics of chapter 3

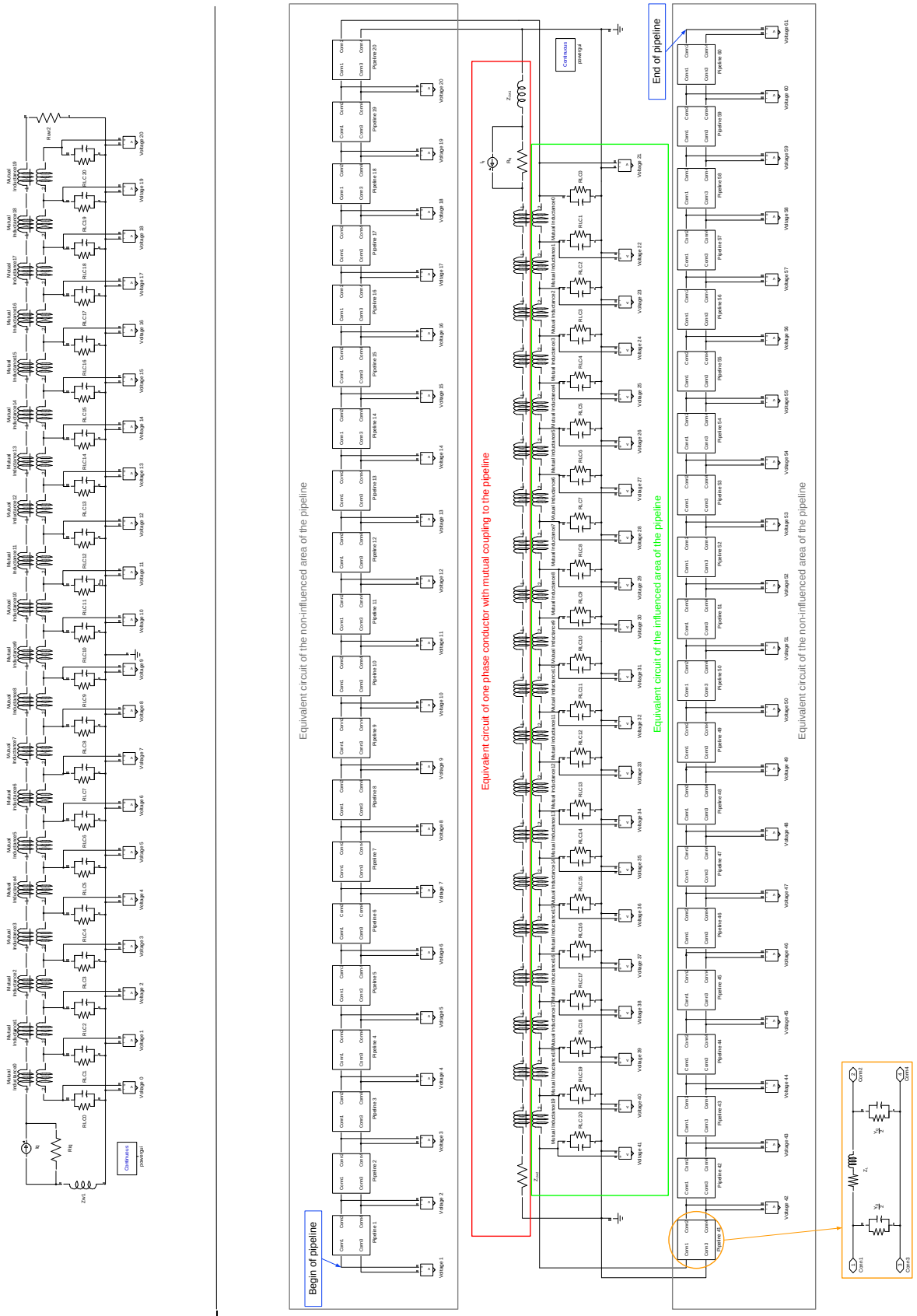

Figure B-1: Full Simulink-model for the interference with pipeline over a) the whole length and b) a partial length

C Additional voltage curves of chapter 4.7.2

C.1 "Ton" pylon 220 kV (PY1) – worst CC

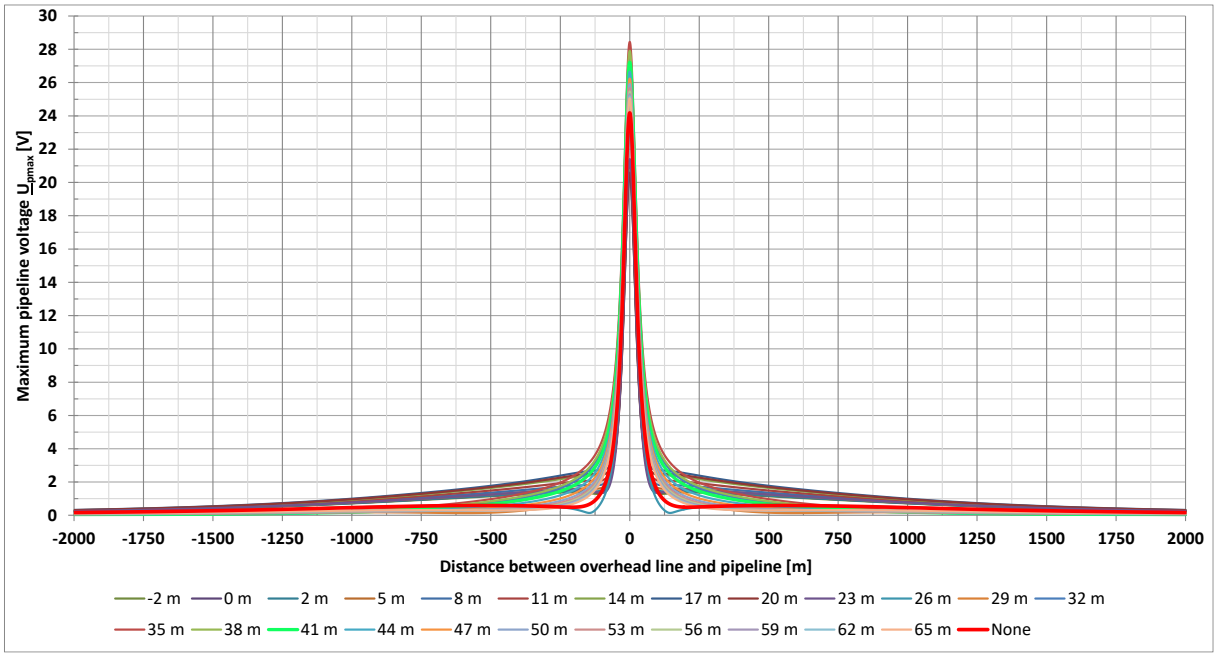

Figure C- 1: Maximum PIVs for the "ton"-pylon with the worst CC at different heights of EC

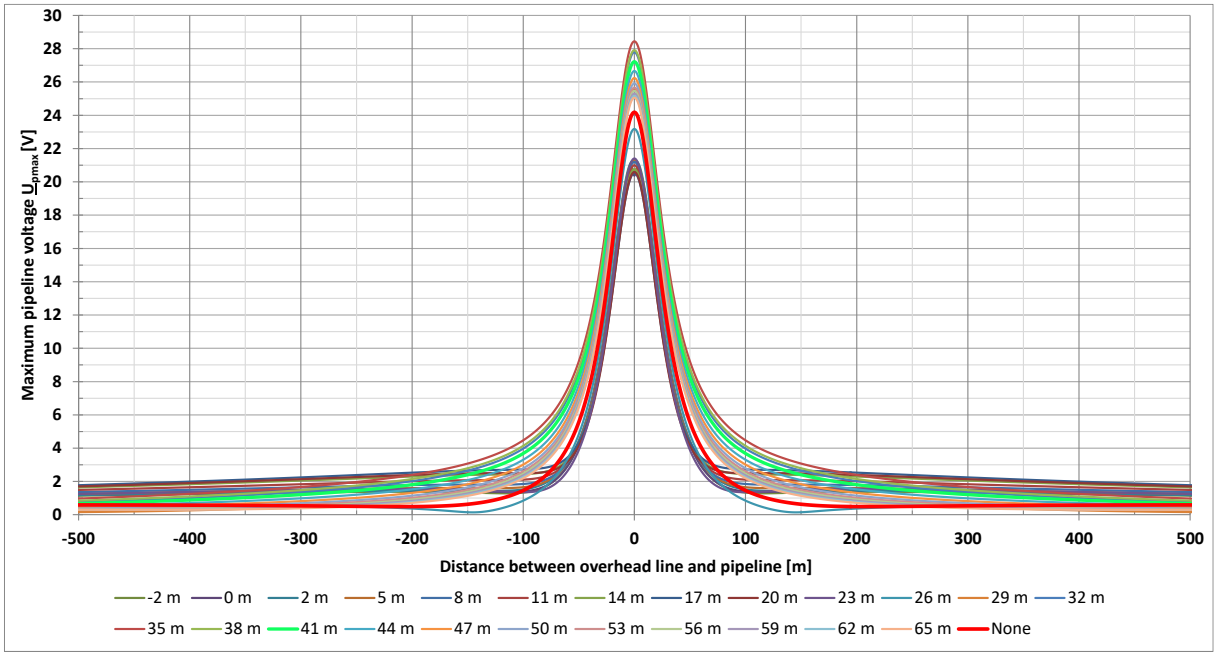

Figure C- 2: Maximum PIVs for the "ton"-pylon with the worst CC at different heights of EC; zoomed variant

C.2 "Tan" pylon 220 kV (PY2) – best CC

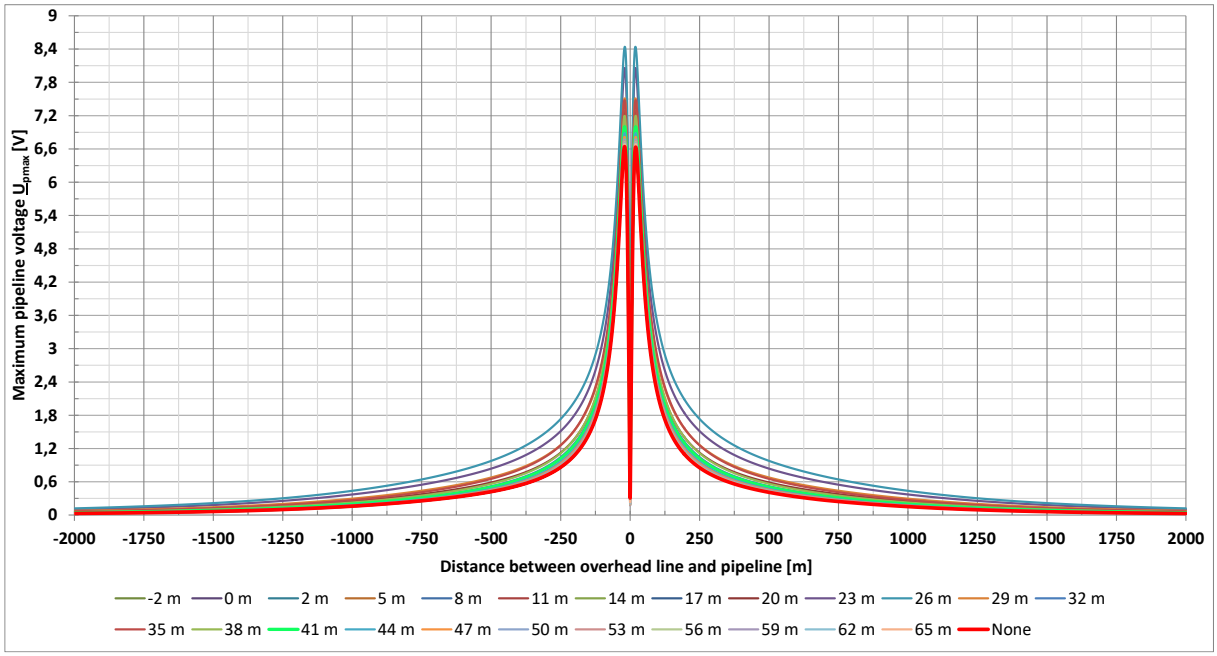

Figure C- 3: Maximum PIVs for the "tan"-pylon with the best CC at different heights of EC

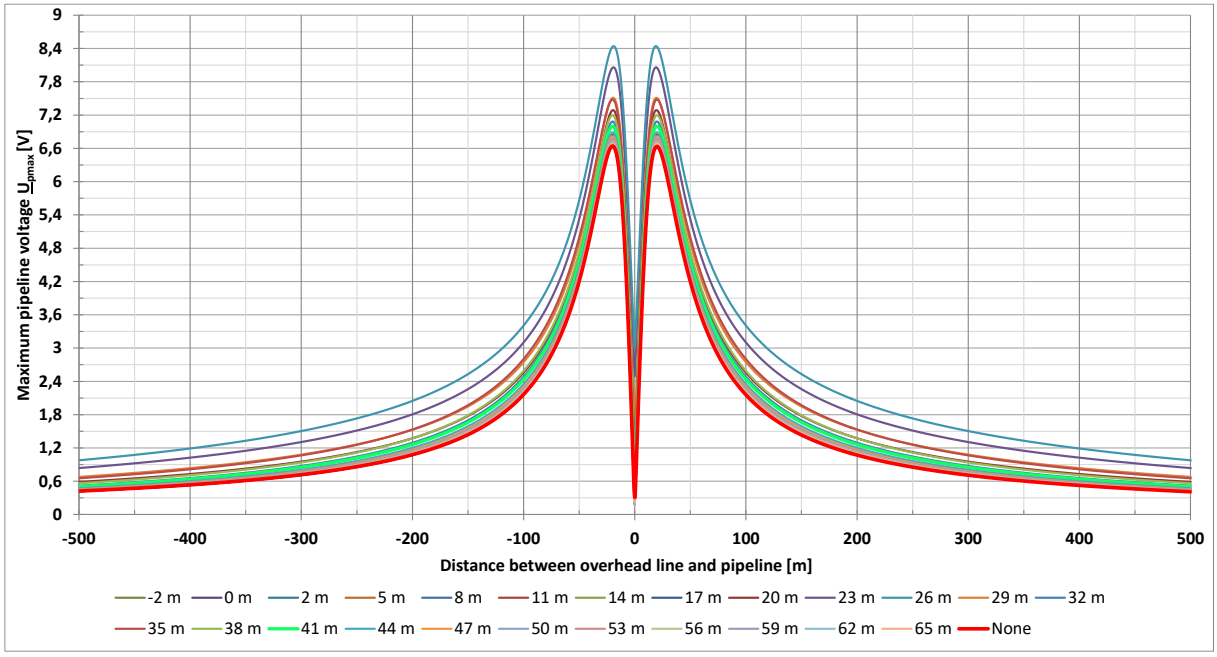

Figure C- 4: Maximum PIVs for the "tan"-pylon with the best CC at different heights of EC; zoomed variant

C.3 "Tan" pylon 220 kV (PY2) – worst CC

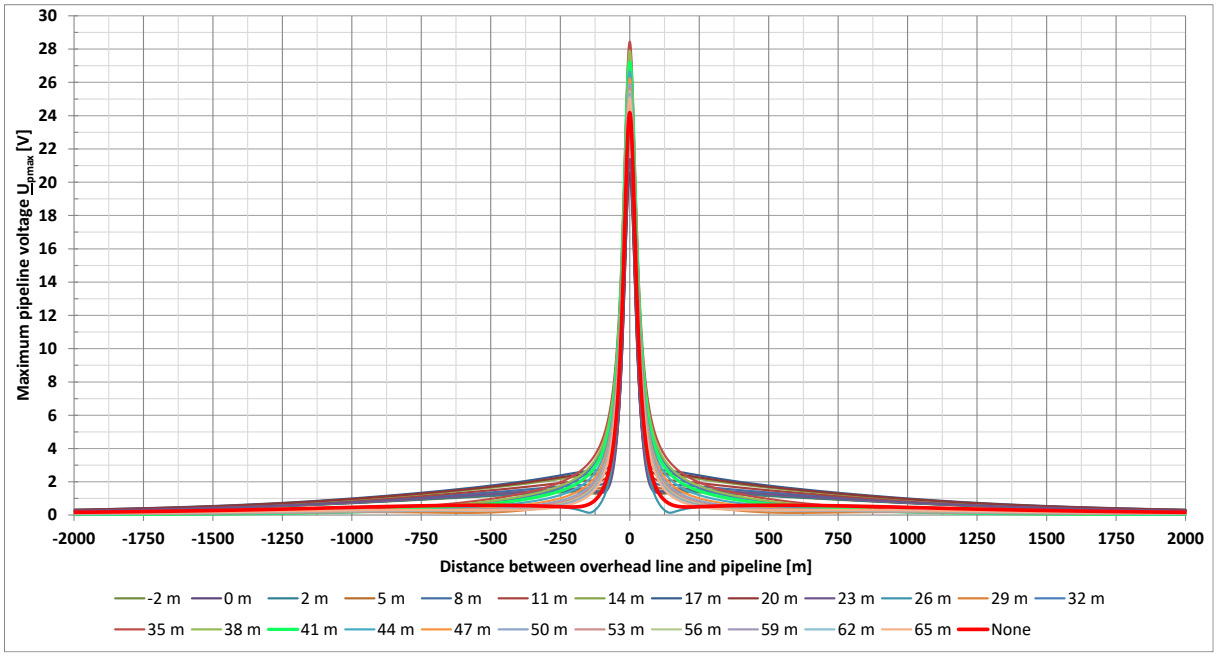

Figure C- 5: Maximum PIVs for the "tan"-pylon with the worst CC at different heights of EC

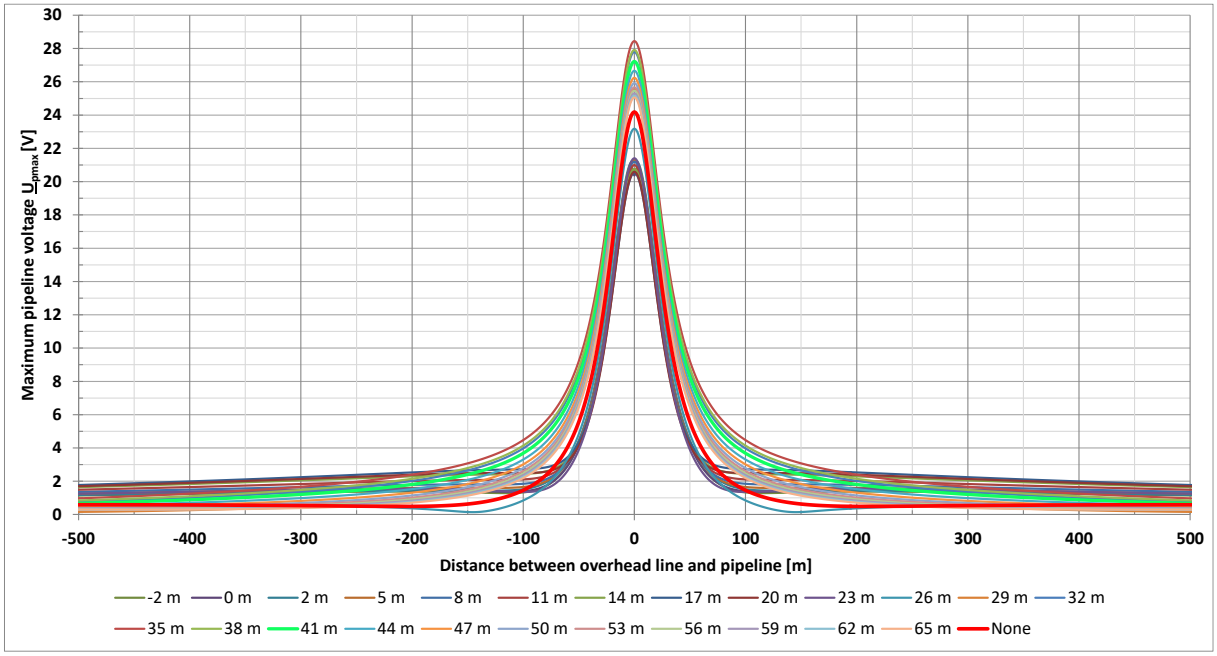

Figure C- 6: Maximum PIVs for the "tan"-pylon with the worst CC at different heights of EC; zoomed variant

C.4 "Danube" pylon 220 kV (PY3) – best CC

The voltage curves in Figure C- 9 and Figure C- 10 serve as a starting point for the voltages in Figure C- 7 and the ratios in Figure C- 8. For this purpose, the calculation method from chapter 4.7.2.1.1 for the vertical profile is used.

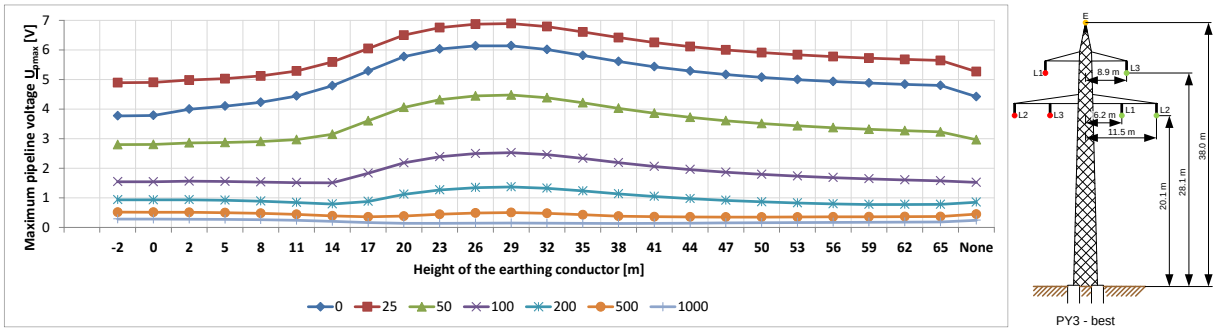

Figure C- 7: Maximum PIVs for the "danube"-pylon at different heights of EC for specific distances

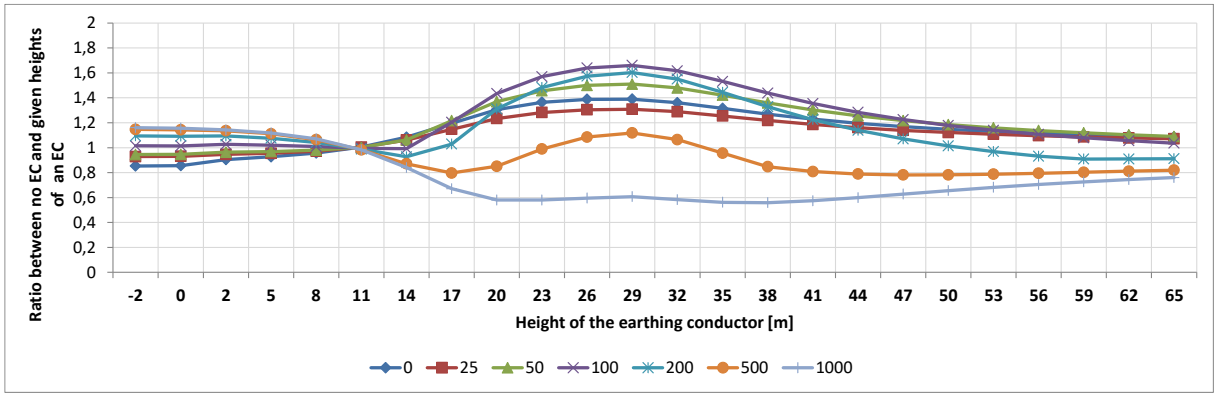

Figure C- 8: Ratio for the "danube"-pylon with the best CC for different heights of the EC for specific distances, where the reference value (value = 1) means using no EC for specific distances

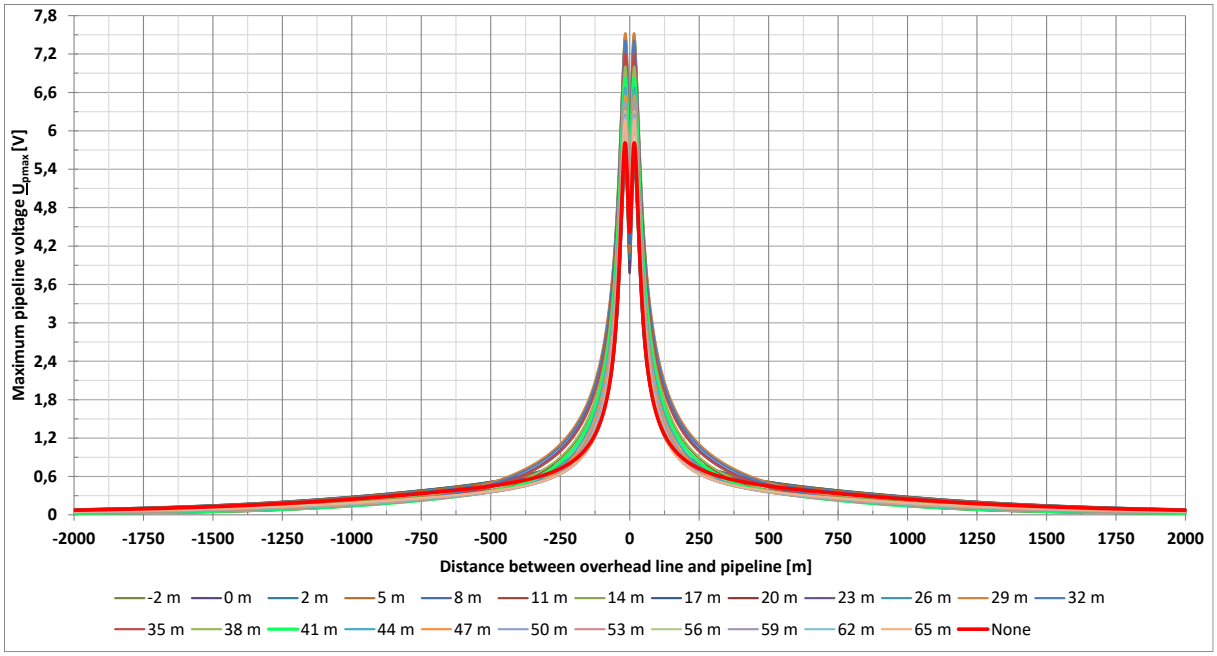

Figure C- 9: Maximum PIVs for the "danube"-pylon with the best CC at different heights of EC

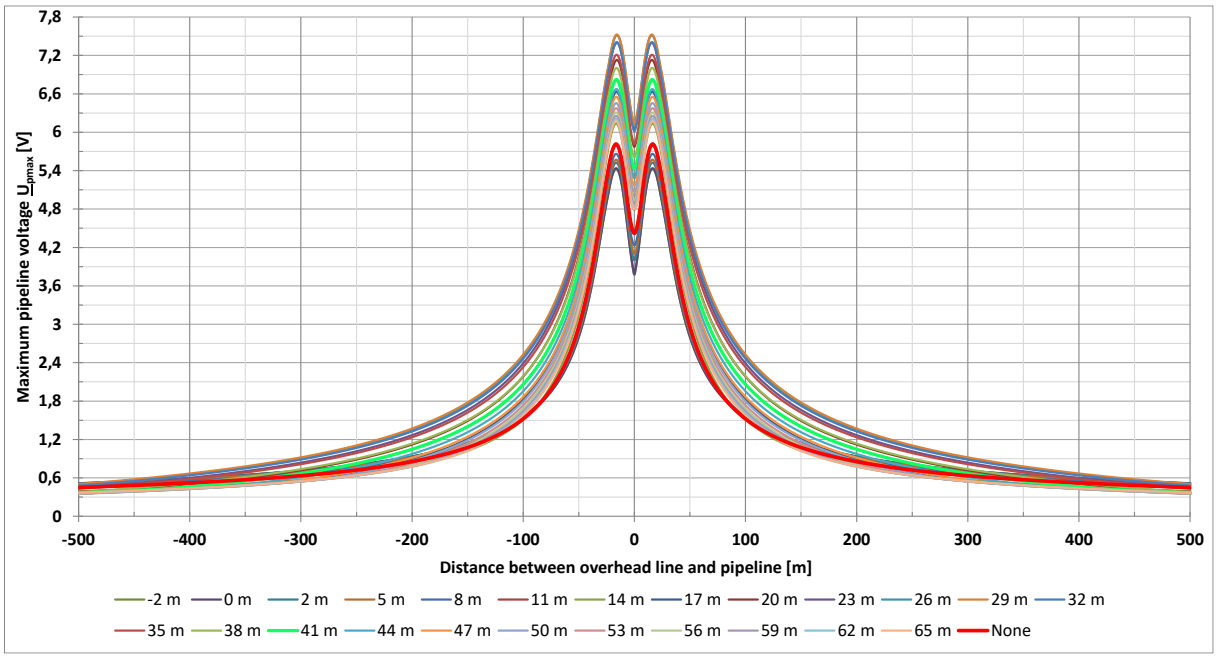

Figure C- 10: Maximum PIVs for the "danube"-pylon with the best CC at different heights of EC; zoomed variant

C.5 "Danube" pylon 220 kV (PY3) – worst CC

The voltage curves in Figure C- 11 and Figure C- 12 serve as a starting point for the voltages in Figure C- 13 and the ratios in Figure C- 14. For this purpose, the calculation method from chapter 4.7.2.1.1 for the vertical profile is used.

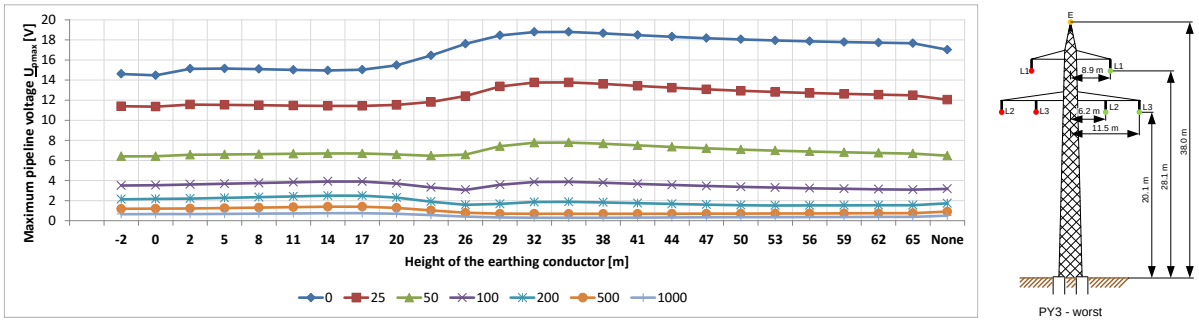

Figure C- 11: Maximum PIVs for the "danube"-pylon at different heights of EC for specific distances

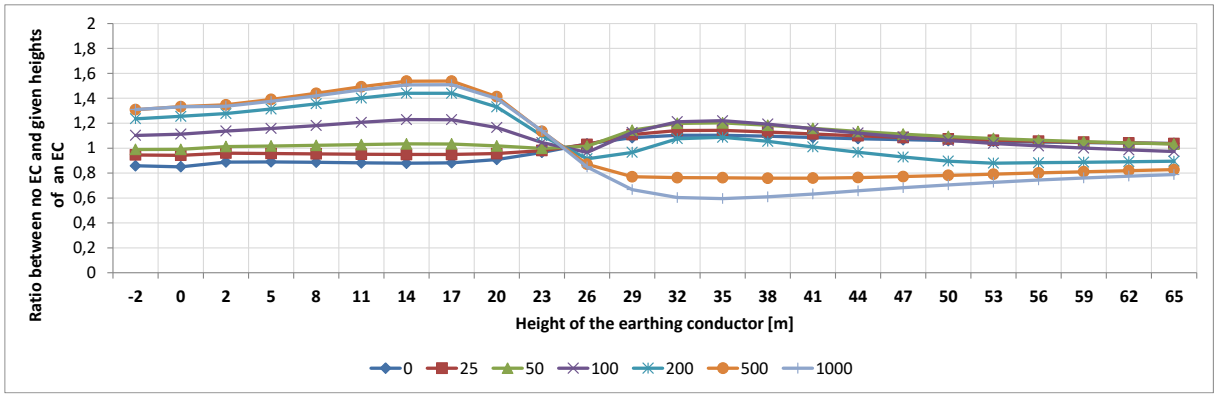

Figure C- 12: Ratio for the "danube"-pylon with the worst CC for different heights of the EC for specific distances, where the reference value (value = 1) means using no EC for specific distances

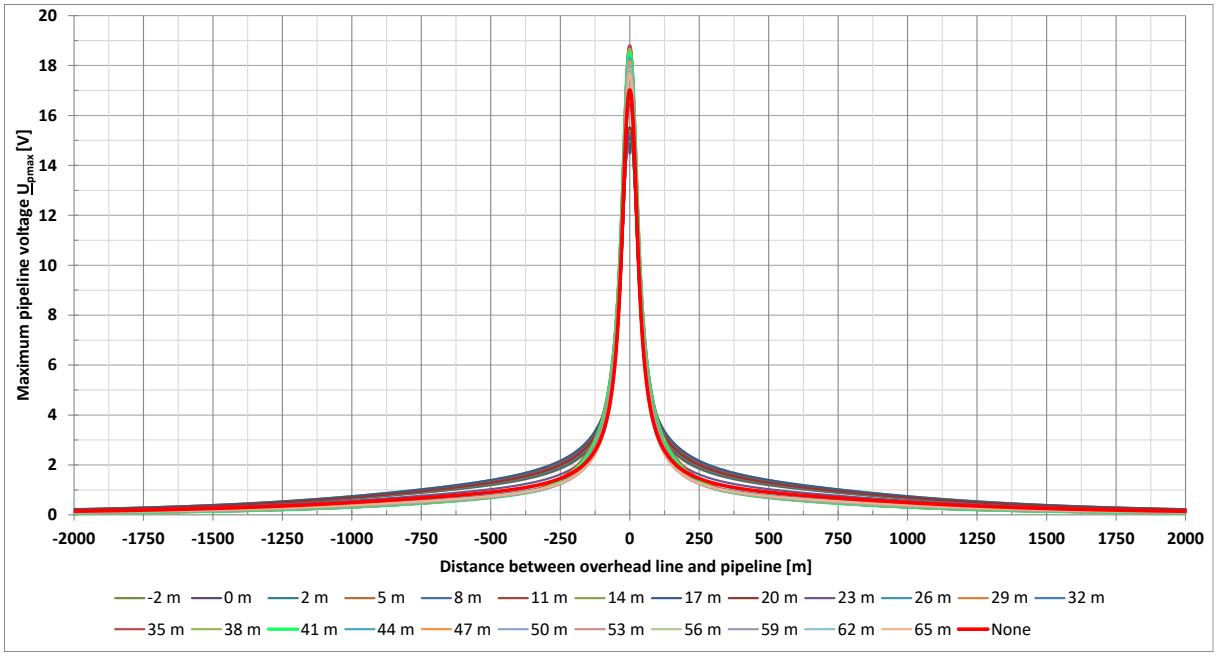

Figure C- 13: Maximum PIVs for the "danube"-pylon with the worst CC at different heights of EC

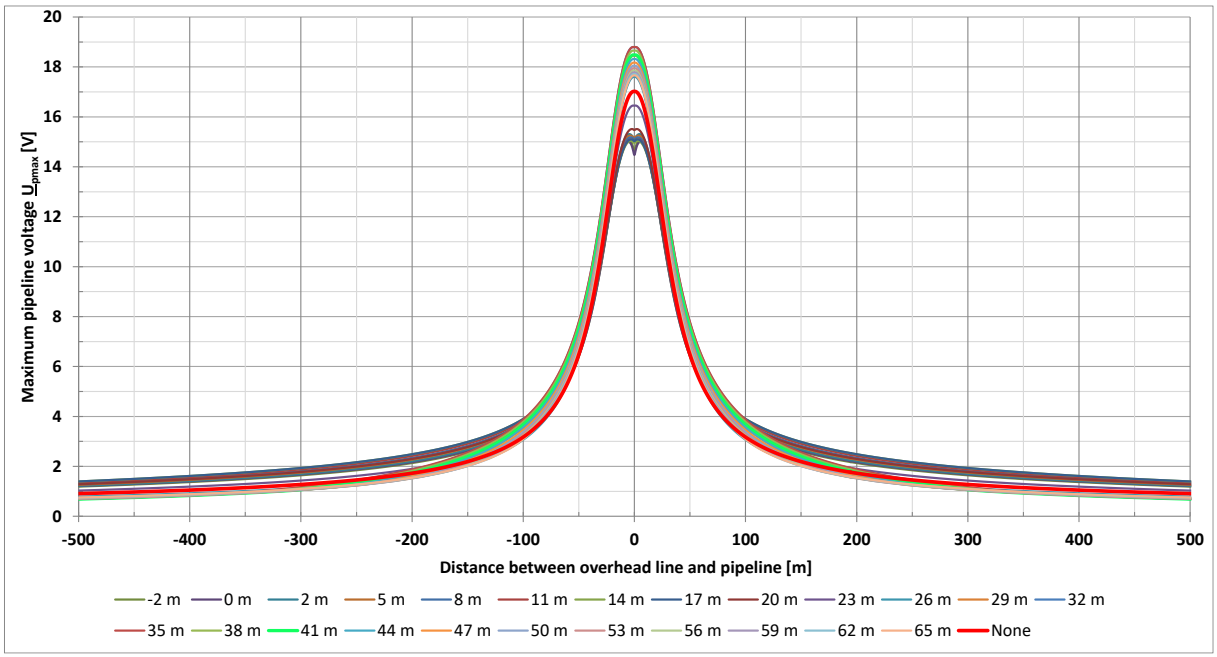

Figure C- 14: Maximum PIVs for the "danube"-pylon with the worst CC at different heights of EC; zoomed variant

C.6 "Single-plane" pylon 220 kV (PY4) – best CC

The voltage curves in Figure C- 15 and Figure C- 16 serve as a starting point for the voltages in Figure C- 17 and the ratios in Figure C- 18. For this purpose, the calculation method from chapter 4.7.2.1.1 for the vertical profile is used.

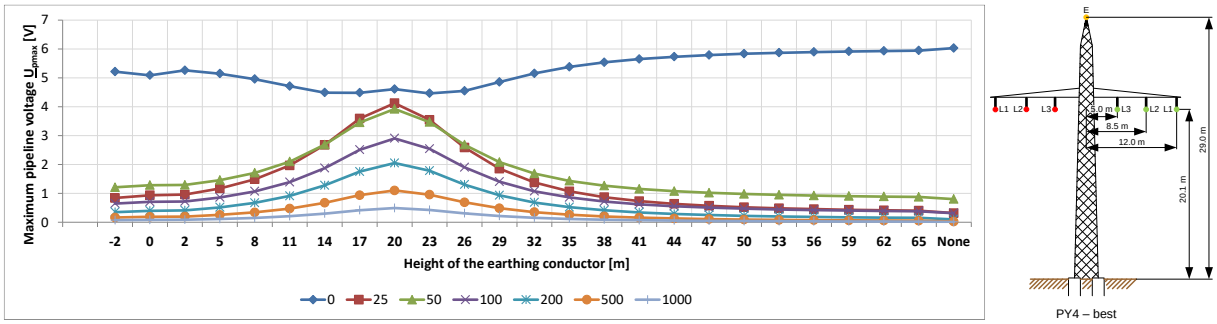

Figure C- 15: Maximum PIVs for the "single-plain"-pylon at different heights of EC for specific distances

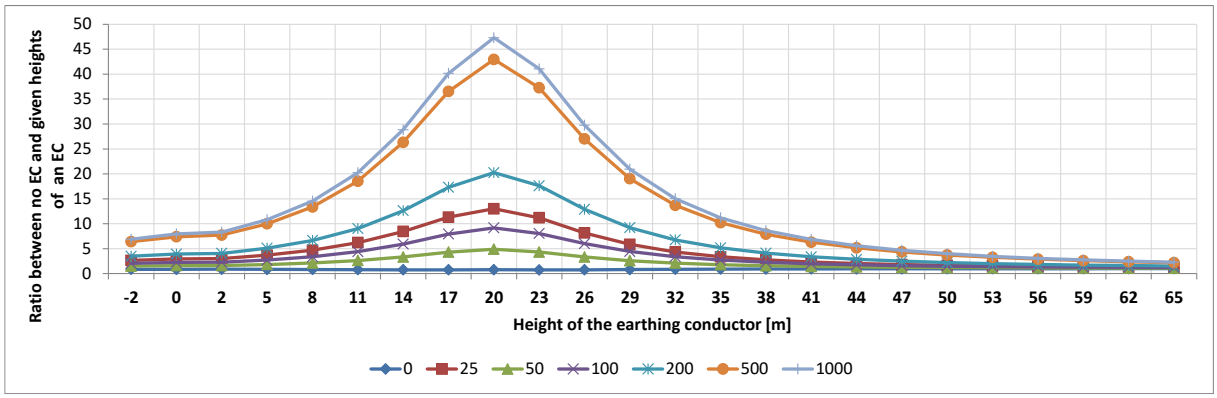

Figure C- 16: Ratio for the "single-plain"-pylon with the best CC for different heights of the EC for specific distances, where the reference value (value = 1) means using no EC for specific distances

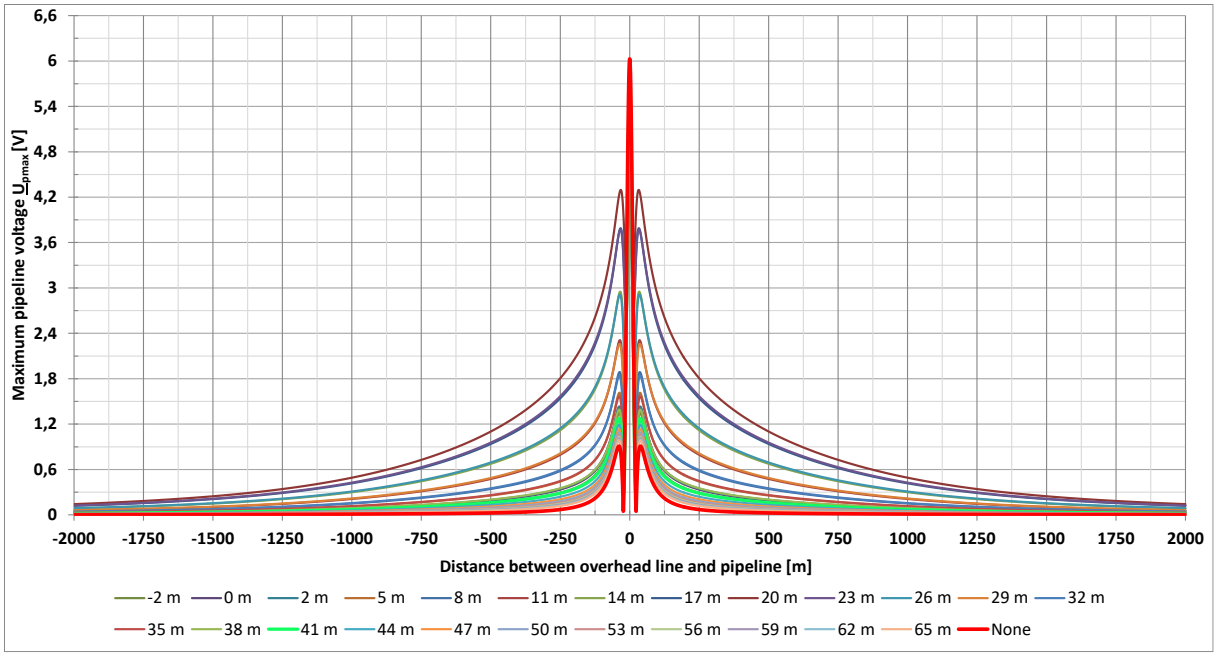

Figure C- 17: Maximum PIVs for the "single-plane"-pylon with the best CC at different heights of EC

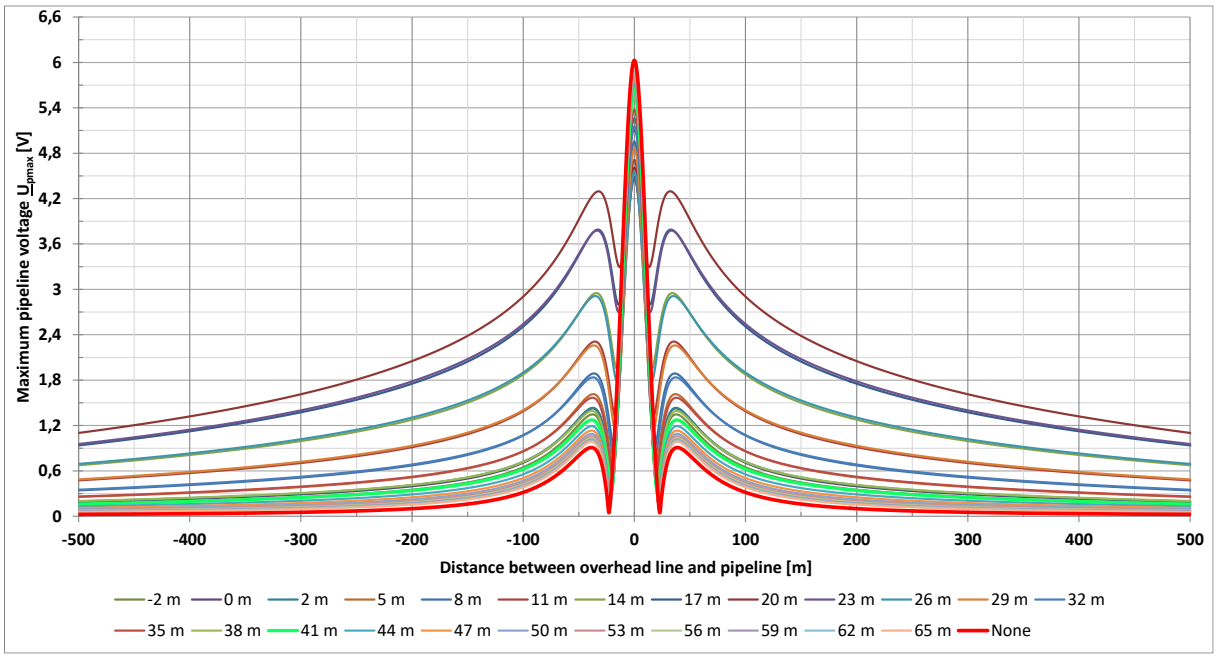

Figure C- 18: Maximum PIVs for the "single-plane"-pylon with the best CC at different heights of EC; zoomed variant

C.7 “Single-plane” pylon 220 kV (PY4) – worst CC

The voltage curves in Figure C- 19 and Figure C- 20 serve as a starting point for the voltages in Figure C- 21 and the ratios in Figure C- 22. For this purpose, the calculation method from chapter 4.7.2.1.1 for the vertical profile is used.

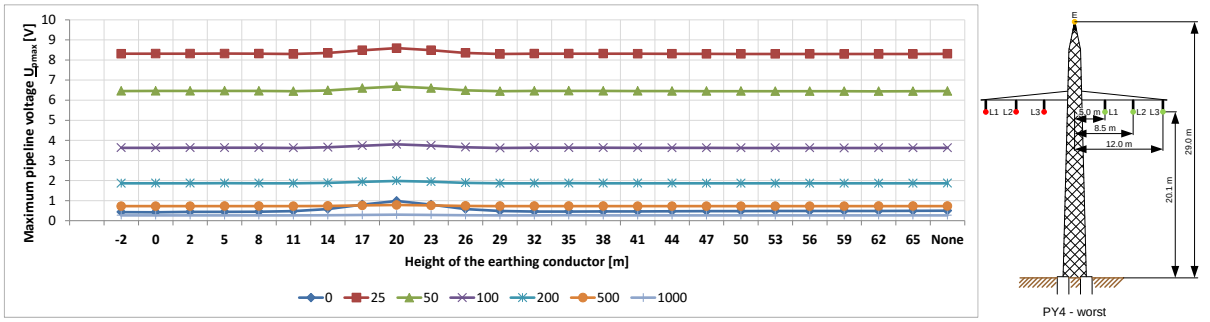

Figure C- 19: Maximum PIVs for the “single-plain”-pylon at different heights of EC for specific distances

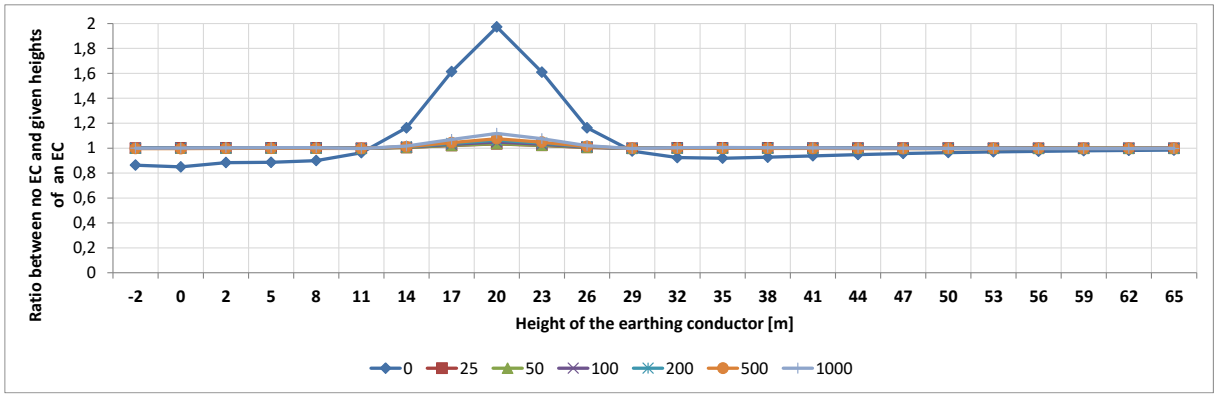

Figure C- 20: Ratio for the “single-plain”-pylon with the worst CC for different heights of the EC for specific distances, where the reference value (value = 1) means using no EC for specific distances

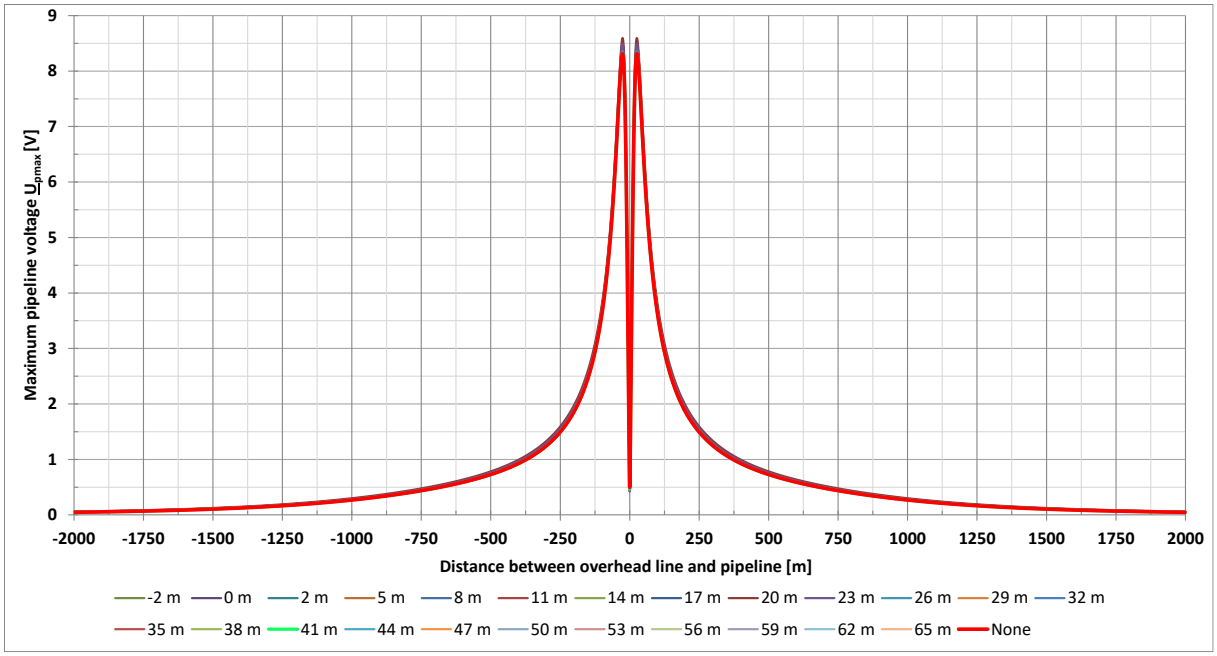

Figure C- 21: Maximum PIVs for the "single-plane"-pylon with the worst CC at different heights of EC

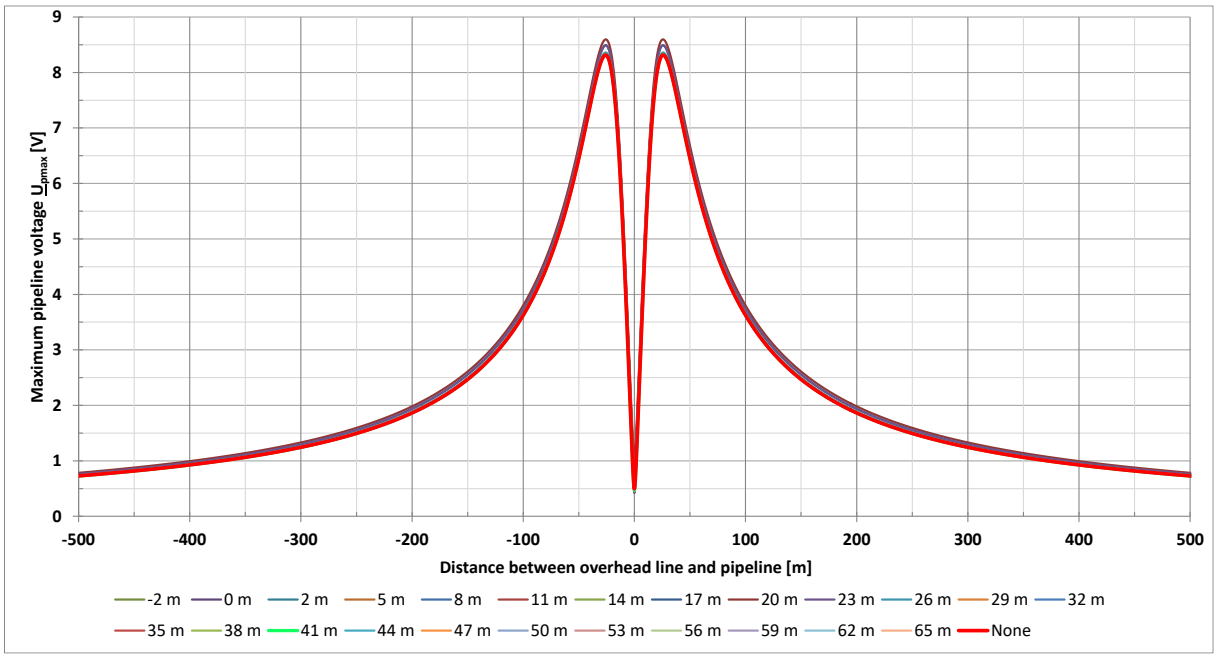

Figure C- 22: Maximum PIVs for the "single-plane"-pylon with the worst CC at different heights of EC; zoomed variant

C.8 "Quadruple" pylon 380 kV (PY6) – best CC

The voltage curves in Figure C- 23 and Figure C- 24 serve as a starting point for the voltages in Figure C- 25 and the ratios in Figure C- 26. For this purpose, the calculation method from chapter 4.7.2.1.1 for the vertical profile is used.

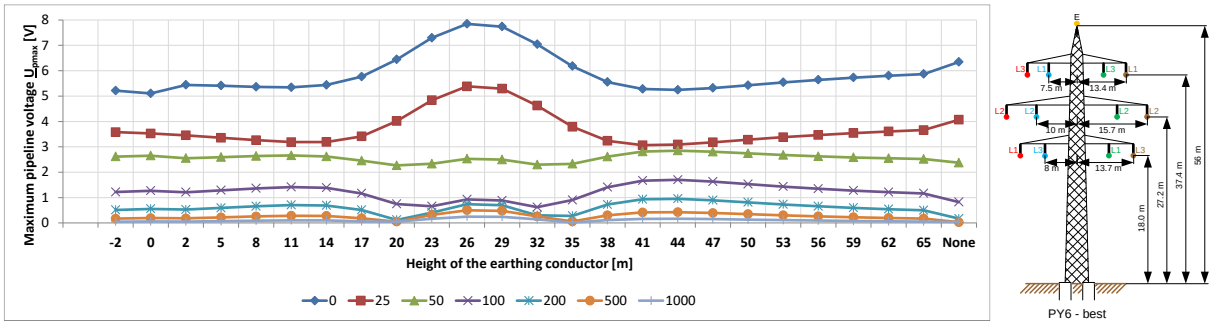

Figure C- 23: Maximum PIVs for the "quadruple"-pylon at different heights of EC for specific distances

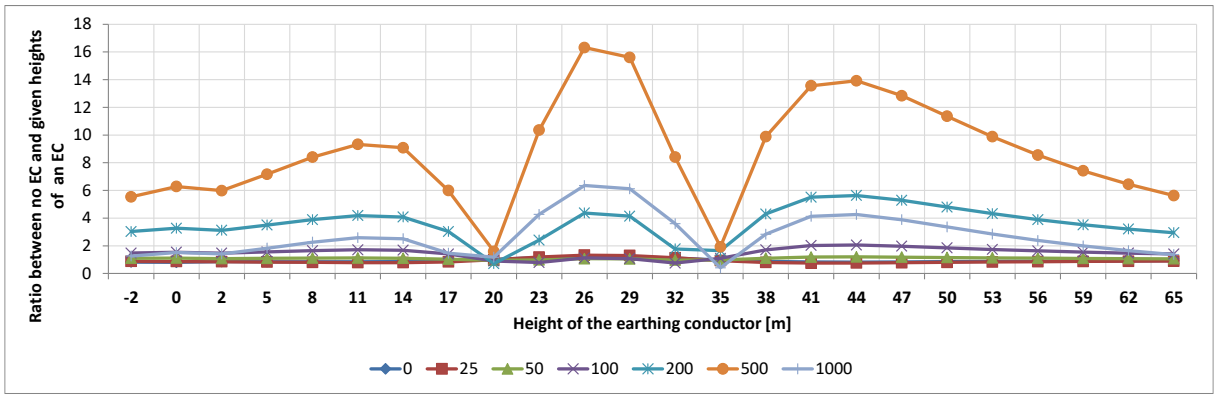

Figure C- 24: Ratio for the "quadruple"-pylon with the best CC for different heights of the EC for specific distances, where the reference value (value = 1) means using no EC for specific distances

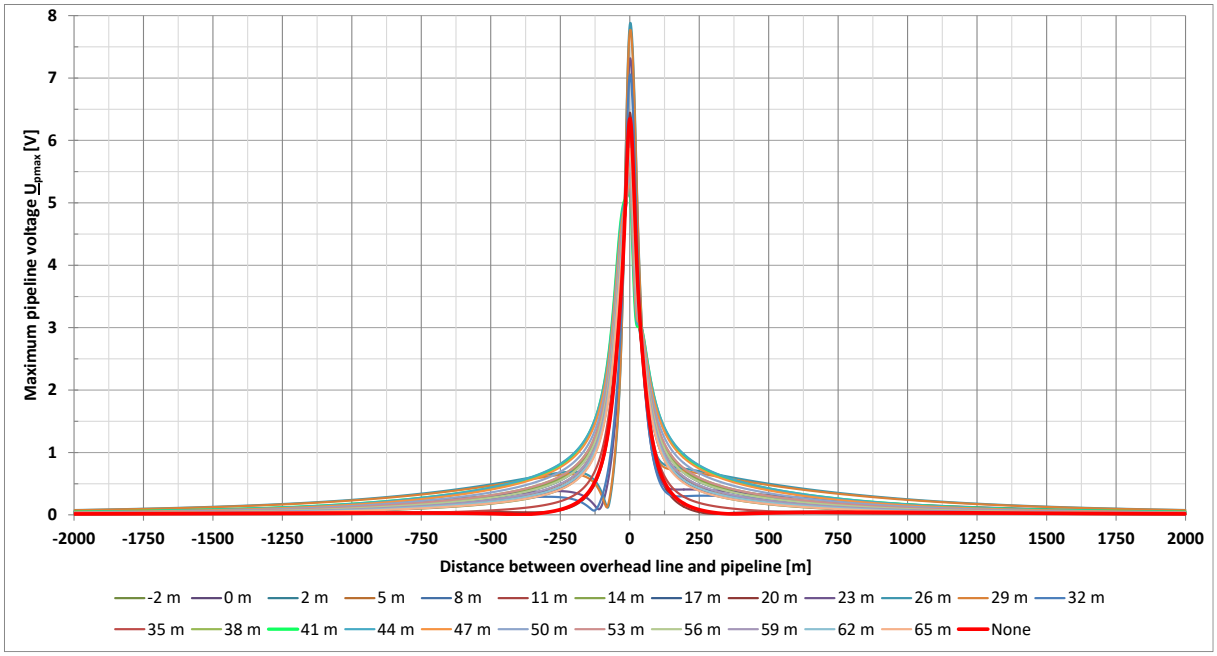

Figure C- 25: Maximum PIVs for the "quadruple"-pylon with the best CC at different heights of EC

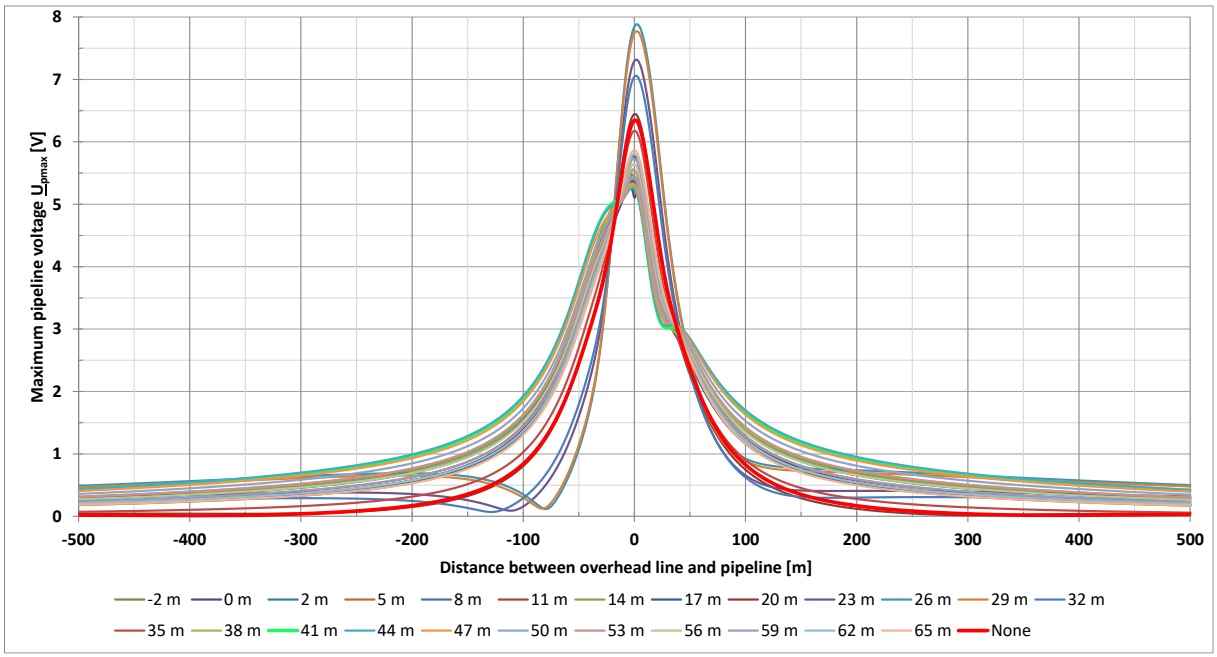

Figure C- 26: Maximum PIVs for the "quadruple"-pylon with the best CC at different heights of EC; zoomed variant

C.9 "Quadruple" pylon 380 kV (PY6) – worst CC

The voltage curves in Figure C- 27 and Figure C- 28 serve as a starting point for the voltages in Figure C- 29 and the ratios in Figure C- 30. For this purpose, the calculation method from chapter 4.7.2.1.1 for the vertical profile is used.

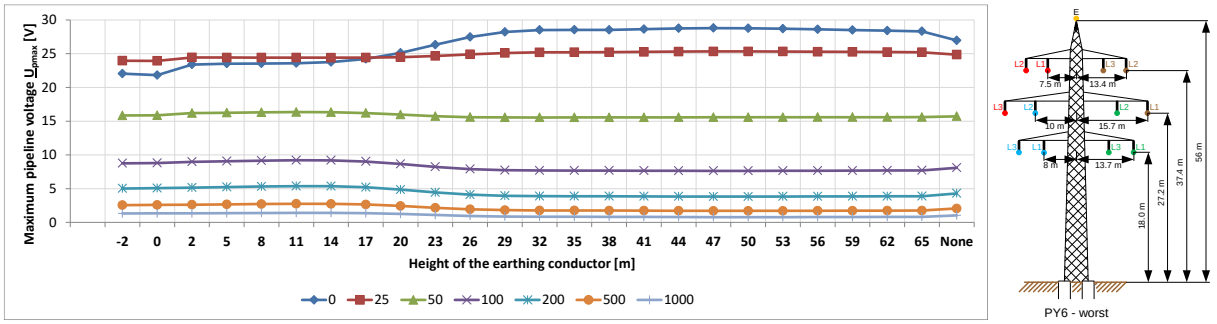

Figure C- 27: Maximum PIVs for the "quadruple"-pylon at different heights of EC for specific distances

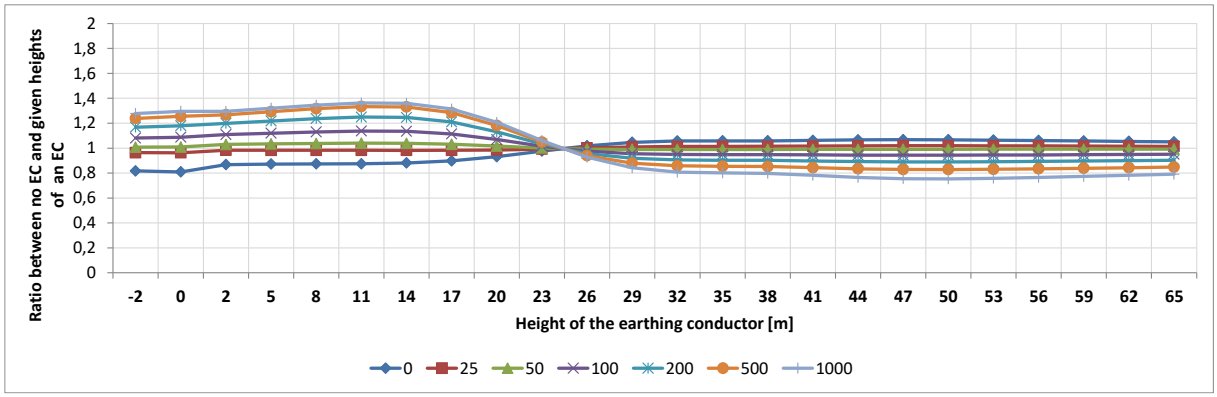

Figure C- 28: Ratio for the "quadruple"-pylon with the worst CC for different heights of the EC for specific distances, where the reference value (value = 1) means using no EC for specific distances

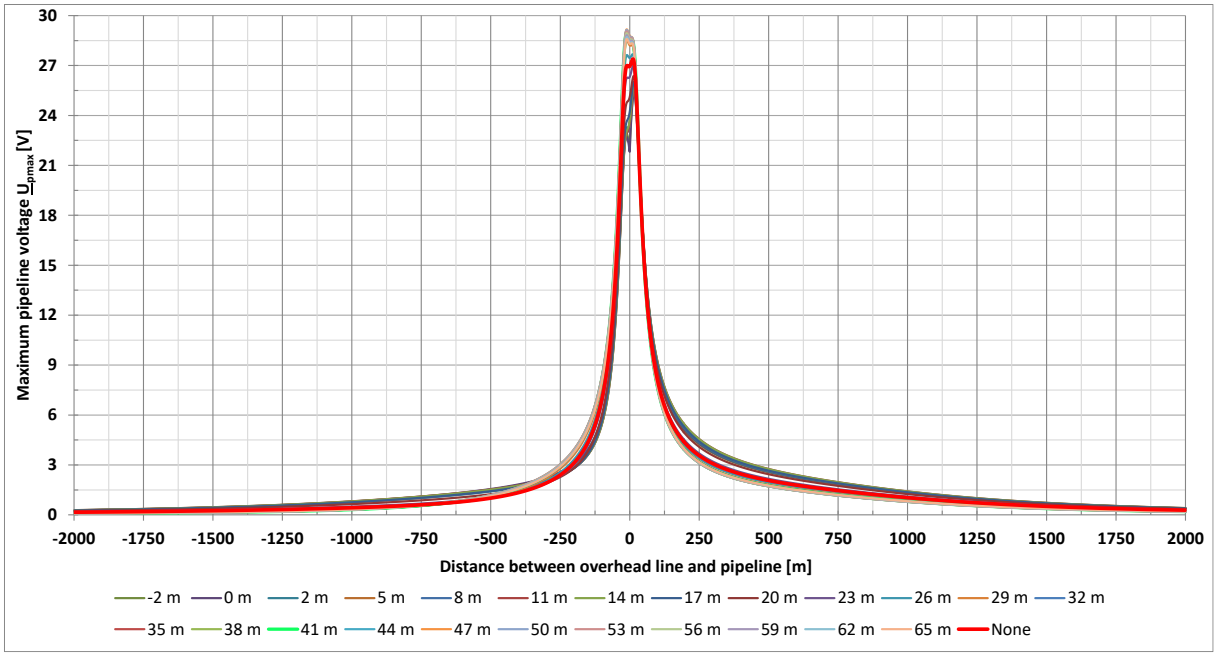

Figure C- 29: Maximum PIVs for the "quadruple"-pylon with the worst CC at different heights of EC

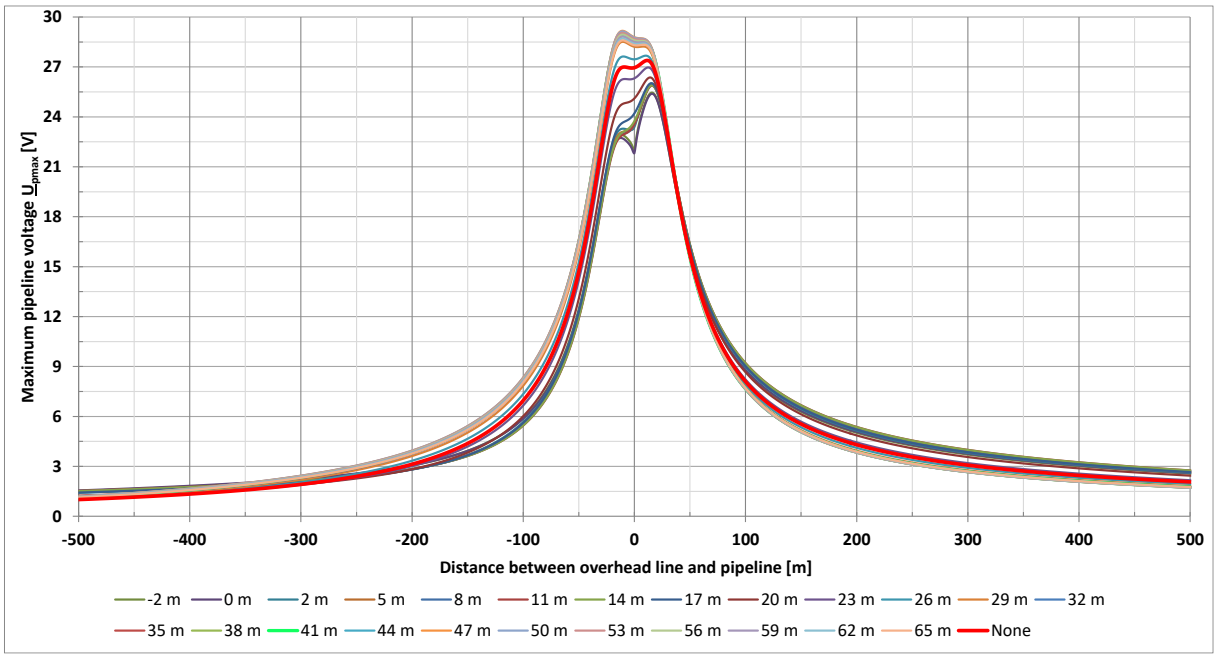

Figure C- 30: Maximum PIVs for the "quadruple"-pylon with the worst CC at different heights of EC; zoomed variant

C.10 "Single-Circuit" pylon 110 kV (PY10)

The voltage curves in Figure C- 31 and Figure C- 32 serve as a starting point for the voltages in Figure C- 33 and the ratios in Figure C- 34. For this purpose, the calculation method from chapter 4.7.2.1.1 for the vertical profile is used.

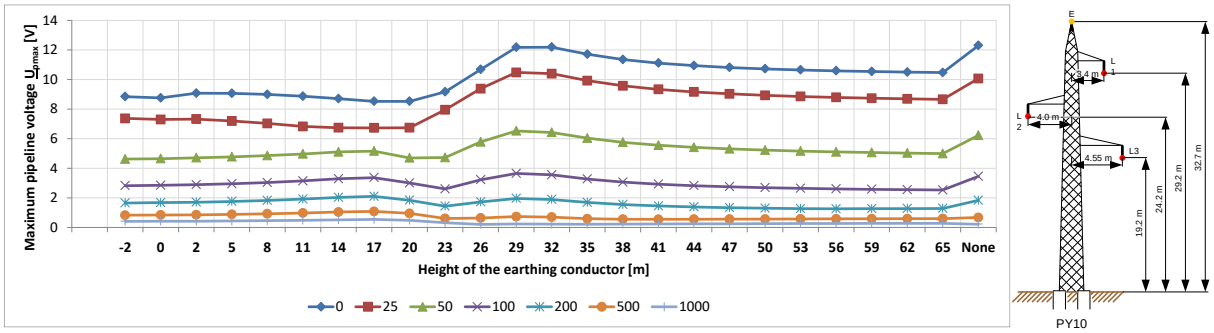

Figure C- 31: Maximum PIVs for the "single-circuit"-pylon at different heights of EC for specific distances

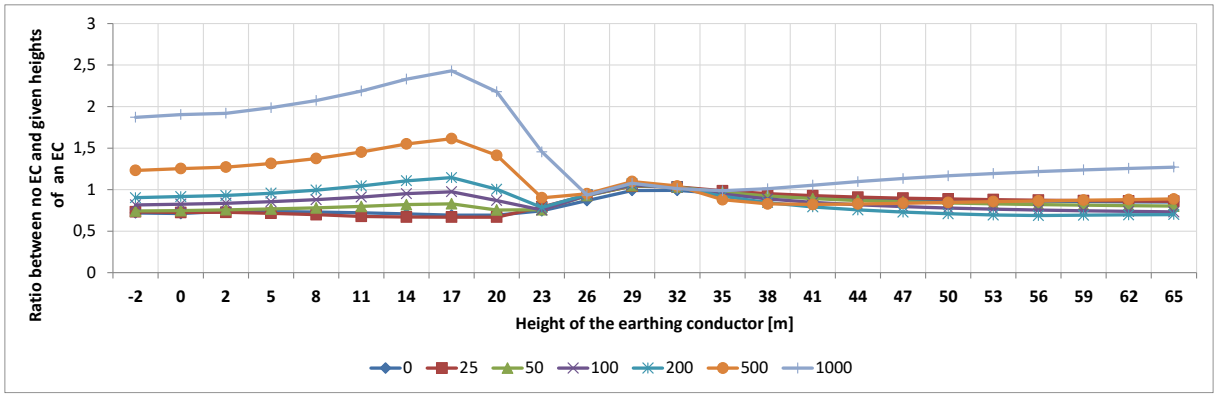

Figure C- 32: Ratio for the "single-circuit"-pylon for different heights of the EC for specific distances, where the reference value (value = 1) means using no EC for specific distances

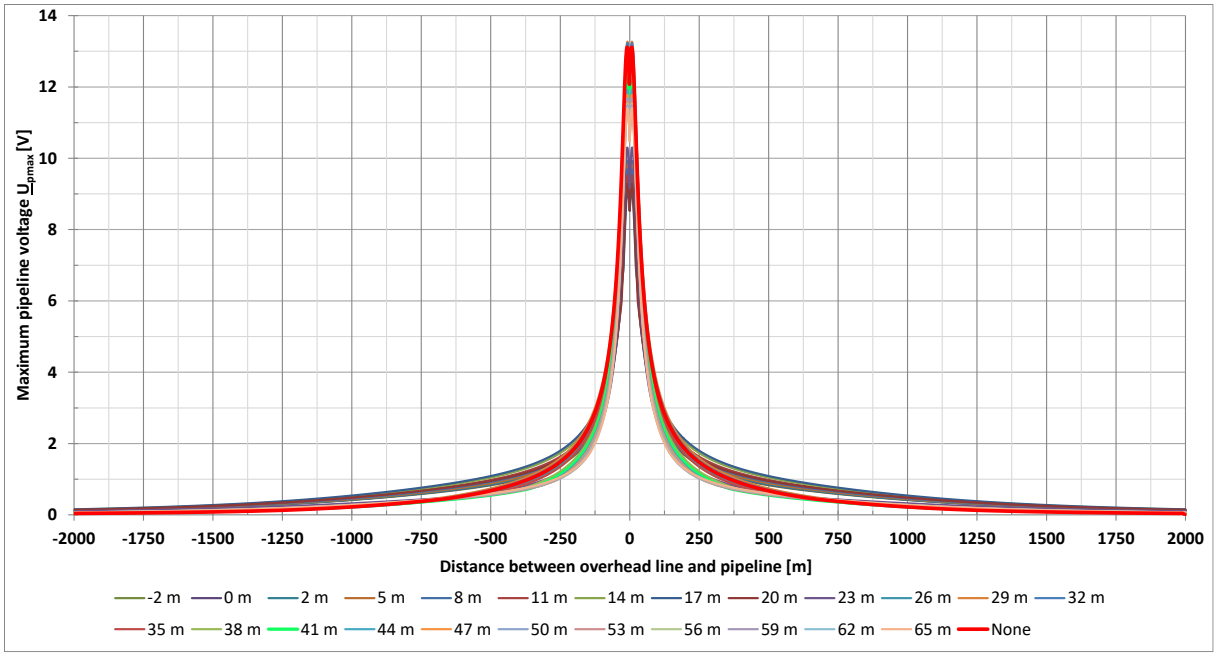

Figure C- 33: Maximum PIVs for the "single-circuit"-pylon with the used CC at different heights of EC

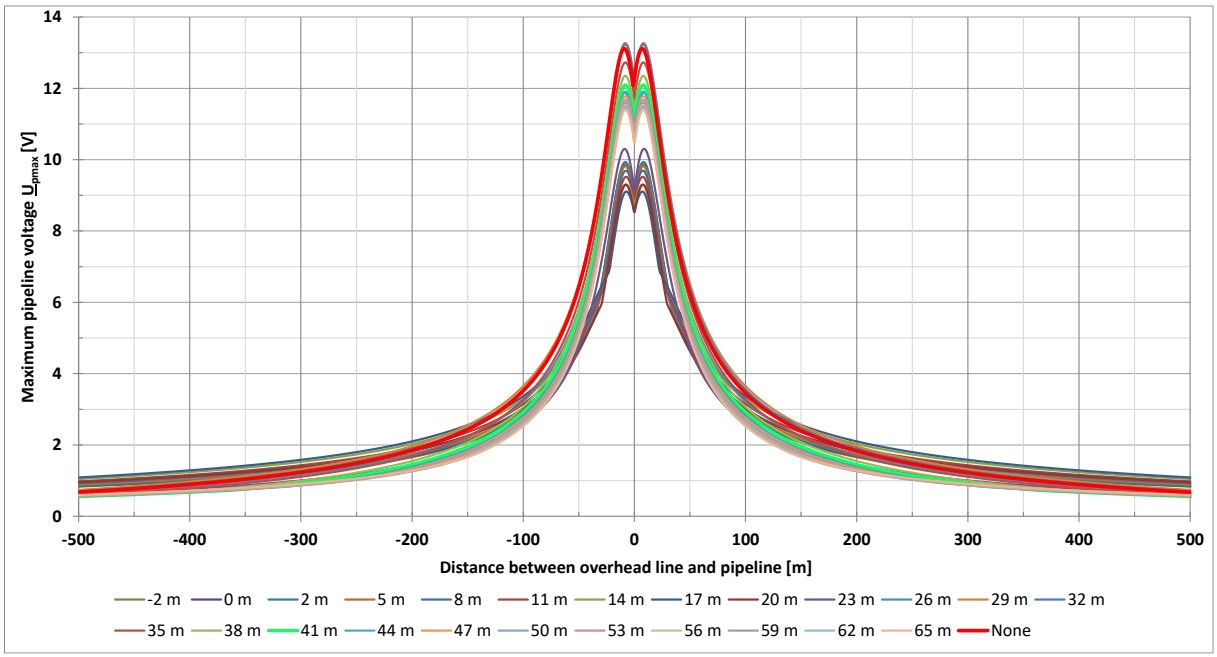

Figure C- 34: Maximum PIVs for the "single-circuit"-pylon with the used CC at different heights of EC; zoomed variant

C.11 “Ton” pylon with two ECs 220 kV (PY11) – best CC

The voltage curves in Figure C- 35 and Figure C- 36 serve as a starting point for the voltages in Figure C- 37 and the ratios in Figure C- 38. For this purpose, the calculation method from chapter 4.7.2.1.1 for the vertical profile is used.

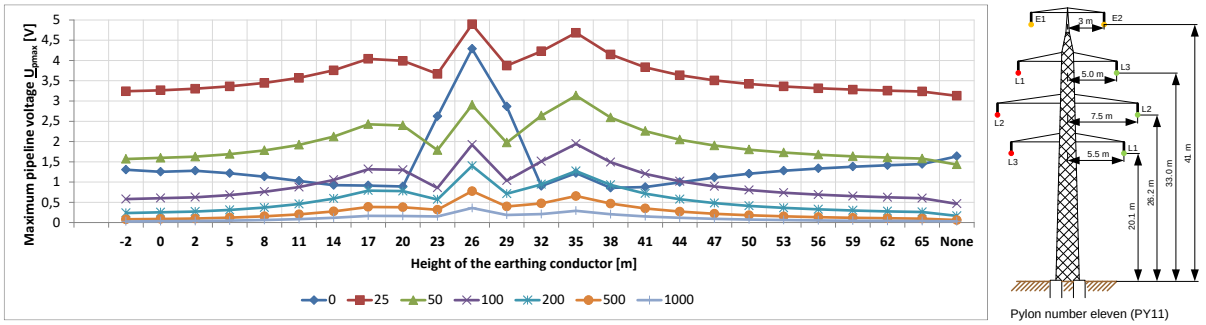

Figure C- 35: Maximum PIVs for the “ton”-pylon with two ECs at different heights of EC for certain distances

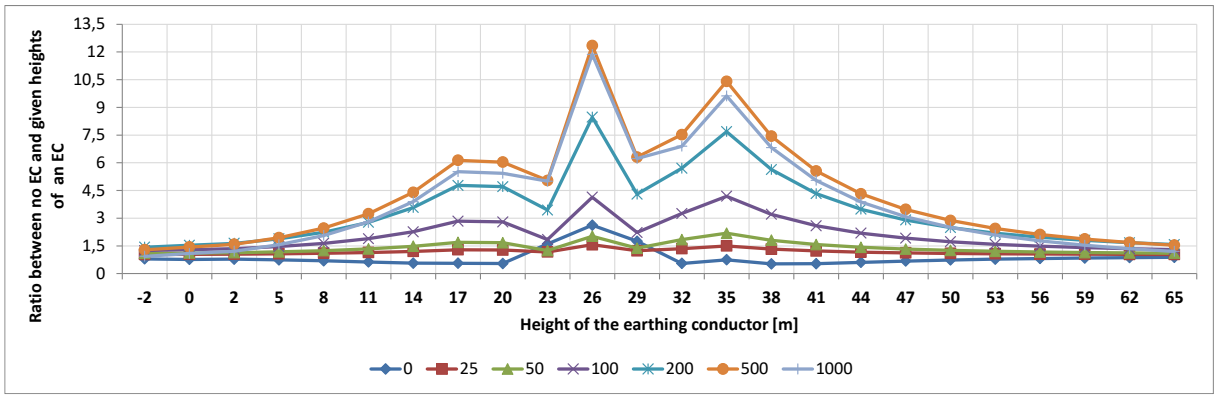

Figure C- 36: Ratio for the “ton”-pylon with two ECs and the best CC for different heights of the EC for certain distances, where the reference value (value = 1) is always the case of using no EC for certain distances

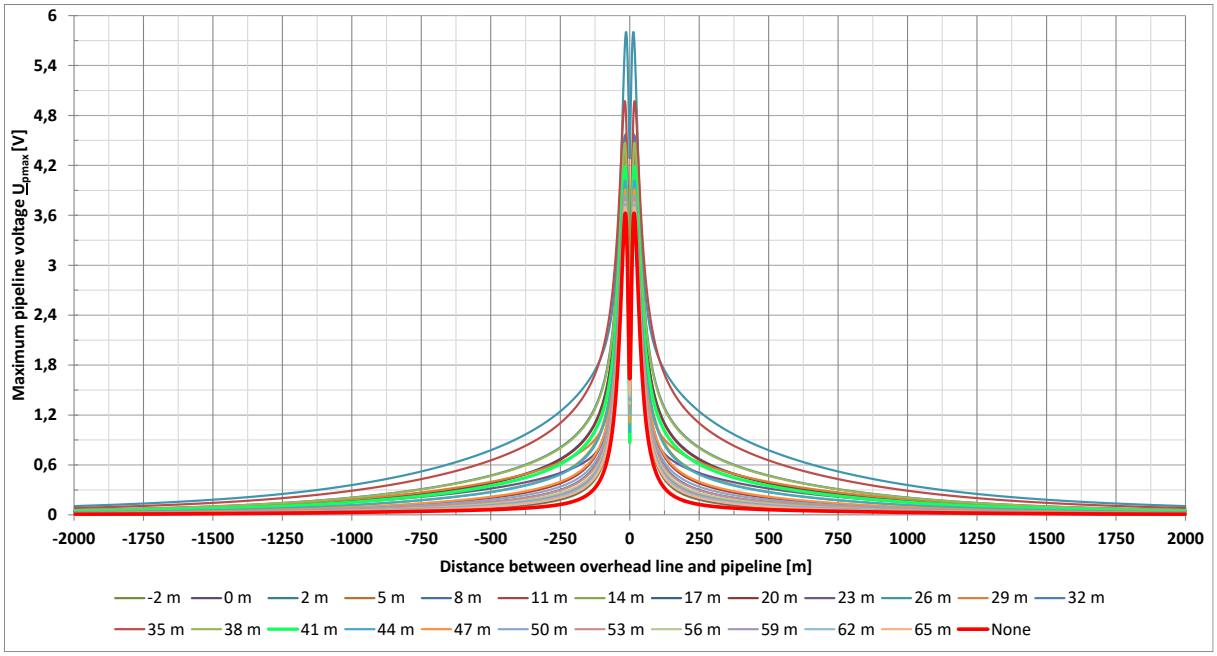

Figure C- 37: Maximum PIVs for the "ton"-pylon with two ECs and the best CC at different heights of EC

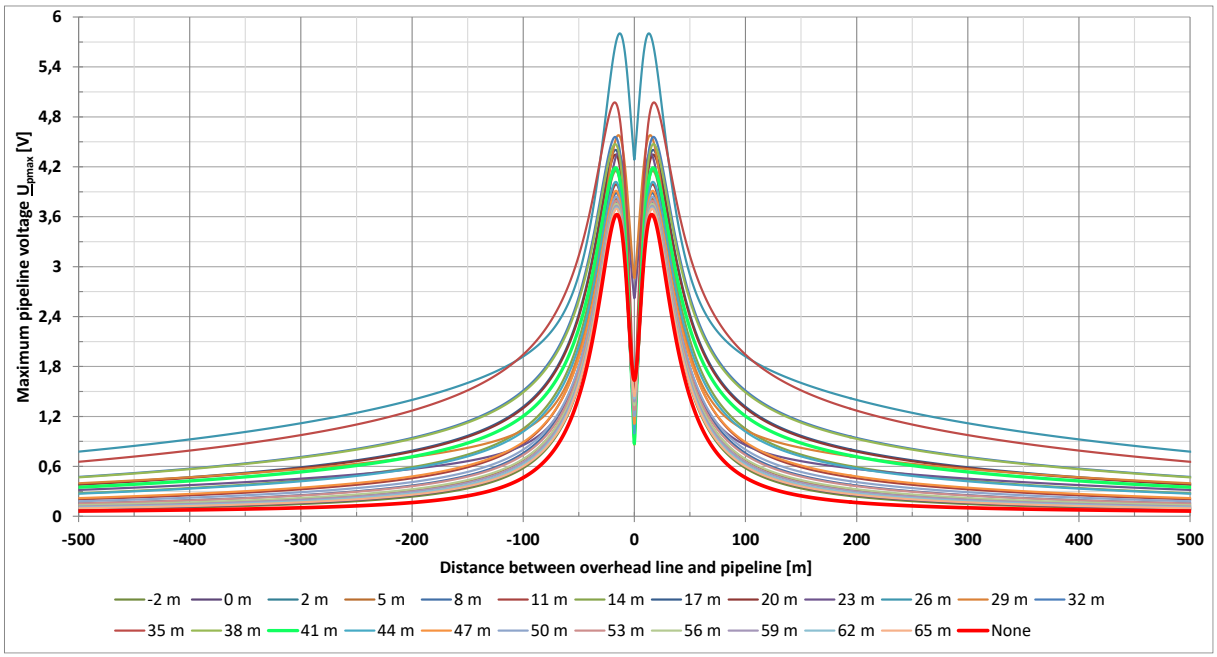

Figure C- 38: Maximum PIVs for the "ton"-pylon with two ECs and the best CC at different heights of EC; zoomed variant

C.12 "Ton" pylon with two ECs 220 kV (PY11) – worst CC

The voltage curves in Figure C- 39 and Figure C- 40 serve as a starting point for the voltages in Figure C- 41 and the ratios in Figure C- 42. For this purpose, the calculation method from chapter 4.7.2.1.1 for the vertical profile is used.

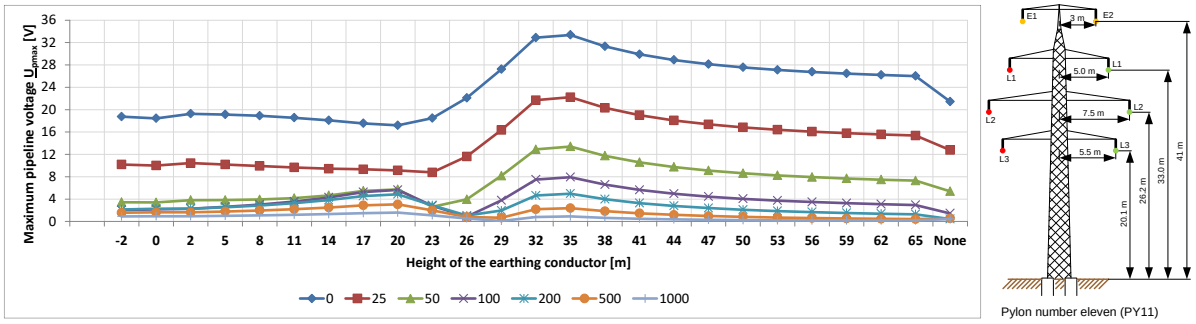

Figure C- 39: Maximum PIVs for the "ton"-pylon with two ECs at different heights of EC for certain distances

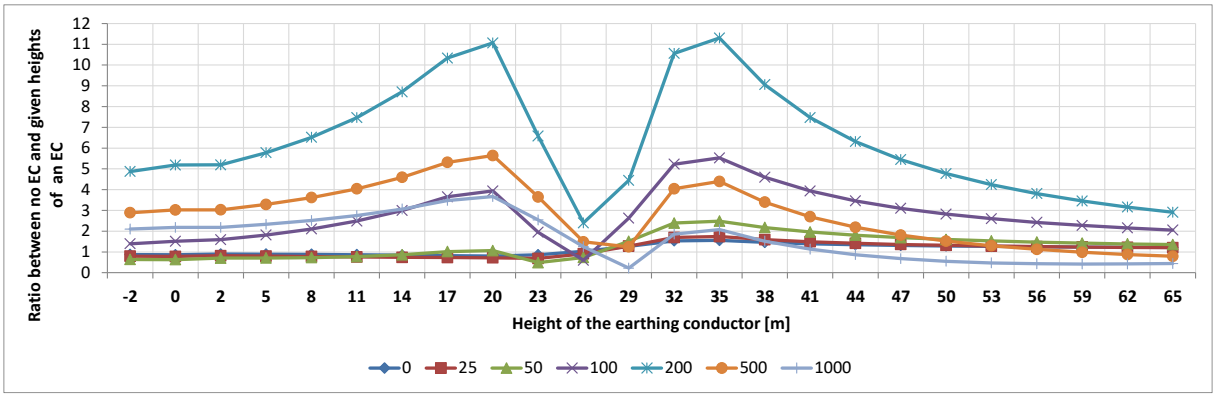

Figure C- 40: Ratio for the "ton"-pylon with two ECs and the worst CC for different heights of the EC for certain distances, where the reference value (value = 1) is always the case of using no EC for certain distances

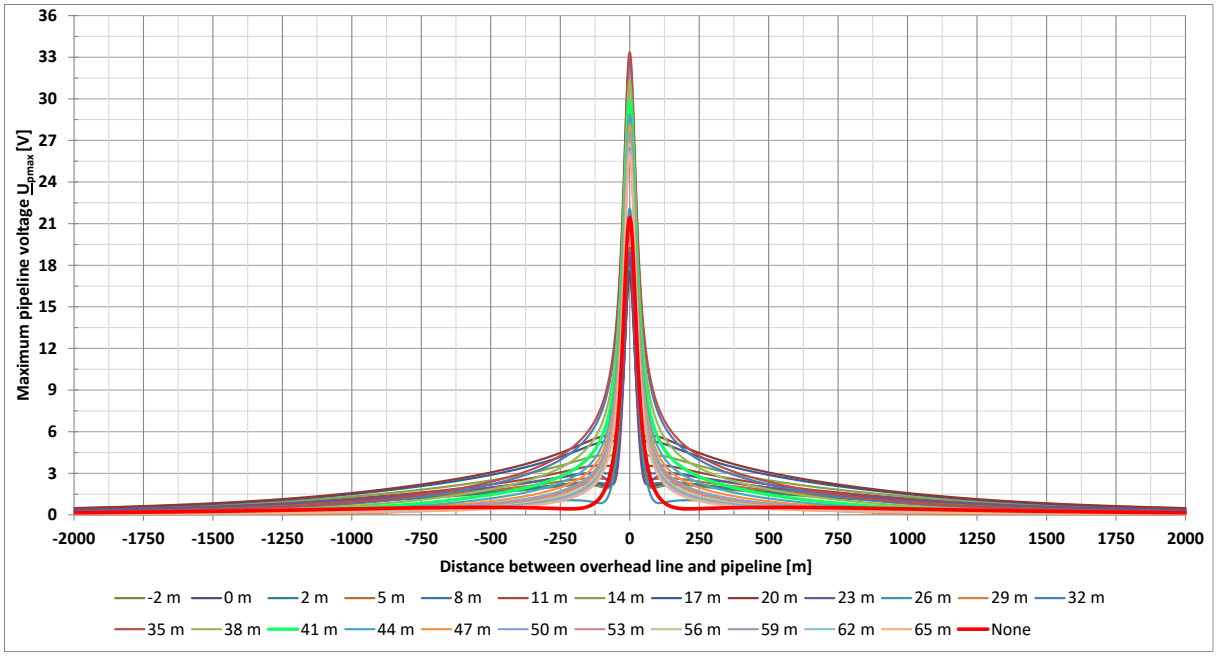

Figure C- 41: Maximum PIVs for the "ton"-pylon with two ECs and the worst CC at different heights of EC

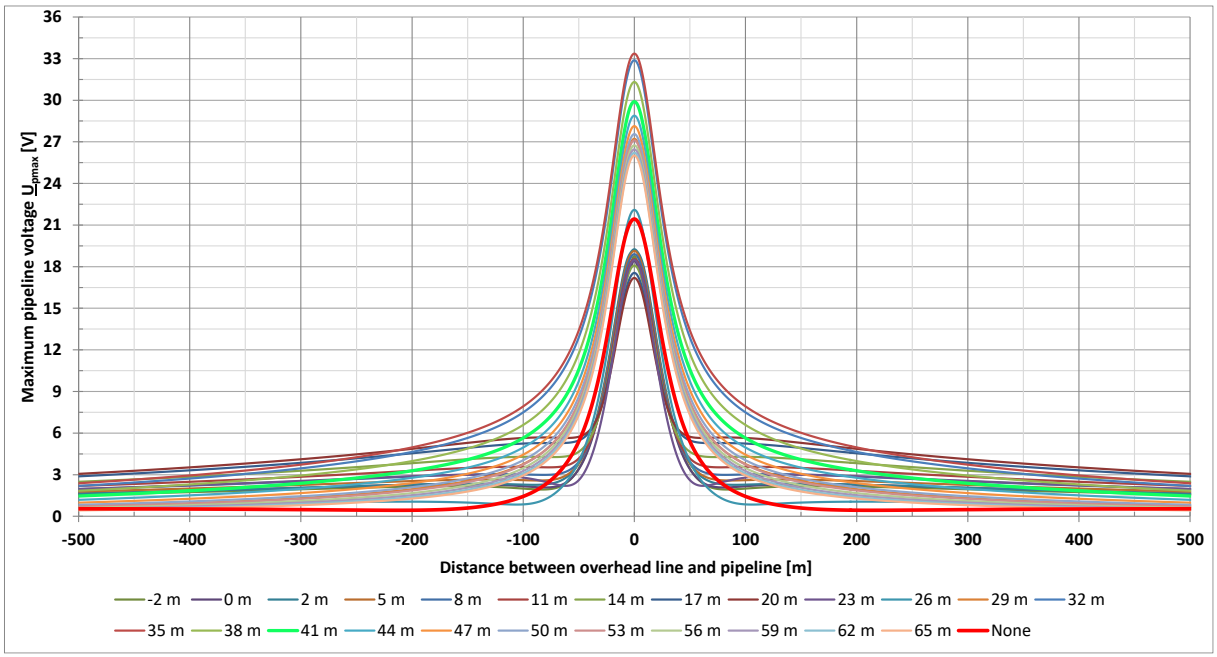

Figure C- 42: Maximum PIVs for the "ton"-pylon with two ECs and the worst CC at different heights of EC; zoomed variant

C.13 “Tan” pylon with two ECs 220 kV (PY12) – best CC

The voltage curves in Figure C- 43 and Figure C- 44 serve as a starting point for the voltages in Figure C- 45 and the ratios in Figure C- 46. For this purpose, the calculation method from chapter 4.7.2.1.1 for the vertical profile is used.

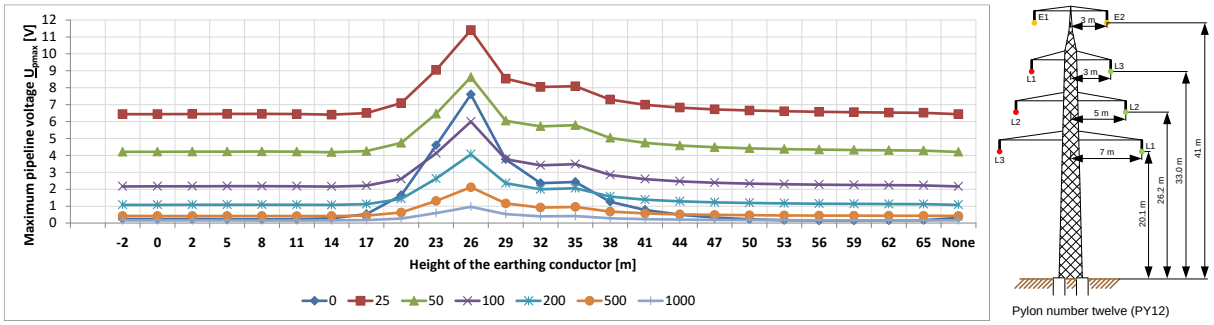

Figure C- 43: Maximum PIVs for the “tan”-pylon with two ECs at different heights of EC for certain distances

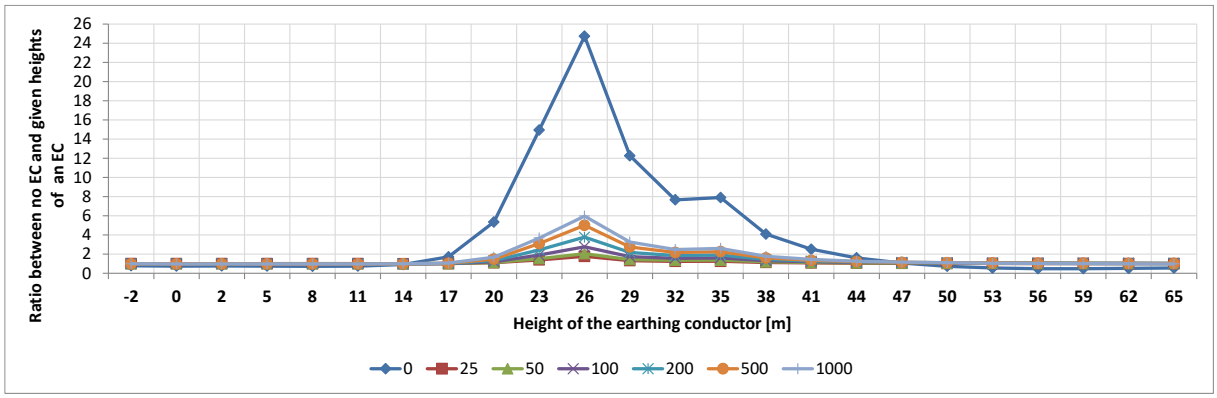

Figure C- 44: Ratio for the “tan”-pylon with two ECs and the best CC for different heights of the EC for certain distances, where the reference value (value = 1) is always the case of using no EC for certain distances

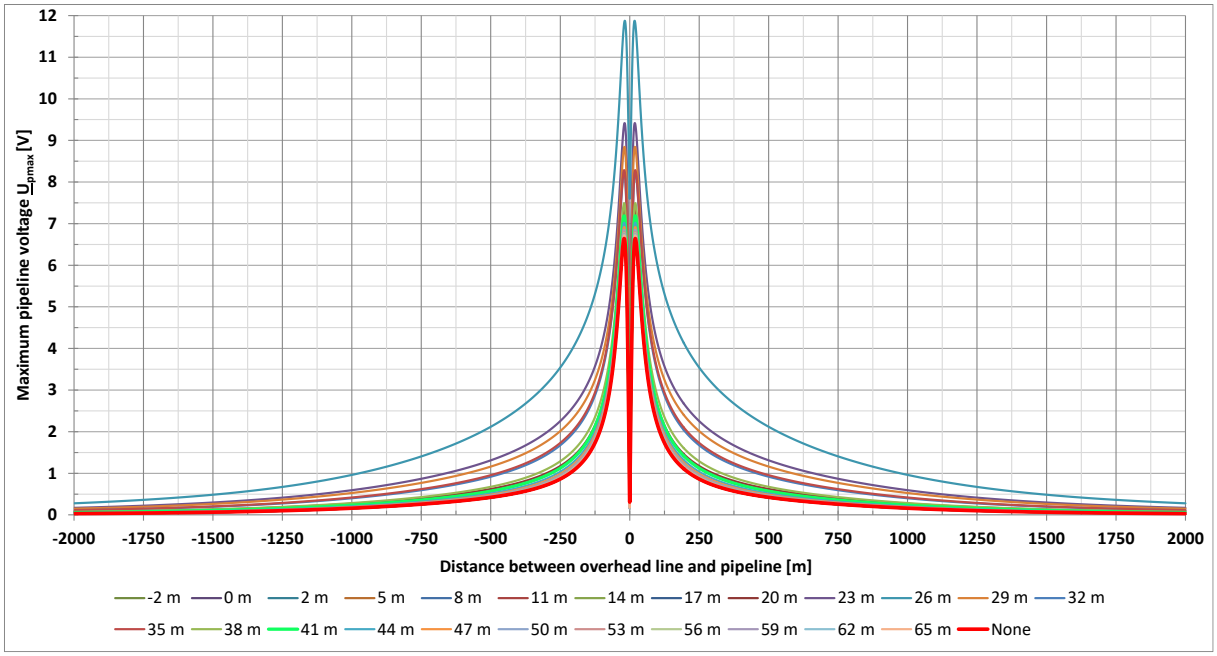

Figure C- 45: Maximum PIVs for the "tan"-pylon with two ECs and the best CC at different heights of EC

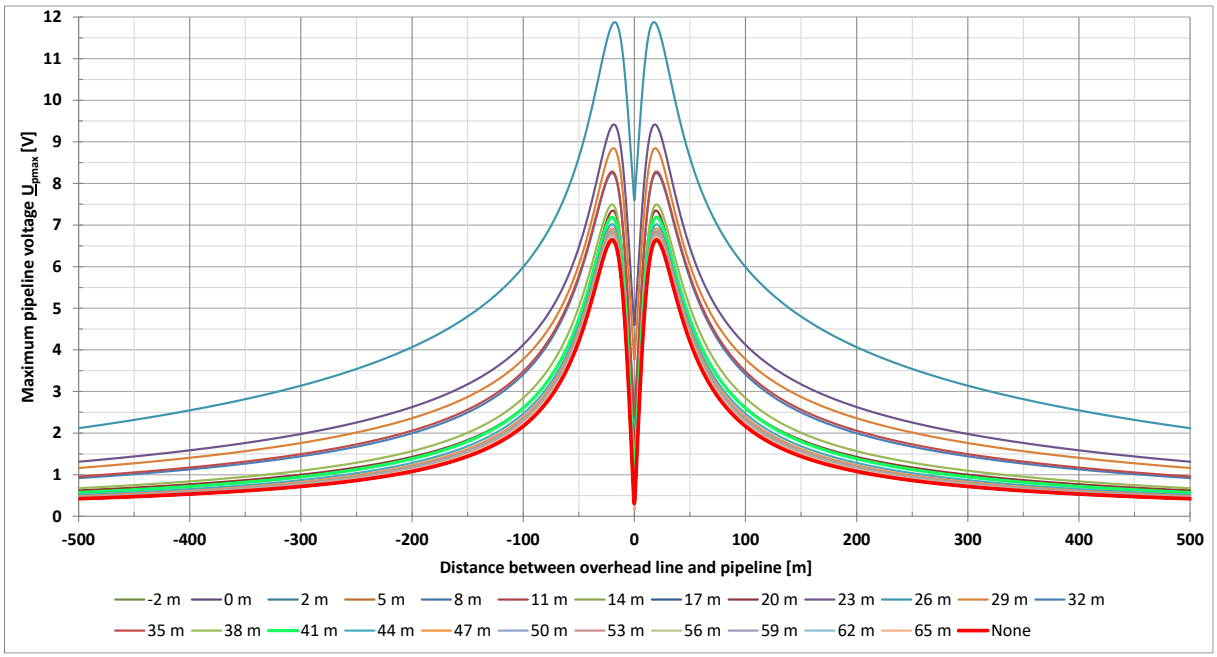

Figure C- 46: Maximum PIVs for the "tan"-pylon with two ECs and the best CC at different heights of EC; zoomed variant

C.14 "Tan" pylon with two ECs 220 kV (PY12) – worst CC

The voltage curves in Figure C- 47 and Figure C- 48 serve as a starting point for the voltages in Figure C- 49 and the ratios in Figure C- 50. For this purpose, the calculation method from chapter 4.7.2.1.1 for the vertical profile is used.

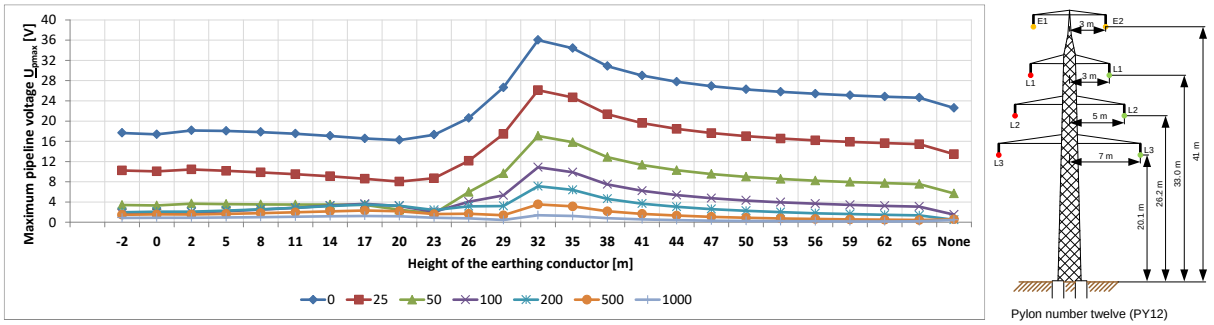

Figure C- 47: Maximum PIVs for the "tan"-pylon with two EC2 at different heights of EC for certain distances

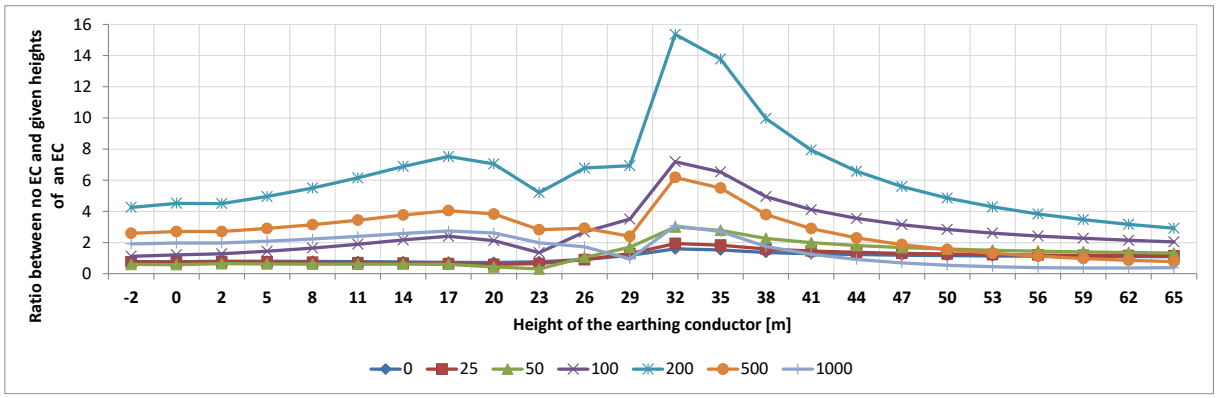

Figure C- 48: Ratio for the "tan"-pylon with two ECs and the worst CC for different heights of the EC for certain distances, where the reference value (value = 1) is always the case of using no EC for certain distances

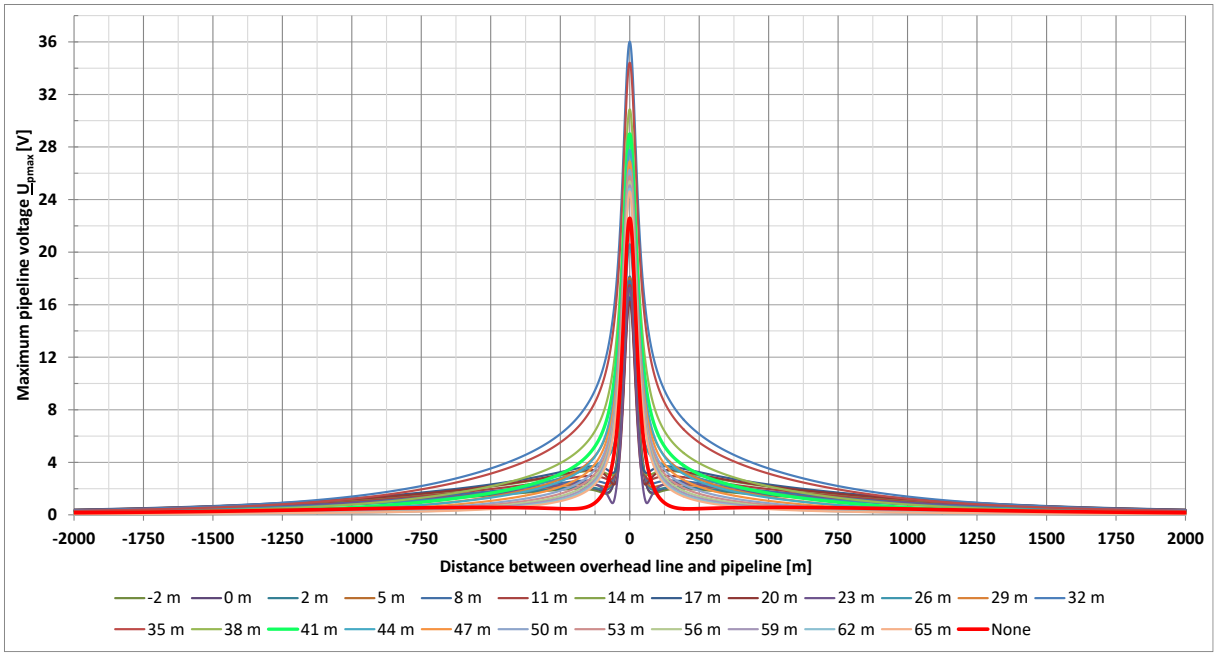

Figure C- 49: Maximum PIVs for the "tan"-pylon with two ECs and the worst CC at different heights of EC

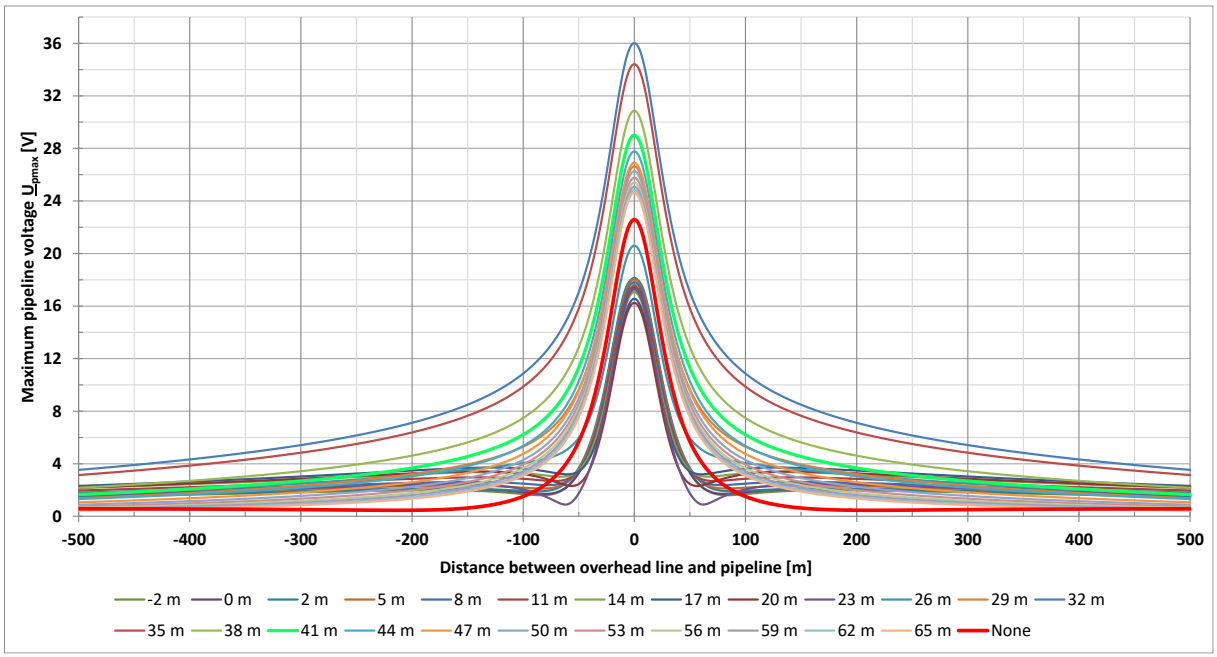

Figure C- 50: Maximum PIVs for the "tan"-pylon with two ECs and the worst CC at different heights of EC; zoomed variant

D Additional voltage curves of chapter 5

D.1 Two parallel overhead lines next to one pipeline

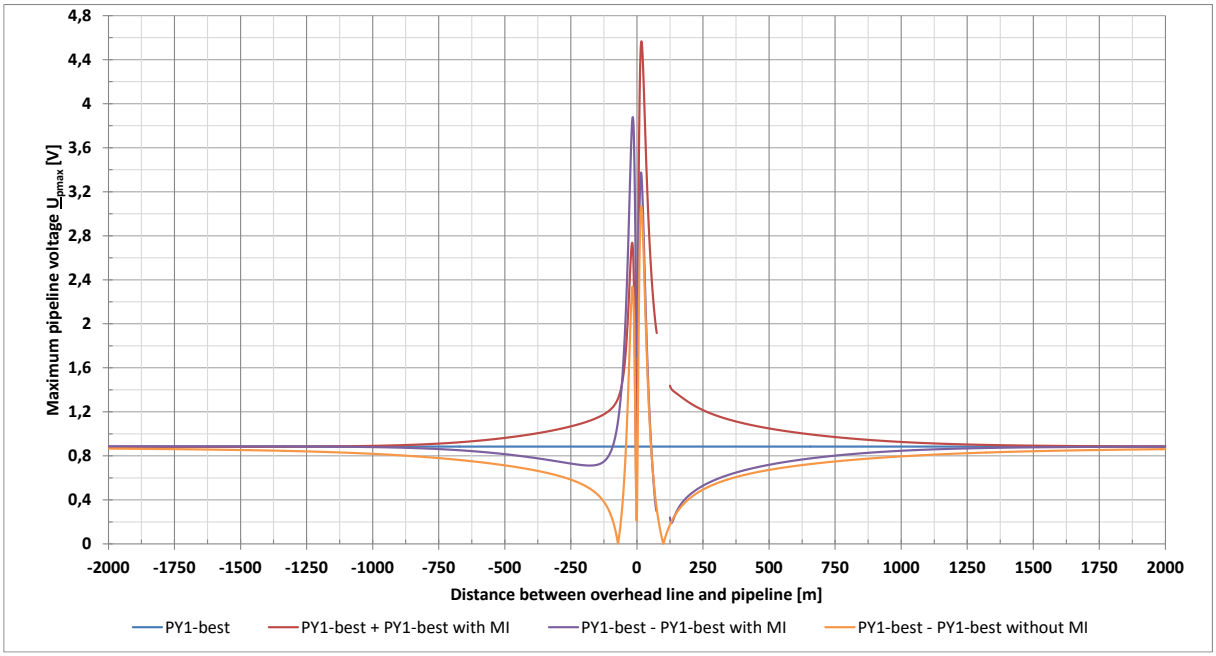

Figure D-1: Maximum PIVs for the combination of PY1-best with PY1-best for the same and the reversed current direction for distances of +/- 2000 m

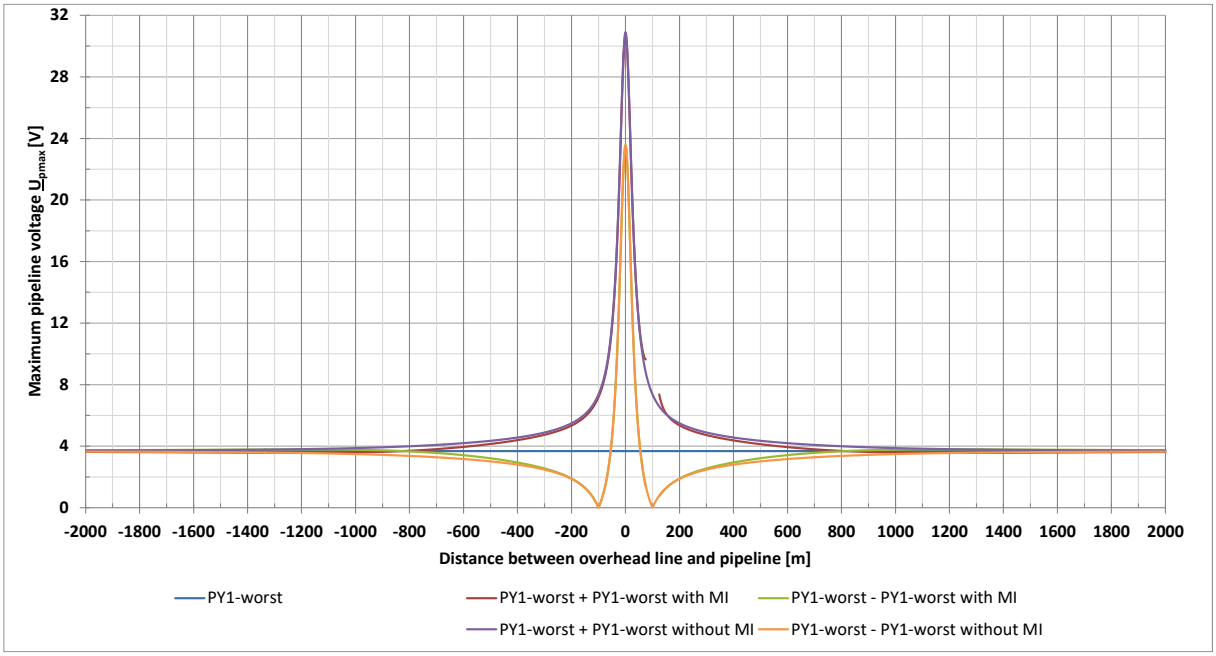

Figure D-2: Maximum PIVs for the combination of PY1-worst with PY1-worst for the same and the reversed current direction for distances of +/- 2000 m

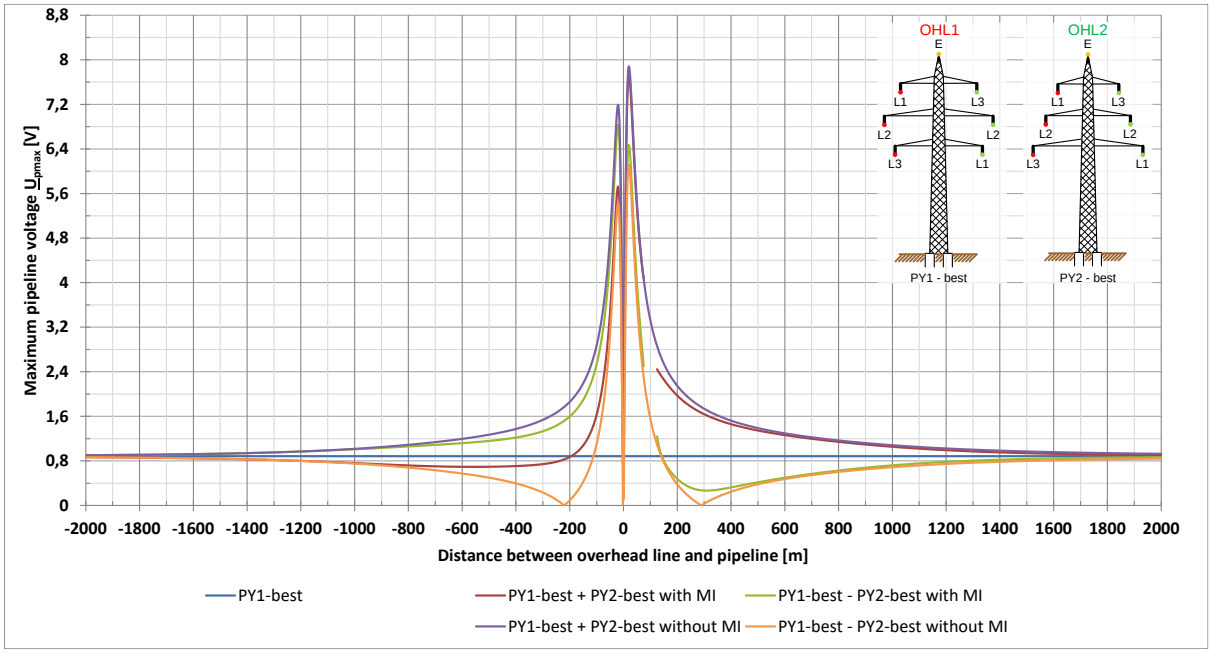

Figure D-3: Maximum PIVs for the combination of PY1-best with PY2-best for the same and the reversed current direction for distances of +/- 2000 m

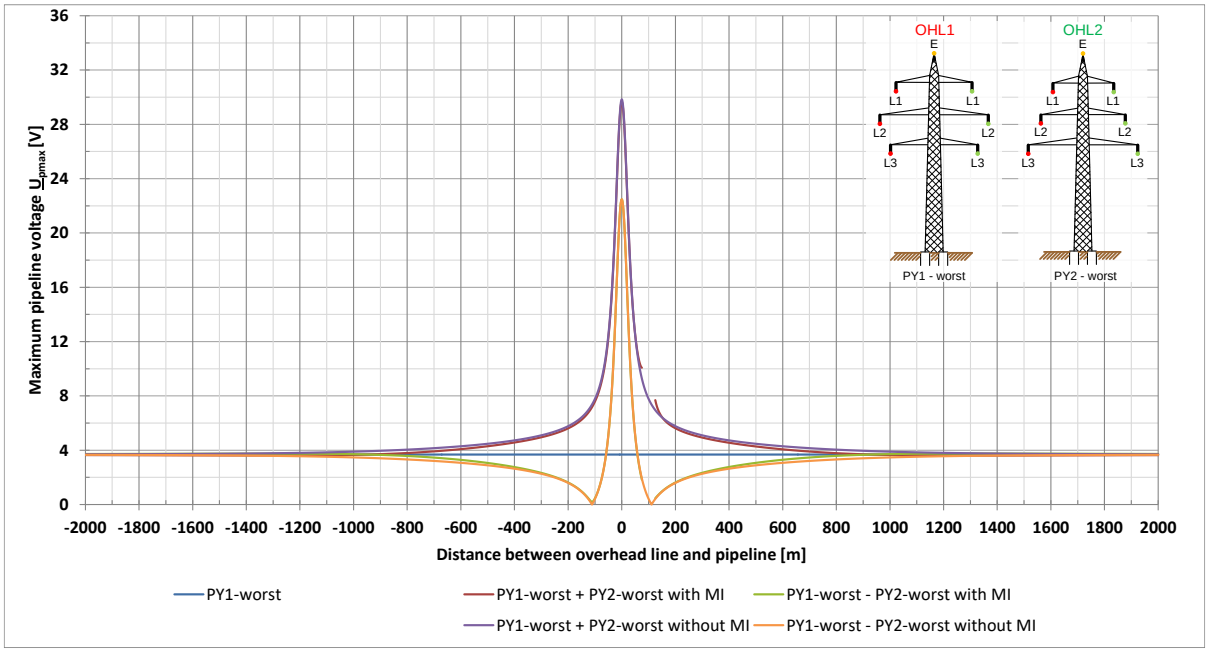

Figure D-4: Maximum PIVs for the combination of PY1-worst with PY2-worst for the same and the reversed current direction for distances of +/- 2000 m

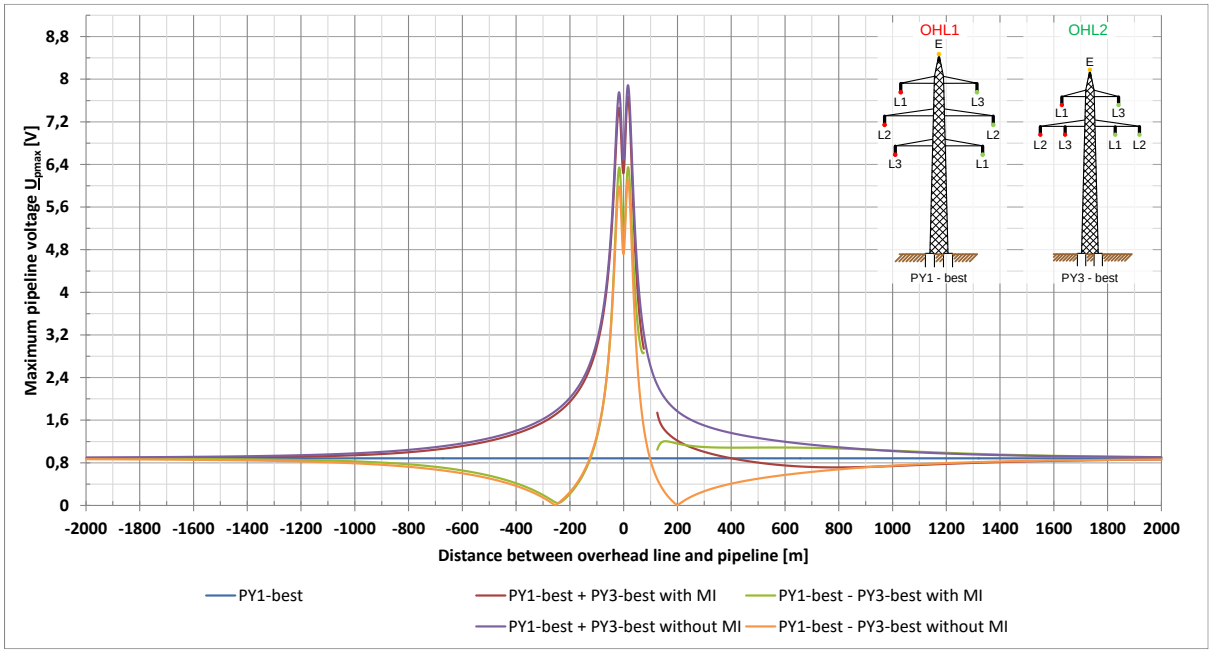

Figure D-5: Maximum PIVs for the combination of PY1-best with PY3-best for the same and the reversed current direction for distances of +/- 2000 m

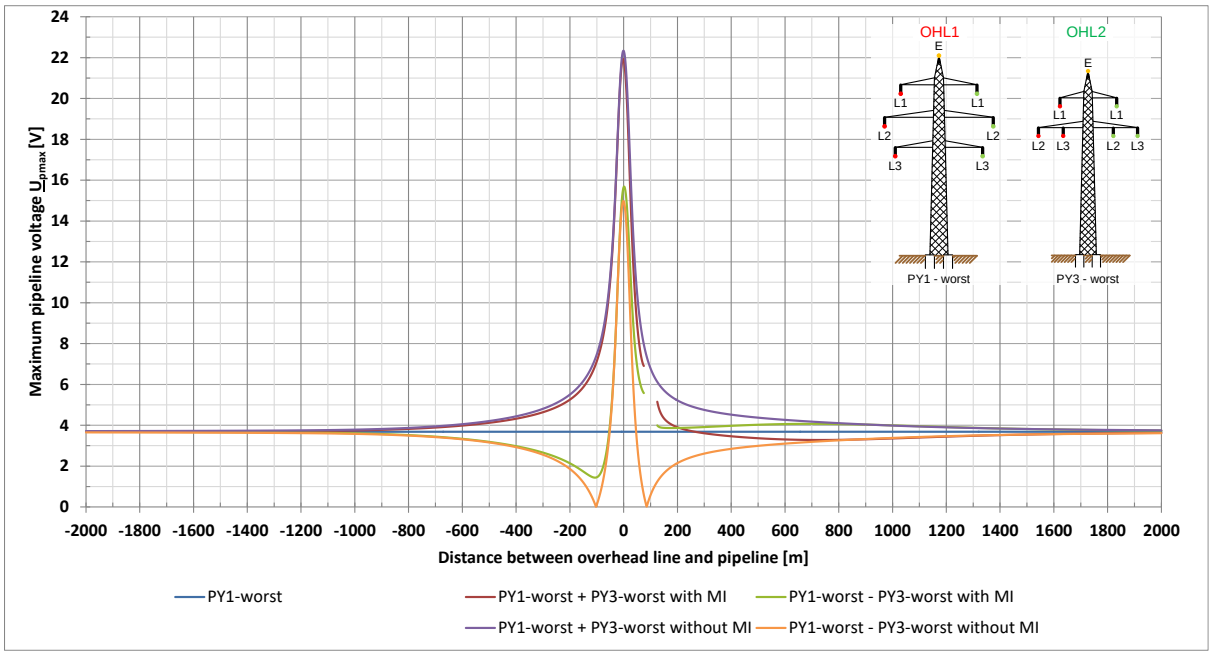

Figure D-6: Maximum PIVs for the combination of PY1-worst with PY3-worst for the same and the reversed current direction for distances of +/- 2000 m

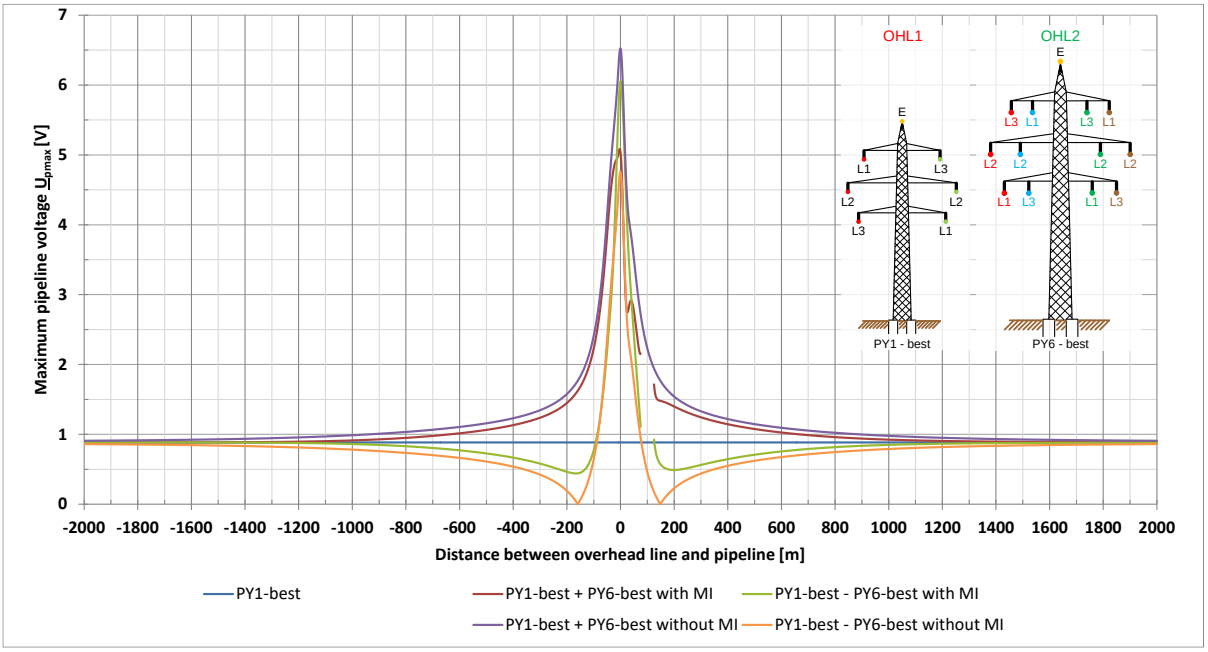

Figure D-7: Maximum PIVs for the combination of PY1-best with PY6-best for the same and the reversed current direction for distances of +/- 2000 m

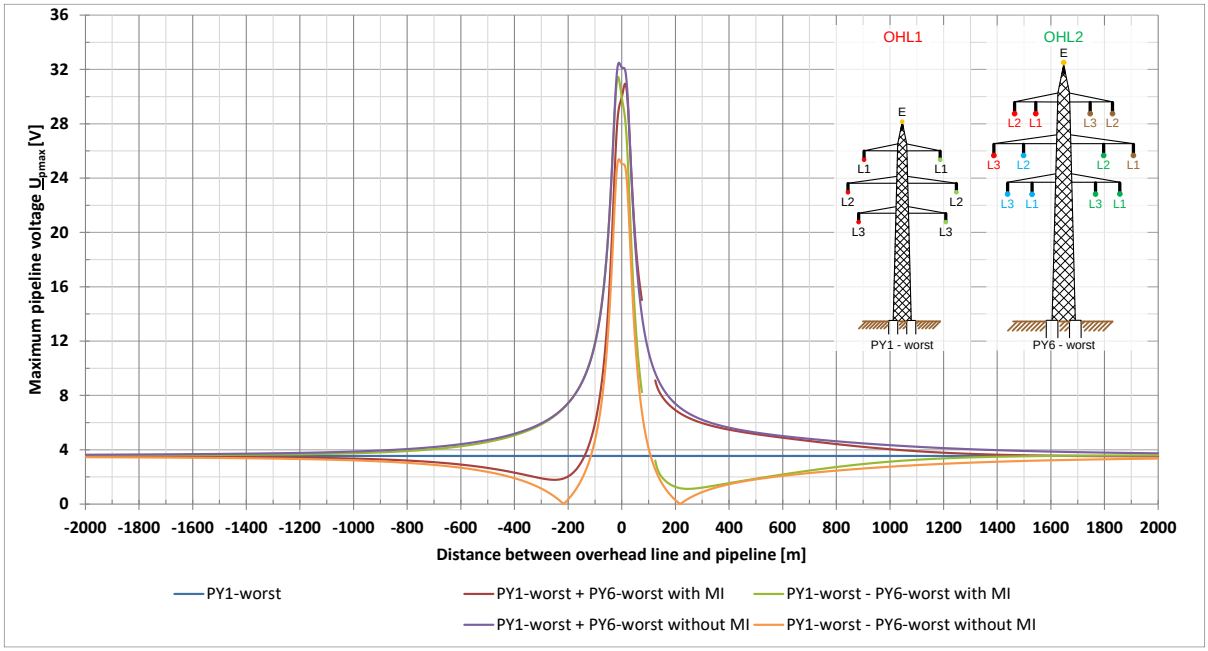

Figure D-8: Maximum PIVs for the combination of PY1-worst with PY6-worst for the same and the reversed current direction for distances of +/- 2000 m